

# FLOW CHARACTERISTICS OF VERTICAL GATES WITH DIFFERENT LIP SHAPES

## A THESIS

*Submitted in partial fulfilment of the  
requirements for the award of the degree*

*of*

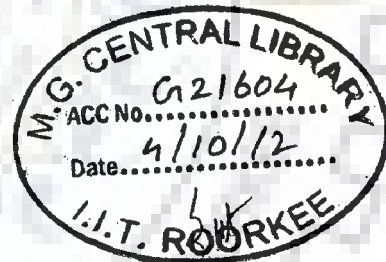
DOCTOR OF PHILOSOPHY

*in*

WATER RESOURCES DEVELOPMENT & MANAGEMENT

*by*

**RAJ AVTAR SINGH**



DEPARTMENT OF WATER RESOURCES DEVELOPMENT & MANAGEMENT  
INDIAN INSTITUTE OF TECHNOLOGY ROORKEE  
ROORKEE-247 667 (INDIA)

JANUARY, 2012



**©INDIAN INSTITUTE OF TECHNOLOGY ROORKEE, ROORKEE-2012  
ALL RIGHTS RESERVED**



# INDIAN INSTITUTE OF TECHNOLOGY ROORKEE ROORKEE

## CANDIDATE'S DECLARATION

I hereby certify that the work which is being presented in the thesis entitled "FLOW CHARACTERISTICS OF VERTICAL GATES WITH DIFFERENT LIP SHAPES" in partial fulfilment of the requirements for the award of the degree of Doctor of Philosophy and submitted in the Department of Water Resources Development and Management of the Indian Institute of Technology Roorkee, Roorkee is an authentic record of my own work carried out during the period from January, 2005 to January, 2012 under the supervision of Professor Gopal Chauhan, Department of Water Resources Development and Management, Dr. C.S.P. Ojha, Professor, and Dr. Ajay Gairola, Associate Professor, Department of Civil Engineering, Indian Institute of Technology Roorkee, Roorkee.

The matter presented in this thesis has not been submitted by me for the award of any other degree of this or any other Institute.

(Raj Avtar Singh)

This is to certify that the above statement made by the candidate is correct to the best of our knowledge.

(Dr. Ajay Gairola)  
Supervisor

(Prof. C.S.P. Ojha)  
Supervisor

(Prof. Gopal Chauhan)  
Supervisor

Date: January 10, 2012

The Ph.D. Viva-Voce Examination of Mr. Raj Avtar Singh, Research Scholar, has been held on

5-7-2012

Signatures of  
Supervisors

Signature of  
Chairman SRC

Signature of  
External Examiner

Head of the Department / Chairman ODC

---

## ACKNOWLEDGEMENTS

---

I feel great privileged to express my deep sense of gratitude to **Prof. Gopal Chauhan** Professor, Water Resources Development and Management, IIT , **Dr. C.S.P.Ojha**, Professor in Department of Civil Engineering and **Dr. Ajay Gairola**, Associate Professor Department of Civil Engineering , I.I.T.Roorkee or giving me an opportunity for doing my Ph.D. work under their sincere, intelligent and honest guidance. This work could have been completed only due to their invaluable guidance, fruitful suggestions, generous help and motivation throughout the present investigation. They have been my key source of inspiration throughout my Ph.D. programme. I am also thankful to **Dr. Nayan Sharma**, Head of Department, Water Resources Development & Management, I.I.T. Roorkee for his valuable guidance and support during my research work. Sincere thanks to **Prof S.K. Tripathi**, and **Dr. Deepak Khare**, Professors at Water Resources Development & Management, IIT Roorkee for the support and guidance extended by them during my research work.

Sincere thanks are due to **Dr. C.S.P.Ojha** , **Dr. U.C.Kothari** , **Dr. K. Hari Prasad**, **Dr. Z. Ahmad**, and **Dr.P.K.Sharma**, **Faculties at Civil Engg.Deptt.**, IIT Roorkee for giving me an opportunity to do experimental work in Hydraulics Laboratory of Civil Engineering Department and their sincere support and invaluable guidance during my experimental work. I am also thankful to Head of Department of my parent organization , Irrigation Department for granting me study/other leaves and all the support for the purpose of my present research work. My sincere thanks are also due to all the members of SRC for their valuable suggestions.

Special thanks are due to the Government for granting me permission for doing this research work at I.I.T. Roorkee without which it could not have become possible to do the present work.

Discussions and immense help extended by friends like **Mr. Manoj Kumar**, Research Scholar, **Mr. Kaushika G.S**, M Tech Student and **Mr. Farookh Omar**, **Mr. Shourya Nautiyal**, **Mr. Sachit**, **Mr. Madhusudan**,. students of IIT Roorkee for their sincere support and assistance in carrying out the experimental work and data analysis.

The assistance extended by the supporting staff of Hydraulics Engineering Laboratory, **Mr. Y. S. Pundir Pundir**, **Mr. Rati Ram**, **Mr. Pramod Kumar**, **Mr. Chhote Lal**, **Mr. Vinod Sharma** and **Mr. Arsad** and others are thankfully acknowledged.

The scientific and moral support from my friends **Mr. K.P. Singh**, S.D.O. Head works Irrigation Department for assisting me from time to time.

Thanks are also due to Mr. Rajendra Singh , Mr. Vinod Gupta and Mr. Imtiyazul Hasan staff of Irrigation Deptt. for their sincere support. The author is also thankful to all other friends and staff who rendered direct and indirect help at different stages of present study.

I feel indebted to my caring wife **Mrs Neetu Singh** who have given me moral support and unconditional affection throughout the period of my research work without which the present work could never be completed.

I wish to extend my thanks to **Mr. Jagvir Singh** and other staff of WRD & M Deptt. for their sincere help from time to time. I wish to extend my unconditional love and affection to my sons **Yashasvi Raj**, and **Aojasvi Raj** for their assistance, throughout the period of my study.

The author feels indebted of his Late father, mother, brother, Late Father in law, Mother in law for their unconditional love and affection.

(Raj Avtar Singh)  
Author  
email: [rajavtaar.singh@gmail.com](mailto:rajavtaar.singh@gmail.com)

---

## ABSTRACT

---

The present work has been mainly an experimental investigation with the broad objectives of studying the discharge and pressure characteristics of vertical gate with different types of non-stream lined and stream lined lip shapes at gate bottom. These lips have been placed at the gate bottom and experiments have been conducted in total for fourteen types of lip shapes and four types of bed conditions including three raised ogee crests, marked by variations in the upstream face and one plane bed. In total, six non-stream lines lip shapes and eight stream lined lip shapes have been tested for their discharge and pressure characteristics.

Certain simplifications to the existing relationships for computation of discharge through gates are done to bring out similarity between these relationships and relationships based on field data. It is also observed that higher discharge coefficients are obtained in the case of weirs located above raised crest. Discharge coefficient variations are found sensitive to the lip effects. To account for lip effects, correction factors are developed which can be used for different bed conditions and lip types. These correction factors, when multiplied with existing relationships of discharge coefficient, lead to a better match with the observed values of discharge coefficient.

Among non-streamlined lip types, lip having equal lip width to lip length is found effective as leads to higher coefficient of discharge than other non-streamlined lip types for a given relative gate opening. For a given lip type, the discharge coefficient is found to be higher when the gate is located above raised crest than the plane bed. This behavior is observed for all the lip types. Regarding pressure variation, the ratio of observed to hydrostatic pressure is found below one. This is influenced by the type of bed profile. For example: ogee weir having upstream face as  $2H: 3V$  is found to experience a lesser pressure

than type 1H: 3V and upstream face vertical. Ratio of observed pressure ( $P$ ) to gate opening ( $a$ ) is found to have an increasing trend with the ratio of upstream specific energy ( $E$ ) to gate opening. Also, this trend is found to be non-linear for different lip types. Only few lip types have been identified which have uniform distribution of pressure across the gate thickness. Based on the  $C_d$  variation, ratio of observed to hydrostatic pressure and uniformity of pressure variation, ranking of overall performance of various lip shapes is done. The best performing lip types are identified among non-stream lined and stream lined lip types.



---

# CONTENTS

---

<b>CANDIDATE'S DECLARATION</b>	<b>i</b>
<b>ACKNOWLEDGEMENTS</b>	<b>iii</b>
<b>ABSTRACT</b>	<b>v</b>
<b>CONTENTS</b>	<b>vii</b>
<b>LIST OF TABLES</b>	<b>xi</b>
<b>LIST OF FIGURES</b>	<b>xiii</b>
<b>LIST OF NOTATIONS</b>	<b>xix</b>
<b>INTRODUCTION</b>	<b>1</b>
1.1 INTRODUCTION AND MOTIVATION	1
1.2 OBJECTIVES OF PRESENT WORK	2
1.3 ORGANIZATION OF THESIS	3
<b>LITERATURE REVIEW</b>	<b>5</b>
2.1 INTRODUCTION	5
2.2 SLUICE GATE LOCATED ABOVE HORIZONTAL FLOOR	5
2.2.1 Discharge Through A Normal Sluice Gate:	5
2.2.2 PRESSURE VARIATIONS	13
2.3 SLUICE GATES LOCATED ABOVE RAISED CREST	15
2.4 USE OF LIP SHAPES	18
2.5 MISCELLANEOUS	19
2.5.1 Flow Characteristics	19
2.5.2 Field Investigations	21
2.6 SUMMARY	23
<b>EXPERIMENTAL SET UP</b>	<b>25</b>
3.1 INTRODUCTION	25
3.2 EXPERIMENTAL SET UP:	25
3.3 GATE	28
3.4 BED CREST SHAPES	28
3.4.1 Plane Bed Crest	28
3.4.2 Ogee Shaped Overflow Crest	29
3.5 SURGE TANK	31
3.6 V-NOTCH	32
3.7 PIEZOMETER	33
3.8 LIP SHAPES	34



3.9	SUMMARY	36
<b>DISCHARGE CHARACTERISTICS OF NON-STREAMLINED LIP SHAPES</b>		<b>37</b>
4.1	INTRODUCTION	37
4.2	DISCHARGE COEFFICIENT CALCULATION	37
4.3	THEORETICAL APPROACHES USED TO COMPUTE VALUES OF DISCHARGE COEFFICIENT	38
4.4	FORMULA FOR OBSERVED $C_d$	38
4.5	THE ANALYSIS OF $C_d$ USING THE SMALL ORIFICE FORMULA FOR WEIR CREST TYPE (1H:3V)	39
4.6	ANALYSIS OF DATA FOR RAISED CREST (2H: 3V)	42
4.7	ANALYSIS OF DATA FOR RAISED CREST WITH UPSTREAM FACE VERTICAL	45
4.8	ANALYSIS OF DATA FOR PLANE BED.	47
4.9	ANALYSIS OF $C_d$ USING LARGE ORIFICE FORMULA	49
4.9.1	Analysis of Data for Raised Crest (1H:3V)	49
4.9.2	Analysis of Data for Other Bed Types	51
4.10	DEVELOPMENT OF CORRECTION FACTOR	52
4.11	COMPARATIVE EVALUATION OF PERFORMANCE OF DIFFERENT NON STREAMLINED LIP SHAPES.	57
4.12	$C_d$ VARIATION AS PER CERTAIN EXISTING MODELS	59
4.12.1	Simplification of Swamee Approach:	59
4.12.2	Simplification of Roth and Hager approach:	60
4.12.3	Habibzadeh et al. Approach	61
4.13	SUMMARY	62
<b>PRESSURE CHARACTERISTICS OF NON-STREAM LINED LIP SHAPES</b>		<b>63</b>
5.1	INTRODUCTION	63
5.2	PRESSURE VARIATIONS	63
5.2.1	Pressure versus Relative Gate Opening	64
5.3	USE OF OTHER DIMENSIONLESS VARIABLES IN PRESSURE PLOTS	71
5.3.1	Critical Depth Based Dimensionless Terms	71
5.3.2	Specific Energy Based Dimensionless Term	75
5.4	UNIFORMITY OF PRESSURE VARIATION	78
5.5	SUMMARY	82
<b>DISCHARGE CHARACTERISTICS OF STREAMLINED LIP SHAPES</b>		<b>83</b>
6.1	INTRODUCTION	83
6.2	VARIATION OF DISCHARGE COEFFICIENT	83
6.2.1	Use of Small Orifice Formula	83

6.2.2	Use of Large Orifice Formula	88
6.3	DEVELOPMENT OF CORRECTION FACTORS	93
6.4	SUMMARY	100
<b>PRESSURE CHARACTERISTICS OF STREAM LINED LIP SHAPES</b>		<b>103</b>
7.1	INTRODUCTION	103
7.2	PRESSURE MEASUREMENTS	103
7.3	VARIATION OF PRESSURE	104
7.3.1	Variation of Observed to Hydrostatic Pressure with Relative Gate Opening	104
7.4	A COMPARATIVE EVALUATION OF STREAMLINED LIP TYPES USING PRESSURES ALONG THE LIP	112
7.5	USE OF OTHER DIMENSIONLESS PLOTS FOR PRESSURE VARIATION	116
7.6	SUMMARY	120
<b>EVALUATION OF PERFORMANCE OF LIPS</b>		<b>121</b>
8.1	INTRODUCTION	121
8.2	METHODOLOGY	121
8.3	EVALUATION OF LIP TYPES	121
8.4	RANKING OF LIP SHAPES	130
<b>CONCLUSIONS</b>		<b>133</b>
9.1	INTRODUCTION	133
9.1.1	Variation of Discharge Coefficient	133
9.1.2	Variation of Pressure	134
9.1.3	Ranking of Lips	135
9.2	LIMITATIONS OF THE STUDY AND FUTURE WORK	135
<b>BIBLIOGRAPHY AND REFERENCES</b>		<b>137</b>





Fig 8.1c	Overall score for different non-streamlined lips on a bed type (vertical)	125
Fig 8.1d	Overall score for different non-streamlined lips on a bed type (plane bed)	126
Fig 8.1e	Overall score for different -streamlined lips on a bed type (1H:3V)	127
Fig 8.1f	Overall score for different streamlined lips on a bed type (2H:3V)	128
Fig 8.1g	Overall score for different streamlined lips on a bed type (Vertical upstream face)	129
Fig 8.1h	Overall score for different streamlined lips on a bed type (plane bed)	130
8.2	Comparative Performance Chart Of Streamlined Lips.	131
8.3	Comparative Performance Chart Of Non Streamlined Lips.	132





	and lip C	
5.6 b	Observed to Hydrostatic Pressure vs. $y_{c2}/h_0$ for raised crest (2H:3V) and lip C	74
5.6 c	Observed to Hydrostatic Pressure vs. $y_{c2}/h_0$ for raised crest (vertical) and lip C	74
5.6d	Observed to Hydrostatic Pressure vs. $y_{c2}/h_0$ for flat bed and lip C	74
5.7a	Ratio of observed to hydrostatic pressure versus $E/a$ for lip C and raised crest type 1H:3V, 2H:3V and vertical and flat bed.	76
5.7 b	Ratio of observed to hydrostatic pressure versus $E/a$ for lip C and raised crest type 2H:3V and vertical and flat bed.	76
5.7c	Ratio of observed to hydrostatic pressure versus $E/a$ for lip C and raised crest type vertical .	77
5.7d	Ratio of observed to hydrostatic pressure versus $E/a$ for lip C and raised crest type and flat bed.	77
5.8a	Variation of $K_B$ for lip C for a raised crest (1H:3V)	79
5.8b	Variation of $K_B$ for lip M for a raised crest (1H:3V)	79
5.8c	Variation of $K_B$ for lip C for a raised crest (2H:3V)	80
5.8d	Variation of $K_B$ for lip M for a raised crest (2H:3V)	80
5.8e	Variation of $K_B$ for lip C for a raised crest (Vertical)	81
5.8f	Variation of $K_B$ for lip M for a raised crest (Vertical)	81
6.1 a	Agreement between observed and computed discharge coefficient using small orifice formula for different lip types in a gate located over a weir of upstream slope 1H:3V	84
6.1 b	Agreement between observed and computed discharge coefficient using small orifice formula for different lip types in a gate located over a weir of upstream slope 1H:3V	85
6.1 c	Agreement between observed and computed discharge coefficient using small orifice formula for different lip types in a gate located over a weir of upstream slope 1H:3V	86
6.1 d	Agreement between observed and computed discharge coefficient using small orifice formula for different lip types in a gate located over a weir of upstream slope 1H:3V	87
6.2 a	Agreement between observed and computed discharge coefficient using small orifice formula for different lip types in a gate located over a weir of upstream slope 1H:3V	89
6.2 b	Agreement of discharge coefficient using large orifice formula for lip types J,K,L and N	90
6.2 C	Agreement of discharge coefficient using large orifice formula for lip types J,K,L and N	91
6.2 d	Agreement between observed and computed discharge coefficient using small orifice formula for different lip types in a gate located over a weir of upstream slope 1H:3V	92
6.3 a	Agreement between observed and computed $C_d$ using correction factors for bed type (1H:3V)	97
6.3 b	Agreement between observed and computed $C_d$ (small orifice formula) for lips J, K, L and N using correction factors for bed type (1H:3V)	98

6.3c	Agreement between observed and computed Cd (large orifice formula) for lips F,G,H and I using correction factors for bed type (1H:3V)	99
6.3 d	Agreement between observed and computed Cd (large orifice formula) for lips J,K,L and N, using correction factors for bed type (1H:3V)	100
7.1a	Variation of observed to hydrostatic pressure for lip types F, G, H and I	105
7.1(b)	Variation of observed to hydrostatic pressure for lip types J, K, L and N	106
7.2a	Variation of observed to hydrostatic pressure in Lip types F,G,H and I for sluice gate placed above raised crest (2H:3V)	107
7.2b	Variation of observed to hydrostatic pressure in Lip types J, K, L and N for sluice gate placed above raised crest (2H:3V)	108
7.3a	Variation of observed to hydrostatic pressure in Lip types F, G, H and I for sluice gate placed above vertical raised crest	109
7.3b	Variation of observed to hydrostatic pressure in Lip types J, K, L and N for sluice gate placed above raised crest (Vertical upstream face)	110
7.4	A typical variation of observed Cd on stream lined lip shapes for gate located above raised crest.	112
7.5 a	Summary graph showing pressure variations for raised crest (1H:3V)	113
7.5 b	Pressure variations along lip H and N (for raised crest 1H:3V)	113
7.6 a	Summary graph showing pressure variations for raised crest (2H:3V)	114
7.6 b	Pressure variations along lip H and N (for raised crest 2H:3V)	114
7.7 a	Summary graph showing pressure variations for raised crest (upstream vertical face)	115
7.7 b	Pressure variations along lip H and N (for raised crest vertical upstream face)	115
7.8 a	Pressure ratio versus $y_{c1}/h_0$ for lip H and raised crest (2H:3V)	116
7.8 b	Pressure ratio versus $y_{c1}/h_0$ for lip H and raised crest (vertical upstream face)	116
7.9 a	Pressure ratio versus $y_{c2}/h_0$ for lip H and raised crest (2H:3V)	117
7.9 b	Pressure ratio versus $y_{c1}/h_0$ for lip H and raised crest (vertical upstream face)	117
7.10 a	P/a versus E/a variation for lip H on ogee crest (1H:3V)	118
7.10 b	P/a versus E/a variation for lip H on ogee crest (2H:3V)	118
7.10 c	P/a versus E/a variation for lip H on ogee crest (upstream vertical face)	119
7.10 d	P/a versus E/a variation for lip H on flat bed	119
Fig 8.1a	Overall score for different non-streamlined lips on a bed type (1H:3V)	123
Fig 8.1b	Overall score for different non-streamlined lips on a bed type (2H:3V)	124



## LIST OF FIGURES

Figure no.	Title	Page no.
2.1	Definition sketch for flow through a sluice gate (Source: Roth and Hager, 1999)	5
2.2	Discharge characteristics of normal sluice gate (Henry, 1950)	7
2.3a	Discharge coefficient $C_d$ as a function of relative gate opening $A$ ,	8
2.3b	Variation of $A_m$ with Reynolds number $R_a$ (Source: Roth and Hager, 1999)	9
2.3c	Variation of $C_{dm}$ as a function of Reynolds number $R_a$	10
2.3d	$D_d$ as a function of $A_n$ ,	10
2.4	Definition sketch for flow under vertical gate in plane bed condition	12
2.5	Shapes and dimensions of tested sills	15
2.6	Definition sketch for gate located over raised crest	16
2.7	Free orifice flow	17
2.8	Lip shapes suggested by Rao and Singla	19
3.1	Photographic view of Flume	26
3.2	Schematic diagram of experimental apparatus	27
3.3	Photographic view of gate Chamber	28
3.4	Schematic diagram of raised crest upstream face vertical	29
3.5	Schematic diagram of raised crest upstream face 1H:3V	30
3.6	Schematic diagram of raised crest upstream face 2H:3V	30
3.7	Schematic diagram of experimental apparatus with raised crest	31
3.8	Photographic view of surge tank	31
3.9	Setup of piezometer tubes	34
3.10 a&b	Schematic diagram of lip shapes and their nomenclatures	35
4.1a	Agreement diagram for raised crest (1H: 3V) for lip A and B	40
4.1b	Agreement diagram for raised crest (1H: 3V) for lip C and D	40
4.1c	Agreement diagram for raised crest (1H: 3V) for lip E and M	41
4.2a	Agreement diagram for raised crest (1H: 3V) for lip A and B	41
4.2b	Agreement diagram for raised crest (1H: 3V) for lip C and D	42
4.2c	Agreement diagram for raised crest (1H: 3V) for lip E and M	42
4.3a	Agreement diagram for raised crest (2H: 3V) for lip A and B	43
4.3b	Agreement diagram for raised crest (2H: 3V) for lip C and D	43
4.3c	Agreement diagram for raised crest (2H: 3V) for lip E and M	43
4.4a	Agreement diagram for raised crest (2H: 3V) for lip A and B	44
4.4b	Agreement diagram for raised crest (2H: 3V) for lip C and D	44
4.4c	Agreement diagram for raised crest (2H: 3V) for lip E and M	44
4.5a	Agreement diagram for raised crest vertical for lip A and B	45

4.5b	Agreement diagram for raised crest vertical for lip C and D	45
4.5c	Agreement diagram for raised crest vertical for lip E and M	46
4.6a	Agreement diagram for raised crest vertical for lip A and B	46
4.6b	Agreement diagram for raised crest vertical for lip C and D	46
4.6c	Agreement diagram for raised crest vertical for lip E and M	47
4.7a	Agreement diagram for plane bed lip A and B	48
4.7b	Agreement diagram for plane bed lip C and D	48
4.7c	Agreement diagram for plane bed lip E	48
4.8a	Agreement diagram for raised crest (1H: 3V) for lip A and B	49
4.8b	Agreement diagram for raised crest (1H: 3V) for lip C and D	50
4.8c	Agreement diagram for raised crest (1H: 3V) for lip E and M	50
4.9a	Agreement diagram for raised crest (1H: 3V) for lip A and B	50
4.9b	Agreement diagram for raised crest (1H: 3V) for lip C and D	51
4.9c	Agreement diagram for raised crest (1H: 3V) for lip E and M	51
4.10a	Agreement diagram for raised crest (1H: 3V) lip A and B	54
4.10b	Agreement diagram for raised crest (1H: 3V) for lip C and D	55
4.10c	Agreement diagram for raised crest (1H: 3V) for lip E and M	55
4.11a	Agreement diagram for raised crest (1H: 3V) for lip A and B	55
4.11b	Agreement diagram for raised crest (1H: 3V) for lip C and D	56
4.11c	Agreement diagram for raised crest (1H: 3V) for lip E and M	56
4.12	Cd variation with relative gate opening for raised crest (1H: 3V)	57
4.13	Cd variation with relative gate opening for raised crest (2H: 3V)	58
4.14	Cd variation with relative gate opening for raised crest (Vertical)	58
4.15	Cd variation with relative gate opening for Plane Bed	59
5.1a	Observed to Hydrostatic Pressure vs. Relative gate Opening	64
5.1b	Observed to Hydrostatic Pressure vs. Relative gate Opening for lip types D, E and M	65
5.2a	Variation of Observed to Hydrostatic Pressure vs. Relative gate Opening for lip type A, B and C	66
5.2b	Variation of pressure ratio for lip D, E and M with upstream face slope of 2H:3V	67
5.3a	Graphical Plot of Observed to Hydrostatic Pressure vs. Relative gate Opening for lips A, B and C.	68
5.3b	Graphical Plot of Observed to Hydrostatic Pressure vs. Relative gate Opening for lip types D, E and M	69
5.4a	Variation of pressure ratio for lip C on a gate located above flat bed.	70
5.4b	Observed to Hydrostatic Pressure vs. Relative gate Opening for lip D	71
5.5 a	Observed to hydrostatic pressure vs. $y_{c1}/h_0$ for raised crest (1H:3V) and lip C	72
5.5b	Graphical Plot of Observed to Hydrostatic Pressure vs. $y_{c1}/h_0$ for raised crest (2H:3V) and lip C	72
5.5c	Observed to Hydrostatic Pressure vs. $y_{c1}/h_0$ for raised crest and lip C	73
5.5d	Observed to Hydrostatic Pressure vs. $y_{c1}/h_0$ for plane bed and lip C	73
5.6a	Observed to Hydrostatic Pressure vs. $y_{c2}/h_0$ for raised crest (1H:3V)	73

*R* ridge  
*s* shock wave  
*u* downstream  
*v* vortex  
*w* wall





## LIST OF NOTATIONS

$A$	relative gate opening
$A_n$	normalized value of $A$
$A_1, A_2$ etc.	Horizontal dimension defining upstream quadrant of the crest.
$a, a_0$	gate opening
$B$	Gate width
$B_1, B_2$ etc.	Vertical dimension defining upstream quadrant of the crest.
$b$	channel width
$C$	Non-dimensional discharge coefficient.
$C_a$	Discharge coefficient as affected by downstream apron.
$C_b$	Discharge coefficient for spillways with breast wall.
$C_c$	contraction coefficient
$C_d$	Coefficient of discharge
$C_g$	Discharge coefficient for flow under the gate.
$C_h$	Discharge coefficient for head $H$ ( other than design head).
$C_s$	Discharge coefficient as affected by submergence of the crest.
$D$	Net opening for the spillway with breast wall
$D_H$	difference of extreme stagnation depths
$D_d$	normalized value of $C_d$
$D_m$	relative reduced shock wave height
$E$	Upstream Specific Energy
$F$	Froude number
$g$	Acceleration due to gravity.
$H$	Upstream flow depth above the flume bed.
$H_1$	Upstream flow depth above the sill crest
$H_o$	approach energy head
$H_p$	relative bottom pressure
$H_{pg}$	normalized gate pressure head
$H_a$	Head due to velocity of approach.
$H_c$	Head from reservoir level up to the centerline of the opening of the gate.
$H_d$	Design head.
$h$	flow depth
$h_o$	approach flow depth
$h_p$	pressure head
$h_{pg}$	gate pressure head
$h_{rm}$	reduced shock wave height
$K_1, K_2$	Variable parameters.
$K_a$	Abutment contraction coefficient.
$K_B$	Pressure uniformity Coefficient
$K_p$	pier contraction coefficient.
$L$	Effective length of overflow crest.
$L$	Net length of overflow crest (excluding thickness of pier).
$M$	Riser of the crest.
$N$	Number of piers.
$n_1, n_2$	variable parameters.

$P$	Sill wetted perimeter.
$P$	bottom pressure at Lip
$Q$	discharge
$q$	Discharge per unit width.
$R_h$	hydraulic radius
$R_a$	Reynolds number
$R_s$	Sill hydraulic radius.
$R$	Radius of abutment.
$R_g$	Radius of crest gate.
$S_f$	friction slope
$T$	shock wave parameter
$U$	relative streamwise velocity
$u$	streamwise velocity component
$V_a$	Approach velocity.
$X, X_1, X_2$	Co-ordinates of the profile
$Y, Y_1, Y_2$	
$X$	relative streamwise coordinate
$X_s$	relative shock maximum position
$x$	streamwise coordinate
$Y$	normalized transverse coordinate
$Y_g$	normalized transverse coordinate
$Y_s$	relative shock wave height
$Z$	relative position above bed
$Z$	Height of the spillway crest measured from the river bed
$z$	vertical coordinate

### Greek Characters

$\alpha$	aspect ratio
$\gamma$	relative gate pressure
$\theta$	shock angle
$\lambda$	relative length of ridge
$\Pi$	force ratio
$\nu$	kinematic viscosity
$\rho$	fluid density
$\Phi$	friction gradient parameter
$\sigma$	surface tension.

### Subscripts

$a$	based on gate opening
$c$	contracted
$E$	anti-vortex element
$g$	gate
$L$	limit
$M$	maximum
$m$	minimum
$o$	base value
$p$	piezometric

---

## INTRODUCTION

---

### 1.1 INTRODUCTION AND MOTIVATION

Flow through vertical gates is encountered in a variety of situations in various hydraulic structures, such as barrage, canals, spillways, and power plant intake. On the upstream side of the gates, there is storage of water which applies hydrostatic pressure on the gates when these are fully closed. However, when the gates are raised to pass the desired discharge, the flowing water generates pressure on the bottom portion of the gate which is named as the lip of the gate. Depending on the magnitude of hydrodynamic force generated, the vibrations are setup in the gate. Engineers are also interested in the smooth closure of the gate. If one considers a situation when the pressure generated on the lip is working in the upward direction, it will offer resistance to the smooth gate closure. For this reason, it is of great practical significance to estimate this upward pressure or thrust acting on the gate. There have been limited studies to modify this up thrust through suitable choice of lip shapes (gate bottom geometry). However, some of the studies (Rao and Singla, 1986) have used electrical analogy to study the relative performance of certain lip shapes. Their work is based on Ohm's law which is valid only when the response of the system is linear. In real situation, the flow is often turbulent below the gates and therefore, it is expected that Ohm's analogy may not be valid. However, the work of Rao and Singla (1986) clearly indicates that lip geometry thus influence the up thrust. It is also known that lips with different geometries will guide the flow in different manner and therefore, it is most likely that for the same bed type and

same gate opening, the discharge passing through lips of different shapes will remain no more same.

In many practical situations, gates operate above horizontal bed. However, there are situations when the gates are located above raised crest. There are many studies which indicate the variation in discharge characteristics of flow through gates and the manner in which they operate above horizontal bed or raised crest. For the same lip shape, if there are two gates having same operating head through the gate, for the same opening of the gate the discharge through both the gates will differ if one is located above the horizontal floor and the other gate is located above the raised crest. Similarly, the pressure characteristics will also differ for the two gates though the lip shapes are same.

Literature review, detailed in next chapter, indicates that there is a need to undertake study on flow characteristics including discharge and pressure variations for different combinations of lip shape and the nature of the bed below gate. The present study is largely based on this need.

## **1.2 OBJECTIVES OF PRESENT WORK**

In view of the above, the objectives of the present study are identified as follows:

- 1 To study the discharge characteristics of vertical gates located above horizontal floor as well as raised crest for streamlined lip shapes.
- 2 To study the discharge characteristics of vertical gates located above horizontal floor as well as raised crest for non-streamlined lip shapes.
- 3 To study pressure characteristic of vertical gates located above horizontal floor as well as raised crest for streamlined lip shapes.



- 4 To study pressure characteristic of vertical gates located above horizontal floor as well as raised crest for non-streamlined lip shapes.
- 5 To identify the lip shape which can pass more discharge and which experiences minimum upward thrust for gates located on horizontal floor as well as raised crest.

### **1.3 ORGANIZATION OF THESIS**

**Chapter 1** deals with the motivation of the present study and outlines the need for further work regarding flow characteristics for streamlined and non- streamlined lip shapes.

**Chapter 2** deals with the literature review related to discharge characteristics for flow through gates located over different types of bed. It also deals with the lip shapes used by earlier investigators and deals with the various equations to compute flow through gates

**Chapter 3** deals with the experimental setup and details of experiments done on gates having different lip shapes. The experiments are organized in four broad categories in terms of the nature of the bed, i.e., horizontal and Ogee crest of three types. For each type of bed condition, eight streamlined lip shapes and six non- streamline lip shapes are considered.

**Chapter 4:** In this chapter the discharge characteristics for four types of bed conditions and eight streamline shapes are evaluated using available equations in the literature. Small orifice and large orifice formulations are used to test the applicability of existing equations. To correctly represent the discharge characteristics suitable correction factors are developed.

**Chapter 5:** In this chapter, the discharge characteristics for four types of bed conditions and six non-streamlined shapes are evaluated using available equations in the literature. Small orifice and large orifice formulations are used to test the applicability of existing

equations. To correctly represent the discharge characteristics, suitable correction factors are developed.

**Chapter 6:** In this chapter the pressure characteristics for four types of bed conditions and eight streamlined shapes are evaluated using available equations in the literature. Lip shape experiencing minimum pressure is identified.

**Chapter 7:** In this chapter the pressure characteristics for four types of bed conditions and six non streamlined shapes are evaluated using available equations in the literature. Lip shape experiencing minimum pressure is identified.

**Chapter 8:** It deals with the evaluation of relative performance of different lip types for different bed conditions.

**Chapter 9:** It deals with the conclusions and salient findings of the present work.

## LITERATURE REVIEW

## 2.1 INTRODUCTION

Sluice gates are widely used in irrigation networks for flow control and measurement. This chapter summarizes the findings of few important investigations on sluice gates. The flow from the gate could be either free or submerged by the tail water. Similarly, the bed below the sluice gate can be a horizontal floor or raised sill or crest. In this work, only the free flow conditions have been investigated. This work focuses on the flow characteristics through a sluice gate having different lip shapes. In the sections to follow, the literature review is confined to the objectives of the study, as indicated in Chapter 1.

## 2.2 SLUICE GATE LOCATED ABOVE HORIZONTAL FLOOR

## 2.2.1 Discharge Through A Normal Sluice Gate:

Fig. 2.1 shows the definition sketch for flow through a Sluice Gate.

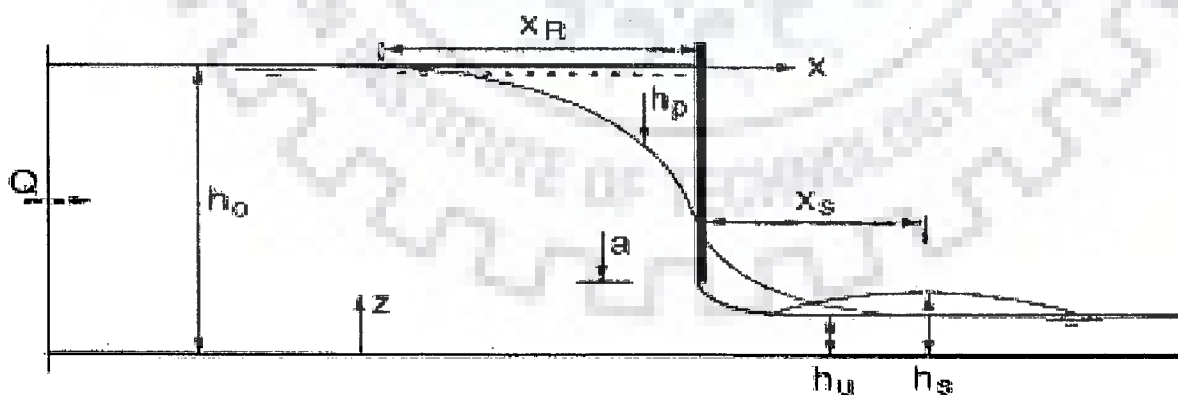
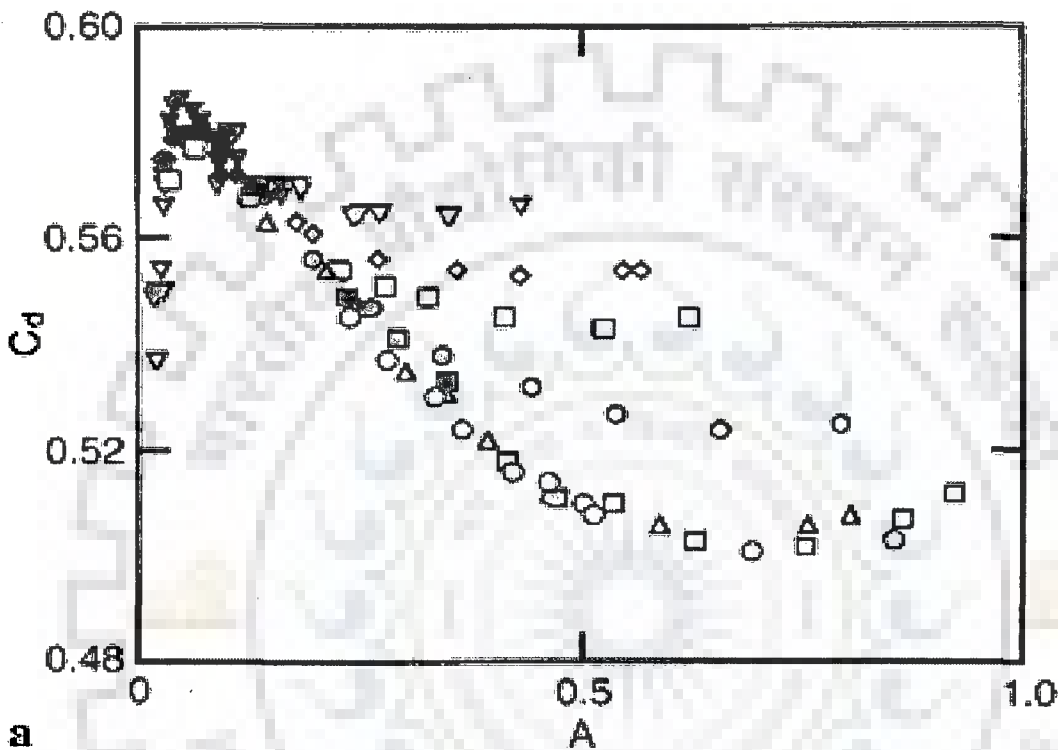


Fig. 2.1: Definition sketch for flow through a sluice gate (Source: Roth and Hager, 1999)

In Fig. 2.1,  $Q$ =discharge,  $h_0$ =approach flow depth,  $a$ =gate opening,  $x$ =stream wise coordinate measured from the gate section,  $z$ =vertical coordinate measured from the channel bottom,

$x_R$  Froude similarity law. For  $a < 50$  mm, the curves  $C_d(A)$  split. However, at lesser gate openings,  $m$  the effects of viscosity become significant, indicating a scale effect. For extremely small values  $ga$  of  $A$ , surface tension dominates the flow, and  $C_d$  decreases sharply.



$a(\text{mm}) = (\nabla) 10, (\diamond) 15, (\square) 20, (\circ) 30, (\triangle) 50, (\square) 80, (\circ) 120$

Fig. 2.3a Discharge coefficient  $C_d$  as a function of relative gate opening  $A$ , (Source: Roth and Hager, 1999)

As stated by Roth and Hager (1999), all curves for  $C_d(A)$  start close to 0.60, decrease to a minimum value  $C_{dm}$  with the corresponding relative gate opening  $A_m$ , and increase again varying essentially with the gate

It Reynolds number  $Ra = a(2ga)^{1/2}v^{-1}$ .

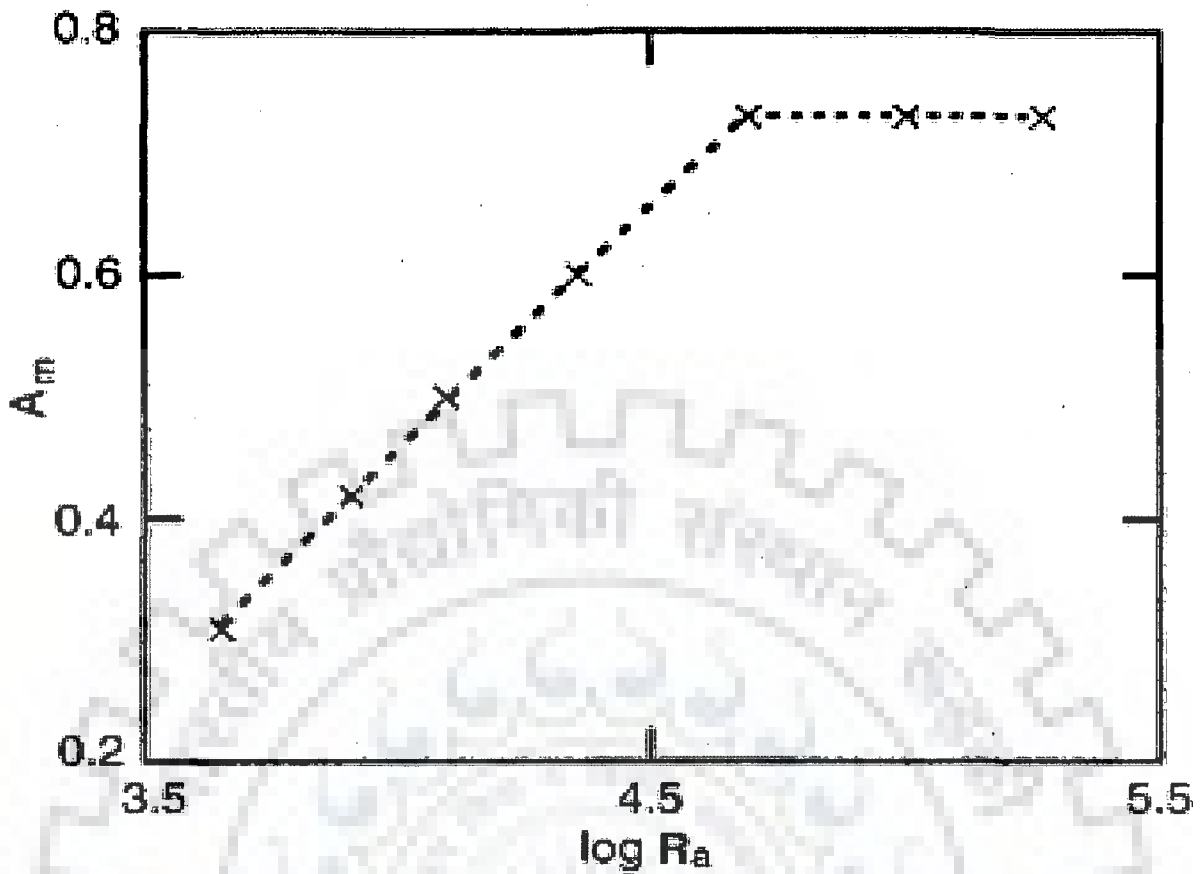


Fig. 2.3b: Variation of  $A_m$  with Reynolds number  $R_a$  (Source: Roth and Hager, 1999)

The curves in Figs. 2.3b and 2.3c are for the Reynolds number  $R_a < 5 \times 10^4$ . Fig 2.3b is governed by Eq. 2.3 and Fig 2.3c is governed by Eq. 2.4

$$A_m = 0.05 + 0.40 \log(R_a/1000) \quad (2.3)$$

$$C_{dm} = 0.60 - \frac{1}{18} \log(R_a/1000) \quad (2.4)$$

Further, substituting  $D_d = (C_d - C_{dm}) / (C_{d0} - C_{dm})$  all data for  $C_d$  can be expressed as a function of  $A_n = A/A_m$ , with  $C_{d0} = 0.594$  as the base value for small  $A_0$ . ( see Fig 2.3d)

$$D_d = (1 - A_n)^2 \quad (2.5)$$

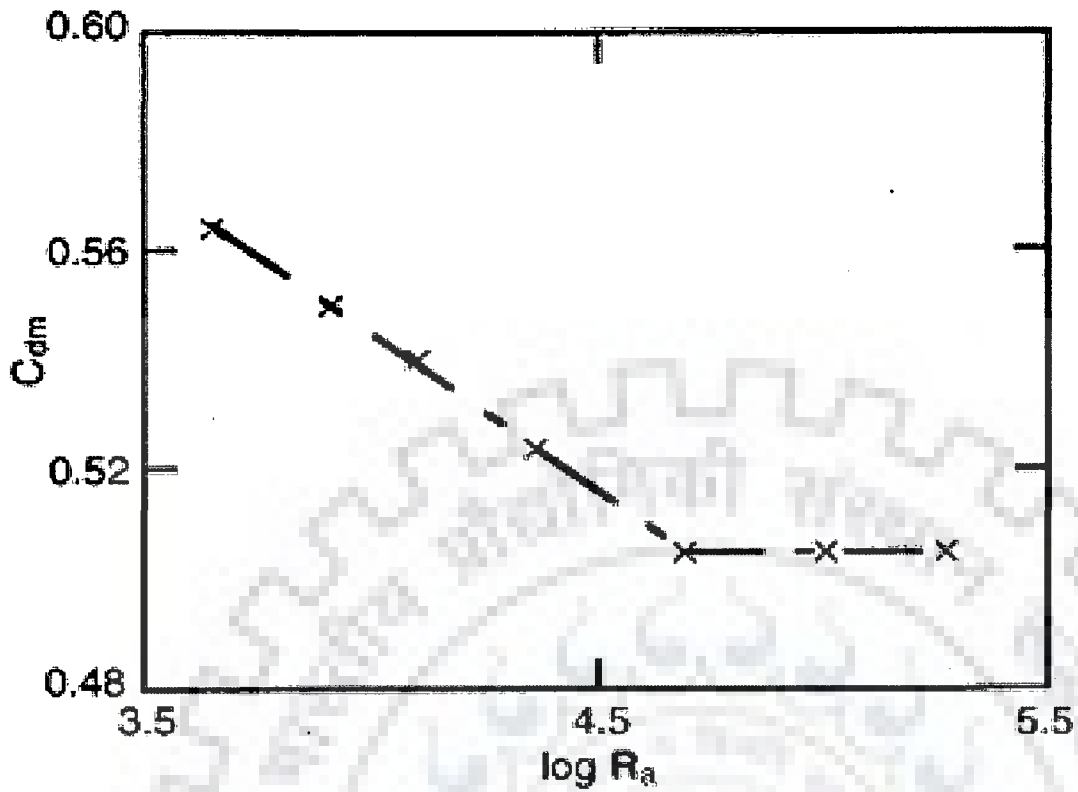
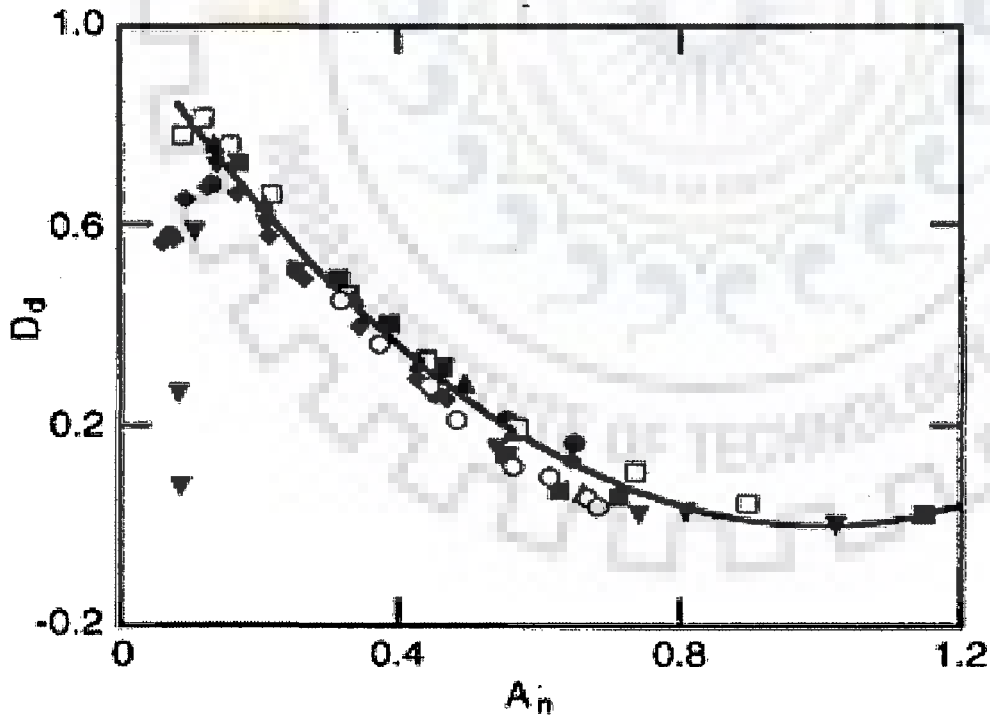


Fig. 2.3c: Variation of  $C_{dm}$  as a function of Reynolds number  $R_a$  (Source: Roth and Hager, 1999)



$\alpha$ (mm) = ( $\nabla$ ) 10, ( $\blacklozenge$ ) 15, ( $\square$ ) 20, ( $\bullet$ ) 30, ( $\blacktriangle$ ) 50, ( $\blacksquare$ ) 80, ( $\circ$ ) 120 (Source: Roth and Hager, 1999)

Fig. 2.3d:  $D_d$  as a function of  $A_n$ ,

LITERATURE REVIEW

2.1 INTRODUCTION

Sluice gates are widely used in irrigation networks for flow control and measurement. This chapter summarizes the findings of few important investigations on sluice gates. The flow from the gate could be either free or submerged by the tail water. Similarly, the bed below the sluice gate can be a horizontal floor or raised sill or crest. In this work, only the free flow conditions have been investigated. This work focuses on the flow characteristics through a sluice gate having different lip shapes. In the sections to follow, the literature review is confined to the objectives of the study, as indicated in Chapter 1.

2.2 SLUICE GATE LOCATED ABOVE HORIZONTAL FLOOR

2.2.1 Discharge Through A Normal Sluice Gate:

Fig. 2.1 shows the definition sketch for flow through a Sluice Gate.

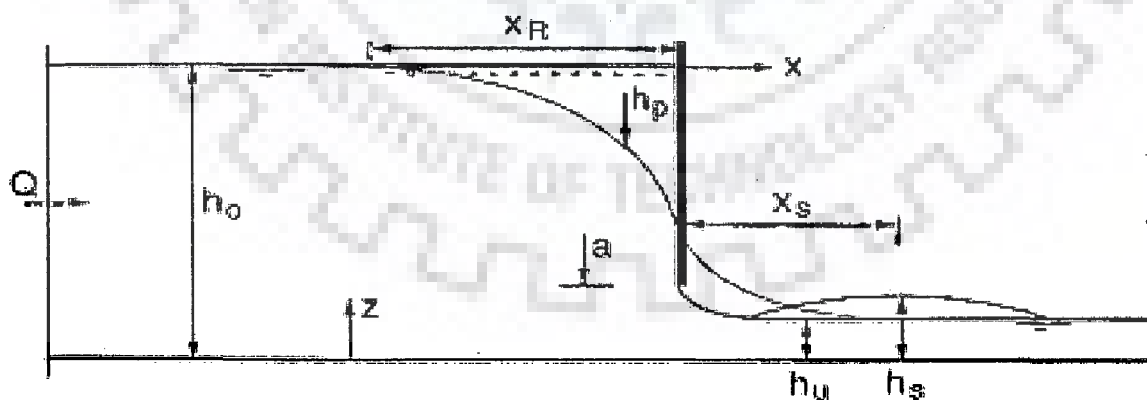


Fig. 2.1: Definition sketch for flow through a sluice gate (Source: Roth and Hager, 1999)

In Fig. 2.1,  $Q$ =discharge,  $h_0$ =approach flow depth,  $a$ =gate opening,  $x$ =stream wise coordinate measured from the gate section,  $z$ =vertical coordinate measured form the channel bottom,

$x_R$  = position of ridge (see below),  $h_p$  = piezometric head on channel bottom,  $x_s$  = position of maximum shock wave height  $h_s$ , and  $h_u$  = axial downstream depth. The general equation for sluice gate discharge is given as,

$$Q = C_d a b \sqrt{2g h_0} \quad (2.1)$$

where  $a$  is the gate opening and  $b$  is the width of the gate and  $C_d$  is the coefficient of discharge.

### 2.2.1.1 Henry's approach (1950)

Henry (1950) suggested curves of  $C_d$  versus  $h_0/a$  with  $h_t/a$  as the third parameter, where  $h_t$  is the tail water depth. The graph plotted is shown in Fig 2.2. Henry's work was authenticated by Rajaratnam and Subramanya (1967). This was further reinforced by Swamee (1992) who developed following equations for Henry's curves for free and submerged flow, respectively:

Free flow

$$C_d = 0.611 \left[ \frac{h_0 - a}{h_0 + 15a} \right]^{0.072} \quad (2.2)$$

For submerged flow

$$C_d = 0.611 \left[ \frac{h_0 - a}{h_0 + 15a} \right]^{0.072} \left\{ 1.032 \left[ \frac{.81 h_t \left( \frac{h_t}{a} \right)^{0.72} - h_0}{h_0 - h_t} \right]^{0.7} \right\}^{-0.1} \quad (2.3)$$

It is to be noted that the equation proposed by Swamee has been reported to give poor results by Sepulveda et al. (2009) and Belaud et al. (2009).



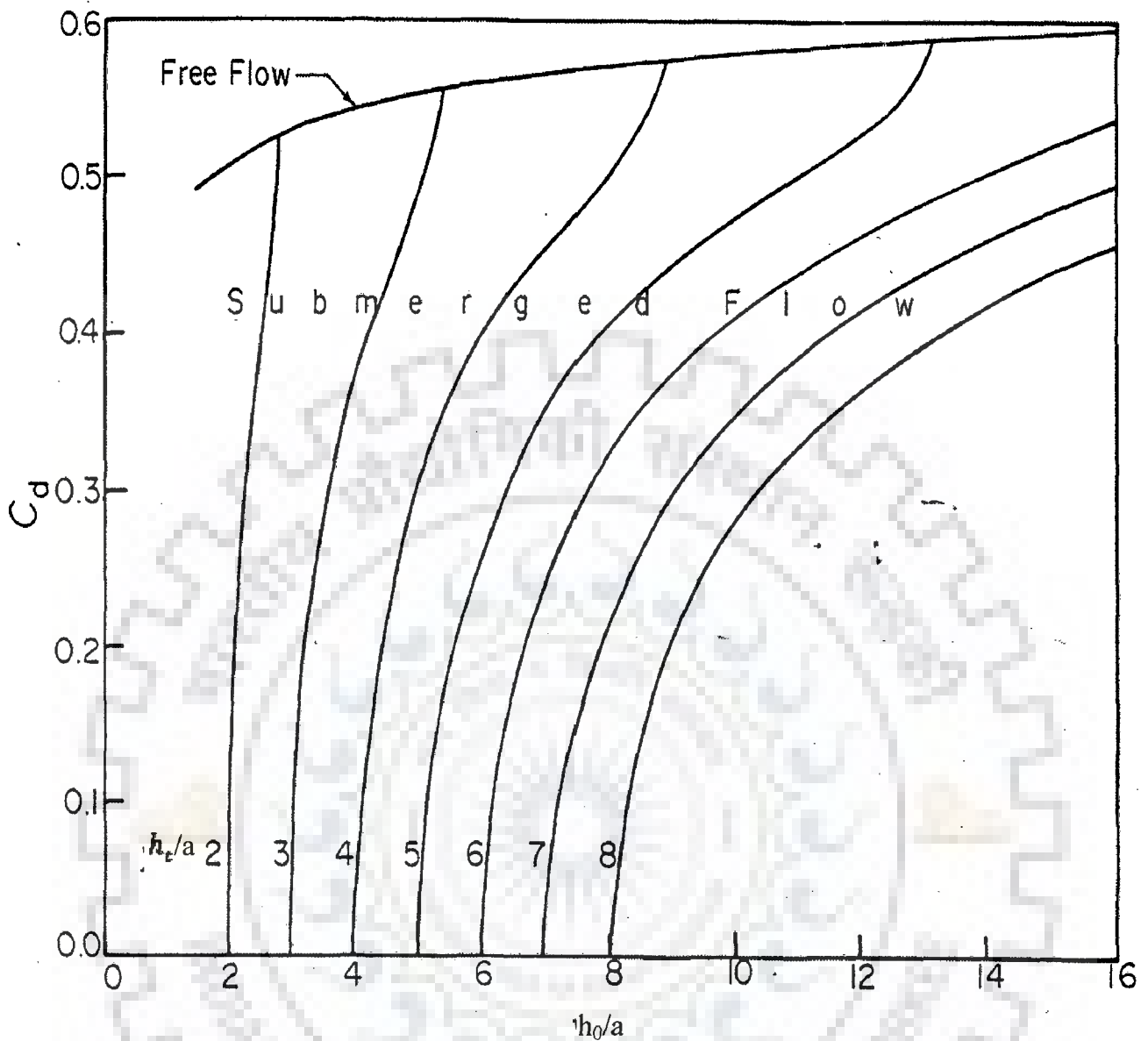


Fig 2.2: Discharge characteristics of normal sluice gate (Henry, 1950)

### 2.2.1.2 Roth and Hager's approach (1999)

This is another useful work on the variation of discharge coefficient which takes care of viscous and surface tension effects. Roth and Hager related discharge coefficient with relative gate opening. Figure 2.3a shows  $C_d$  as a function of  $(A)$ , where  $A=a/h_0$ =relative gate opening. It was observed by authors that for gate opening  $a \geq 50$  mm, all data follow a single curve, based on the

Froude similarity law. For  $a < 50$  mm, the curves  $C_d(A)$  split. However, at lesser gate openings, the effects of viscosity become significant, indicating a scale effect. For extremely small values of  $A$ , surface tension dominates the flow, and  $C_d$  decreases sharply.

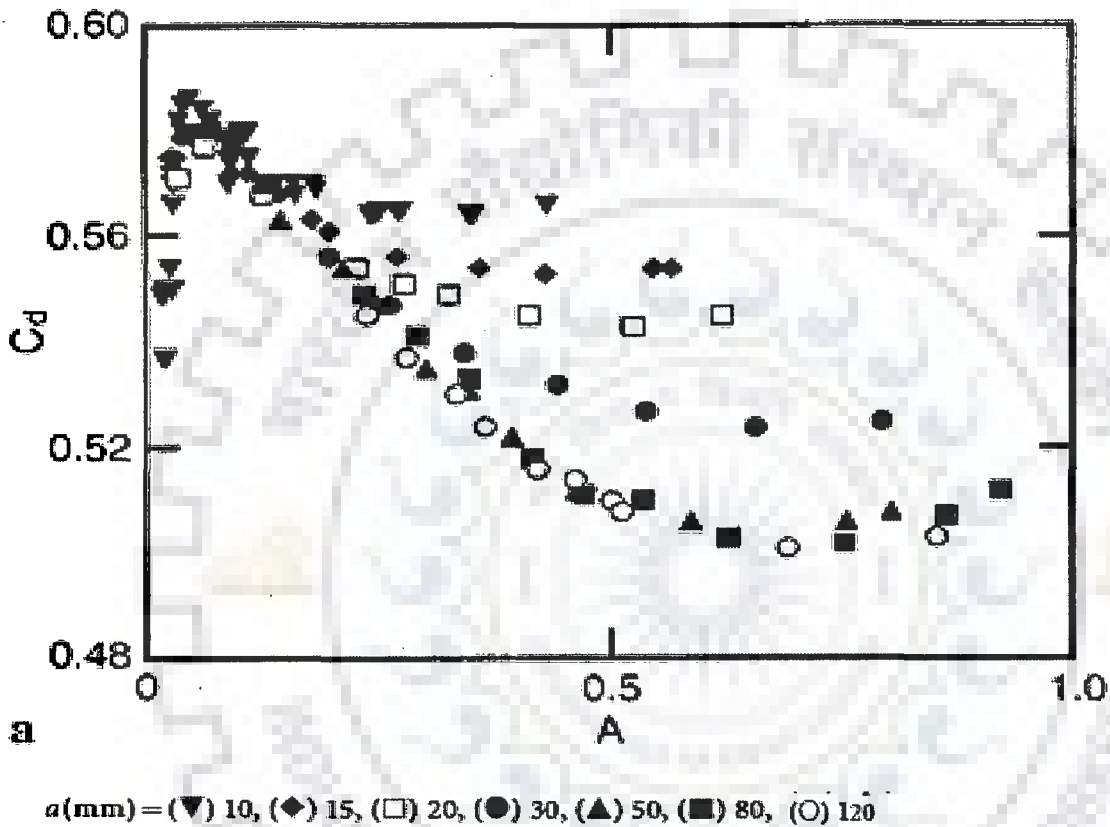


Fig. 2.3a Discharge coefficient  $C_d$  as a function of relative gate opening  $A$ , (Source: Roth and Hager, 1999)

As stated by Roth and Hager(1999), all curves for  $C_d(A)$  start close to 0.60, decrease to a minimum value  $C_{dm}$  with the corresponding relative gate opening  $A_m$ , and increase again varying essentially with the gate Reynolds number  $Ra = a(2ga)^{1/2}v^{-1}$ .

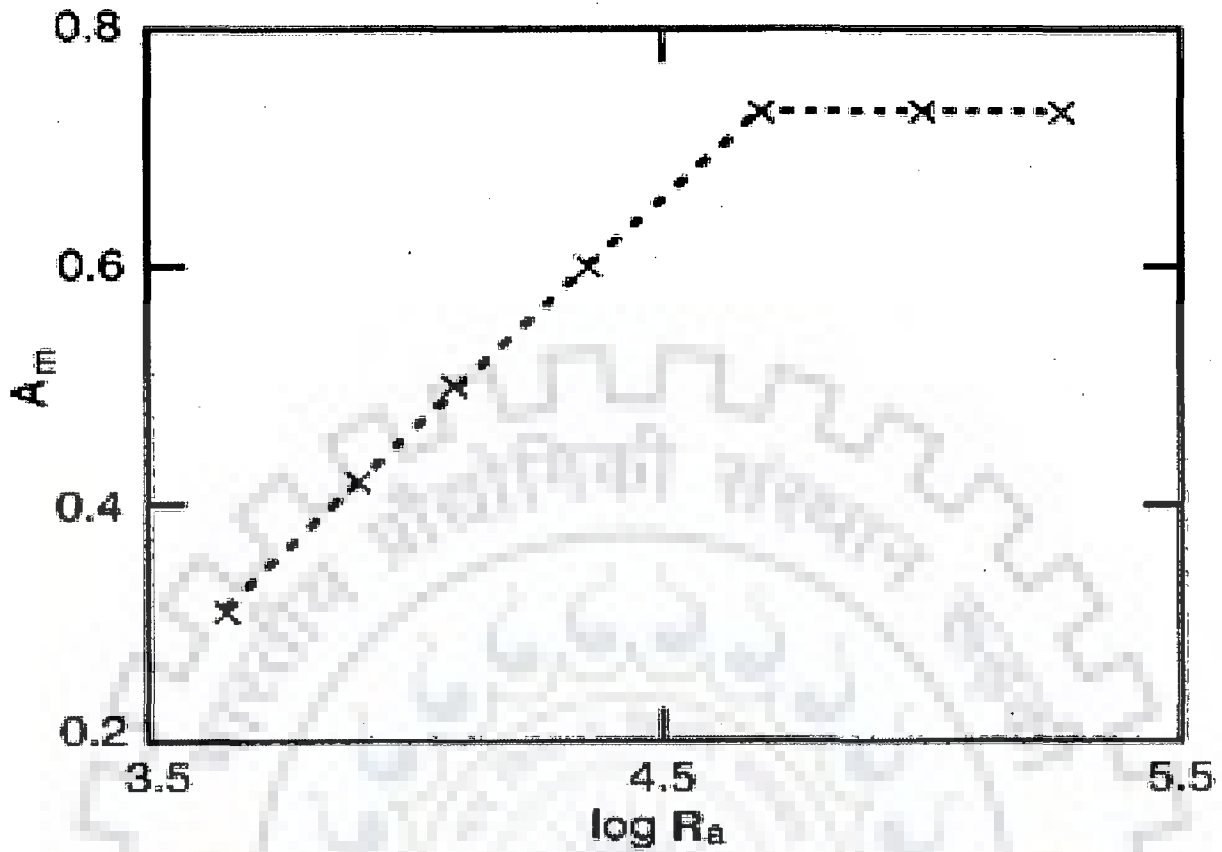


Fig. 2.3b: Variation of  $A_m$  with Reynolds number  $R_a$  (Source: Roth and Hager, 1999)

The curves in Figs. 2.3b and 2.3c are for the Reynolds number  $R_a < 5 \times 10^4$ . Fig 2.3b is governed by Eq. 2.3 and Fig 2.3c is governed by Eq. 2.4

$$A_m = 0.05 + 0.40 \log(R_a/1000) \quad (2.3)$$

$$C_{dm} = 0.60 - \frac{1}{18} \log(R_a/1000) \quad (2.4)$$

Further, substituting  $D_d = (C_d - C_{dm}) / (C_{d0} - C_{dm})$  all data for  $C_d$  can be expressed as a function of  $A_n = A/A_m$ , with  $C_{d0} = 0.594$  as the base value for small  $A_0$ . (see Fig 2.3d)

$$D_d = (1 - A_n)^2 \quad (2.5)$$

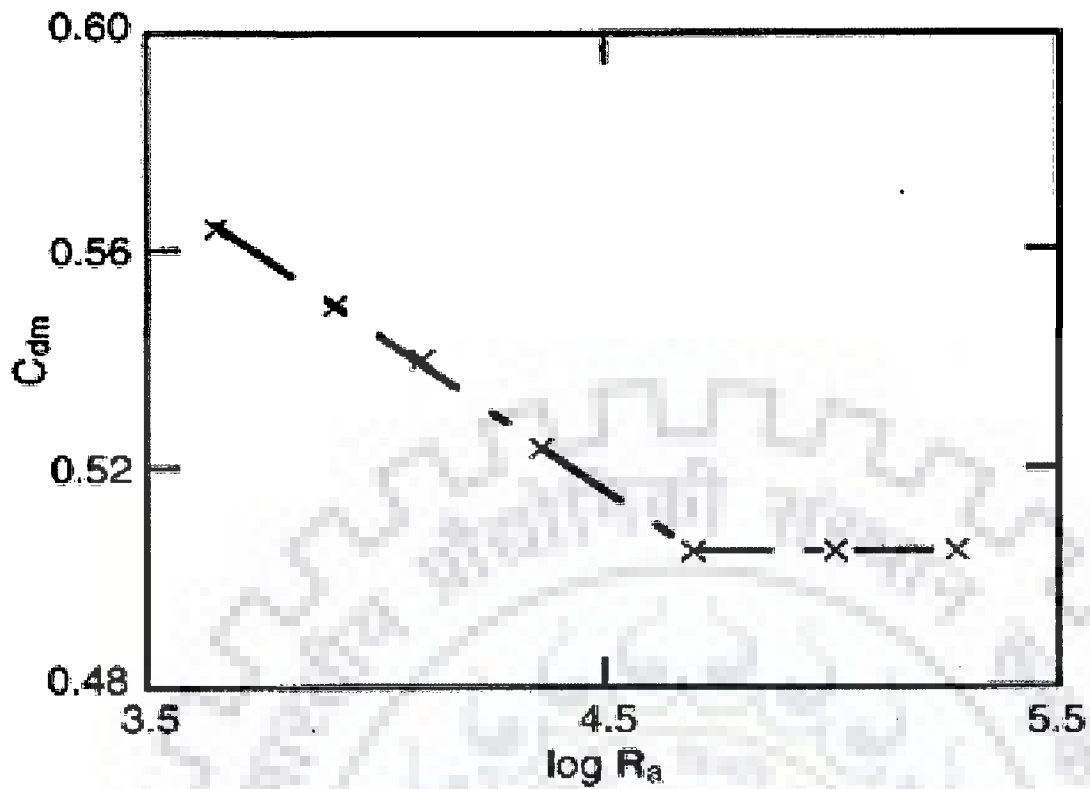
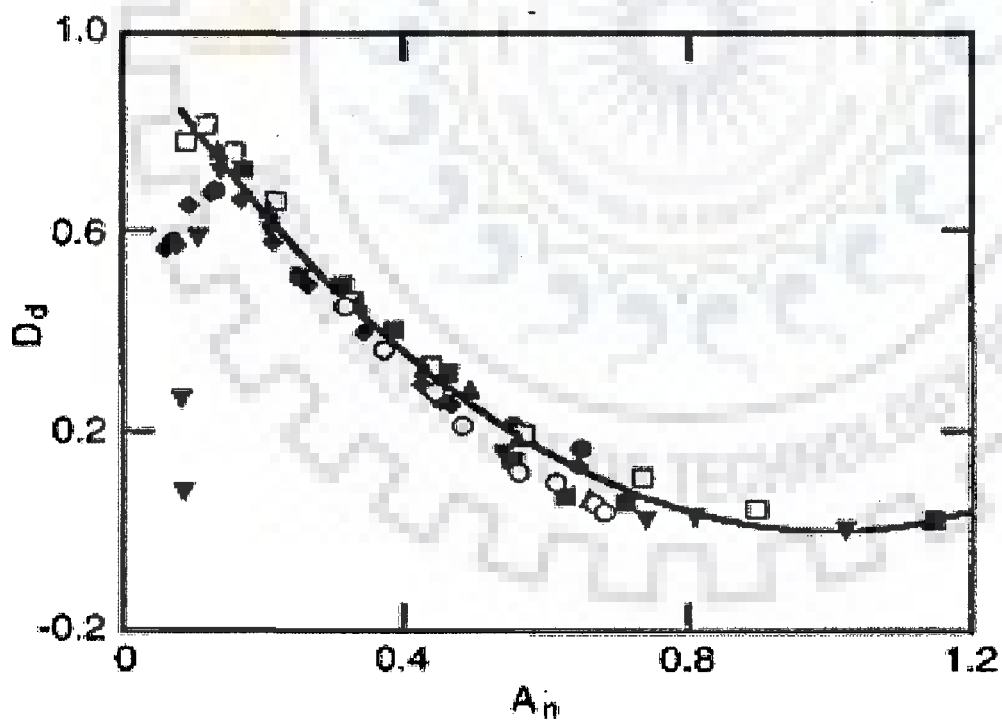


Fig. 2.3c: Variation of  $C_{dm}$  as a function of Reynolds number  $R_a$  (Source: Roth and Hager, 1999)



$\alpha$ (mm) = ( $\nabla$ ) 10, ( $\blacklozenge$ ) 15, ( $\square$ ) 20, ( $\bullet$ ) 30, ( $\blacktriangle$ ) 50, ( $\blacksquare$ ) 80, ( $\circ$ ) 120 (Source: Roth and Hager, 1999)

Fig.2.3d:  $D_d$  as a function of  $A_n$ ,

For  $b=500$  mm, the gate opening must be at least  $a=50$  mm for satisfying the Froude similarity law. Equation 2.5 is a generalization, including both gravitational and viscous effects.

### 2.2.1.3 Habibzadeh et al. Approach (2011)

Based on theoretical considerations, Habibzadeh et al. (2011) theoretically derived an equation for discharge coefficient of sluice gates in rectangular channels under orifice-flow (both free and submerged conditions) as shown in Fig 2.4.

The discharge coefficient for free flow through a sluice gate can be obtained as follows.

$$C_d = C_c \sqrt{\left(1 - \frac{1}{\beta}\right) / (1 + k - 1/\beta^2)} \quad (2.6)$$

where  $C_d$ = Coefficient of discharge,  $C_c$ =Contraction coefficient,  $\beta$ =Dimensionless parameter, and  $k$ =energy loss factor.

The validity of the discharge coefficient relationship for the discharge equation of free and submerged sluice gate was investigated using the experimental data of Rajaratnam and Subramanya (1967) which covered a wide range of Froude number from just greater than 1 up to 11.1 and submergence from 0.12 to 4.5. A comparison between the calculated  $C_d$  values using the relation presented by Swamee (1992) as well as proposed model with the experimental results of Rajaratnam and Subramanya (1967) showed that a value of 0.611 was assigned to  $C_c$  where as the value of  $k$  was found to be 0.062 on the basis of minimum sum of absolute deviations method.

Authors also attributed the main source of energy loss in a free flow condition due the large scale turbulence structure in the upstream pool, i.e., the recirculating region. The turbulent part of this region which occupies most of it is responsible for the velocity gradient that in turn produces

turbulence and results in energy loss. For submerged flows, a flow entrainment of approximately 25 % in terms of discharge per unit width occurs within the distance between the gate and the vena contracta (Rajaratnam and Subramanya, 1967). This entrainment of the shear layer is believed to be turbulent, considering the large magnitude of entrainment in a short length. The excess energy loss in the submerged flow is attributed to this shear-layer action that results in a larger value of the energy-loss factor  $k$ . Comparing the values of  $k$  for free and submerged flows, it is concluded that the energy loss in the shear layer causes an increase in  $k$  of approximately 42%, which is a representation of the contribution of the shear layer to the energy-loss process. One of the important observation of this study was that the value of the energy-loss factor  $k$  depends on the geometry of the sluice gate edge .

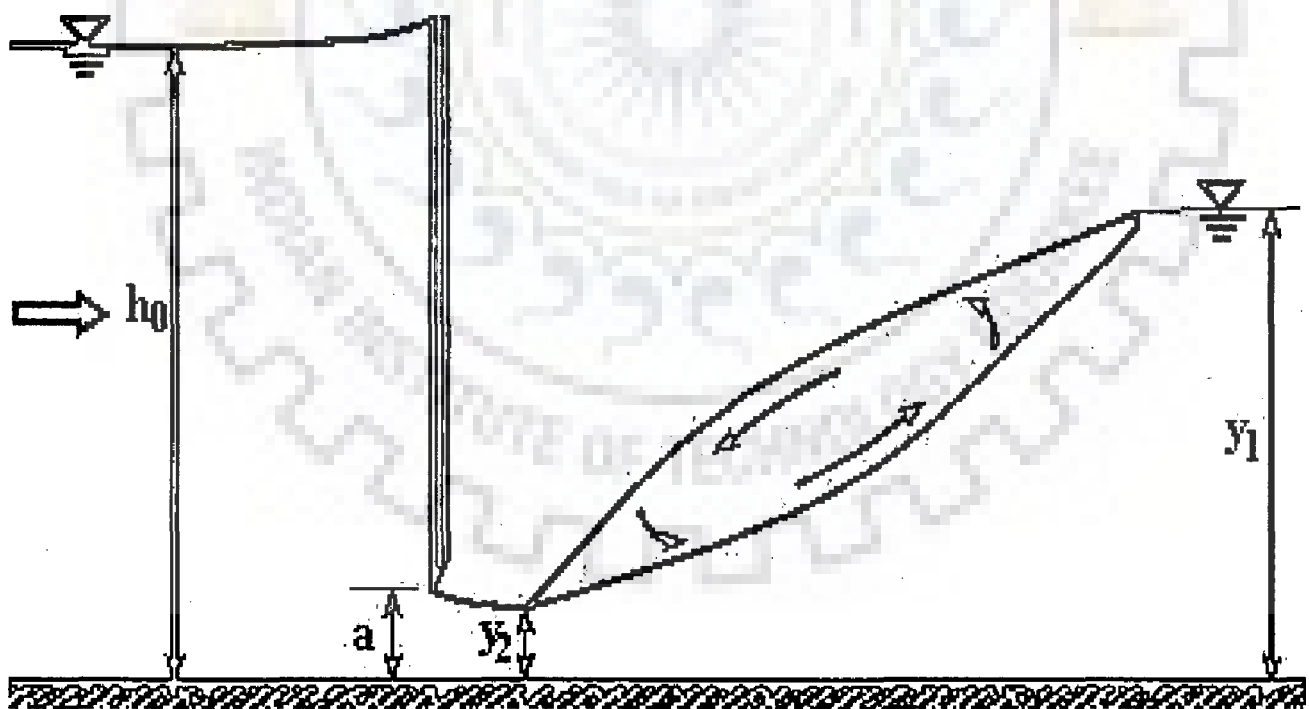


Fig.2.4 Definition sketch for flow under vertical gate in plane bed condition (Free flow)

## 2.2.2 PRESSURE VARIATIONS

### 2.2.2.1 Discharge Through a Normal Sluice Gate

The studies on pressure variations are very much limited. The work of Roth and Hager (1999) provides useful information on the variation of bottom pressure head along the channel length covering a region from upstream of gate to sufficiently downstream from the gate section. The authors defined a dimensionless pressure head term as

$$H_p = \frac{(h_p - h_o)}{(h_o - h_w)} \quad (2.7)$$

Where  $h_p$  is the pressure head at gate bottom;  $h_o$  is the approach flow depth,  $h_w$ , tail water depth

The authors plotted  $H_p$  as a function of dimensionless location  $X=x/a$ , where  $x$  is the distance measured with respect to gate and  $a$  is the gate opening.

$$H_p = 1 - \exp\left(\frac{-1}{3}(X - 1.7)^2\right) \quad (2.8)$$

Authors also observed that Eq. 2.8 better reproduced the data than the work of Montes (1997), who did not consider the flow with a scale effect.

### 2.2.2.2 Gate Pressure Variation

Roth and Hager (1999) considered the variation of gate pressure and observed that the ratio  $\Pi$  of effective to hydrostatic pressure force varies exclusively with relative gate opening,  $A$ , provided viscous flow effects are excluded. The relationship proposed is as follows:

$$\Pi = 0.75 + 0.25 \exp(-2.15 A^{1.15}) \quad (2.9)$$

Where,  $A = a/h_o$ . For small  $A$ ,  $\Pi$  is very close to 1 and for large gate openings,  $\Pi$  decreases to about 0.80.

Belaud et al. (2009) used energy and momentum balance to estimate pressure force on the upstream face of the gate as well as the variation of contraction coefficient. Their expression for pressure force includes an integral term and involves dependence on the relative gate opening, upstream Froude number and contraction coefficient. Thus, it lacks the simplicity of Roth and Hager(1999) approach. For free flow, the contraction coefficient is theoretically obtained as 0.6182. They also reported that Swamee (1992) relationship did not perform well in their study domain. A good discussion on the scale effects is also provided by authors because the experimental values of contraction coefficient were observed to be higher than the theoretical predictions. Authors also supported this mismatch by providing support from the work of Speerli and Hager (1999), where at smaller laboratory scales, fluid viscosity, surface tension, relative boundary roughness and exact geometry may be important. These effects can be further pronounced at lower values of gate Reynolds number, as shown by Roth and Hager (1999) and Clemmens et al. (2003).

### 2.2.2.3 Pressure Variation at the Vena Contracta

Rajaratnam and Subramanya (1967) observed that pressure at vena contracta can also deviate from hydrostatic pressure distribution. The authors showed that pressure deviation from hydrostatic varies linearly with  $z$ , the vertical distance measure from the bed. If the depth of water at vena contracta is  $h_v$ , the pressure deviation  $\Delta p$  can be expressed as

$$\Delta p \approx \lambda \left(1 - \frac{z}{h_v}\right) \rho \frac{Q^2}{2h_v^3 B^2} \text{ for } 0 \leq z \leq h_v, \Delta p=0 \text{ otherwise} \quad (2.10)$$

In eq. 2.10,  $Q$  is the flow rate through a gate of width  $B$  and  $\rho$  is the mass density of the water. The value of  $\lambda$  was assigned as 0.08 and the vena contracta was observed at a distance of 1.25 times of the gate opening. Belaud et al. (2009) used Eq. 2.10 in developing an expression for the pressure distribution on gate.



### 2.3 SLUICE GATES LOCATED ABOVE RAISED CREST

The presence of sill under sluice gate has a positive effect on the flow characteristics as it increases the coefficient of discharge no matter what shape is used. Both shape and height plays an important role in the enhancement of the discharge coefficient. For the shapes tested, (see Fig 2.5) it is concluded by Alhamid et.al.,(1999) that circular sill is the most effective shape compared to all other shapes and triangular shape is the most effective compared to other polygonal sill shapes. An equation for computing the flow discharge was developed for both silled and non-silled gate conditions.

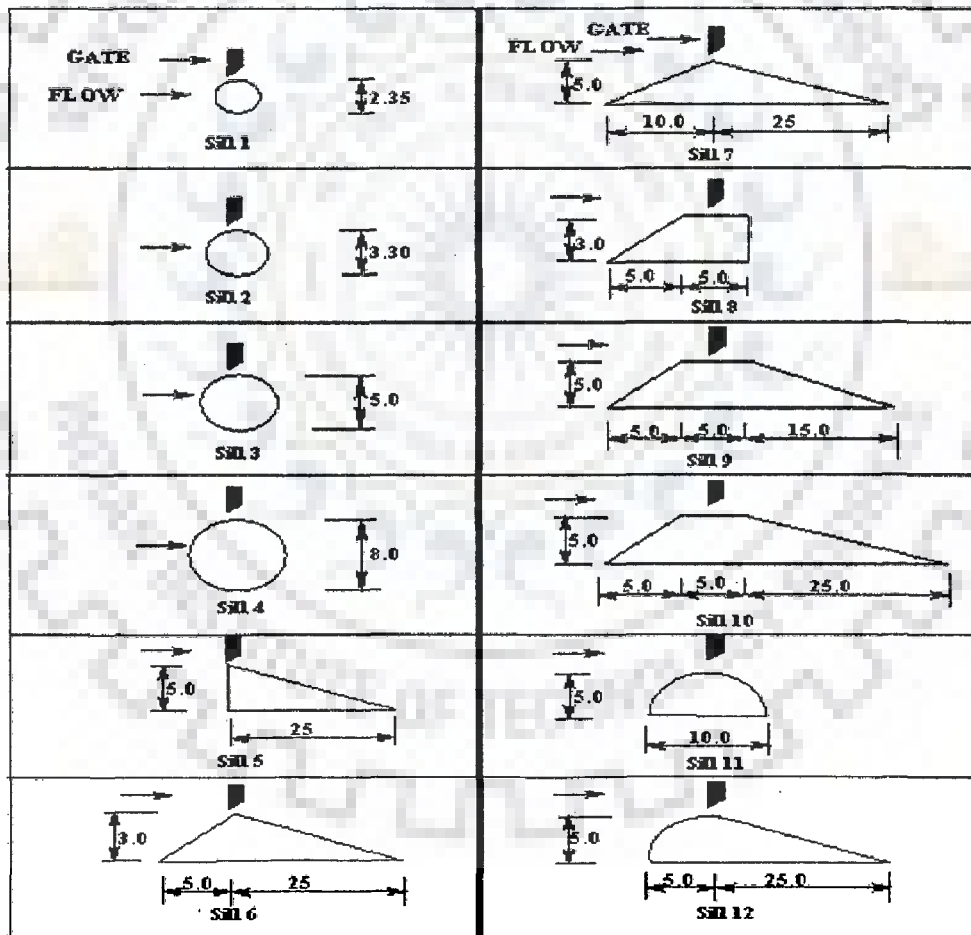


Fig. 2.5 Shapes and dimensions of tested sills

Sills located under the gates are used mainly to reduce height of the gate and consequently its weight. Many investigators have studied the effect of sills on the free out flow characteristics, e.g., Ranga Raju and Visavadia (1979), Salama (1987), Negm et.al. (1993), and Negm (1995),. These studies have experimentally investigated the effect of trapezoidal sills of different dimensions on the coefficient of discharge. Generally, these studies showed that the presence of sills under the gates increases the coefficient of discharge and this increase depends on sill dimensions.

This work presents the results of an experimental investigations on the effect of sill height and shape, including polygonal and non polygonal shapes, located under sluice gate on the coefficient of discharge. A definition sketch relevant to a gate located over a sill is shown in Fig.2.6. Experiments were carried out in a horizontal rectangular flume for free gate out flow conditions. Also, an equation for the evaluation of the coefficient of discharge for both silled and non-silled gates were developed and its performance was compared with data of other investigators.

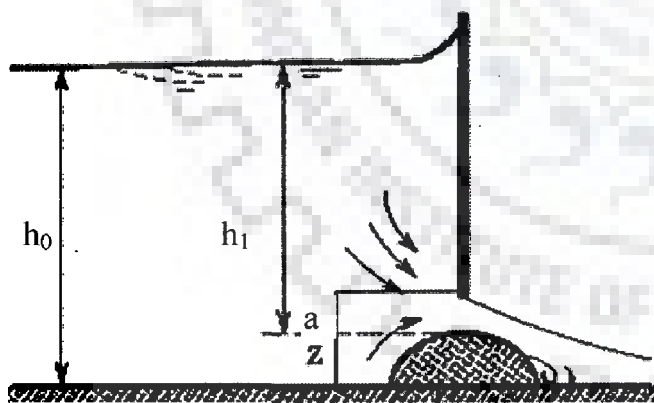


Fig.2.6 Definition sketch for gate located over raised crest (source:Alhamid1999)

Similar to an ordinary sluice gate, the discharge below gates located over sills in rectangular channels may be expressed as:

$$q = C_d a \sqrt{2g(h_0 - Z)} \quad (2.11)$$

Where 'q' is the discharge per unit width, 'h<sub>0</sub>' is the upstream flow depth above the channel bed, 'a' is the gate opening, 'Z' is the sill height above the bed, 'g' is the gravitational acceleration and 'C<sub>d</sub>' is the coefficient of discharge. For this study, C<sub>d</sub> was computed using Eq. (2.11) and effect of sill shape and height are discussed hereafter,

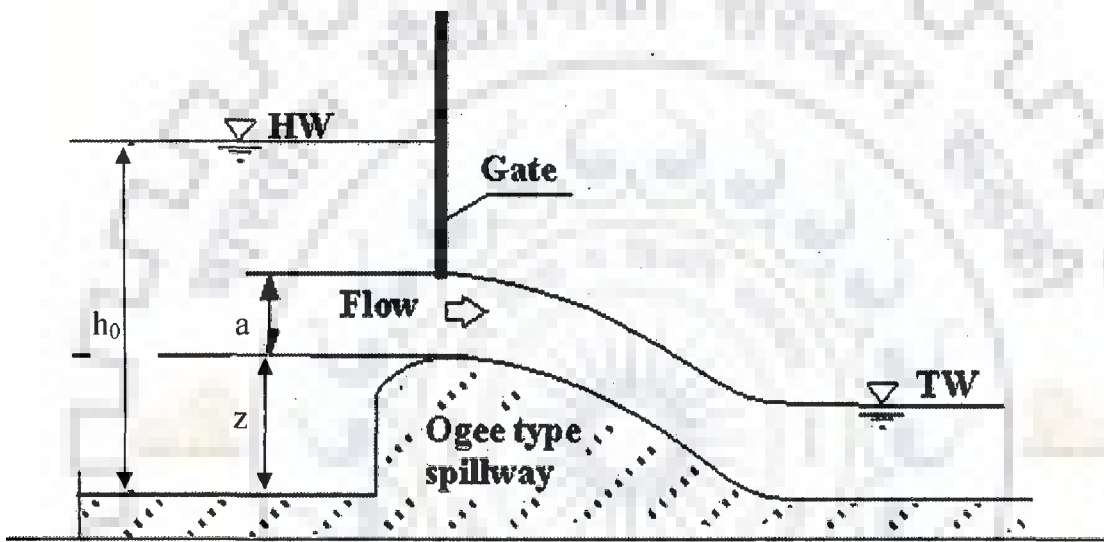


Fig. 2.7 Free orifice flow

Many polygonal sills, upstream slope, downstream slope and crest shape are the main shape parameters, while for non-polygonal, the above are invalid. Hence, a common shape factor, or factors, are required to represent all shapes.

Many shape parameters were tried by author to represent the different shapes efficiently. Finally, the sill wetted parameter 'P', and sill hydraulic radius 'R<sub>s</sub>=A/P' where 'A' is the sill cross sectional area, were found as suitable shape factors.

Using non linear regression analysis, an equation was obtained in the following form:

$$C_d = 0.63 \left( \frac{h_0 - a}{h_0 + 15a} \right)^{0.0649} \frac{\left(1 + \frac{Z}{a}\right)^{0.3618} \left(1 + \frac{h_0 - a}{P}\right)^{0.0434}}{\left(1 + \frac{R_s}{a}\right)^{0.5169} \left(1 - \frac{R_s}{h_0 - a}\right)^{0.3887}} \quad (2.12)$$

According to Alhamid (1999), this equation can be used for both silled and non silled free gate flow and can predict  $C_d$  values with a maximum error of less than 6%. For non silled gate, 'Z' will be equal to zero, 'P' will be infinity and head is equal to  $h_0$ , however, equation (2.12) will reduce to an equation which is different than Swamee's equation for free flow, i.e., Eq. 2.2.. In Indian conditions, different sill types are already in use and these are shown in Fig. 2.5. To the best of knowledge, there is no work reported on the performance of gates located above raised crest type, as shown in Fig. 2.7 with different lip shapes.

#### 2.4 USE OF LIP SHAPES

Hydraulic gates are subjected to flow-induced vertical vibrations which may cause serious accidents unless designed adequately against these vibrations. Design engineers are interested in reducing this effect by suitably shaping the gate bottom in vertical lift gates. The different lip shapes including flat lip, upstream curve,  $45^\circ$  wedge,  $45^\circ$  wedge with curve and vertical lip and stream line shapes were tested by Rao and Singla (1986). It was found that streamline lip gives smooth flow under the gate, less pulsating force and good bearing surface. It is also concluded that it is practicable and preferable to other lip shapes. Some of the lip shapes, as used by Rao and Singla (1986) are shown in Fig. 2.8.

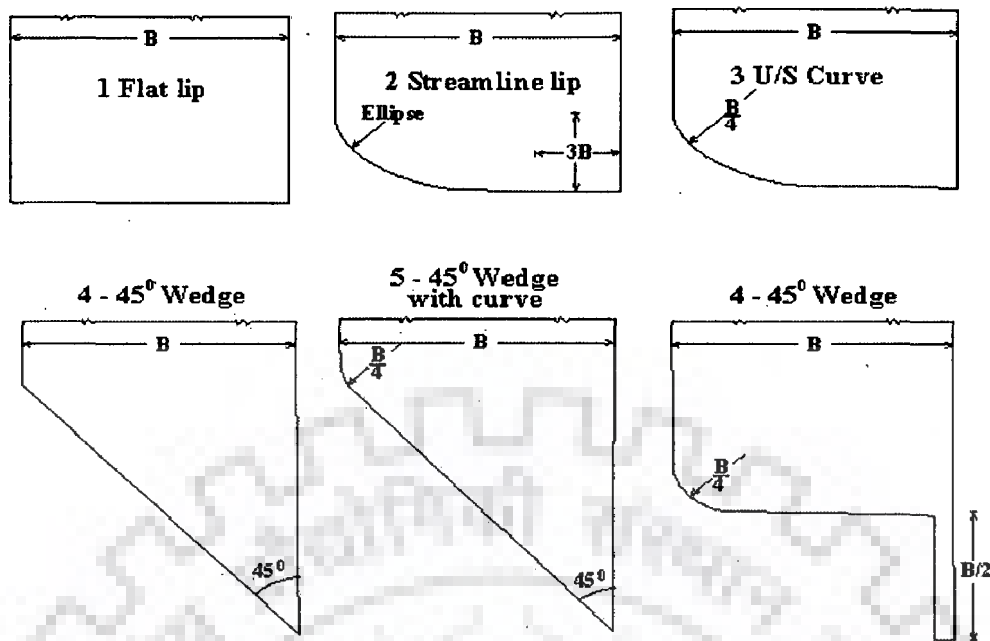


Fig. 2.8. Lip shapes tested by Rao and Singla (1986)

Rao and Singla tested the performance of lip shapes using electrical model. However, their work was limited to only few lip shapes. Also, authors did not investigate the discharge characteristics of gates having these lip shapes.

## 2.5 MISCELLANEOUS

In this section of the review, certain studies which are not directly linked with the objectives of the present work are included. The purpose of inclusion of these studies is that these describe the latest information available on the flow through sluice gate and may provide useful insight for future investigations. Also, field based investigations provide the need for developing simple relationships for computation of discharge coefficient only in terms of relative gate opening.

### 2.5.1 Flow Characteristics

Montes (1997) looked into irrotational flow and real fluid effects under planar sluice gates. Based on his analysis, he observed that the trend of the computed contraction coefficients for the

gravity-affected flow is quite different from the no-gravity case. Also, there is a continuous decrease of  $C_c$  with an increase in  $a/E$ , a trend opposite to the no-gravity case with similar geometry. Here,  $E$  is the upstream energy. Other flow parameters calculated from the inverse method included the surface profiles, velocity, and inclination distributions, as well as the pressure distribution along the bottom of the channel and along the gate. The comparison of the potential flow solution with experimental data revealed that real fluid effects appear to have only slight influence on the velocity and pressure distributions, which seem to be in good agreement with the small amount of experimentation available. The contrast of the coefficient of contraction with the experimental data was found less favorable. Boundary shear effects were found to be a feature of real fluid flow, and they increased the magnitude of the coefficient of contraction with respect to the potential flow values. Author argued that this difference can be best explained by considering the energy loss introduced by the maintenance of a vortex region upstream of the gate. This argument was also indirectly supported by the calculations performed on the development of the boundary layer along the gate and on the channel bottom. The study concluded that the displacement thickness on the gate and on the channel below the gate is too small to account for the experimental deviation of the coefficient of contraction from the inviscid flow values.

Ohtsu and Yasuda (1994) focussed on investigations related to understanding of flow characteristics below sluice gate. The results of the theoretical and experimental study on characteristics of supercritical flow and the jump location below a sluice gate in a horizontal smooth rectangular channel were summarized as follows:

1. The one-seventh power-law velocity distribution in the boundary layer is confirmed.

2. The distribution of the relative turbulence intensity ( $\sqrt{u'^2_{\text{rms}}}/U'$ ) in the boundary layer is similar to that of the boundary layer in airflow with zero pressure gradients. Further, the low-turbulence intensity always occurs in the flow outside the boundary layer.
3. The velocity distribution in the fully developed flow is approximated by the one-seventh power law, and the distribution of the relative turbulence intensity ( $\sqrt{u'^2_{\text{rms}}}/U'$ ) for the fully developed flow is similar to that of an uniform open-channel flow.
4. The predicted boundary-layer growth is verified by the accurate measurements of mean velocities and turbulence intensities.
5. For the developing flow and the fully developed flow, the calculated water-surface profile is verified experimentally. Furthermore, the critical point is determined.
6. The inflow condition of the hydraulic jump below a sluice gate is predicted from the boundary-layer growth and the water-surface profile.
7. From the exact analysis of the water-surface profile, the movement of the location of a hydraulic jump to variation in tail water level is determined.

### 2.5.2 Field Investigations

Lozano et al. (2009) undertook a massive field investigation where in four rectangular sluice gates were calibrated for submerged-flow conditions using nearly 16,000 field-measured data points. G1, G2, G3, and G4 are vertical sluice check gates with rectangular opening and separate the main canal from the pools as discussed in Lozano et al. (2009). The Energy-Momentum (E-M) method underestimated discharge under the gates when it was applied using a contraction coefficient equal to 0.61. The calibration of this coefficient using the field-measured data yielded values greater than 0.61 (between 0.629 and 0.652, depending on the gate). The use of calibrated

contraction coefficients eliminated the under estimation of discharge that was observed with  $C_c$  equal to 0.61. For gates G2, G3, and G4, the performance of the E-M method (a physically based method) with a calibrated, constant contraction coefficient was almost as good as the performance of the best-performing conventional, empirical discharge equation with discharge coefficient varying with gate opening and/or water levels. Only at gate G1, a gate with non regular canal approach, use of a constant contraction coefficient did not give satisfactory results.

Authors concluded that provided that calibration data are available to determine the empirical parameter values, the conventional discharge equation can be applied to rectangular sluice gates when the hydraulic variables  $\Delta h$  and  $a$  are within certain ranges. The variation of the discharge coefficient,  $C_d$ , with the head differential,  $\Delta h$ , and the vertical gate opening,  $a$ , suggested that  $C_d$  can be expressed as a function of these two variables. This research demonstrated that, for the sluice gates considered in the case study, the best empirical fit was obtained by expressing  $C_d$  as a parabolic function of the gate opening,  $a$ .

Therefore, the conventional discharge equation, with a discharge coefficient expressed as a function of hydraulic variables, is more advisable than the E-M method when the gate placement results in a water flow regime different from that for which the E-M method was derived. The case of gate G1 in this study is one such example.

A remarkable result was the offset of the calibrated  $C_d$  for the gate structure at the head of the canal (G1) when an old gate was substituted by a new one with the same dimensions. This observation reflected the sensitivity of  $C_d$  to changes in the gate structure and thus the need to check the calibration periodically or whenever changes in the structure are introduced.



Based on this data set, the uncertainty of calibrated sluice gate measurements was found to be the order of 5–15%. The greatest uncertainty in the variables considered in this study was in the calculated coefficient of discharge. The discharge uncertainty in each of the four gates in this study decreased with increasing gate opening, and it decreased slightly with increasing upstream-downstream differential heads.

## 2.6 SUMMARY

It can be seen from the review of literature that even for free flow conditions and simple gate (with flat bottom), discharge relationships differ. It is also not known how these relationships will behave in case of gate having different lip shapes. The problem is more interesting when the sill types used also differ. Apparently, no work appears to have been done on gates having different lip shapes located above raise weir crest. Thus, there is a need to study the flow characteristics of such gates and to evaluate their performance using various relationships for discharge coefficient and pressure.



---

### EXPERIMENTAL SET UP

---

#### 3.1 INTRODUCTION

In this Chapter the experimental setup is designed. Different lip shapes (eight streamlined and six non streamlined) were fabricated and were used in the experimental studies. The experiments were performed with different lip shapes placed at gate bottom and piezometric pressures were measured by piezometers placed at gate bottom lip. The experimental studies were carried out at four types of beds viz. plane bed and three types of raised crest (ogee type). In this setup different lip shapes are used for investigation namely plane, inclined and vertical. The experiments were performed with different crest types for different lip shapes and the instrument used to measure the pressure is piezometer.

#### 3.2 EXPERIMENTAL SET UP:

The experimental setup as shown in photograph (see Fig.3.1) was designed and fabricated in Hydraulics laboratory of Civil engineering department of IIT Roorkee. A schematic diagram of the experimental setup is shown in Fig 3.2. It consists of a rectangular flume of 0.30 m wide and 0.55 m high with Plexiglas walls provided on both side of the flume having a length of 7.1 m. The top of flume was open to atmospheric pressure so that it gives an effect of an open channel flow in this flume. At the inlet of rectangular flume, a surge tank made of concrete of size 1m length x 1 m wide x 1.5 m height was provided such that the water coming from overhead tank placed at the roof of the laboratory, become stabilized before entering into open channel flume through trash rack and gated channel. The plexi glass rectangular open channel was connected to the rectangular concrete surge tank for supplying water to the vertical gate. The gate chamber was placed at down stream end of the flume at a distance of 7.1 metre from the tank through the

aforesaid plexi wall open channel. The slope of the open channel was kept negligible for 7.1 m length and in the downstream of the gate, a slope of 2 cm for 1 m length was provided for free flow condition. In the gate chamber, a vertical sluice gate was placed and was operated by electric motor of 0.28 hp and gate was raised and lowered by a geared arrangement to provide different gate openings from 0.025 m to 0.7 m from the bottom of the open channel.

The height of water ( $h_o$ ) upstream of the gate was measured by a pointer gauge placed in the open channel at different gate openings (a). The flow downstream of the gate was in a free flow condition. It was possible to measure the gate openings through a linear scale attachment over the gate having a least count of 1 mm. The dimension of vertical sluice gate was 0.30 m width, 1.2 cm thickness and 0.70 m height. The experiment was conducted for different lip shapes attached at the bottom of the gate by means of screw arrangement. The piezometer was placed to measure the pressure head at gate bottom. The discharge was measured at a V-notch tank placed in the downstream side of open channel at an accuracy of  $\pm 0.001$  m by measuring the height of water at V-notch. Then the water is pumped to over head tank and again the procedure was repeated for different lip shapes.

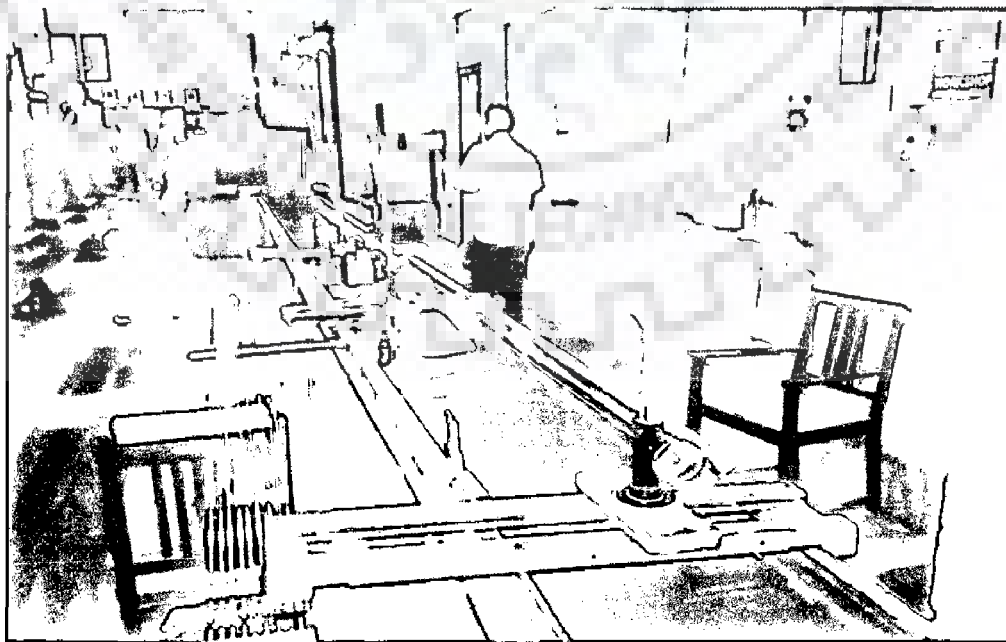


Fig. 3.1 Photographic view of Flume

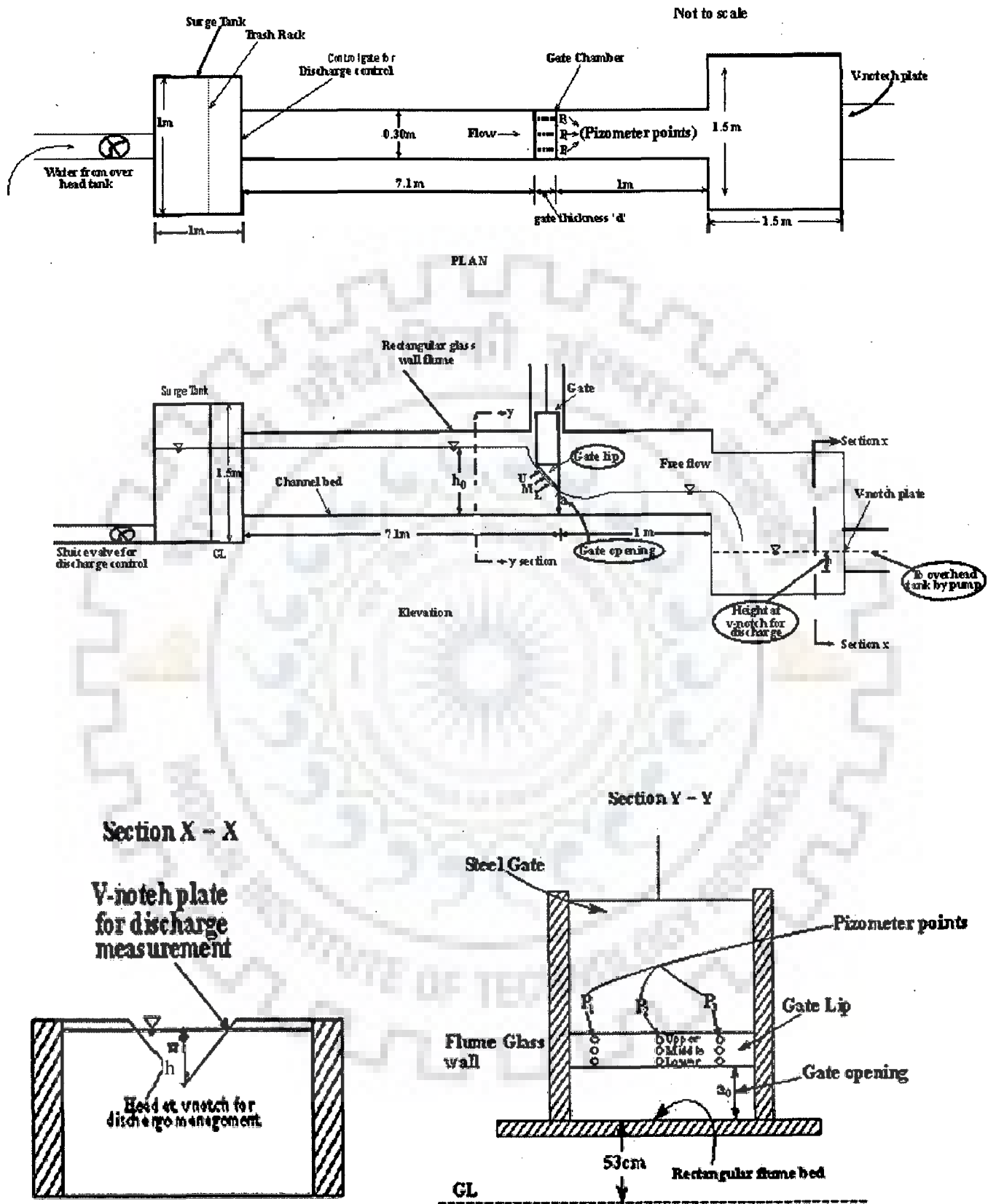


Fig.3. 2 :Schematic diagram of experimental apparatus

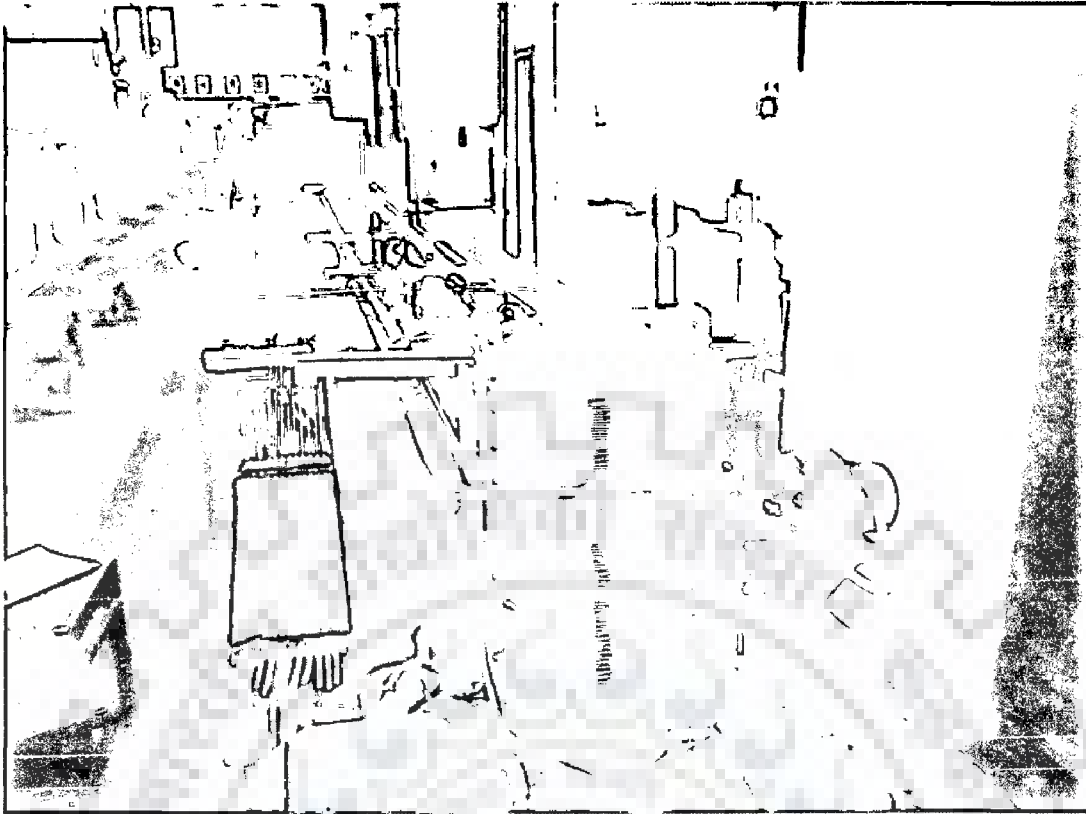


Fig. 3.3 Photographic view of gate Chamber

### **3.3 GATE**

It consists of a steel vertical gate of 30 cm width a rack fixed on side of the gate on downstream side of the gate so that the gate could raised and lowered by means of the pinion operated by an electric motor ,as shown in Fig. 3.3. The bottom of the gate is fixed with different lip shapes attached to the gate bottom by means of screw fasteners. A linear scale is fastened with a gate body which moves along with the gate movement. The gate openings from the bed level are measured by this linear scale through a fixed pointer placed with flume walls.

### **3.4 BED CREST SHAPES**

#### **3.4.1 Plane Bed Crest**

A plane horizontal rectangular Channel bed was used under the gate and observations were taken at various gate openings from 0.025m to 0.07m by moving the gate in upward and downward directions

### 3.4.2 Ogee Shaped Overflow Crest

Ogee shaped over flow crests as shown in Fig.3.4, Fig.3.5 & Fig.3.6, were used as per IS specification code IS 6934 to conduct the studies. There were three types of Ogee crest shapes used in the study and they were placed under the vertical sluice gate on the bed of open channel(see Fig 3.7). The gate was placed on the top of the crest and piezometric pressures were observed at different gate openings similar to the plain bed gate opening

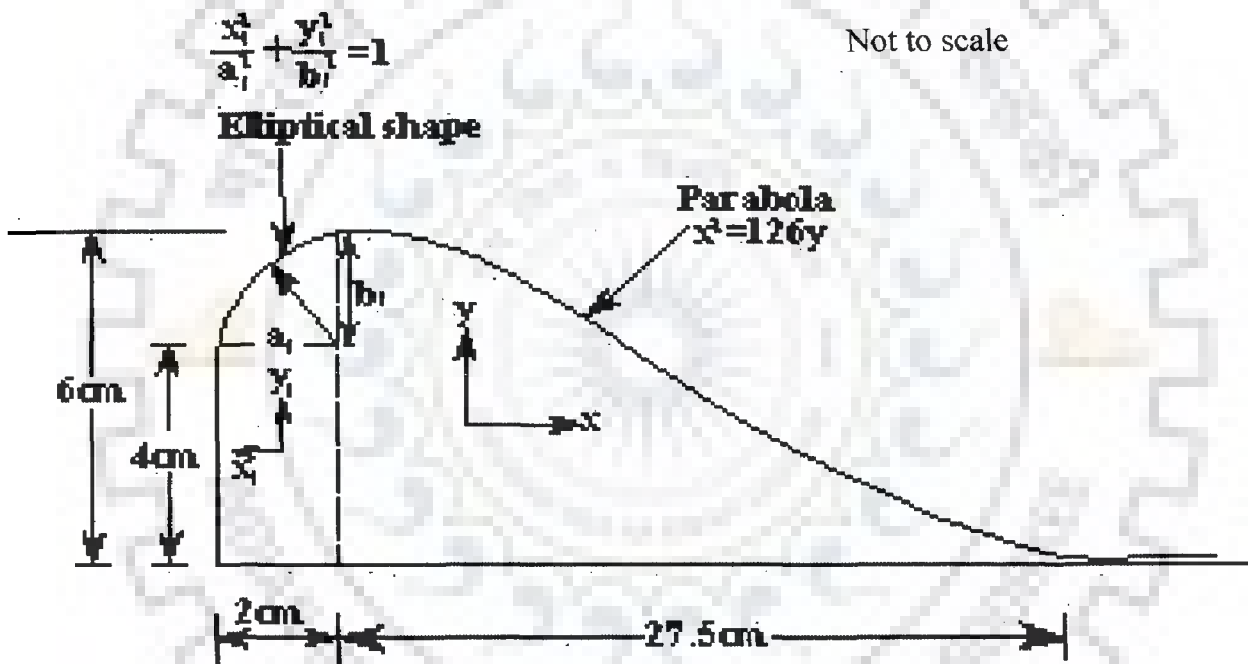


Fig.3.4 Schematic diagram of raised crest upstream face vertical

Note to scale

**Raised Crest as per  
IS code: 6934**

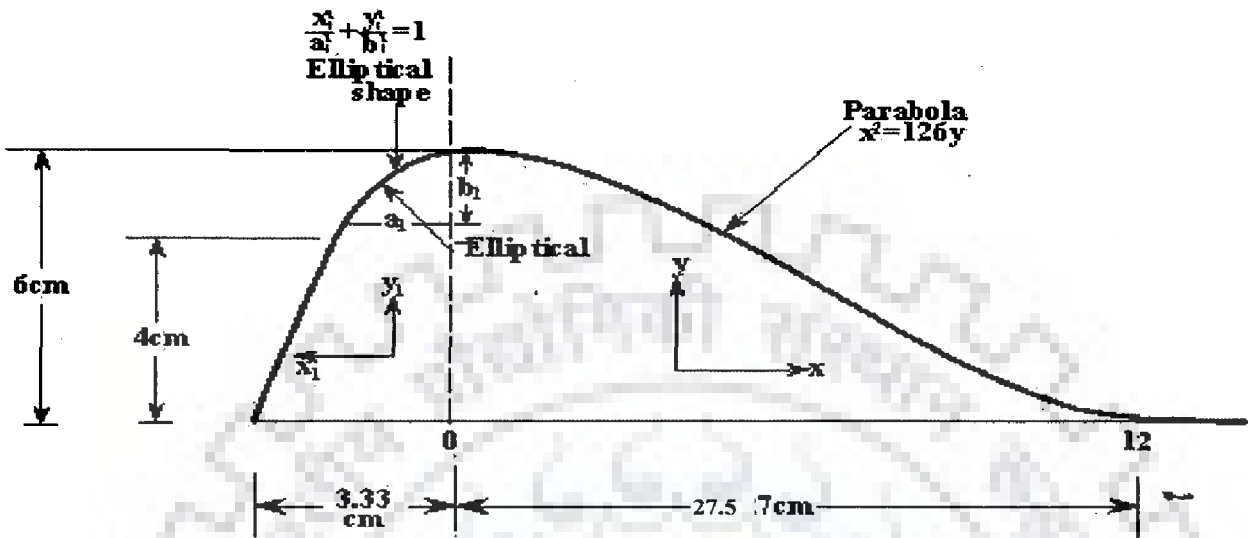


Fig.3.5 Schematic diagram of raised crest upstream face 1H:3V

Not to scale

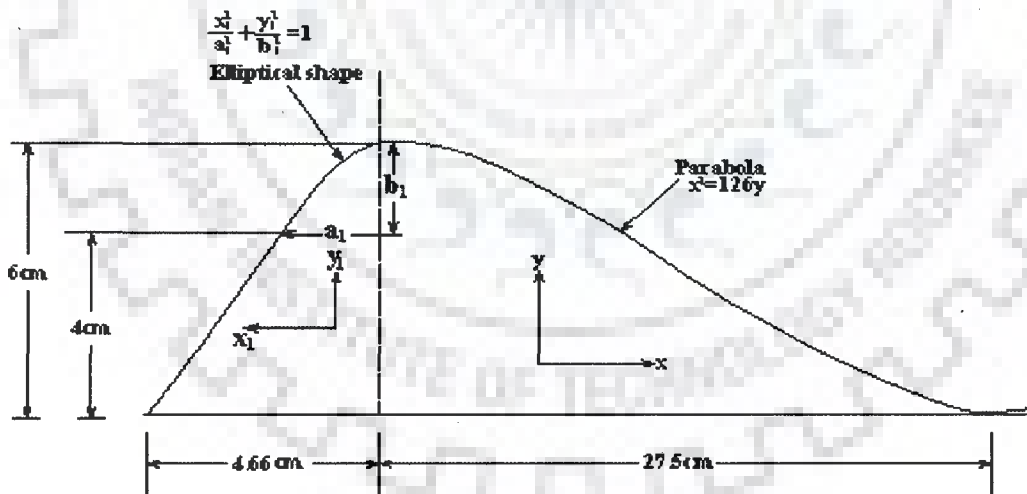


Fig.3.6 Schematic diagram of raised crest upstream face 2H:3V



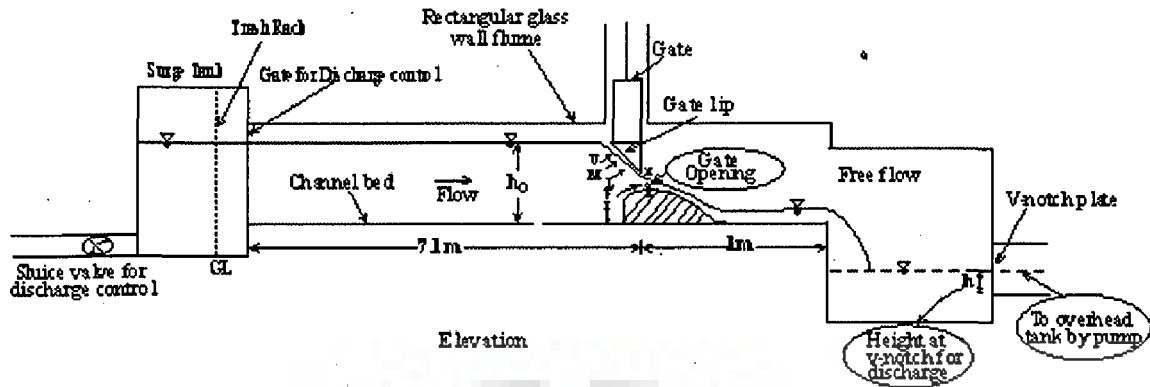


Fig.3.7 Schematic diagram of experimental setup with raised crests placed below Gate

### 3.5 SURGE TANK

It is made of concrete and it stabilizes the flow of water before entering to the flume. It also creates a head of water to the flume. Bottom of the surge tank is connected to incoming waterpipe from overhead tank through sluice valve to control the discharge to the surge tank. Photographic view of surge tank is shown in Fig.3.8.

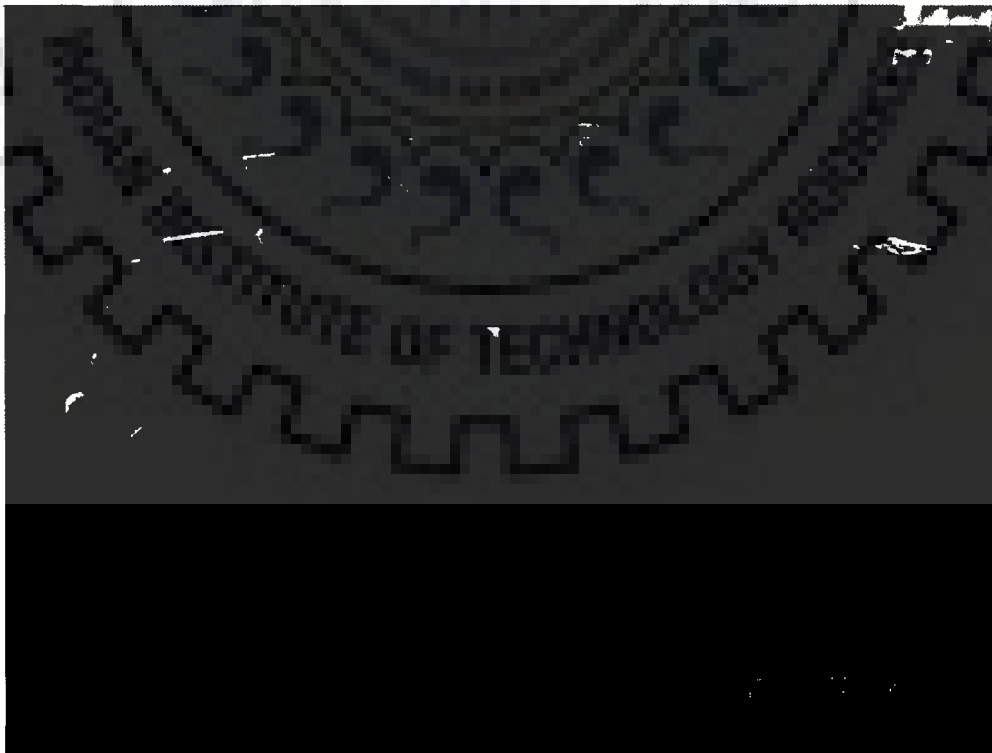


Fig.3.8 Photographic view of surge tank

### 3.6 V-NOTCH

At the outlet of the flume a V-notch (see Fig.3.2) is placed to measure the discharge of water flowing under the gate. The discharge was measured at a V-notch placed in the downstream side of open channel at an accuracy of  $\pm 0.001$  m by measuring the height of water at V-notch as given in Table no.3.1. The formula to calculate the discharge is the one recommended by the U.S Department of the Interior, Bureau of Reclamation in their *Water Measurement Manual* for calculations with a fully contracted,  $90^\circ$  V-Notch, sharp crested weir with free flow conditions.

The discharge was measured at V-notch tanks by measuring the height of head of water 'h' at V-notch by means of a pointer gauge so that the discharge is computed by Eq.3.1.

$$Q = 1.36h^{2.48} \quad (3.1)$$

where, Q = discharge in  $m^3/sec$  and

h = head of water at V-notch tanks in m.

The sensitivity of discharge "Q" with reference to the unit change in the value of head can be computed as below.

Differentiating Eq. (3.1),

$$dQ = 1.36 \times 2.48h^{1.48} dh \quad (3.2)$$

Dividing Eq.3.2 by 3.1,

$$\frac{dQ}{Q} = \frac{1.36 \times 2.48h^{1.48} dh}{1.36 h^{2.48}} \quad (3.3)$$

Simplifying Eq.3.3, we get,

$$\frac{\Delta Q}{Q} = 2.48 \frac{\Delta h}{h} \quad (3.4)$$

The discharge calculated for a head of 0.1500m using Eq. 3.1 is obtained as 0.012309 m<sup>3</sup>/sec.

On substituting in Eq.3.4, an increase of 1 mm as  $\Delta h$  causes a corresponding increase of 0.000204m<sup>3</sup>/sec in the value of discharge.

### 3.7. PIEZOMETER

It is used to measure the pressure head at the bottom of the gate by means of placing nine piezometer tubes at three equidistant points ( $P_1$ ,  $P_2$  and  $P_3$ ) along the channel width as shown in Fig. 3.2 (plan). It is also placed along the bottom thickness of the gate at equidistance perpendicular to the bottom surface of lip profile as shown in Fig.3.2 (section Y-Y). The piezometer tubes of 3 mm diameter were welded to lip surface and this piezometer points at bottom of the gate were connected to the piezometer placed at a height of 58 cm above the ground level. Its dimension is 28.6 cm stand height at piezometric tubes and tubes were inclined at an angle of  $13.9^\circ$  from horizontal surface. Piezometer head was measured in cms of water by the tubes laid on the surface of the piezometer parallel to its base. Fig.3.9 shows the photograph of piezometric tube set up.



Fig.3.9 Setup of piezometer tubes

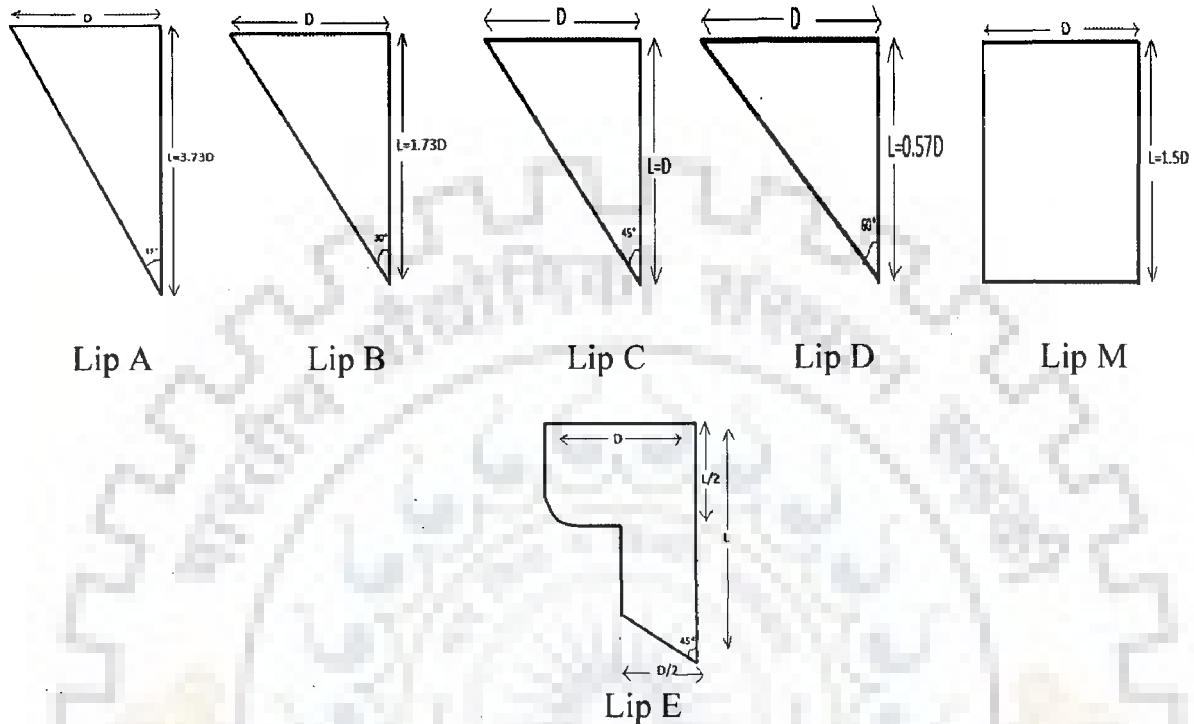
### 3.8 LIP SHAPES

Fourteen lip shapes were used in the present experimental investigations and readings of pressure at the bottom were measured at different discharges at different bed conditions in the open channel.

In order to provide various geometrical shapes at the bottom of the gate, fourteen types of lip shapes, as shown in Fig.3.11 were fabricated. The lip shapes were made up of mild steel so that they do not deform due to hydraulic pressure. Different lip shapes were fastened at the bottom of the gate in order to take observations of pressure under the gate by means of piezometers. Three combinations of lip shapes were used. They are (1) flat angular lip shapes with angles varying  $30^{\circ}$ ,  $45^{\circ}$ ,  $60^{\circ}$  and  $75^{\circ}$  (2) compound lip shapes with combination of angular surface and curved surface. (3) different lip shapes having only curved shapes. The lip shapes were broadly classified into streamlined and non streamlined types. The figures of the lip shapes are drawn below. The

thickness of each lip shape was kept equal to the thickness of the gate and pizometers point were drilled along the perpendicular to surface of Lip bottom.

**(a). Non-streamlined Lip Shapes:-**



**(b). Streamlined Lip Shapes:-**

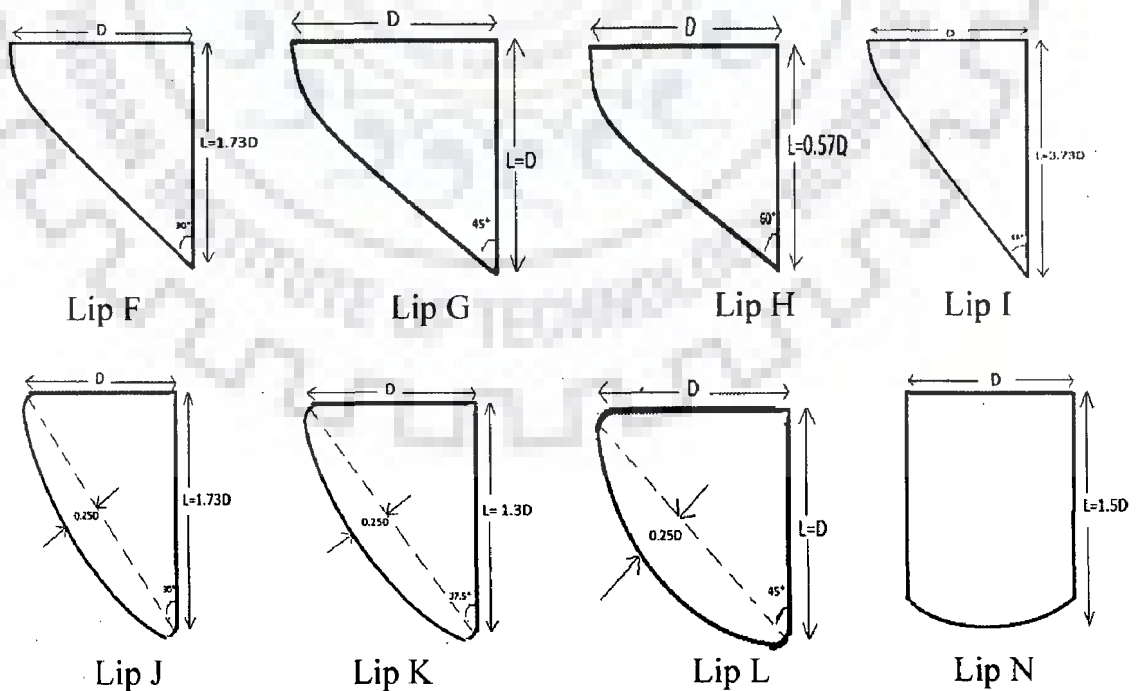


**Figure No. 3.10 a and b: Schematic diagrams of Lip Shapes & their nomenclatures**

### 3.9 SUMMARY

The experiments were formed for different lip shapes. Pressures head were measured at different location of gate for different lip shapes. The data collected from the experiments were used for further processing and used for determining the coefficient of discharge.

The maximum error in pressure measurement was restricted upto 5% and the error in discharge measurements was restricted to 2.5%.



---

DISCHARGE CHARACTERISTICS OF NON-STREAMLINED LIP

SHAPES

---

4.1 INTRODUCTION

The discharge characteristics of sluice gates having non-streamlined lip shape will be dealt in this chapter. The variation of discharge coefficient with relative gate opening will be analyzed. The idea is to find the lip shapes which give maximum value of discharge coefficient throughout the operational range of relative gate opening. The variables which have been changed to see the corresponding effect on discharge are (1) upstream head (2) gate opening and (3) channel bed profile under the sluice gate. The variation of discharge coefficient has been plotted against various parameters to identify the dependence of discharge coefficient on those parameters. The shape of the lip, as determined by the observational data, plays an important role in the discharge coefficient of the sluice gate.

4.2 DISCHARGE COEFFICIENT CALCULATION

The measurements of the discharge have been taken using a V-notch in the downstream of the flume. The formula to calculate the discharge is the one recommended by the U.S Department of the Interior, Bureau of Reclamation in their *Water Measurement Manual* for calculations with a fully contracted, 90<sup>0</sup> V-Notch, sharp crested weir with free flow conditions. The discharge was controlled using sluice valve. Six discharges have been analyzed with ten different gate openings each, thus making sixty readings for each combination of a lip and bed profile.

### 4.3 THEORETICAL APPROACHES USED TO COMPUTE VALUES OF DISCHARGE COEFFICIENT

The observed  $C_d$  has been compared with the computed coefficients of discharge as given by Swamee (1992), Roth and Hager (1999), Alhamid (1999), Ansar and Chen (2009) and Habibzadeh et al. (2011). The details about the theory and formulae suggested by these authors have been extensively covered in Chapter 2. The approaches subscribed by Swamee, Roth & Hager, and Habibzadeh et al. do not incorporate the cases for raised crest. The work by Alhamid (1999) and Ansar & Chen (2009) takes into account the cases where a raised crest is provided under a sluice gate. Nevertheless, none of these studies deal with the effect of the sluice gate lip.

### 4.4 FORMULA FOR OBSERVED $C_d$

Two formulae have been used to calculate the observed coefficient of discharge. The formula which is only accurate for small openings, for now on referred to as small orifice formula, is used by all the previous investigators:

$$Q = C_d a B (2gh_0)^{0.5} \quad (4.2)$$

In Eq. 4.2,  $a$  = gate opening and  $h_0$  = the head above the bottom of the gate,  $g$  = acceleration due to gravity and  $B$  = gate width, measured perpendicular to flow. Integrating elementary discharge equation through a strip of thickness  $dh$  between the limits  $h_0$  and  $h_0 - a_0$ , leads to Eq. 4.3, which is more appropriate to use for large gate openings.

$$Q = 2.9 C_d B \left[ (h_0)^{1.5} - (h_0 - a_0)^{1.5} \right] \quad (4.3)$$

The small orifice formula has been used by all the previous investigators including Swamee (1992), Roth and Hager (1999), and Habibzadeh et al. (2011). The existing formulae have not been developed for gates having different lip shapes. It was discussed in Chapter 1 that the

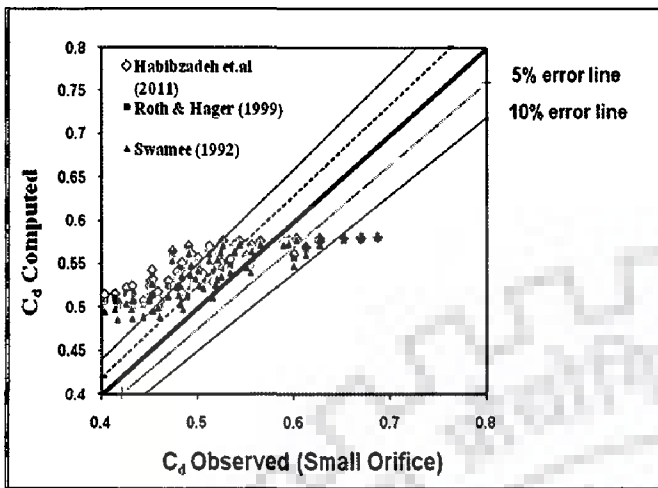


discharge characteristics will vary with the lip shapes and the types of bed below the gate. If one considers the use of small orifice or large orifice formula, the coefficient of discharge,  $C_d$  is likely to be estimated differently, particularly at larger gate openings. To have a feel about the performance of some of the relationships for discharge computations, an attempt is made to compute discharge coefficient using existing formulae and compare this with the observed  $C_d$  values computed using equation (4.2).

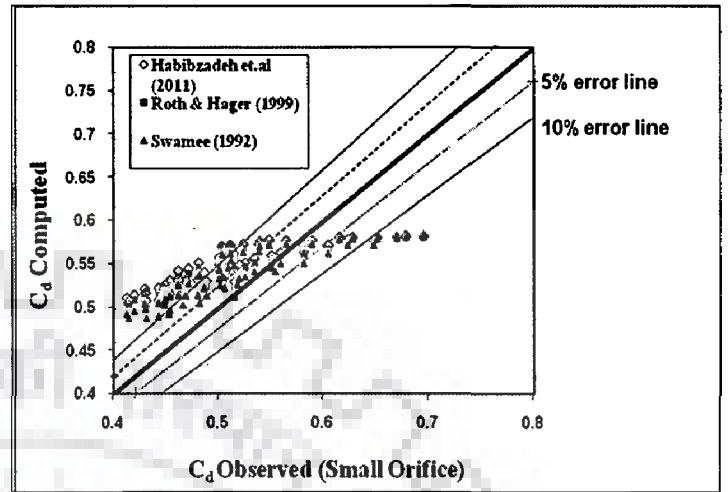
#### **4.5 THE ANALYSIS OF $C_d$ USING THE SMALL ORIFICE FORMULA FOR WEIR CREST TYPE (1H:3V)**

The agreement diagram for raised crest (1H:3V) is shown in Fig.4.1 for lip shapes A,B,C,D,E and M using the relationships of Swamee (1992), Roth and Hager (1999), and Habibzadeh et al. (2011). It is noted that a considerable part of the data falls beyond an error band width of  $\pm 10\%$  line. Fig. 4.1 also indicates the tendency of these relationships towards over prediction of discharge coefficient in majority of the situations. Thus, there is concentration of points more above the line of perfect agreement than that below the line of perfect agreement. The relationship of Swamee (1992), relatively does better than Roth and Hager (1999), and Habibzadeh et al. (2011) relationships. However, the difference between the computed  $C_d$  between these three approaches is not in wide disagreement with each other.

One can argue that the relationships of Swamee (1992), Roth and Hager (1999), and Habibzadeh et al. (2011) are not meant for gates located on raised crest. For this reason, two relationships, which have been exclusively developed for gate located above raised crest are used to compute  $C_d$ . Fig 4.2 shows the agreement between  $C_d$  computed and  $C_d$  observed using the relationships of Alhamid (1999) and Ansar & Chen (2009). A comparison of Figs 4.1 and 4.2 presents a very interesting behavior. The  $C_d$  relationships which are meant to perform better in case of gates located above raised crest fail to do so, as seen from Fig. 4.2.

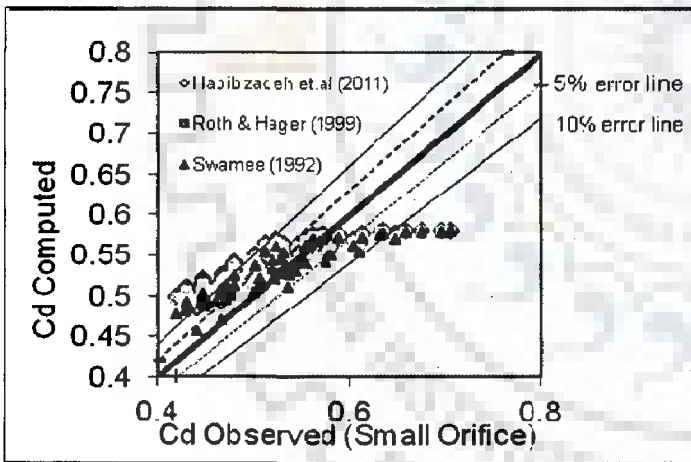


Lip A

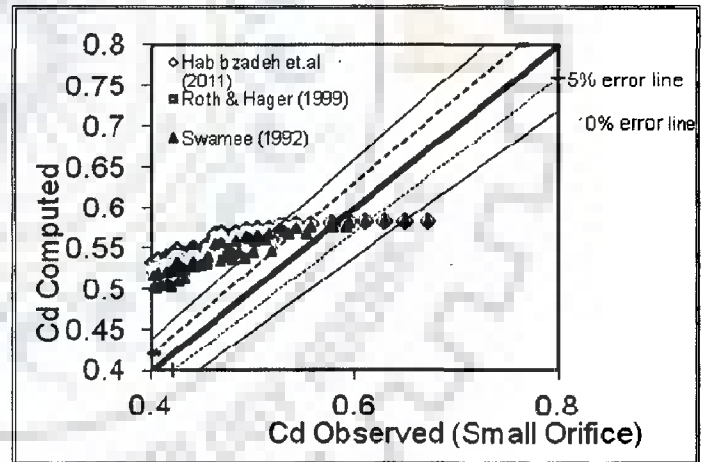


Lip B

Fig.4.1a: Agreement diagram for raised crest (1H: 3V) for lip A and B for Habibzadeh et Al, Roth and Hager and Swami

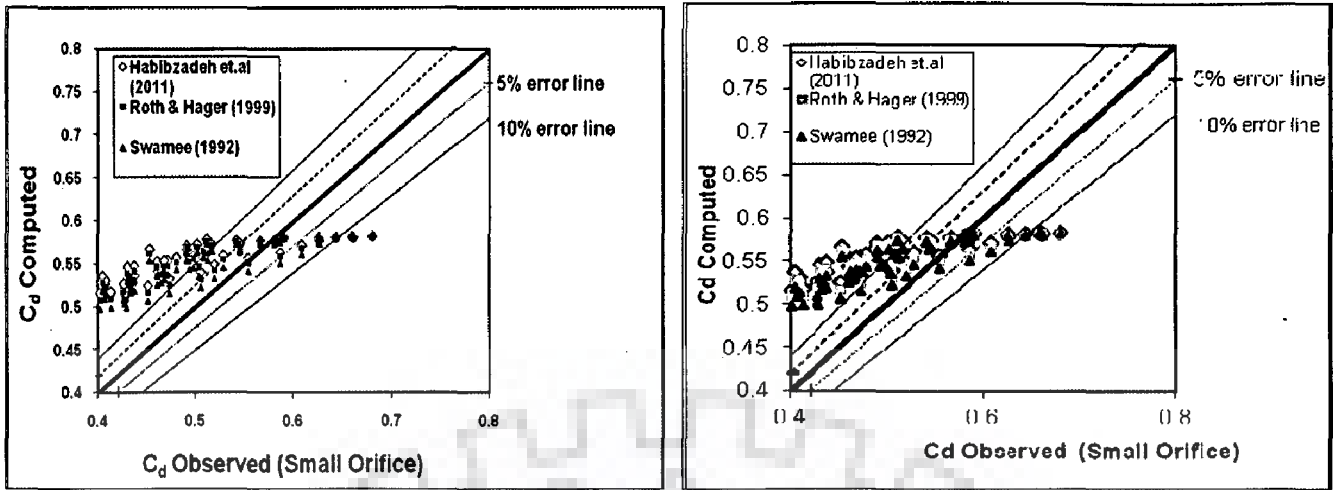


Lip C



Lip D

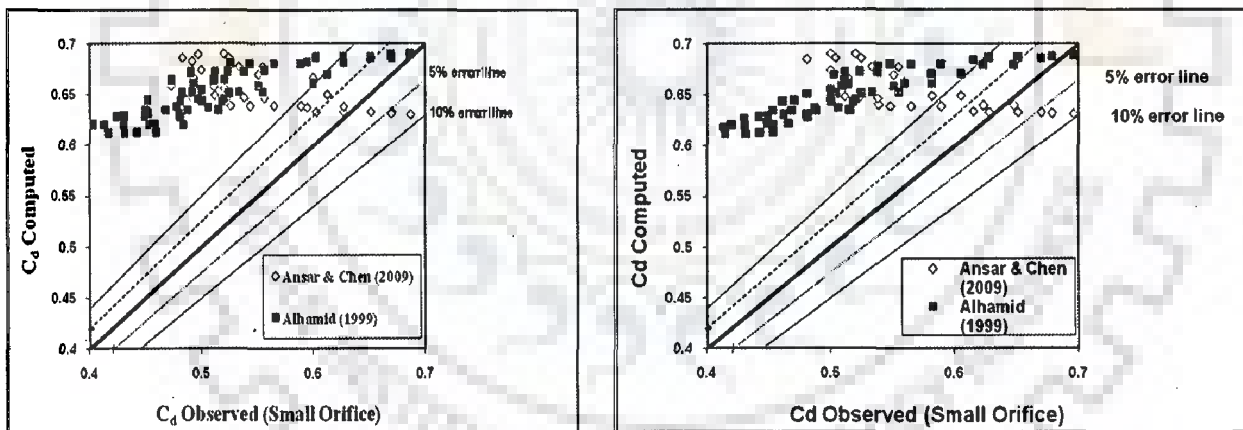
Fig.4.1b: Agreement diagram for raised crest (1H: 3V) for lip C and D for Habibzadeh et Al, Roth and Hager and Swami



Lip E

Lip M

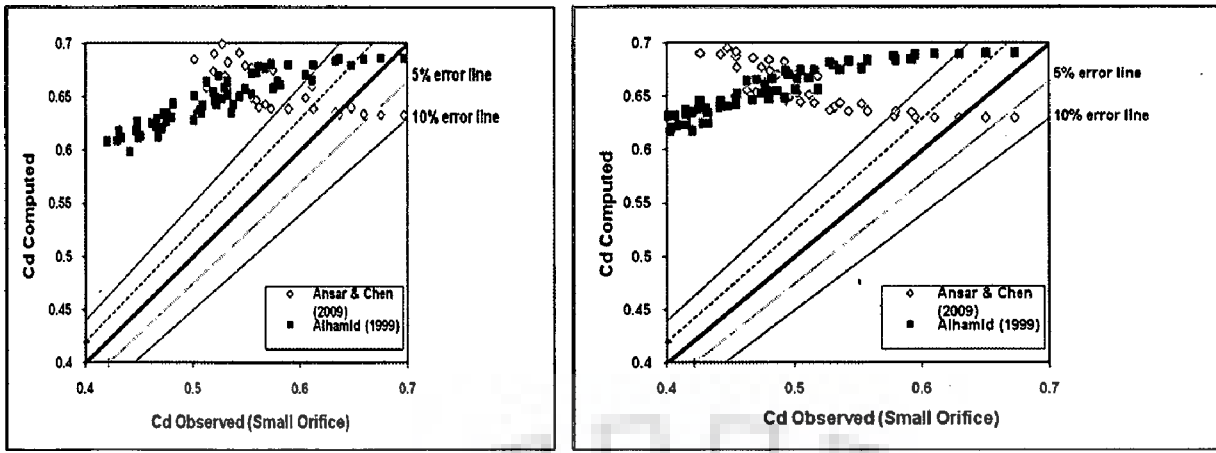
Fig.4.1c: Agreement diagram for raised crest (1H: 3V) for lip E and M for Habibzadeh et Al, Roth and hager and Swami



Lip A

Lip B

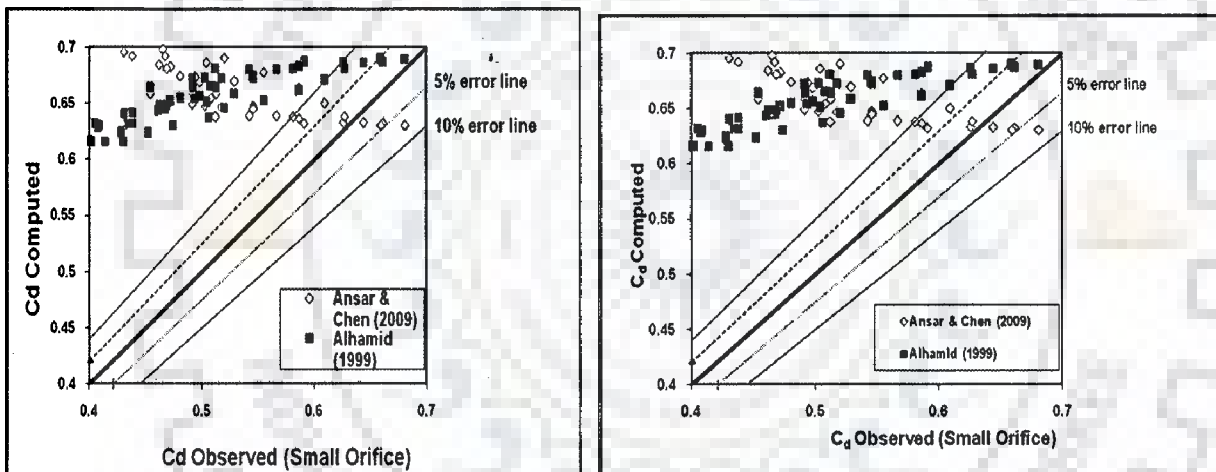
Fig.4.2a: Agreement diagram for raised crest (1H: 3V) for lip A and B for Ansar and Chen, Alhamid



Lip C

Lip D

Fig.4.2b: Agreement diagram for raised crest (1H: 3V) for lip C and D for Ansar and Chen, Alhamid



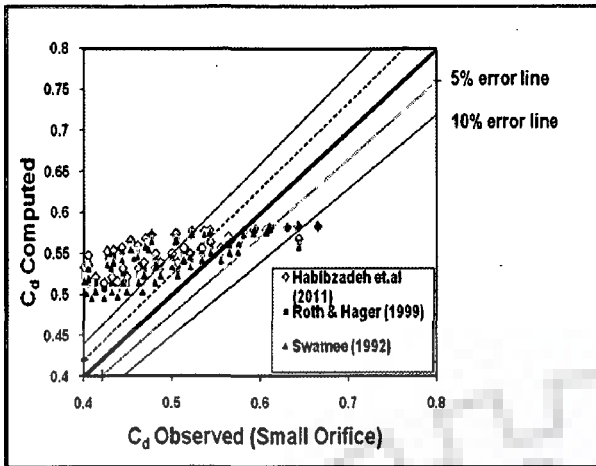
Lip E

Lip M

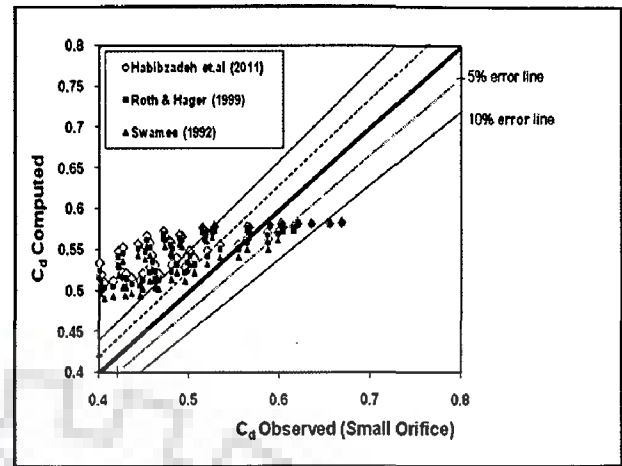
Fig.4.2c: Agreement diagram for raised crest (1H: 3V) for lip E and M for Ansar and Chen, Alhamid

#### 4.6 ANALYSIS OF DATA FOR RAISED CREST (2H: 3V)

Figs. 4.3 and 4.4 are shown to indicate agreement between computed and observed discharge coefficient. It can be seen that none of the relationships including Alhamid (1999) and Ansar & Chen (2009) have performed well for the raised crest type (2H:3V).

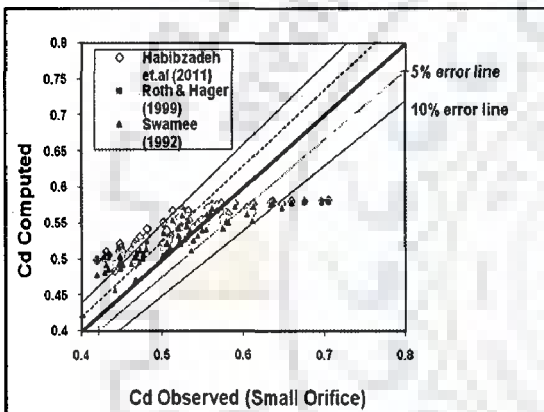


Lip A

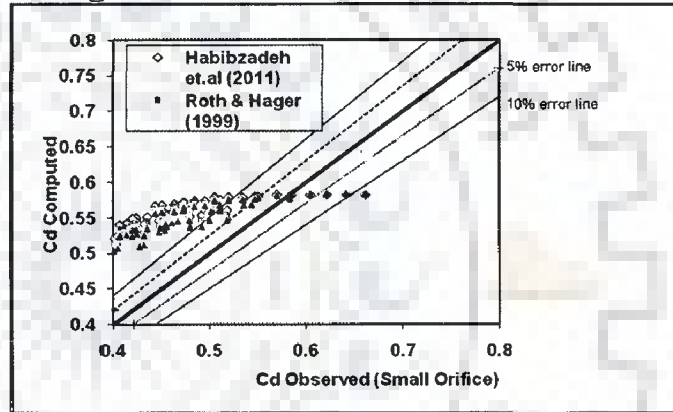


Lip B

Fig.4.3a: Agreement diagram for raised crest (2H: 3V) for lip A and B for Habibzadeh et Al, Roth and Hager and Swami

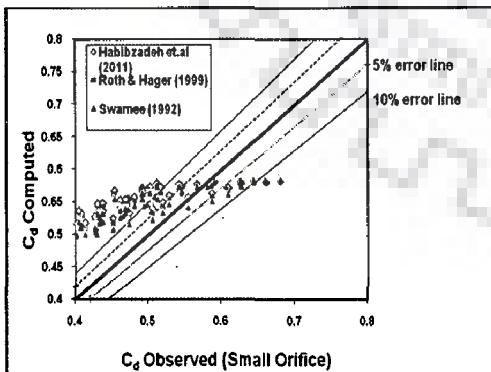


Lip C

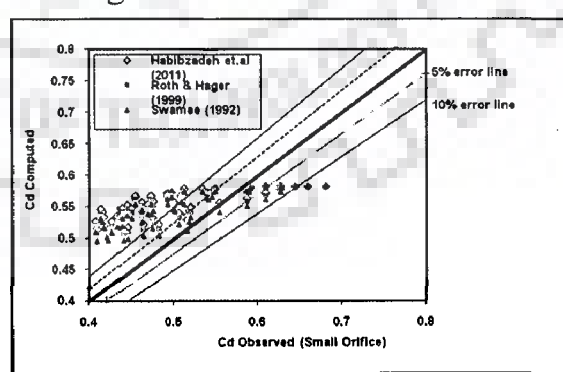


Lip D

Fig.4.3b: Agreement diagram for raised crest (2H: 3V) for lip C and D for Habibzadeh et Al, Roth and Hager and Swami

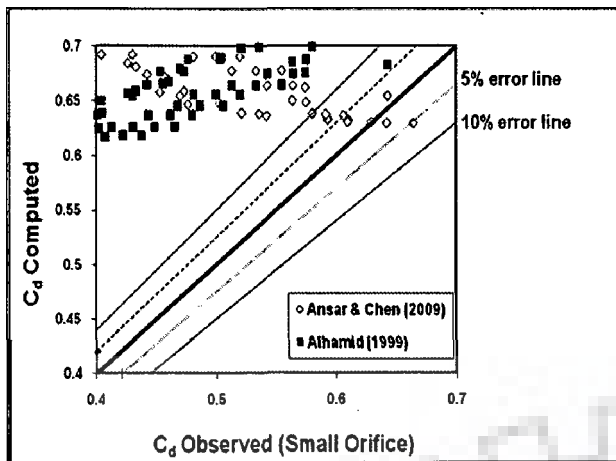


Lip E

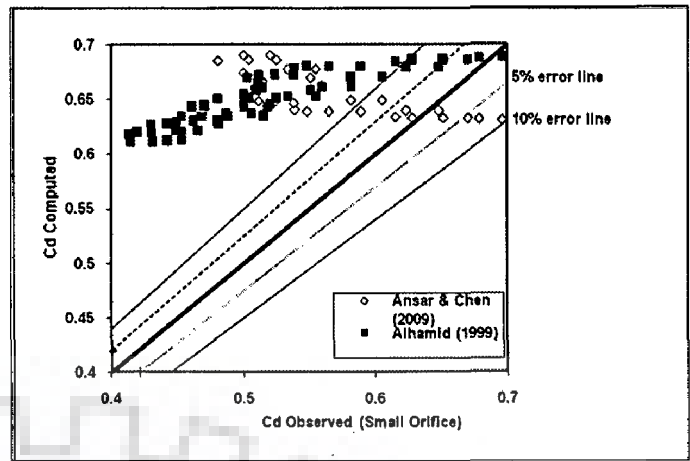


Lip M

Fig.4.3c: Agreement diagram for raised crest (2H: 3V) for lip E and M for Habibzadeh et Al, Roth and Hager and Swami

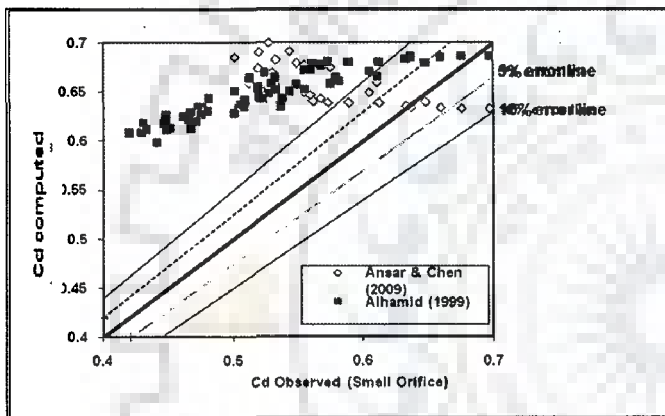


Lip A

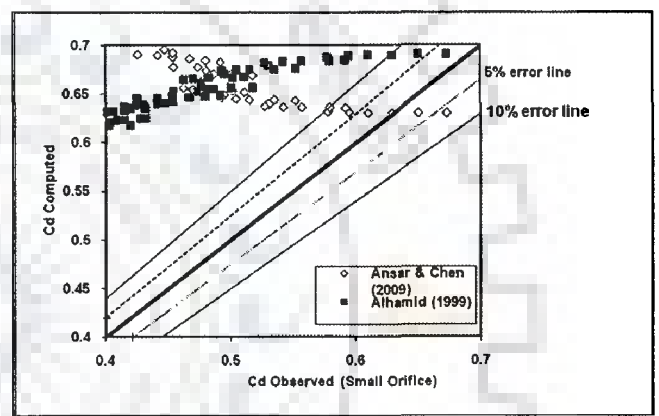


Lip B

Fig.4.4a: Agreement diagram for raised crest (2H: 3V) for lip A and B D for Ansar and Chen, Alhamid

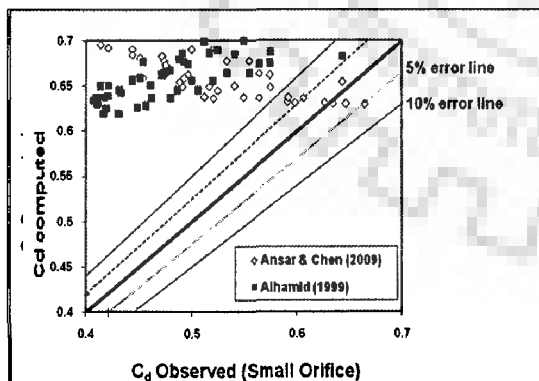


Lip C

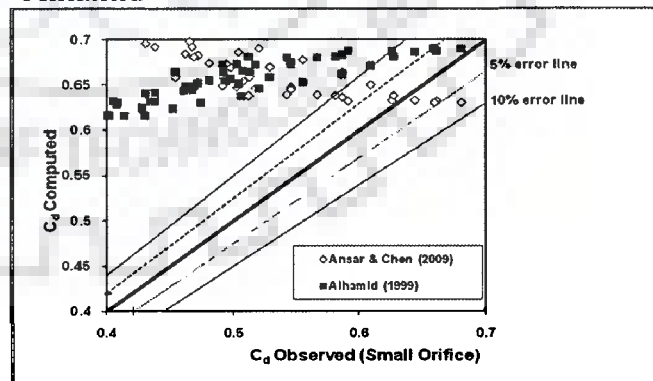


Lip D

Fig.4.4b: Agreement diagram for raised crest (2H: 3V) for lip C and D D for Ansar and Chen, Alhamid



Lip E



Lip M

Fig.4.4c: Agreement diagram for raised crest (2H: 3V) for lip E and M D for Ansar and Chen, Alhamid

## 4.7 ANALYSIS OF DATA FOR RAISED CREST WITH UPSTREAM FACE VERTICAL

The third profile of Ogee weir which has been tested in this work has a raised crest in which upstream face is vertical. Fig 4.5 and 4.6 again show the comparison between  $C_d$  computed by different relationships. Once again, the performance of this relationship is very similar to what has been reported with reference to Figs. 4.1 to 4.4.

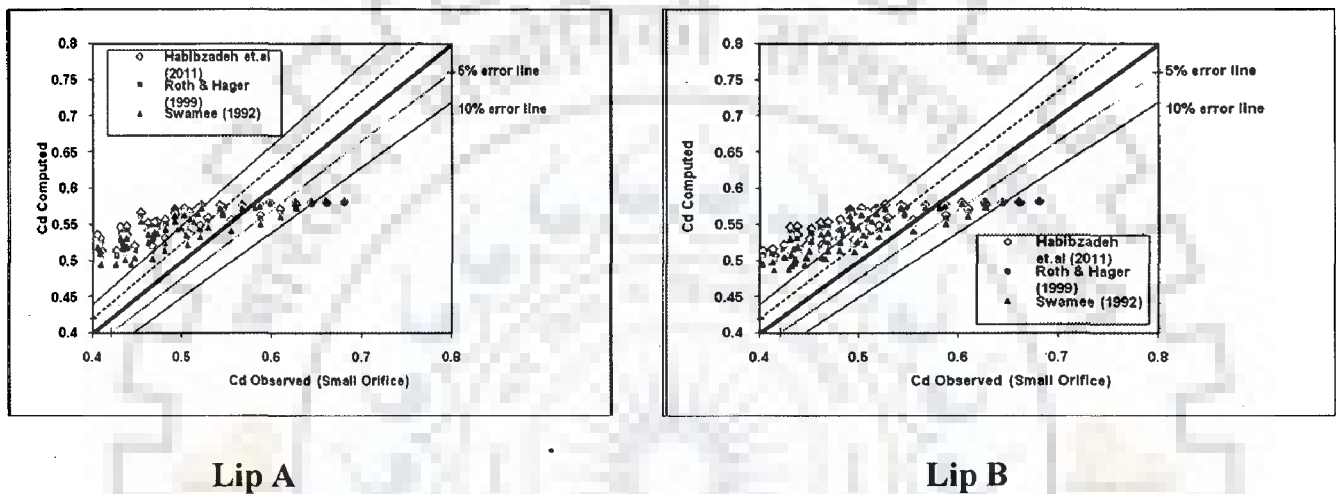


Fig.4.5a: Agreement diagram for raised crest vertical for lip A and B for Habibzadeh et Al, Roth and Hager and Swami

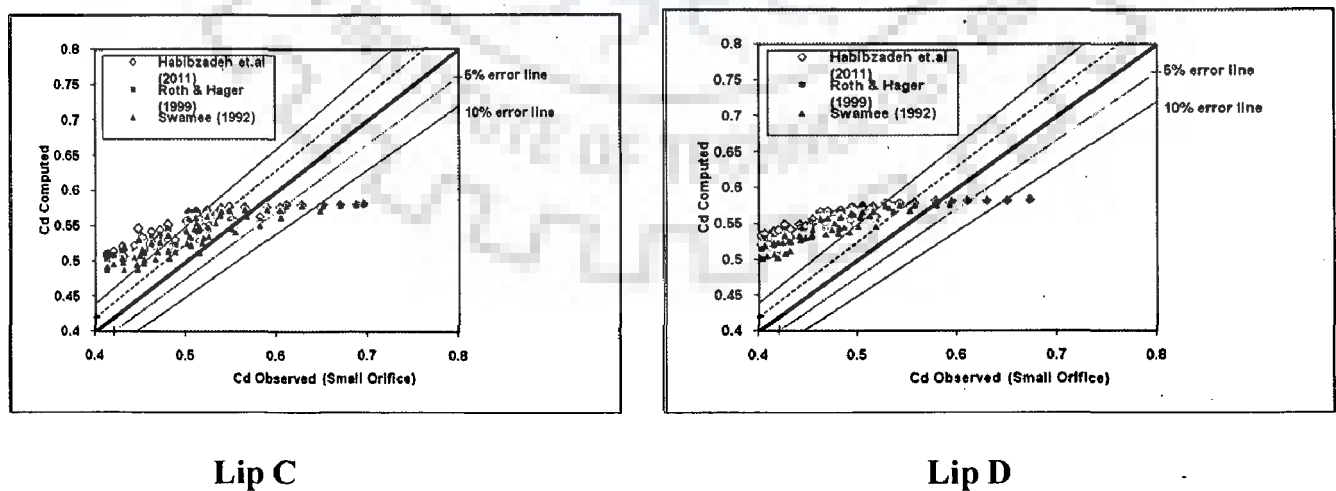
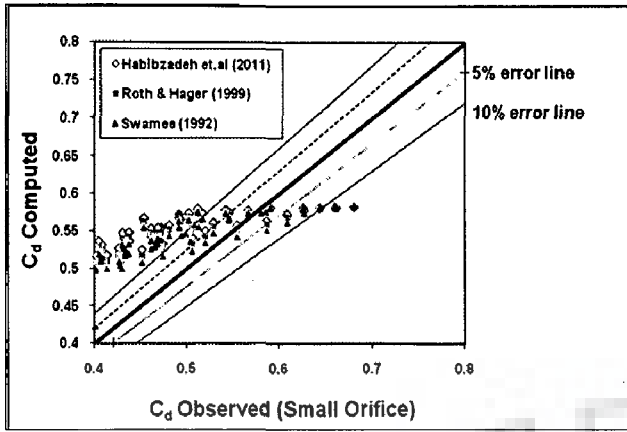
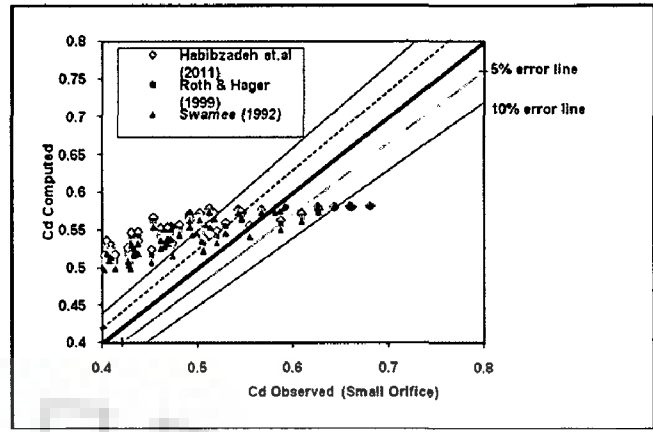


Fig.4.5b: Agreement diagram for raised crest vertical for lip C and D for Habibzadeh et Al, Roth and Hager and Swami

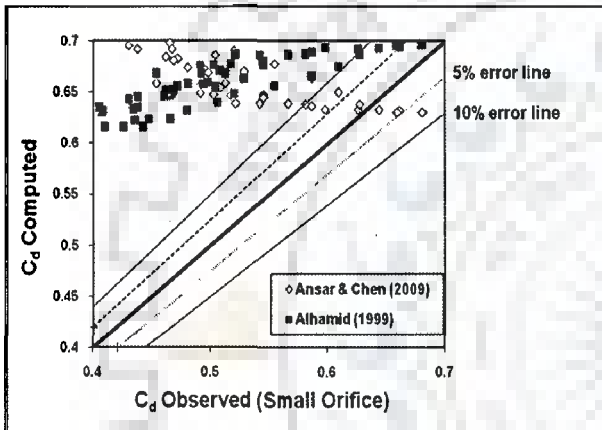


Lip E

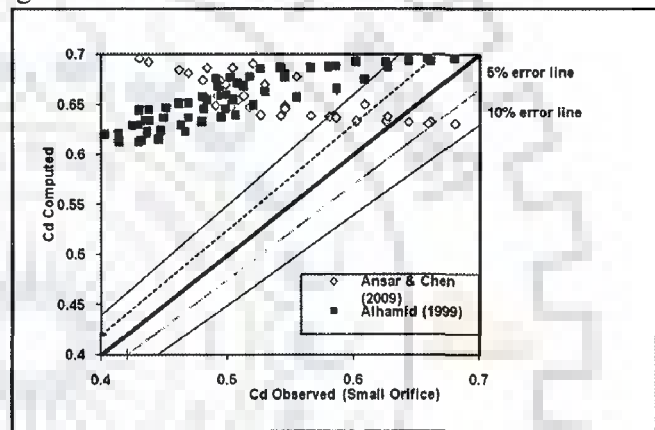


Lip M

Fig.4.5c: Agreement diagram for raised crest vertical for lip E and M for Habibzadeh et Al, Roth and Hager and Swami

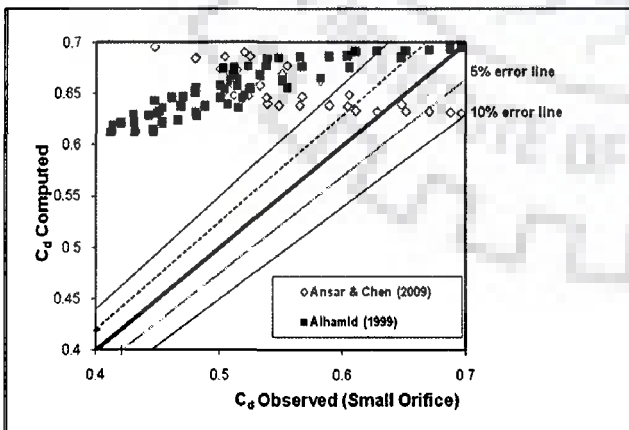


Lip A

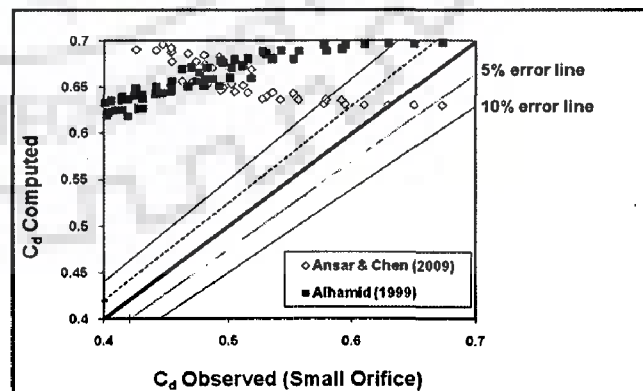


Lip B

Fig.4.6a: Agreement diagram for raised crest vertical for lip A and B D for Ansar and Chen, Alhamid



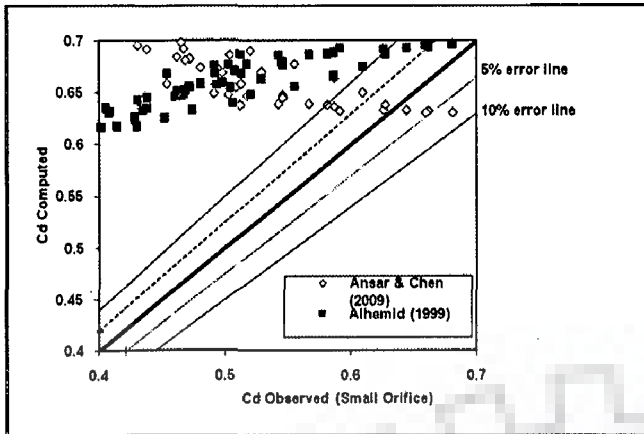
Lip C



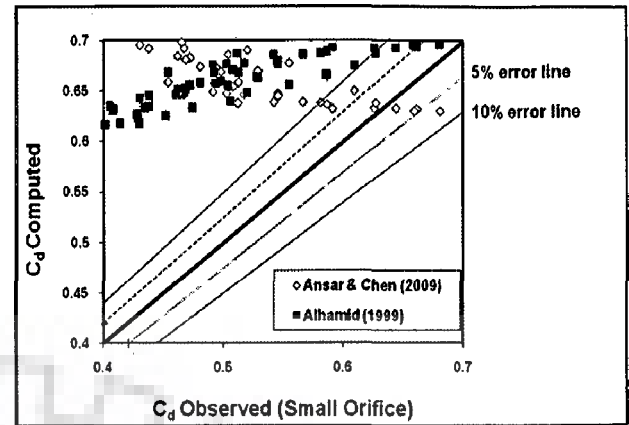
Lip D

Fig.4.6b: Agreement diagram for raised crest vertical for lip C and D for Ansar and Chen, Alhamid





Lip E



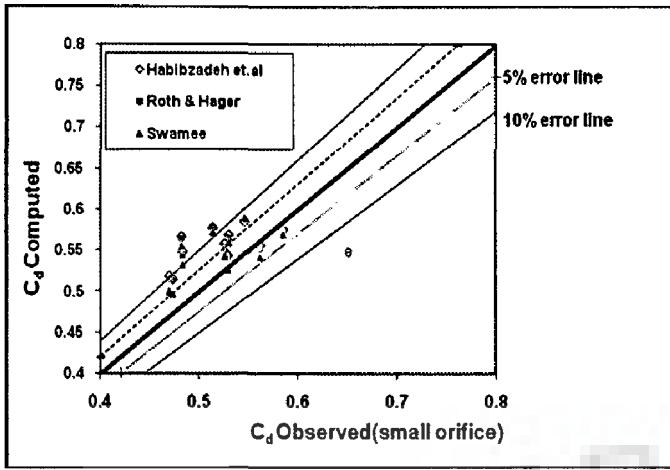
Lip M

Fig.4.6c: Agreement diagram for raised crest vertical for lip E and M for Ansar and Chen, Alhamid

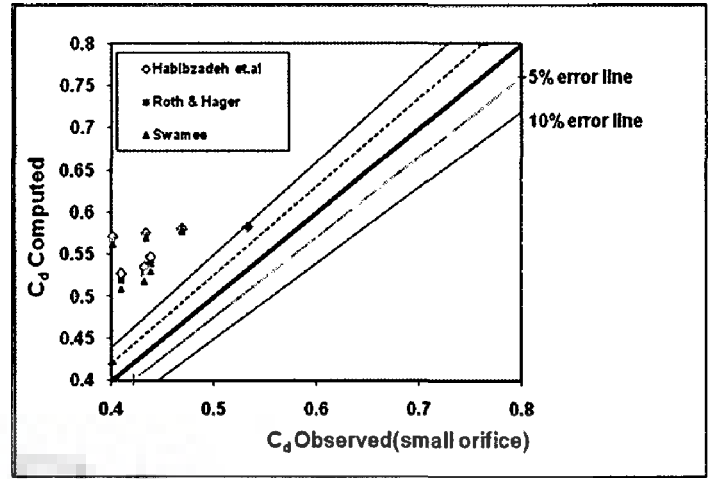
#### 4.8 ANALYSIS OF DATA FOR PLANE BED.

Certain experiments were also planned for flow through gates located above horizontal plane bed. The idea was that for such beds, the relationships of Swamee (1992), Roth and Hager (1999), and Habibzadeh et al. (2011) may do well if lip effects are not significant.

Figs. 4.7a-c show the agreement diagram between computed and observed  $C_d$  for few lip shapes. It can be seen that this relationship predicts the  $C_d$  in general within an error band of  $\pm 10\%$ . However, looking at the relative comparison between computed and observed  $C_d$  for different lip types, one tends to infer that the  $C_d$  values are being influenced by the lip shapes. For example, for lip A, there is tendency for  $C_d$  being over predicted and tendency for lip B is also over predicted, while the tendency for Lip C only being under predicted. In lips D and E, the computed  $C_d$ 's are being under as well as over predicted. If one compared the magnitude of  $C_d$  values for a given  $a/h_0$  value, the difference in  $C_d$  values for either of the gate locations whether above raised crest or plane bed, the lip effects are noticeable.

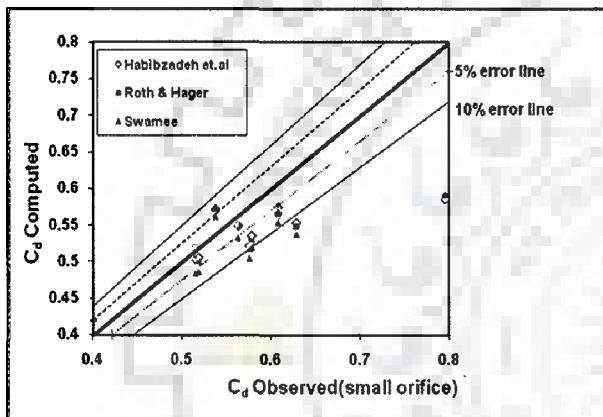


Lip A

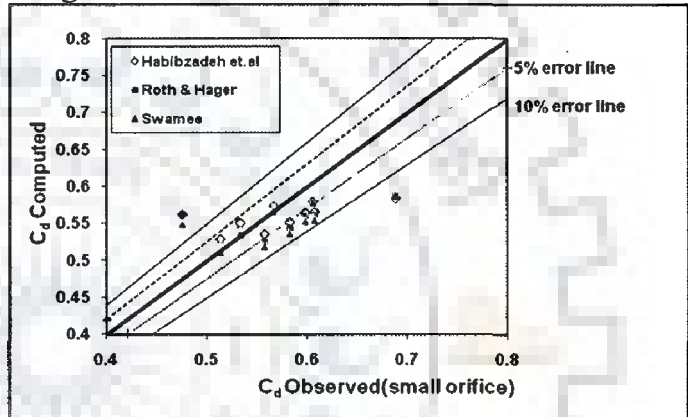


Lip B

Fig. 4.7a: Agreement diagram for plane bed lip A and B for Habibzadeh et Al, Roth and Hager and Swami

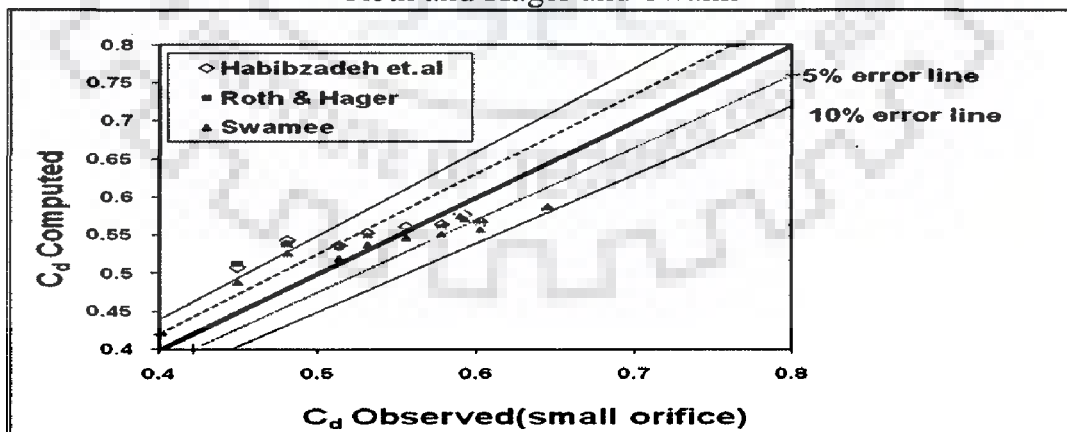


Lip C



Lip D

Fig.4.7b: Agreement diagram for plane bed lip C and D for Habibzadeh et Al, Roth and Hager and Swami



Lip E

Fig.4.7c: Agreement diagram for plane bed lip E for Habibzadeh et Al, Roth and Hager and Swami

## 4.9 ANALYSIS OF $C_d$ USING LARGE ORIFICE FORMULA

### 4.9.1 Analysis of Data for Raised Crest (1H:3V)

The major objective of this section is to assess where the large orifice formulation can lead to a better match with the observed  $C_d$  values. To investigate this, the agreement diagrams are developed for raised crest (1H:3V) for lip shapes A,B,C,D,E,M, as shown in Figs. 4.8a-c using Swamee (1992), Roth and Hager (1999), and Habibzadeh et al. (2011) relationships. Similarly, Figs. 4.9 a-c are developed using Alhamid (1999) and Ansar & Chen (2009) relationships. From Figs. 4.8 to 4.9, following points are worth notable.

Compared to small orifice formulation, the large orifice formulation helps in reducing the over prediction of the  $C_d$  values. This feature is observed in Figs. 4.8a-c and can be well appreciated using a comparison with Figs. 4.1a-c. Also, Fig. 4.9 indicates that Alhamid (1999) relationship has performed relatively better with the large orifice formulation.

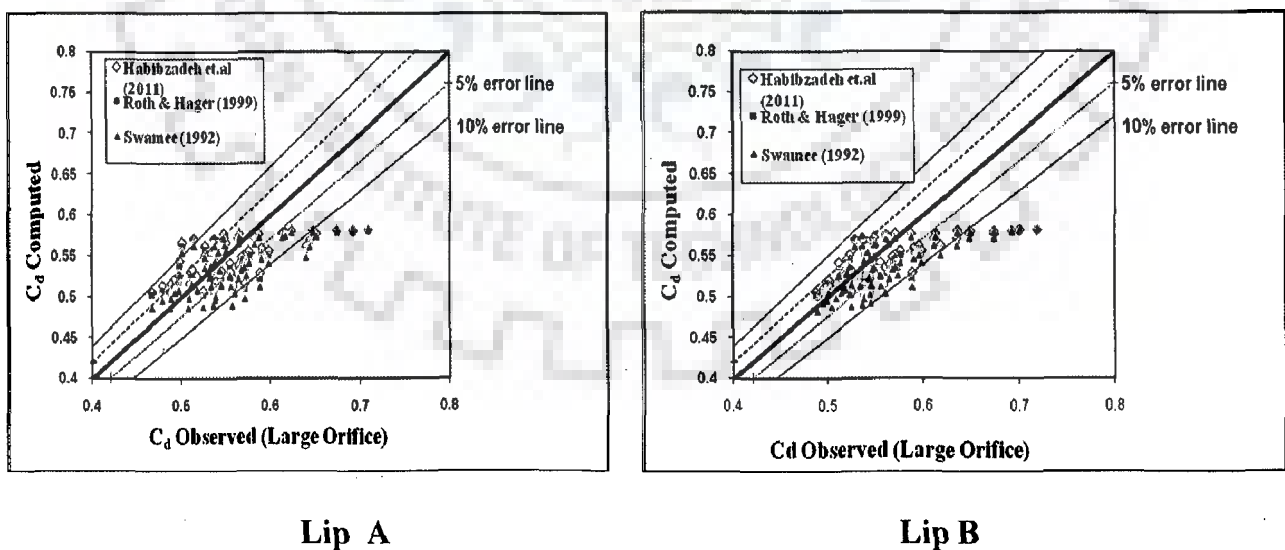
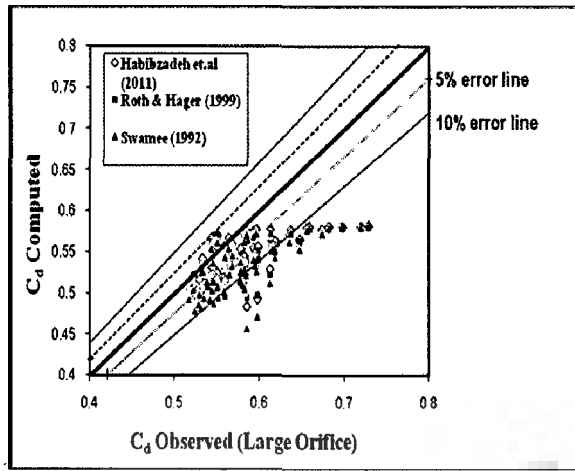
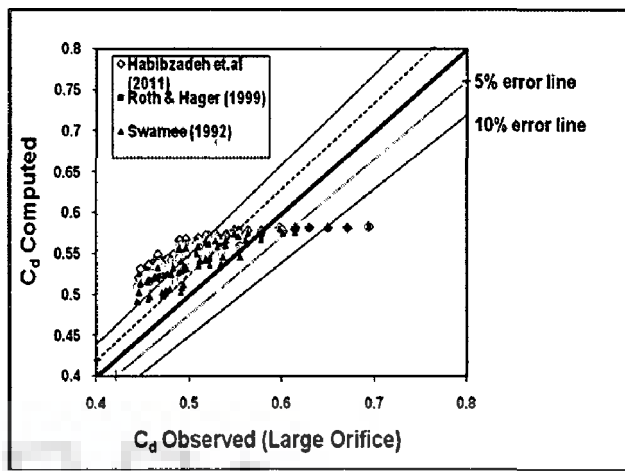


Fig.4.8a: Agreement diagram for raised crest (1H: 3V) for lip A and B for Habibzadeh et Al, Roth and Hager and Swami

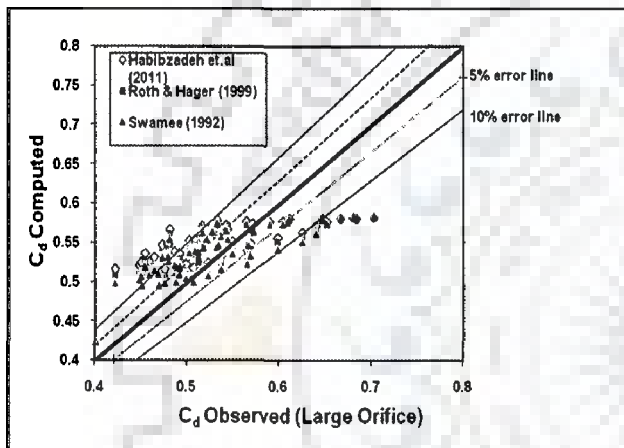


Lip C

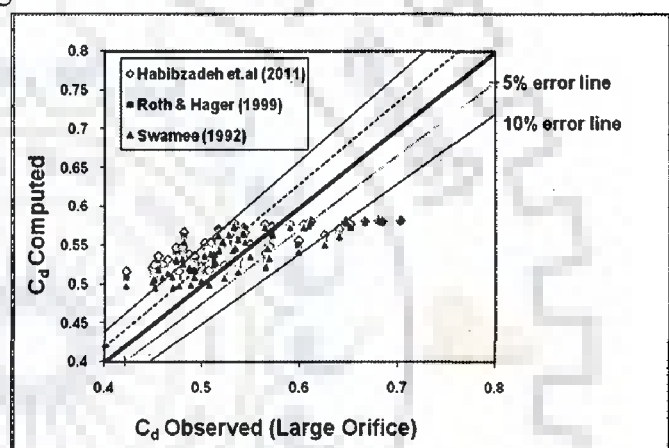


Lip D

Fig.4.8b: Agreement diagram for raised crest (1H: 3V) for lip C and D for Habibzadeh et Al, Roth and Hager and Swami

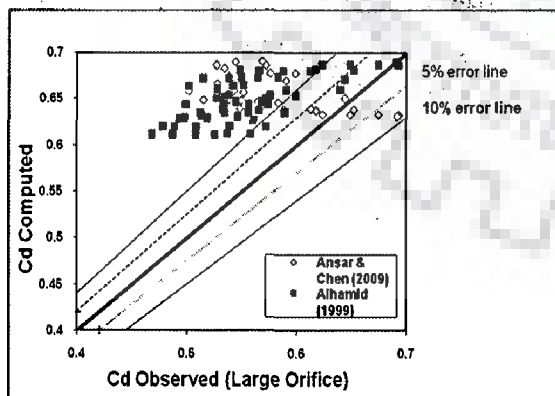


Lip E

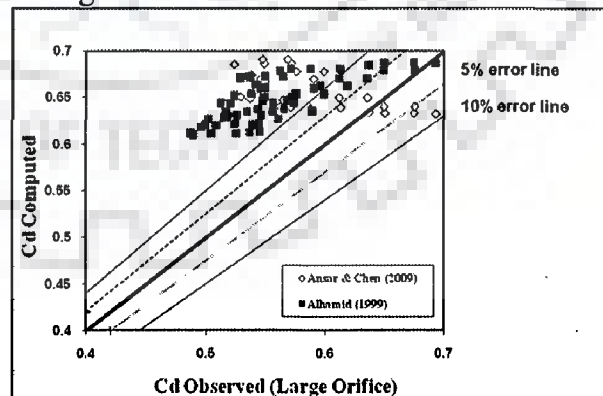


Lip M

Fig.4.8c: Agreement diagram for raised crest (1H: 3V) for lip E and M for Habibzadeh et Al, Roth and Hager and Swami

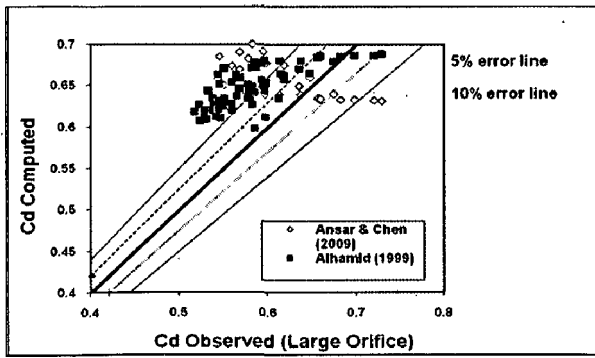


Lip A

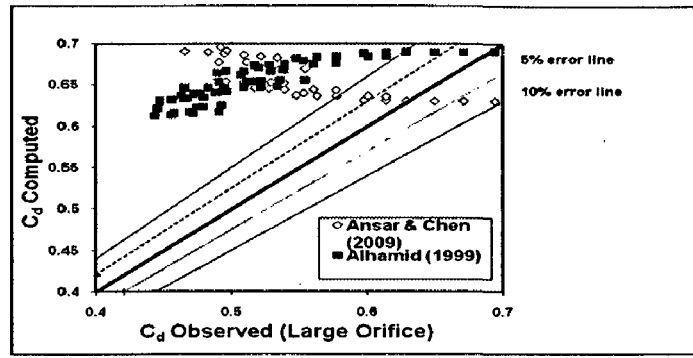


Lip B

Fig.4.9a: Agreement diagram for raised crest (1H: 3V) for lip A and B for Ansar and Chen, Alhamid

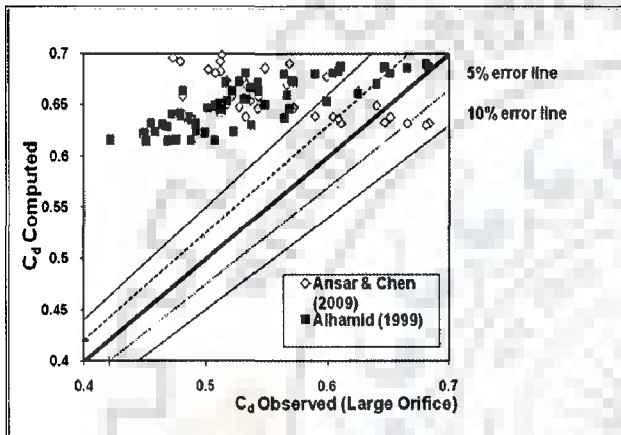


Lip C

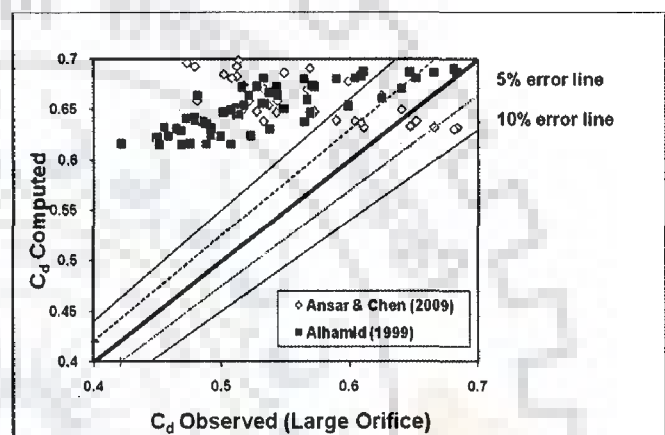


Lip D

Fig.4.9b: Agreement diagram for raised crest (1H: 3V) for lip C and D for Ansar and Chen, Alhamid



Lip E

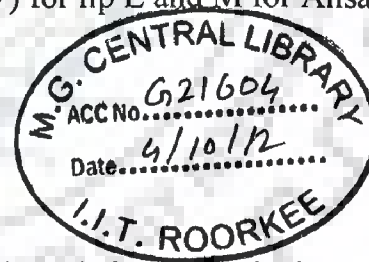


Lip M

Fig.4.9c: Agreement diagram for raised crest (1H: 3V) for lip E and M for Ansar and Chen, Alhamid

#### 4.9.2 Analysis of Data for Other Bed Types

Performance of large orifice formulation is also evaluated for other bed types and similar behavior is observed, as for bed type 1H:3V. To avoid repetition, figures for other bed types are given in Appendix attached in C.D. form with the present Thesis. The performance of Swamee (1992), Roth and Hager (1999), and Habibzadeh et al. (2011) as well as Alhamid (1999) and Anwar and Chen (2009) is very similar to that shown in Figs. 4.8 and 4.9.



#### 4.10 DEVELOPMENT OF CORRECTION FACTOR

It can be seen from Figs 4.1 to 4.9 that there is a need to improve the predictions for discharge coefficient for various lip shapes and bed profile combinations for large as well as small orifice formulations. For the relationships of Alhamid (1999), the correction factors have been developed because there is Alhamid (1999) only who had given equations of flow characteristics on different types of raised crest profiles located under vertical sluice gates in literature. To develop the correction factors, the ratio of observed to computed discharge coefficient was plotted with respect to relative gate opening and then, these trends were fitted.

Tables 4.1 to 4.4 present the correction factors which can be used with the relationship of Alhamid for computing discharge through the gates located above raised crest. Multiplying these correction factors with the  $C_d$  computed using Alhamid, one can predict  $C_d$  values which are in close agreement with the observed  $C_d$  values.

**Table 4.1: Correction Factors for Raised Profile (1H: 3V)**

Lip Shape	Correction Factor (Large Orifice)	Correction Factor (Small Orifice)
Lip A	$1.2703 A^{0.0497}$	$1.6119 A^{0.1285}$
Lip B	$1.2805 A^{0.0599}$	$1.6278 A^{0.1397}$
Lip C	$1.1838 A^{0.0381}$	$1.5325 A^{0.1264}$
Lip D	$1.511 A^{0.0947}$	$1.8655 A^{0.1614}$
Lip E	$1.4836 A^{0.1051}$	$1.8404 A^{0.1742}$
Lip M	$1.4836 A^{0.1051}$	$1.8404 A^{0.1742}$

**Table 4.2: Correction factors for Raised Profile (2H: 3V)**

Lip Shape	Correction	Factor	Correction	Factor
	(Large Orifice)		(Small Orifice)	
Lip A	$1.4238 A^{0.0709}$		$1.7689 A^{0.1404}$	
Lip B	$1.3288 A^{0.0433}$		$1.6687 A^{0.1173}$	
Lip C	$1.2867 A^{0.0434}$		$1.6268 A^{0.1205}$	
Lip D	$1.5357 A^{0.0825}$		$1.8847 A^{0.1464}$	
Lip E	$1.4273 A^{0.0743}$		$1.7701 A^{0.1429}$	
Lip M	$1.4105 A^{0.0698}$		$1.757 A^{0.1405}$	

**Table 4.3: Correction factors for Raised Profile (Vertical)**

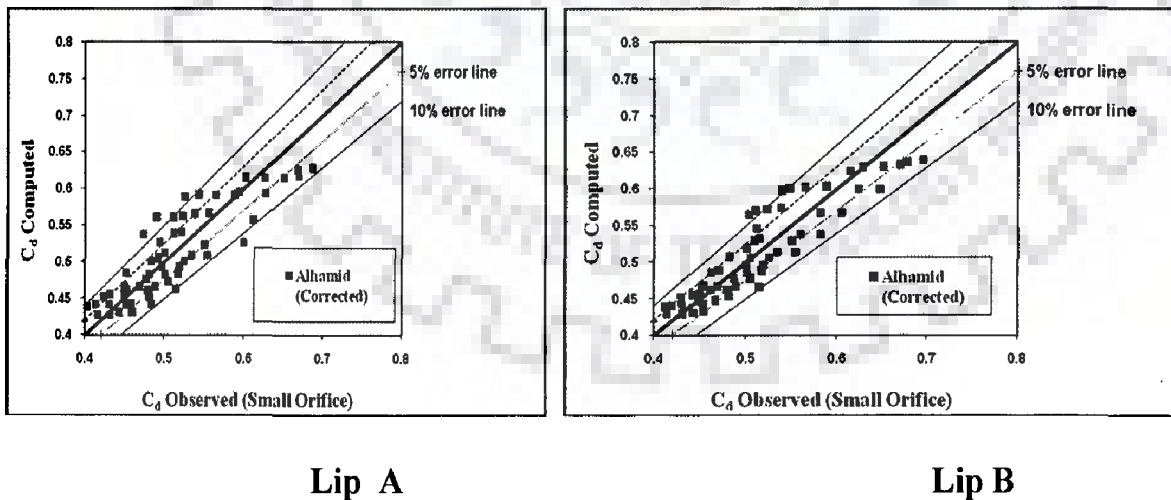
Lip Shape	Correction	Factor	Correction	Factor
	(Large Orifice)		(Small Orifice)	
Lip A	$1.1368 A^{0.0102}$		$1.8035 A^{0.163}$	
Lip B	$1.323 A^{0.057}$		$1.6709 A^{0.1338}$	
Lip C	$1.2851 A^{0.0555}$		$1.6332 A^{0.1353}$	
Lip D	$1.5084 A^{0.0909}$		$1.8623 A^{0.1576}$	
Lip E	$1.4809 A^{0.1012}$		$1.837 A^{0.1703}$	
Lip M	$1.4809 A^{0.1012}$		$1.837 A^{0.1703}$	

Table 4.4 shows the correction factors to be used with the relationship of Swamee (1992).

**Table 4.4: Correction factors for Plane Bed**

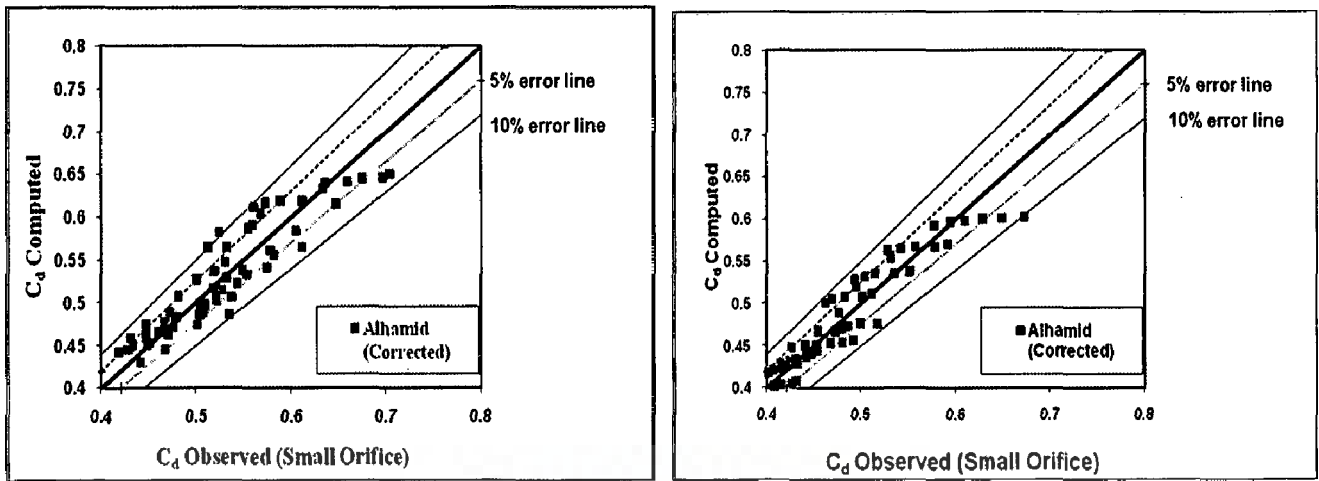
Lip Shape	Correction (Large Orifice) Factor	Correction (Small Orifice) Factor
Lip A	$0.8759 A^{-0.0596}$	$1.0867 A^{0.015}$
Lip B	$0.7562 A^{-0.0378}$	$0.9542 A^{0.0354}$
Lip C	$0.7412 A^{-0.0526}$	$0.9398 A^{0.0295}$
Lip D	$0.7848 A^{-0.0628}$	$0.9818 A^{0.0173}$
Lip E	$0.9327 A^{0.0099}$	$1.1264 A^{0.0709}$

For bed type 1H:3V, Figs. 4.10a-c and 4.11 a-c show the agreement between the computed  $C_d$  and observed  $C_d$  using correction factors for small as well as large orifice formulations. It can be seen from these figures that use of correction factors is helpful to compute discharge under various lip shapes.



**Fig.4.10a: Agreement diagram for raised crest (1H: 3V) lip A and B for Small Orifice**

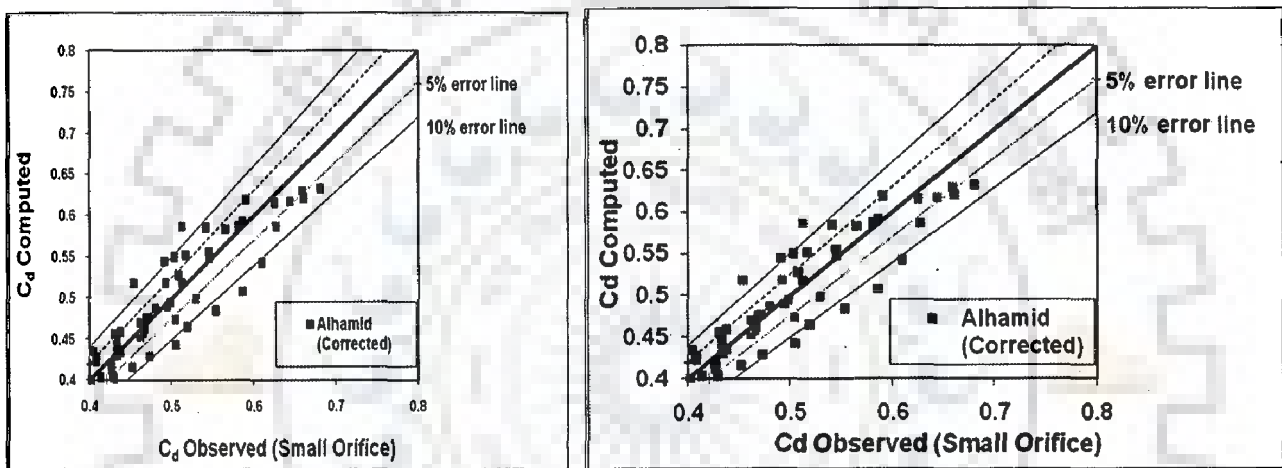




Lip C

Lip D

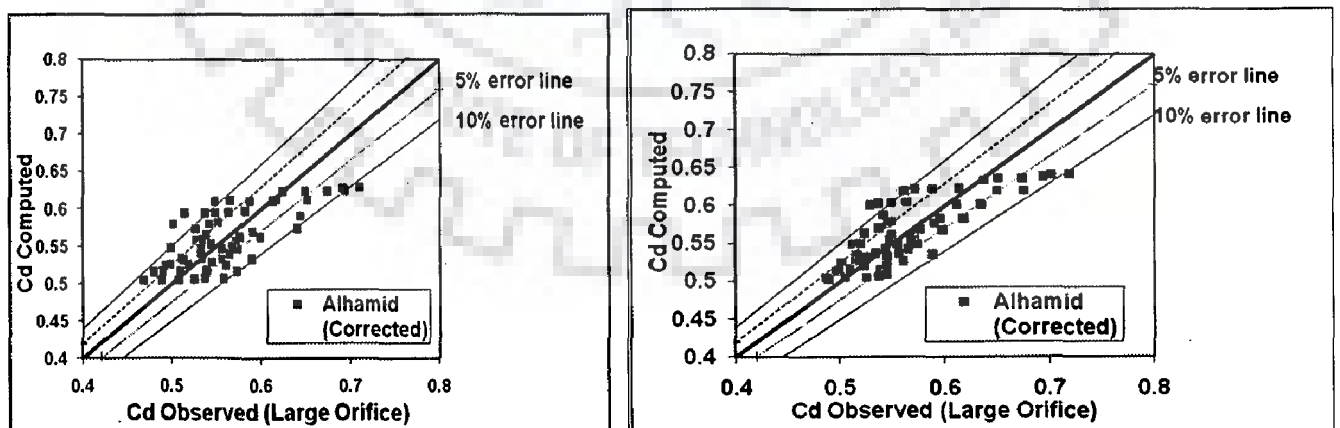
Fig.4.10b: Agreement diagram for raised crest (1H: 3V) for lip C and D for Small Orifice



Lip E

Lip M

Fig.4.10c: Agreement diagram for raised crest (1H: 3V) for lip E and M for Small Orifice



Lip A

Lip B

Fig.4.11a: Agreement diagram for raised crest (1H: 3V) for lip A and B for Large Orifice

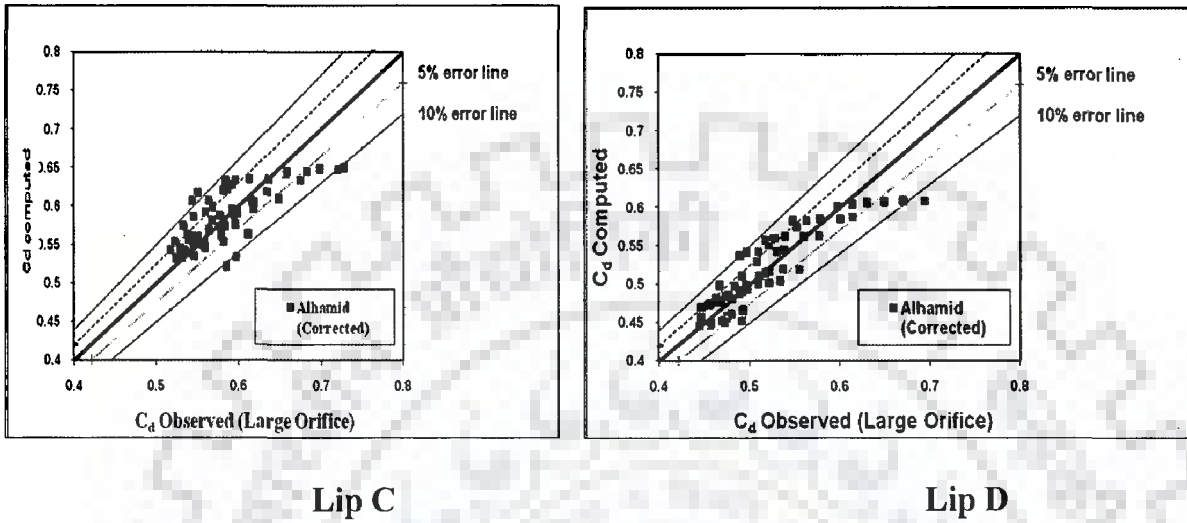


Fig.4.11b:Agreement diagram for raised crest (1H: 3V) for lip C and D for Large Orifice

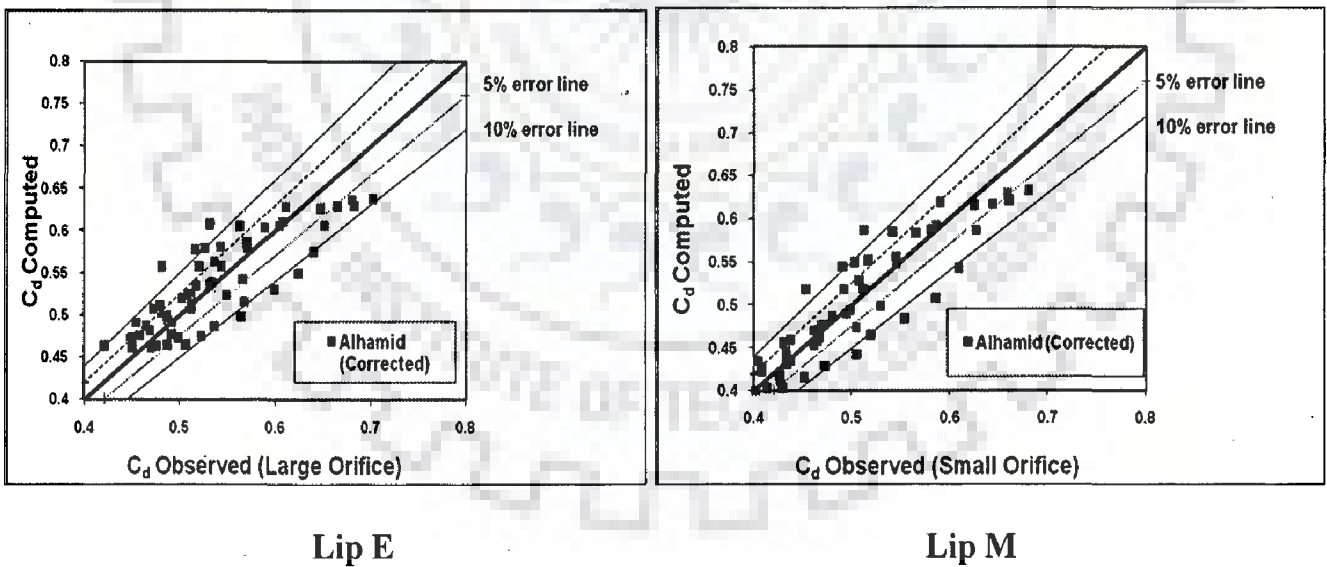


Fig.4.11c: Agreement diagram for raised crest (1H: 3V) for lip E and M

The formula as proposed by Alhamid (1999) can be multiplied with the correction factors generated from experimental data for various lip and bed profile combinations.

#### 4.11 COMPARATIVE EVALUATION OF PERFORMANCE OF DIFFERENT NON STREAMLINED LIP SHAPES.

It is of interest to identify a lip shape which can maximize coefficient of discharge for the same gate opening. For three types of raised crest and plane bed, the  $C_d$  variations have been shown with relative gate openings and Figs 4.12 to 4.15 present the combined variations of discharge coefficients for various lip shapes. It can be seen from Fig 4.12 to 4.15 that lip C has the higher  $C_d$  values at various relative gate openings. Thus, this can be considered as the best shape among non-streamlined lip shapes investigated in this chapter.

The better performance of lip C is further justified by ranking of the lips as can be seen in Chapter 8.

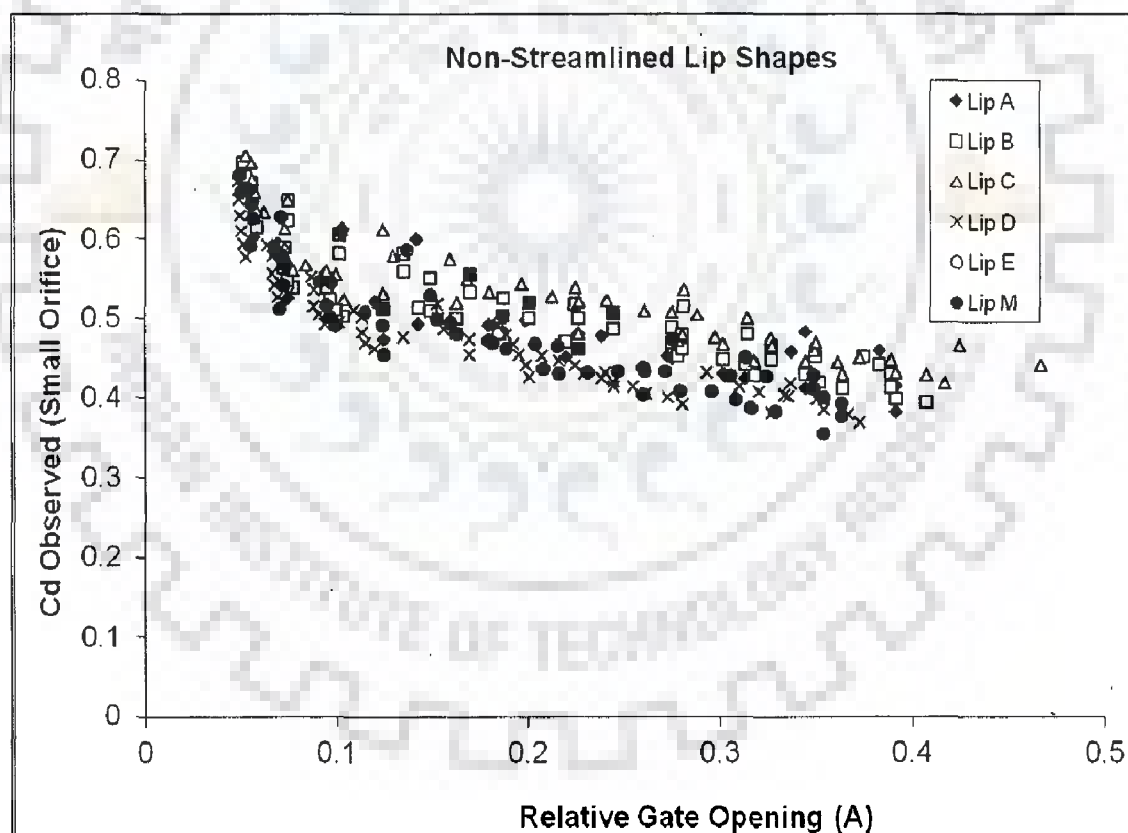


Fig. 4.12:  $C_d$  variation with relative gate opening for raised crest (1H: 3V)

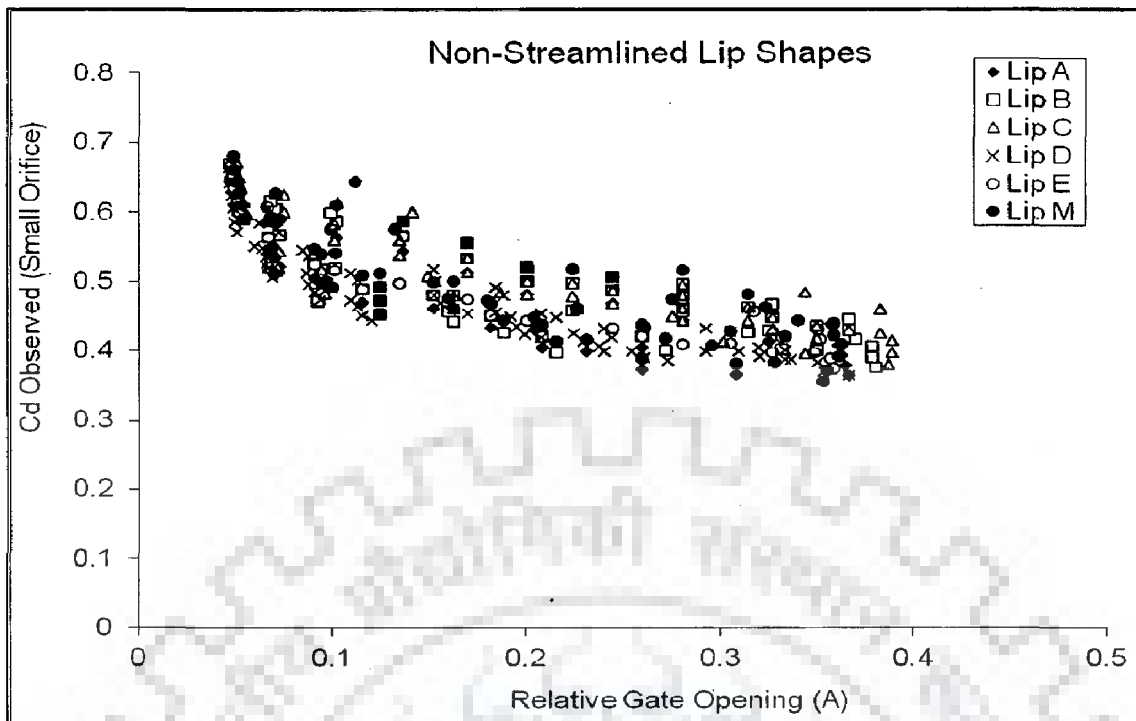


Fig.4.13:  $C_d$  variation with relative gate opening for raised crest (2H: 3V)

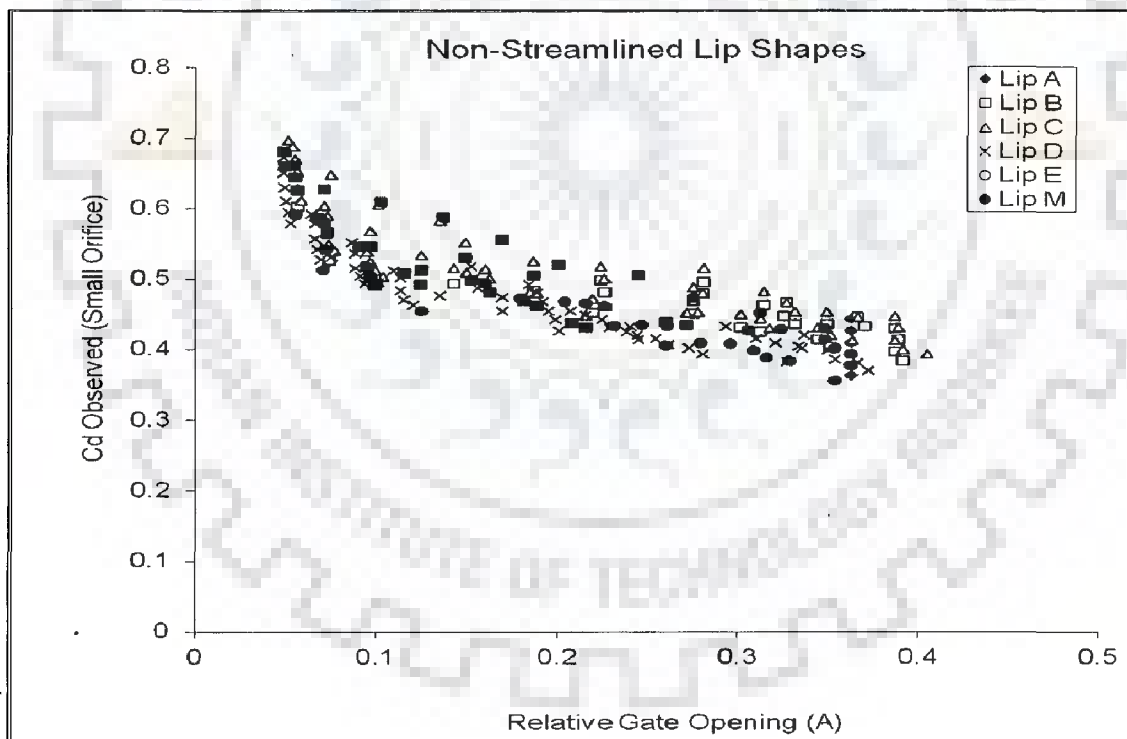


Fig.4.14:  $C_d$  variation with relative gate opening for raised crest (Vertical)

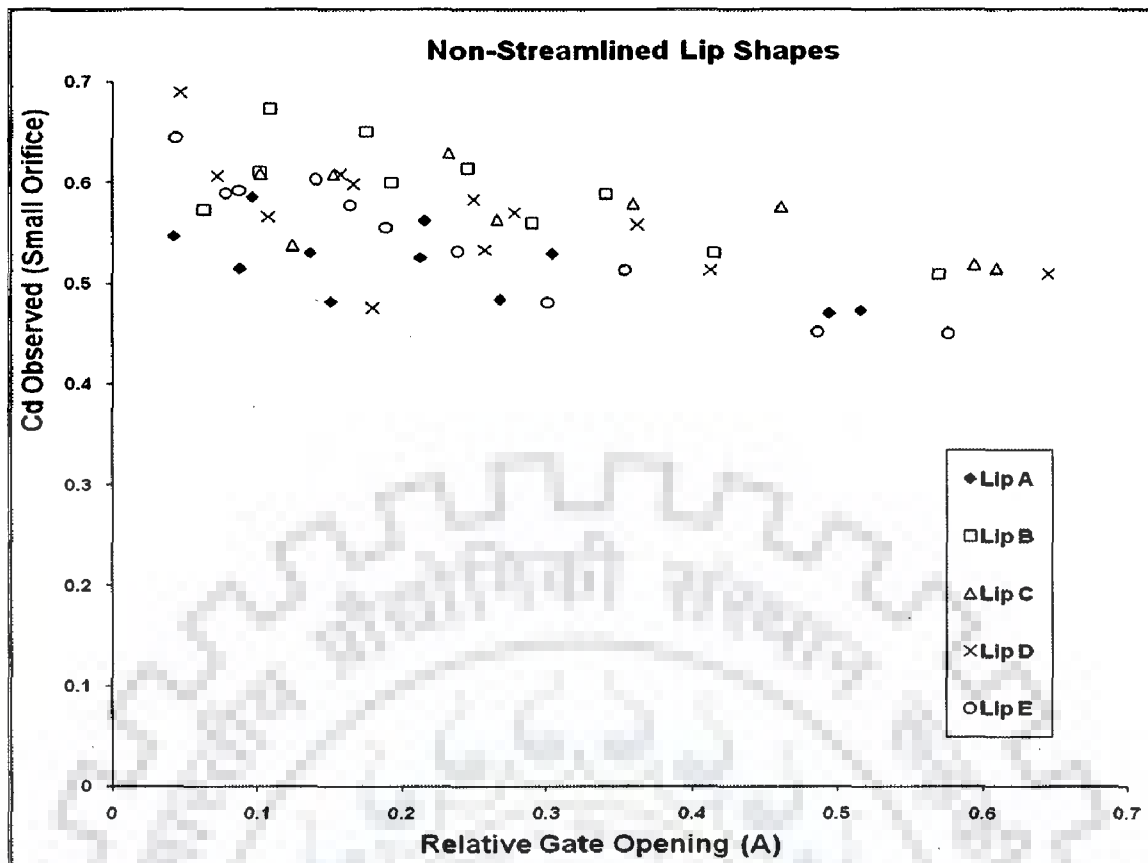


Fig.4.15:  $C_d$  variation with relative gate opening for Plane Bed

#### 4.12 $C_d$ VARIATION AS PER CERTAIN EXISTING MODELS

To assess the potential and power of different approaches such as Swamee(1992), Roth and Hager (1999); Habibzadeh et.al.(2011) this section looks into simplification of various approaches and tries to identify the relative merits of using various approach formulations comparatively .

##### 4.12.1 Simplification of Swamee Approach:

The equation proposed by Swamee for the variation of discharge coefficient under free flow condition can be written as:

$$\frac{C_d}{0.611} = \left[ \frac{1 - \frac{a}{h_0}}{1 + 15 \left( \frac{a}{h_0} \right)} \right]^{0.072} \quad (4.4)$$

In equation 4.4,  $a$  is the gate opening and  $h_0$  is the approach flow depth u/s of the gate.

Using binomial expansion, the numerator and denominator in Eq. 4.4 can be linearised.

Considering the first two terms of the binomial expansion, Eq.4.4 becomes

$$C_d = 0.611 \left[ 1 - 0.072 \left( \frac{a}{h_0} \right) \right] \left[ 1 - 0.072 \times 15 \left( \frac{a}{h_0} \right) \right] \quad (4.5)$$

Eq. 4.5 can be written as:

$$C_d = 0.611 \left[ 1 - \alpha_1 \left( \frac{a}{h_0} \right) \right] \left[ 1 + \alpha_2 \left( \frac{a}{h_0} \right) \right] \quad (4.6)$$

Where  $\alpha_1 = 0.072$  and  $\alpha_2 = -0.072 \times 15$  . Eq.4.6 further simplifies to:

$$C_d = 0.611 \left[ 1 - (\alpha_1 + \alpha_2) \left( \frac{a}{h_0} \right) + \alpha_1 \alpha_2 \left( \frac{a}{h_0} \right)^2 \right]$$

$$C_d = 0.611 \left[ 1 - 1.152 \frac{a}{h_0} + 0.07776 \left( \frac{a}{h_0} \right)^2 \right] \quad (4.7)$$

#### 4.12.2 Simplification of Roth and Hager approach:

In Roth and Hager approach,  $C_d$  is related with relative gate opening. In Chapter 2, relevant equations and charts were provided to use this approach. For the sake of presentation, some of the key equations are reproduced here.

$$A_m = 0.05 + .40 \left( \log \left( \frac{R_a}{1000} \right) \right) \quad (4.8 a)$$

$$C_{d_m} = 0.60 - \frac{1}{18} \log(R_a/1000) \quad (4.8 b)$$

$$D_d = (C_d - C_{d_m}) / (C_{d_0} - C_{d_m}) \quad (4.8 c)$$

$$D_d = (1 - A_n)^2 \quad \text{where } A_n = A/A_m \quad (4.8 d)$$

$$(C_d - C_{d_m}) = [0.6 - C_{d_m}] [1 + A_n^2 - 2A_n] \quad (4.6 e)$$

Combining the above equations and simplifying , one obtains

$$C_d = \left[ 0.60 - \frac{1}{18} \log \left( \frac{R_g}{1000} \right) \right] + \left( \frac{1}{18} \log \left( \frac{R_g}{1000} \right) \right) \left[ 1 + \frac{1}{A_n^2} \left( \frac{a}{h_0} \right)^2 - \frac{2}{A_n} \left( \frac{a}{h_0} \right) \right] \quad (4.7)$$

or

$$C_d = \left[ a_0 + a_1 \left( \frac{a}{h_0} \right) + a_2 \left( \frac{a}{h_0} \right)^2 \right] \quad (4.8)$$

In Eq 4.8,  $a_0=0.6$  and,

$$a_1 = \frac{1}{18} \log \left( \frac{R_a}{1000} \right) \left[ \frac{-2}{0.65 + 0.40 \log \left( \frac{R_a}{1000} \right)} \right] \quad (4.8 a)$$

$$a_2 = \frac{1}{18} \log \left( \frac{R_a}{1000} \right) \left[ \frac{1}{0.65 + \log \left( \frac{R_a}{1000} \right)^2} \right]^2 \quad (4.8 b)$$

#### 4.12.3 Habibzadeh et al. Approach

Habibzadeh et al. (2011) proposed the following equation for variation of discharge coefficient,  $C_d$

$$C_d = C_c \left( 1 - \frac{1}{\beta} \right)^{0.5} \left( 1 + k - \frac{1}{\beta^2} \right)^{-0.5} \quad (4.9)$$

In eq. 4.9,  $C_c$  is coefficient of contraction and is normally taken as 0.61.  $k$  is a constant and equals 0.062.

For free flow.  $\beta$  is defined as

$$\beta = \frac{h_0}{0.61 \times a} \quad (4.10)$$

Substituting for  $\beta$  in Eq. 4.9 and simplifying, one obtains

$$C_d = C_c \left[ 1 - 0.5k + \frac{0.5k}{\beta^2} - \frac{0.5}{\beta} + \frac{0.25k}{\beta} - \frac{0.25k}{\beta^3} \right] \quad (4.11)$$

Using binomial expansion of the terms in {}, and retaining first two terms, one obtains,

$$C_d = \left[ a_0 + a_1 \frac{a}{h_0} + a_2 \left( \frac{a}{h_0} \right)^2 + a_3 \left( \frac{a}{h_0} \right)^3 \right] \quad (4.13)$$

Where,

$$a_0 = \frac{2-k}{2} \quad (4.13 a)$$

$$a_1 = -0.5k \times 0.611 \quad (4.13 b)$$

$$a_2 = 0.5k \times 0.611^2 \quad (4.13 c)$$

$$a_3 = -0.25k \times 0.611^3 \quad (4.13 d)$$

It can be seen from the present analysis that Eq. (4.13) has better potential than Eq.(4.8) and Eq.(4.7). This is because Eq. (4.13) is a third order polynomial and has a better ability to fit the data than a second or the first order polynomial.

#### 4.13 SUMMARY

In this chapter the discharge characteristics of non-streamlined lip shapes are evaluated. It is observed that in the presence of lip the existing relationship for discharge coefficient computations deviate from the observed values. To include the effect of lip in discharge coefficient computation correction factors have been proposed. The agreement between computed and observed discharge coefficient using correction factors is found to work well. Among various non-streamlined lip shapes, lip C which has a  $45^{\circ}$  inclination from the horizontal and same lip length and same lip width is found to give higher value of discharge coefficient than the other lip types tested in this study. Relationships of Swamee, Roth and Hager and Habibzade et al. are revisited to look into similarity in their functional forms and it is observed that these relationship show similar variation between the discharge coefficient and relative gate opening. Swamee (1992) ,Roth and Hager (1999) relationship are governed by a second order polynomial relationship between discharge coefficient and relative gate opening where as the Habibzade et al.(2011) relationship is governed by a third order polynomial relationship. Simplification of these relationships also supports the field based variations between discharge coefficient and relative gate opening, as suggested by Lozano et al. (2009).



---

# PRESSURE CHARACTERISTICS OF NON-STREAM LINED LIP SHAPES

---

### 5.1 INTRODUCTION

The pressure characteristics of sluice gates having non-stream lined lip shape are considered in this chapter. Six types of non-stream lined shapes are analysed for pressure variations. The idea is to find the lip shape which experiences minimum upward/downward pressure throughout the operational range of relative gate opening. The variables which have been changed to see the corresponding effect on pressure are (1) discharge, (2) gate opening and (3) channel bed profile under the sluice gate. Four types of channel bed profiles are considered. Three bed profiles are top surface profiles of ogee shaped weirs. The upstream slope of these ogee weirs varies and is considered as 1H:3V, 2H:3V and vertical face. The fourth profile is a flat or plane bed. This chapter deals with variation of pressure with a range of dimensionless parameters, including relative gate opening.

### 5.2 PRESSURE VARIATIONS

The measurements of the pressure have been taken using a peizometer. Each lip was provided with nine holes for pressure measurement connected to a peizometer each. The arrangement of these holes is symmetric; three holes each on the extreme edges of the lip and three at the center of the lip. The average of these nine readings has been taken as the average pressure on the lip. In actual practice, sluice gates are usually operated within the range of 0-0.5 relative gate opening. Therefore, experiments have been done within this range of relative gate opening.

### 5.2.1 Pressure versus Relative Gate Opening

Rather than plotting pressure as a function of the actual opening, the plot has been made against relative gate opening  $A$ . In this work, relative gate opening is represented as

$$A = a/h_o \tag{5.1}$$

Therefore, for a particular upstream depth and gate opening, one can compare the pressure experienced by each lip shape. This comparison yields the lip shape with minimum pressure.

#### 5.2.1.1 Raised crest (1H: 3V)

For this situation, pressure variation for three lip shapes is shown in Fig. 5.1 a.

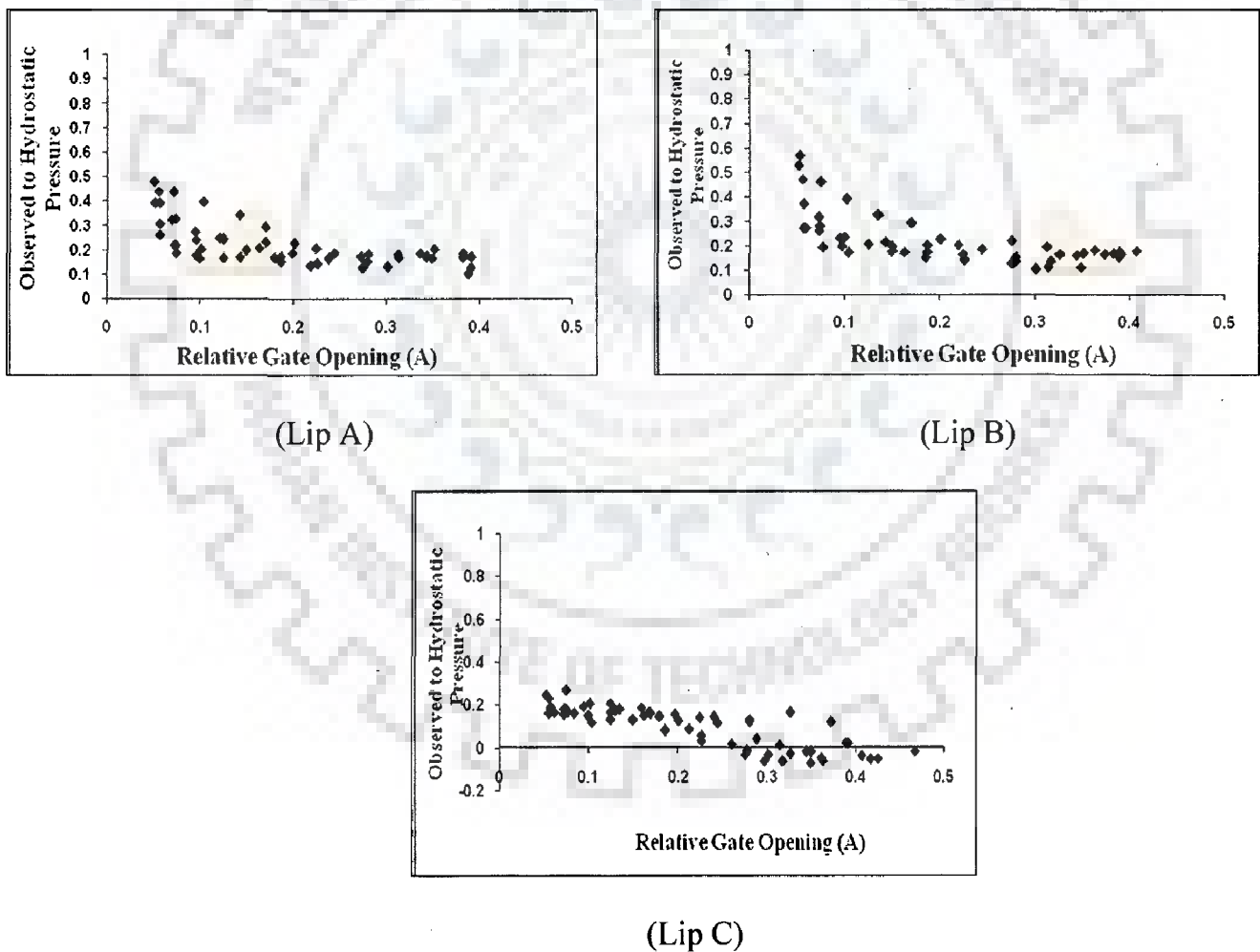
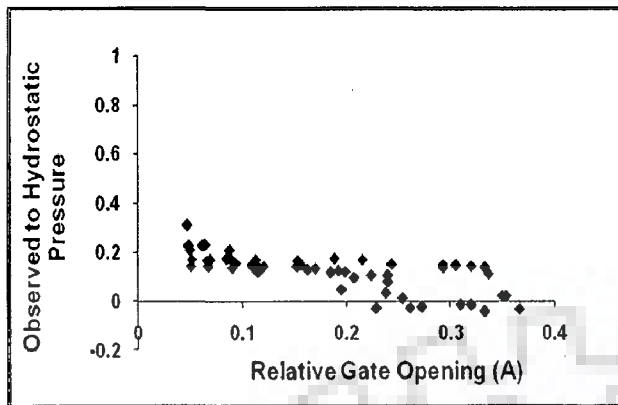
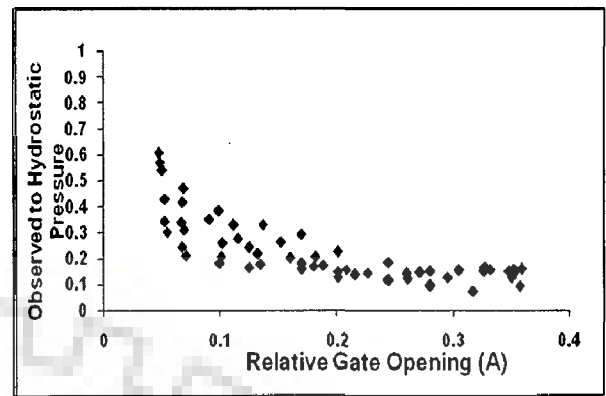


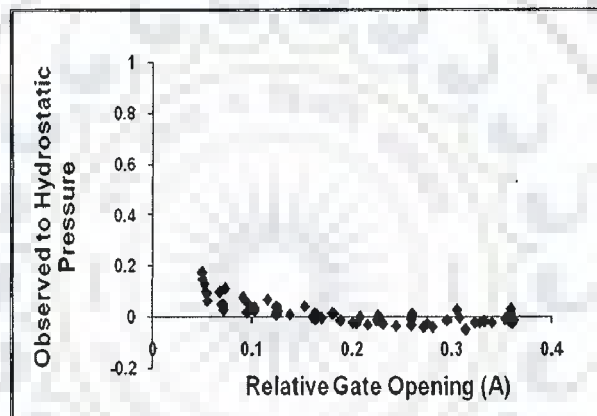
Fig. 5.1a Observed to Hydrostatic Pressure vs. Relative gate Opening



(Lip D)



(Lip E)



(Lip M)

**Fig. 5.3b Graphical Plot of Observed to Hydrostatic Pressure vs. Relative gate Opening for lip types D, E and M**

A comparison of Figs. 5.1-5.3 indicates that increasing the slope of the upstream face helps in reducing the observed pressure on the lip. For example, for lip shape C, the ratio of observed to hydrostatic pressure is close to 0.4 at smaller relative gate opening in Fig. 5.2 a, whereas it is below 0.3 in case of Figs. 5.1 a and 5.3 a. As Figs. 5.1a and 5.3a pertain to situations where slope of upstream face is steeper than that for Fig. 5.2a, the increase in the slope of upstream face is certainly supported. However, Fig. 5.1a and 5.3a indicates that there is not much reduction in pressures if upstream face slope is changed from 1H:3V to vertical.

Comparative evaluations of performance of different lip types in terms of pressure variations indicated the better performance of lip C. Although the lip D appears to work better in terms of pressure, however, it is not good in terms of discharge. Further, for a given gate thickness, lip D has a longer lip length. A longer length will also mean more hydrostatic pressure. In case of lip C, lip length is same as gate width. Thus, in case of lip C, a lesser hydrostatic pressure will exist on the gate than in case of lip type gate D.

#### 5.2.1.4 Plane bed

As lips C and D did better in terms of pressure distribution in case of raised crest, performance of only these two lip shapes are reported here. In case of plane bed, profile M was also excluded from experimentation as the literature indicated existence of non-uniform pressure distribution on the gate bottom and thus, lip type M is more prone to creating vibration of the gate which is undesired due to instability. Thus, for lips C and D, variation of observed to hydrostatic pressure is shown in Fig. 5.4 a and Fig. 5.4b.

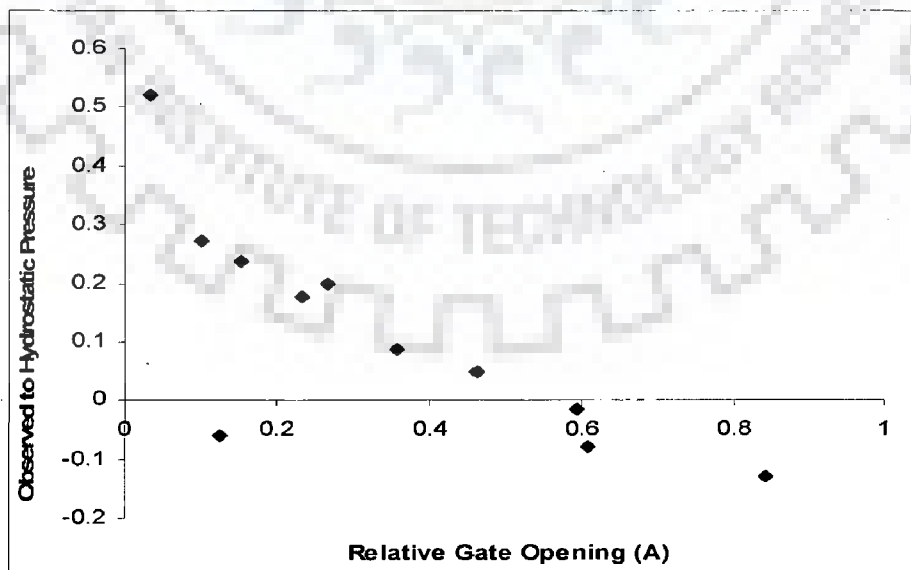


**Fig. 5.4a: Variation of pressure ratio for lip C on a gate located above flat bed.**

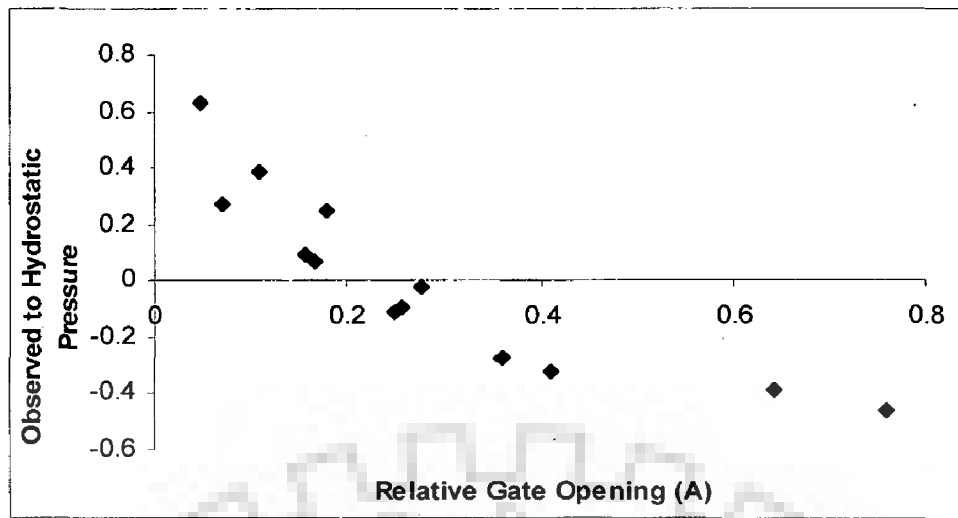


**Fig. 5.4b Observed to Hydrostatic Pressure vs. Relative gate Opening for lip D**

A comparative evaluation of Figs. 5.4 a and b only reveals the better performance of lip C than lip D.

### 5.3 USE OF OTHER DIMENSIONLESS VARIABLES IN PRESSURE PLOTS

#### 5.3.1 Critical Depth Based Dimensionless Terms

Ansar and Chen (2009) used two depth terms to express the variation of discharge. These depth terms are represented as  $y_{c1}$  and  $y_{c2}$  and can be expressed as:

$$y_{c1} = \left( \frac{Q}{B\sqrt{g}} \right)^{1/3} \quad (5.1)$$

In eq. 5.1, Q is the discharge, B is the width of gate and g is the acceleration due to gravity.

$$y_{c2} = D^{2/3} (h_0 - z_0)^{1/3} \left( c_1 + c_2 \frac{D}{h_0 - z_0} \right) \quad (5.2)$$

In eq.5.2,  $h_0$  is the upstream water depth with respect to lip of weir,  $z_0$  is the height of the weir crest,  $c_1=0.91$  and  $c_2=0.28$ . D is expressed as

$$D = \min(a, h_0 - z_0) \quad (5.2a)$$

The critical depth is a function of discharge and increases with increase in discharge. Thus, such a graphical representation provides the idea of the variation of discharge with increase in the critical depth; thus, it was assumed that this can be also a reasonable choice to study the variation of pressure. With this in consideration, dimensionless plots between observed to hydrostatic pressure are shown using two dimensionless terms  $y_{c1}/h_0$  and  $y_{c2}/h_0$ . As the objective is to see whether such plots are able to reduce the scatter, only plots in respect of lip type C are given. Figs. 5.5 and 5.6 show the variation of pressure ratio, with the use of  $y_{c1}/h_0$  and  $y_{c2}/h_0$ , respectively. Each of these Figures includes four types of bed conditions, as discussed earlier.

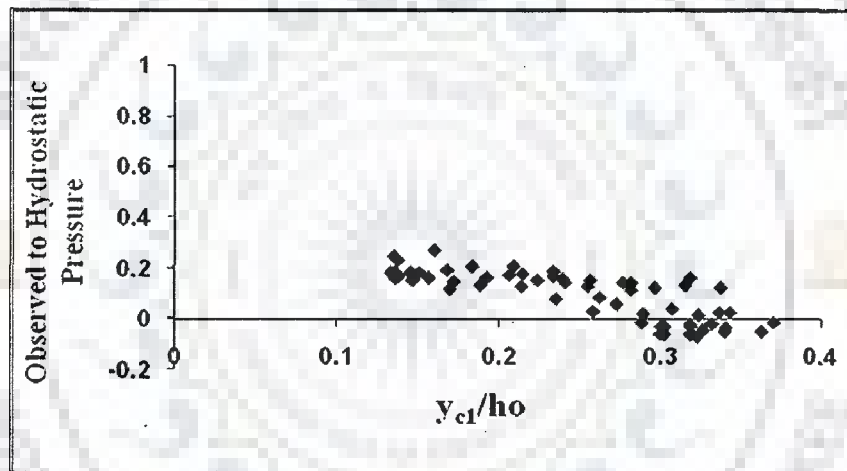
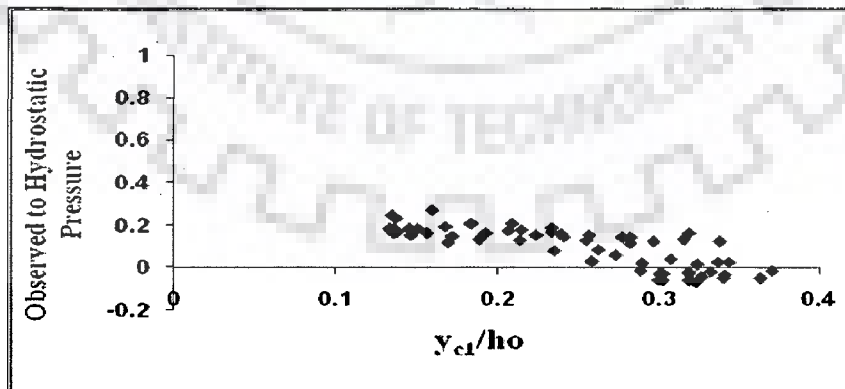


**Fig.5.5 a: Observed to hydrostatic pressure vs.  $y_{c1}/h_0$  for raised crest (1H:3V) for lip C**



(Lip C)

**Fig. 5.5b Graphical Plot of Observed to Hydrostatic Pressure vs.  $y_{c1}/h_0$  for raised crest (2H:3V) for lip C**

It can be seen from Fig. 5.1a that for lip A, the plot is initially scattered but converges as the relative gate opening area increases and the ratio of observed to hydrostatic pressure varies from 0.5 to 0.1. For lip B, the situation is similar to that for lip A. The initial value of relative gate opening sees an increase in the observed to hydrostatic pressure ratio which varies from 0.5 to 0.1. For lip C, the value of the pressure ratio remains below 0.3 throughout. Also, the pressure ratio attains a negative value with an increase in relative gate opening area value above 0.25. For other three lip types, i.e. D, E and M, the variation of observed to hydrostatic pressure is shown in Fig. 5.1 b.

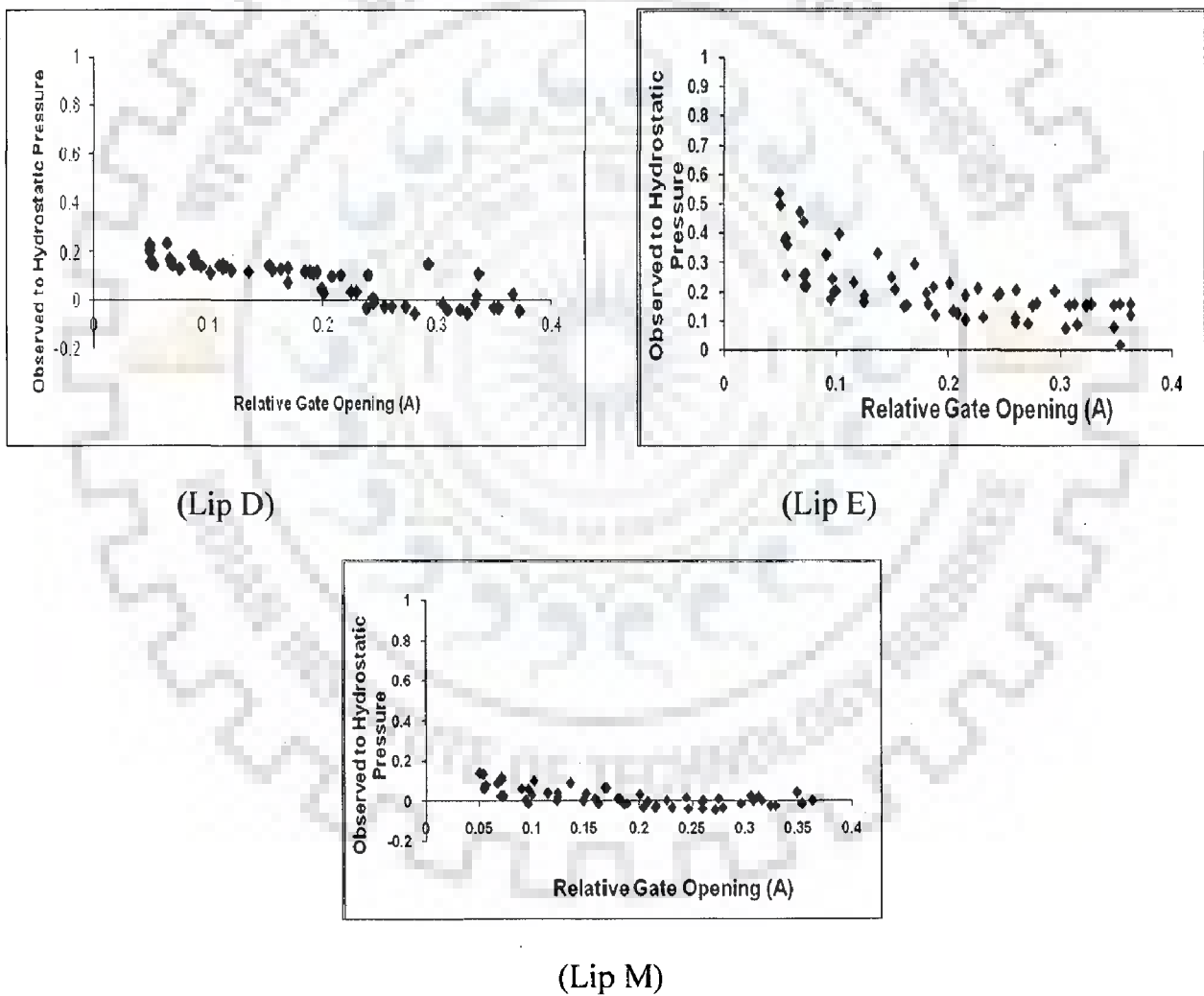
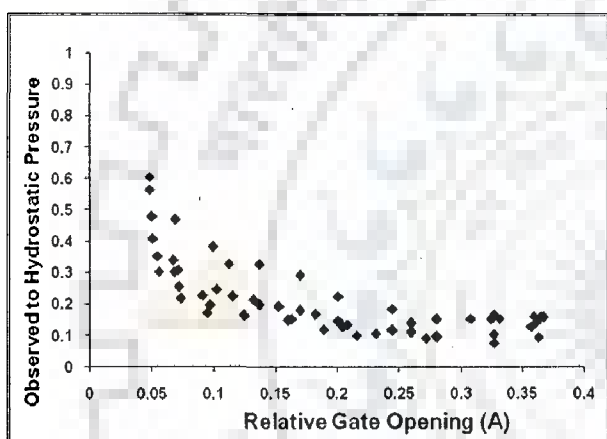


**Fig. 5.1b: Observed to Hydrostatic Pressure vs. Relative gate Opening for lip types D, E and M**

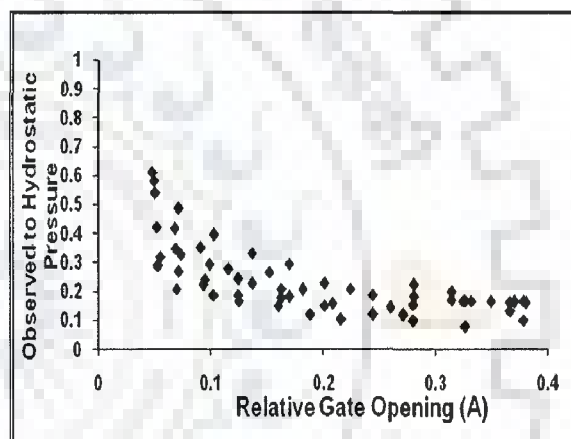
In lip D, the ratio of observed to hydrostatic pressure drop further when compared with lip C. Lip E experiences the values of pressure ratio below 0.6 but the values remain positive, though the plot has a scatter. In lip M, the observed to hydrostatic pressure values show less variation and remain within a range of  $\pm 0.20$ .

### 5.2.1.2 Raised crest (2H : 3V)

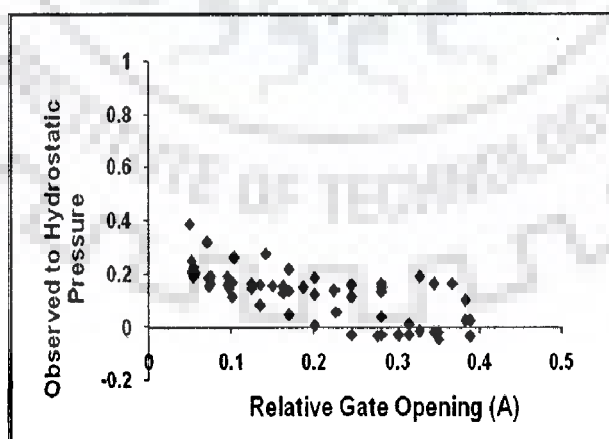
An upstream slope of ogee weir with 2H:3V slope indicates a milder slope than 1H:3V. To see the effect of this change in the upstream slope, the pressure distribution is shown for lip type A, B and C in Fig. 5.2a.



(Lip A)



(Lip B)



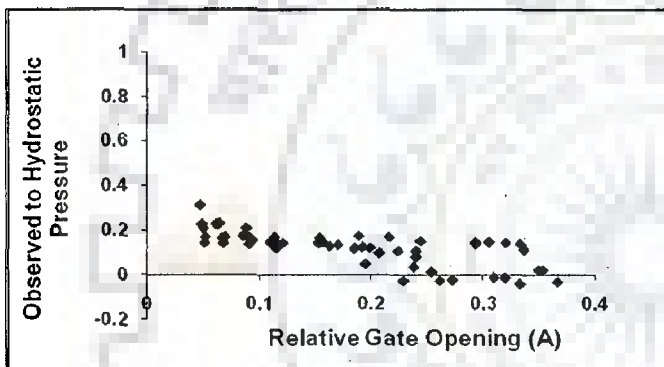
(Lip C)

**Fig. 5.2a Variation of Observed to Hydrostatic Pressure vs. Relative gate Opening for lip type A, B and C**

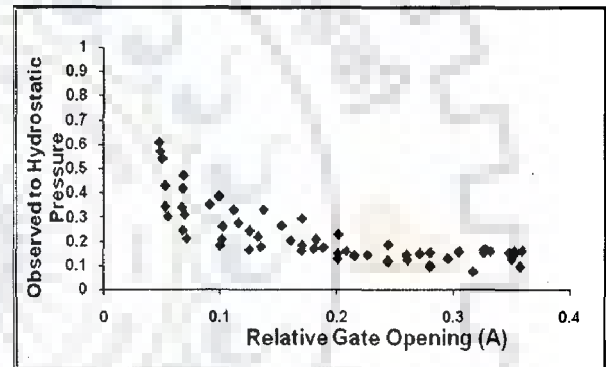


It can be seen from Fig. 5.2a that change in the upstream slope leads to an increase in the pressure on lips. For example, for Lip A, the initial value of the pressure ratio corresponding to lowest gate opening is increased from 0.5 to 0.65. Similarly, for Lip B, there is increase in the initial value from 0.6 to 0.656 and for Lip C from 0.3 to 0.4.

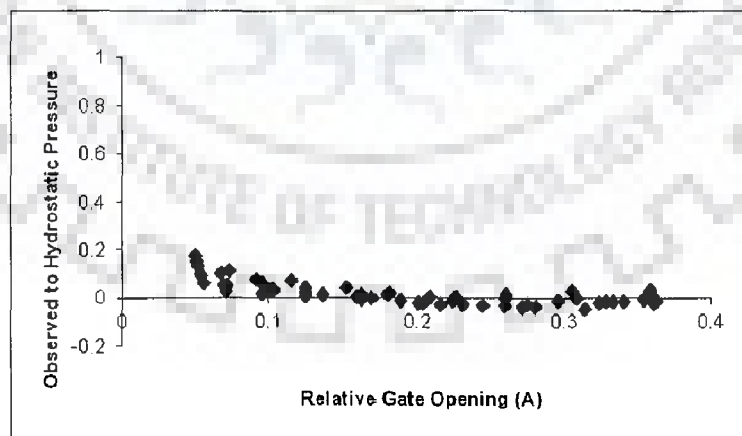
For lip types D, E and M, the corresponding plots are shown in Fig. 5.2 b. A comparison between Figs. 5.1 b and 5.2 b indicates that for lip D, again the slope reduction of the upstream face of the ogee leads to an increase in the pressure. This is further supported by variation shown for lip E. However, for lip M, there is not much difference between values of pressure ratio for Figs. 5.1 b and 5.2 b.



(Lip D)



(Lip E)



(Lip M)

**Fig. 5.2b : Variation of pressure ratio for lip D, E and M with upstream face slope of 2H:3V**

### 5.2.1.3 Raised crest (Vertical)

From the preceding sections, it has been seen that change of the slope of the upstream face affects the pressure on a lip. Just to probe further, a third situation where the upstream face of the weir is kept vertical was considered. The main consideration in such experimentation was to see if further pressure reductions are possible.

Thus, pressure variations are shown for different lip types, as shown in Figs. 5.3a and 5.3b.

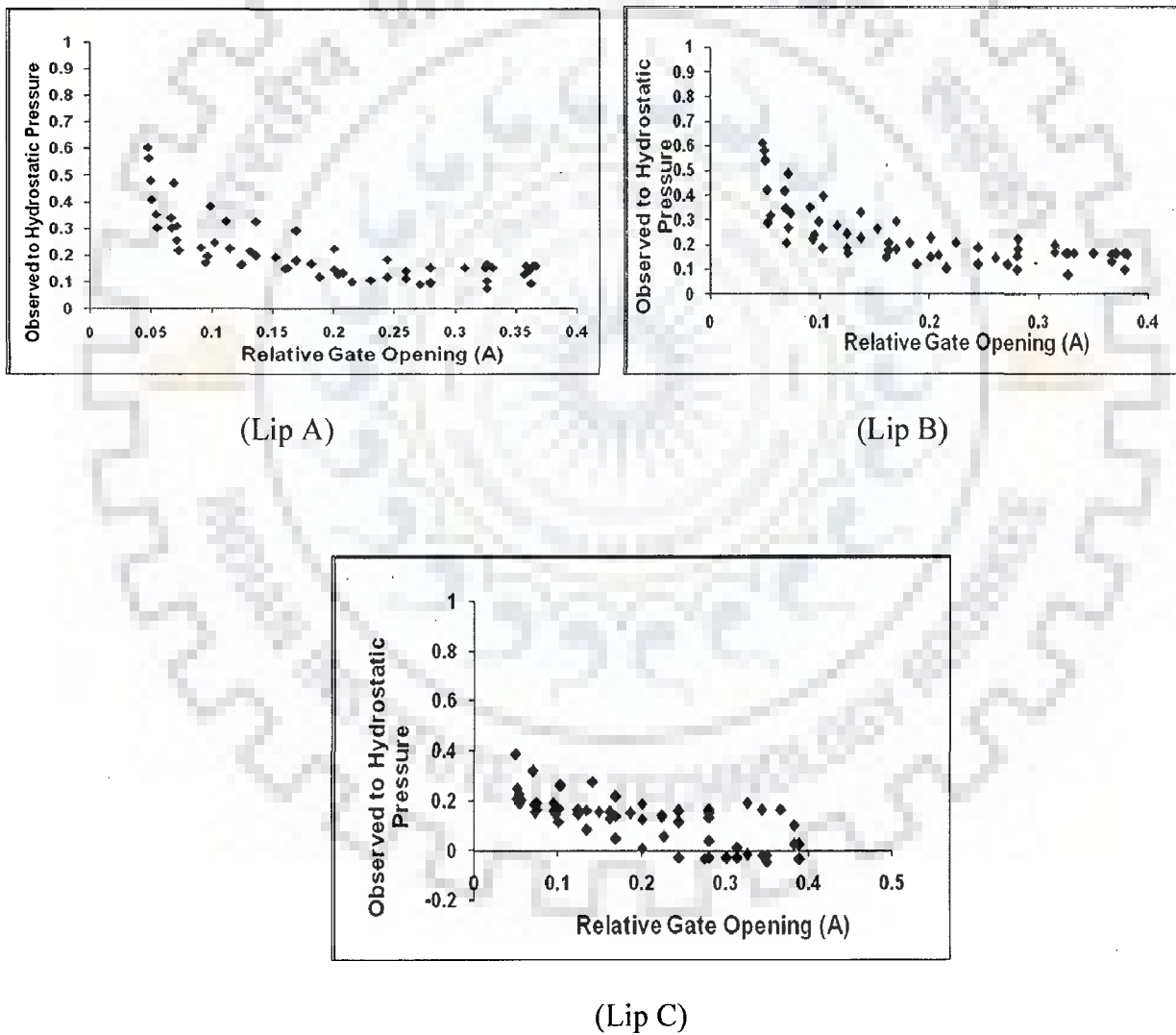
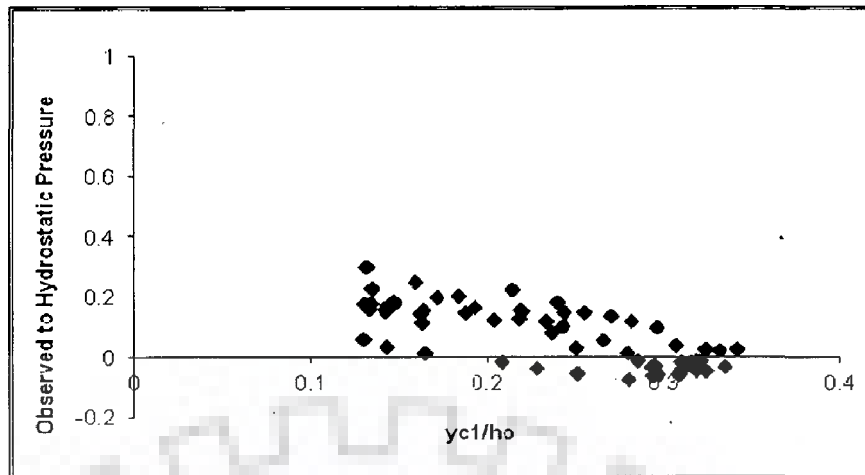


**Fig. 5.3a Graphical Plot of Observed to Hydrostatic Pressure vs. Relative gate Opening for lips A, B and C.**



(Lip C)

**Fig. 5.5c: Observed to Hydrostatic Pressure vs.  $y_{c1}/h_0$  for raised crest(vertical) for lip C**

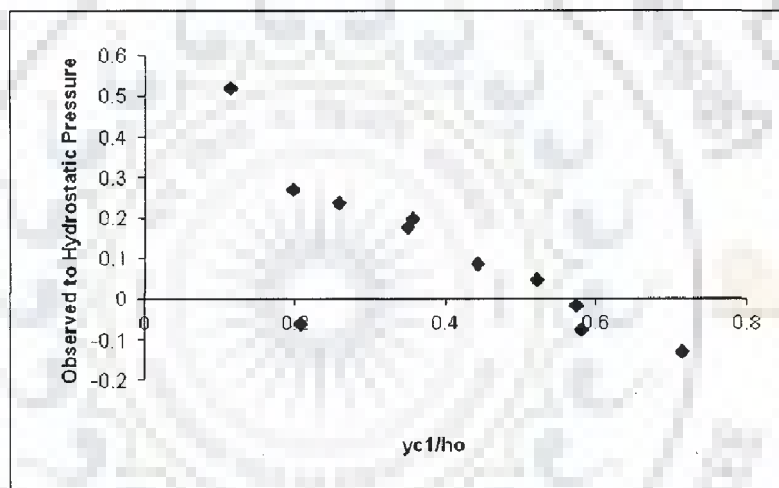
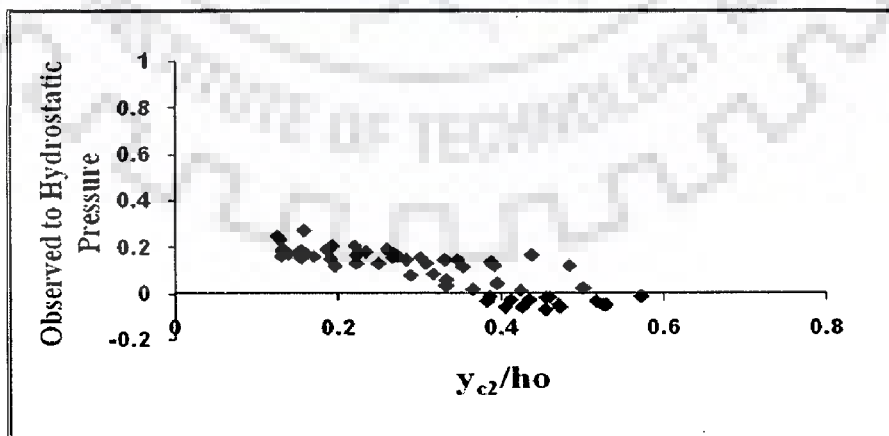


**Fig. 5.5d: Observed to Hydrostatic Pressure vs.  $y_{c1}/h_0$  for plane bed and lip C**



(Lip C)

**Fig. 5.6a: Observed to Hydrostatic Pressure vs.  $y_{c2}/h_0$  for raised crest (1H:3V) and lip C**

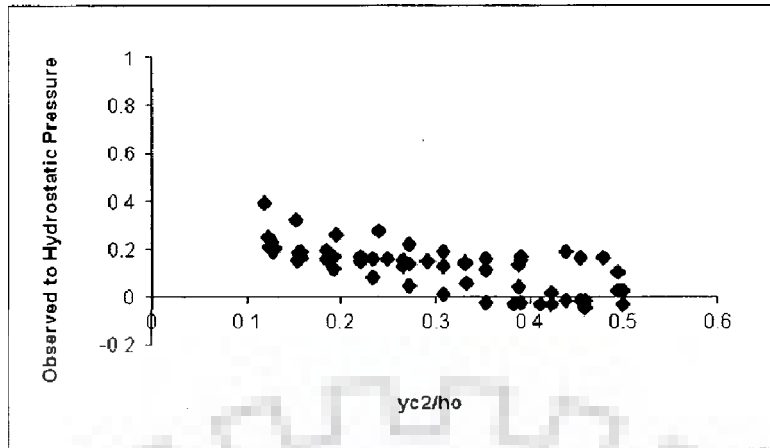


**Fig. 5.6 b: Observed to Hydrostatic Pressure vs.  $y_{c2}/h_0$  for raised crest (2H:3V) and lip C**

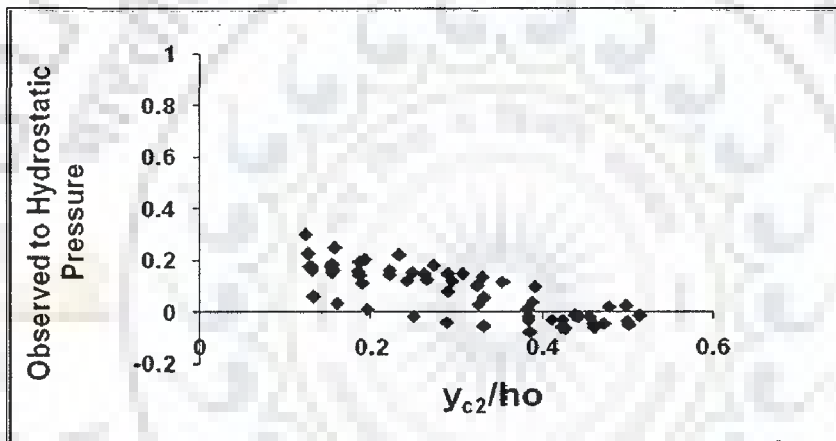
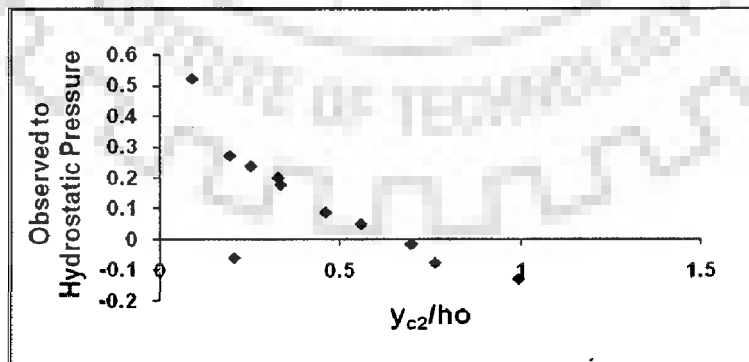


**Fig. 5.6 c: Observed to Hydrostatic Pressure vs.  $y_{c2}/h_0$  for raised crest (vertical) and lip C**



**Lip C**

**Fig. 5.6d: Observed to Hydrostatic Pressure vs.  $y_{c2}/h_0$  for flat bed and lip C**

### 5.3.2 Specific Energy Based Dimensionless Term

It is shown in the literature that the bottom pressure below the gates follows a liner variation between 'p/γa' and 'E/a'. Here p is the pressure, a is the gate opening and E is the upstream specific energy defined as

$$E = h_0 + \frac{v_0^2}{2g} \quad (5.3)$$

In eq. 5.3 ,v<sub>0</sub> is the velocity corresponding to flow rate Q and the flow depth h<sub>0</sub>

When  $\frac{v_0^2}{2g}$  is small, Eq. 5.3 can be approximated as

$$E = h_0 \quad (5.4)$$

For the linear variation between  $\frac{p}{\gamma a}$  and  $\frac{E}{a}$ , as shown in Fig. 9 of Montes (1997), one can write the following expression.

$$\frac{p}{\gamma a} = \alpha_1 + \alpha_2 \frac{E}{a} \quad (5.5)$$

From Eq. 5.4 and 5.5, one has

$$\frac{p}{\gamma h_0} = \alpha_1 \frac{a}{h_0} + \alpha_2 a \quad (5.6)$$

The left hand side in Eq. 5.6 indicates the ratio of observed to hydrostatic pressure as  $\alpha_1$  and  $\alpha_2$ , which are shown to be positive for flat bed and flat gate bottom. Thus, the use of the plot between the ratio of observed to hydrostatic pressure versus dimensionless energy term can also convert to ratio of pressure versus relative gate opening plot if  $\alpha_2$  is zero.

The purpose of the above analysis is just to indicate some commonality between the use of relative gate opening vis a vis E/a as an abscissa to relate the ratio of observed to hydrostatic

pressure. To have an idea about the trend of variation for different bed conditions, lip C has been considered.

Figs. 5.7a-d present the plots between ratio of observed to hydrostatic pressure versus  $E/a$  for raised crest type 1H:3V, 2H:3V and vertical and flat bed.

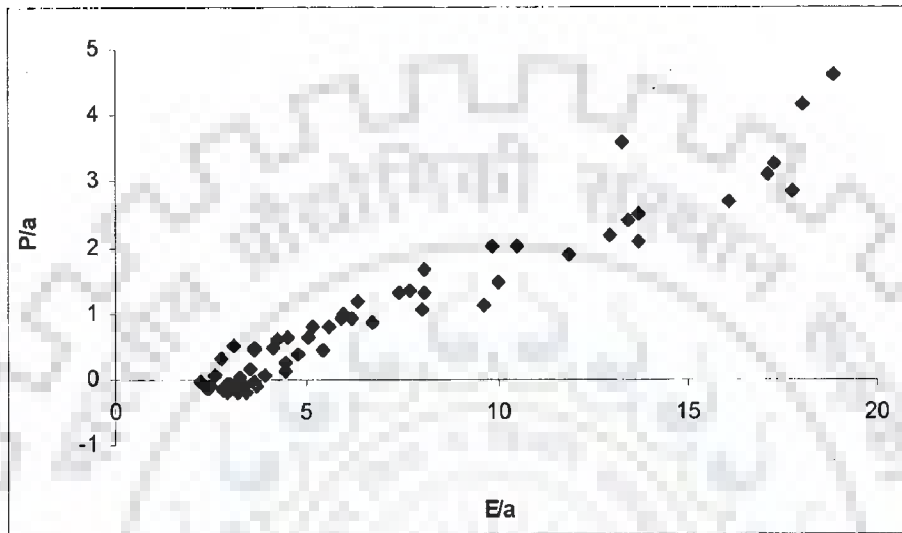


Fig. 5.7a: Ratio of observed to hydrostatic pressure versus  $E/a$  for lip C and for raised crest type 1H:3V.

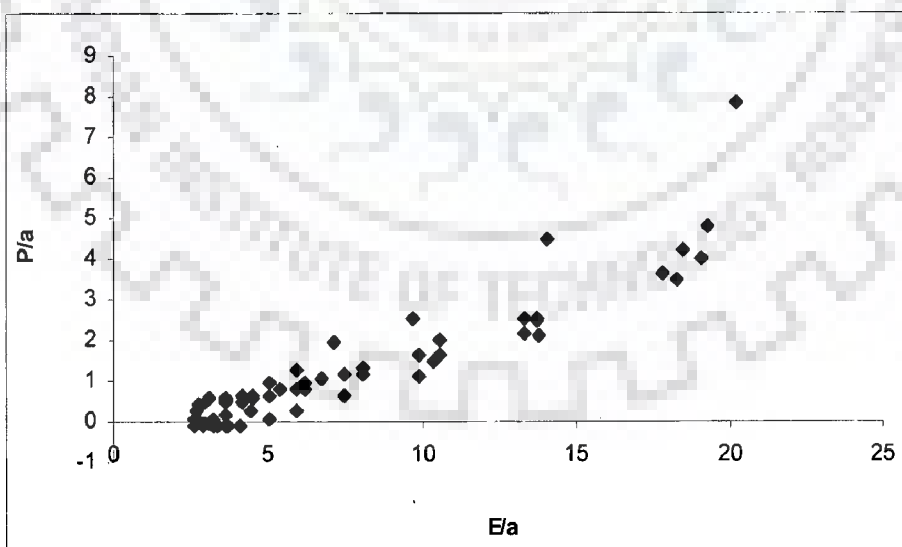


Fig. 5.7 b: Ratio of observed to hydrostatic pressure versus  $E/a$  for lip C and for raised crest type 2H:3V.

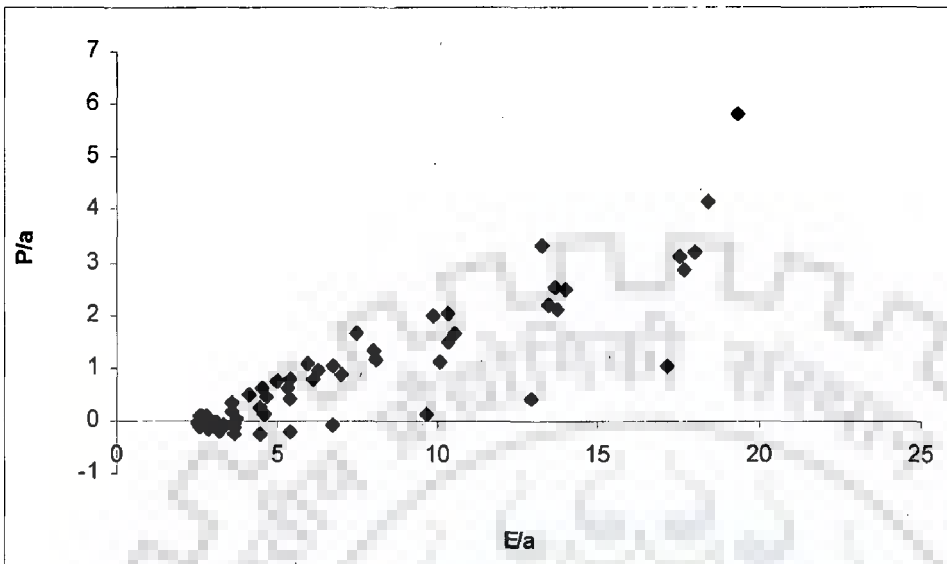


Fig. 5.7c: Ratio of observed to hydrostatic pressure versus  $E/a$  for lip C and for raised crest type vertical .

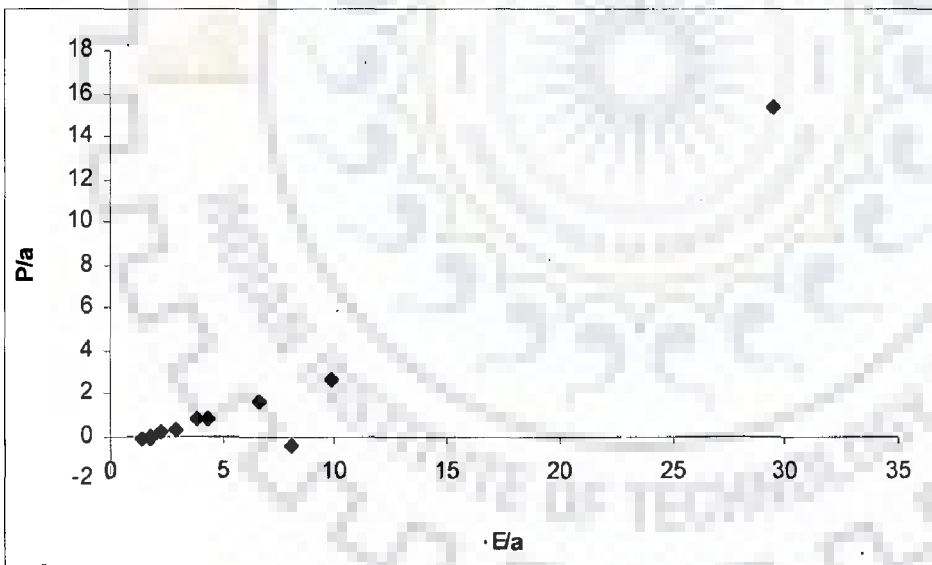


Fig. 5.7d: Ratio of observed to hydrostatic pressure versus  $E/a$  for lip C for plane bed.

From Figs. 5.7a-d, one can observe that in general, the variations are non-linear for raised crest while the variation between pressure ratio term and  $E/a$  is linear for plane bed. Literature also

indicates that for flat bed and flat lip shape, negative values of  $p$  are not present (Montes, 1994). Thus, occurrence of negative values is only due to lip effect.

#### 5.4 UNIFORMITY OF PRESSURE VARIATION

Uniformity of pressure distribution has been viewed as one of the important criteria to select lip shape. If the pressure deviates from average pressure, this also signifies that gate will experience more vibration because of non-uniform pressure distribution along the lip base. With this in view, certain uniformity diagrams are presented in terms of a factor  $K_B$  defined as:

$$K_B = 2(h_o - h)/(\rho v_o^2) \quad (5.7)$$

Where  $h_o$  = Hydrostatic Pressure Head;

$h$  = Observed Pressure Head;

$\rho$  = Density of water and

$v_o$  = Velocity of water in the flume

The units of  $K_B = m^2 s^2 / kg$  It can be converted to dimensionless  $k_B$  where  $k_B = \rho g K_B$



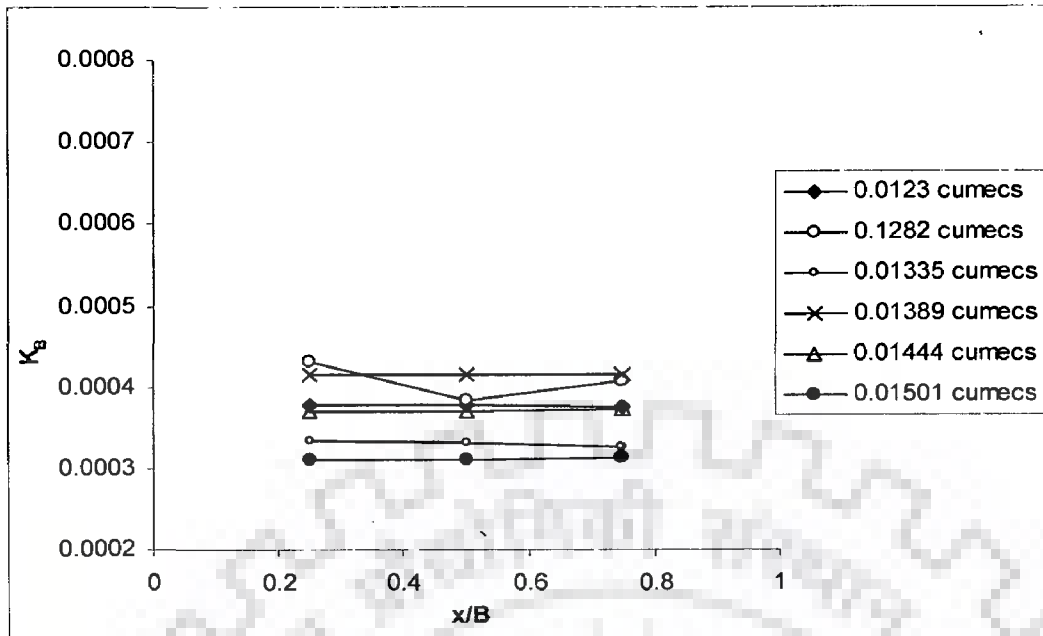


**Fig. 5.8a: Variation of  $K_B$  for lip C for a raised crest (1H:3V)**

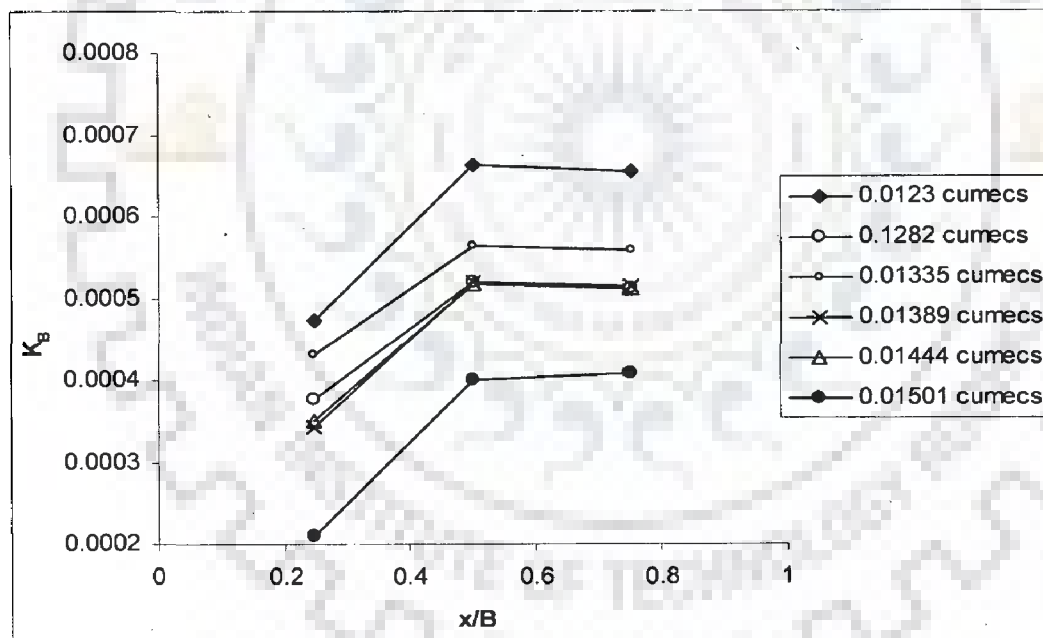


**Fig. 5.8b: Variation of  $K_B$  for lip M for a raised crest (1H:3V)**

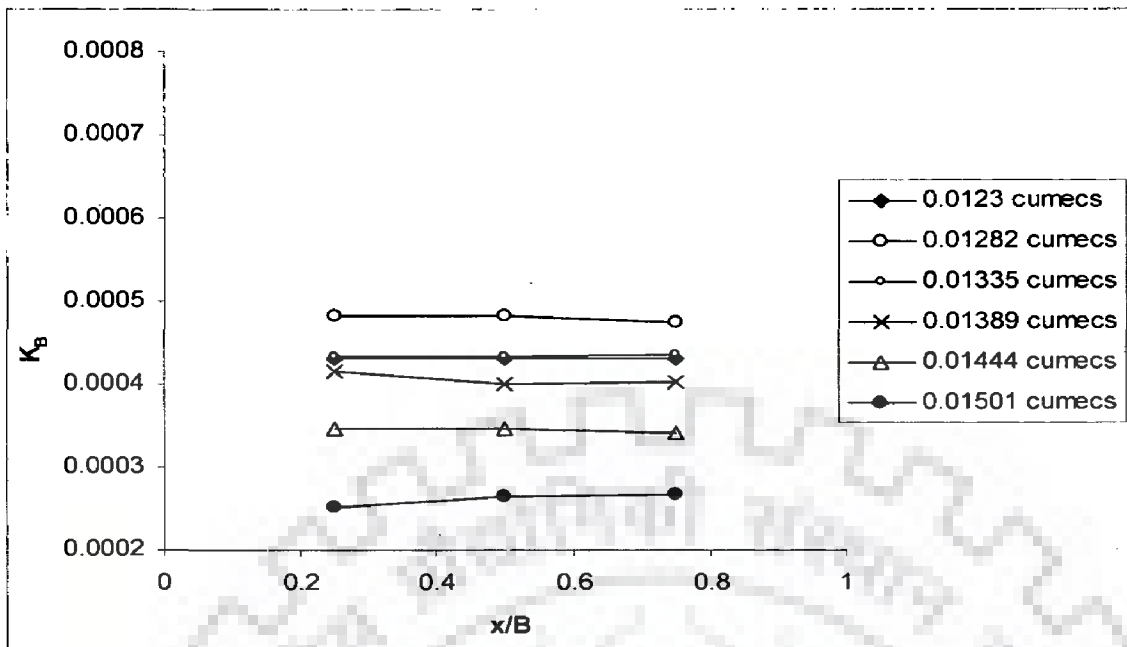


**Fig. 5.8c: Variation of  $K_B$  for lip C for a raised crest (2H:3V)**

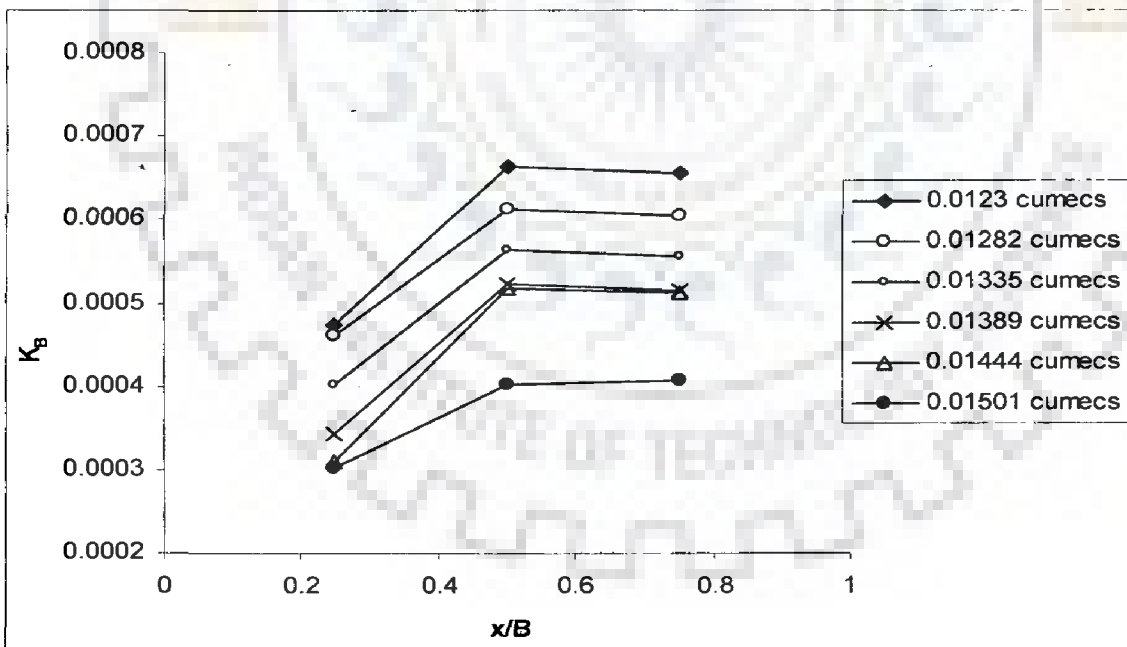


**Fig. 5.8d: Variation of  $K_B$  for lip M for a raised crest (2H:3V)**

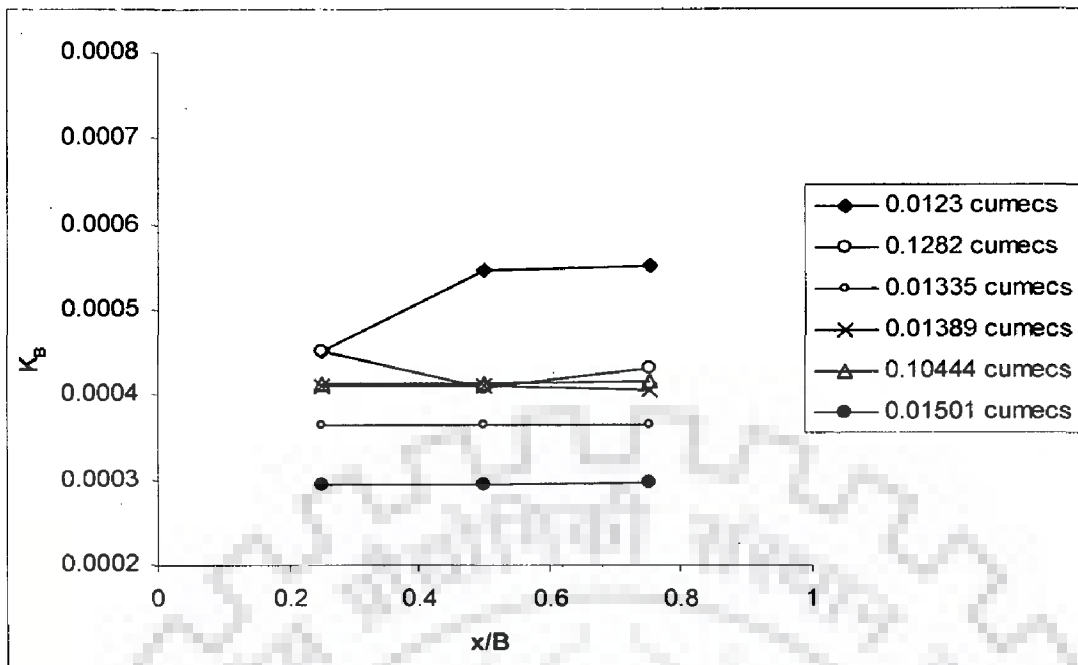


**Fig. 5.8e: Variation of  $K_B$  for lip C for a raised crest (Vertical)**

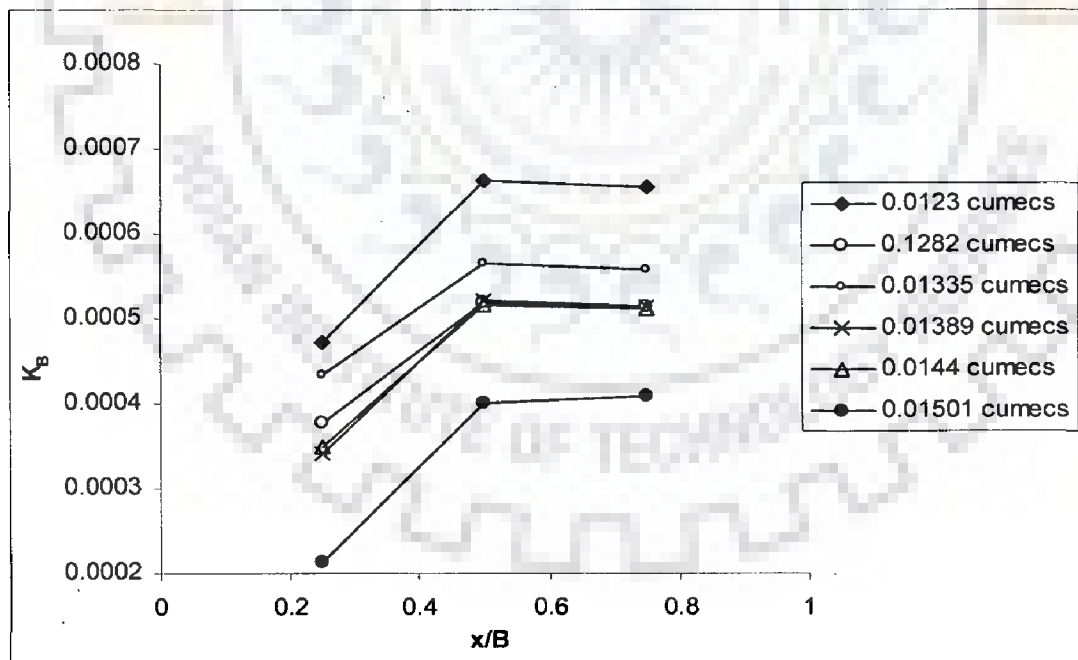


**Fig. 5.8f: Variation of  $K_B$  for lip M for a raised crest (Vertical)**

All the above uniformity diagrams, as given in Fig. 5.8a-f, suggest that lip C experiences in general uniform pressure along the lip base and for this reason, if pressure variation is accepted as a sole criteria to select suitable non-stream lined lip type, one can favor the lip C as a desirable lip type.

## 5.5 SUMMARY

Evaluation of six non-stream lined lip types is done when these lips are attached to the gate bottom. For different types of bed conditions, it is observed that lip type C which has same lip width as lip length is the best performing lip considering the uniformity of pressure distribution along the lip base as well as magnitude of pressure. The pressures on lip are observed to be influenced by the bed conditions below the gate. Bed with ogee profile having upstream face slope as 1H:3V achieves lesser pressure in comparison to the the bed with ogee profile having steeper upstream face slope. Use of pressure to gate opening ( $a$ ) versus upstream specific energy ( $E$ ) to gate opening diagram seems no more linear, as was perceived in the literature for flat beds and flat gate bottom. A linkage between the ratio of observed to hydrostatic pressure versus relative gate opening as well as between the ratio of observed to hydrostatic pressure versus  $E/a$  is also established

---

**DISCHARGE CHARACTERISTICS OF STREAMLINED LIP SHAPES**

---

**6.1 INTRODUCTION**

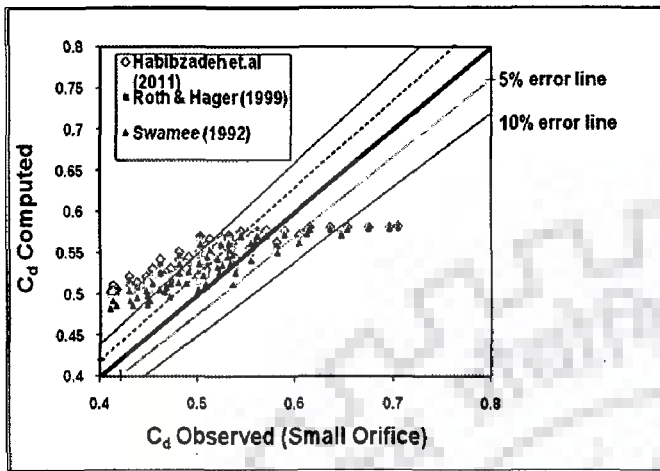
Use of streamlined shapes has found lot of attention in the literature. The existing perception is that such lip shapes allow a smooth passage of flow and therefore these shapes may help in reducing the losses. This may be helpful in increasing the discharge for a given operating head and gate opening. In view of this, eight type of stream lined shapes are considered for gate located over four type of bed including raised crest (1H: 3V), raised crest (2H: 3V), raised crest (with upstream vertical face), and flat bed. The variation of discharge coefficient has been plotted against various parameters to identify the dependence of discharge coefficient on bed and lip types.

**6.2 VARIATION OF DISCHARGE COEFFICIENT**

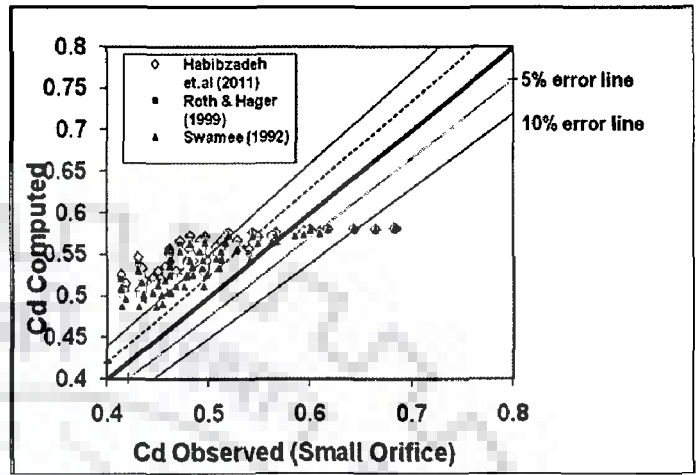
The computation of discharge coefficient can be done either using a small orifice formula or large orifice formula, as described in Chapter 4. To see the effectiveness of the small as well as large orifice formula agreement diagram were developed for different type of lip shapes and bed condition. The presentation in this section is organized as follows.

**6.2.1 Use of Small Orifice Formula**

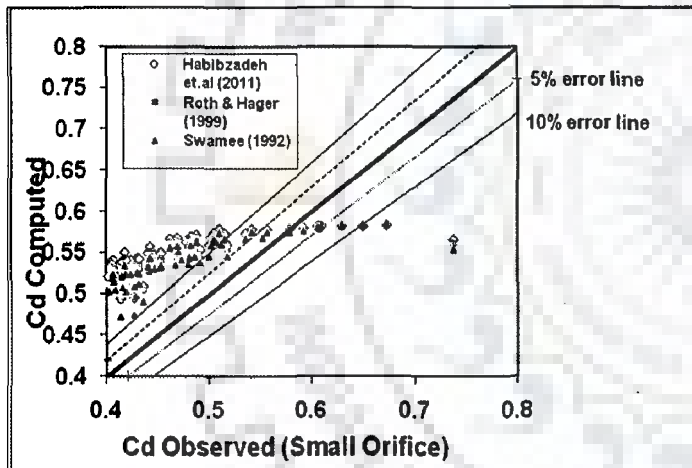
Using small orifice formula, the agreement diagrams using Habibzadeh et al. (2011), Roth and Hager (1999) and Swamee (1992), for raised crest (1H: 3V) is presented for eight streamlined types i.e. lip F, G, H, I in Fig. 6.1a and lip type J, K, L and N in Fig. 6.1 b. Similarly, Figs. 6.1c and 6.1d show the agreement using Ansar and Chen(2009) and Alhamid (1999) for lip types F,G,H and I, and for lip shapes J,K,L and N, respectively.



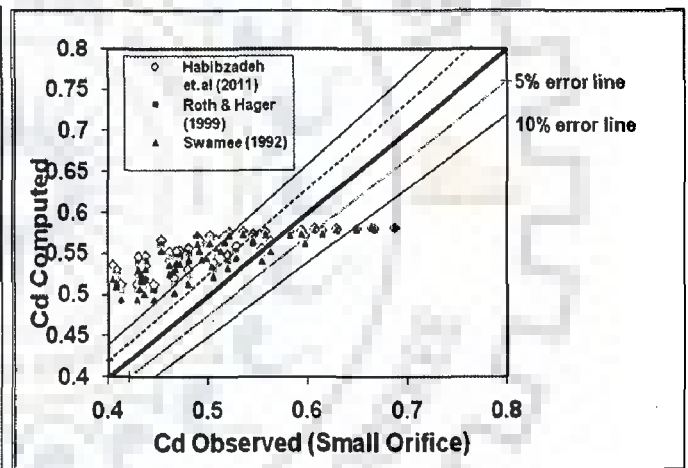
Lip F



Lip G

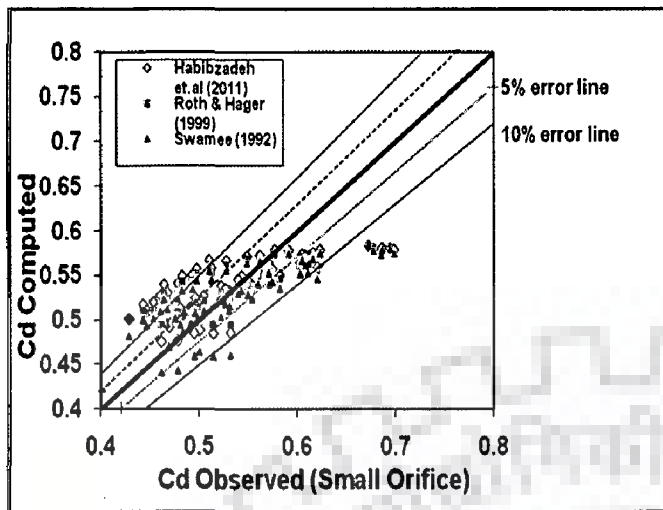


Lip H

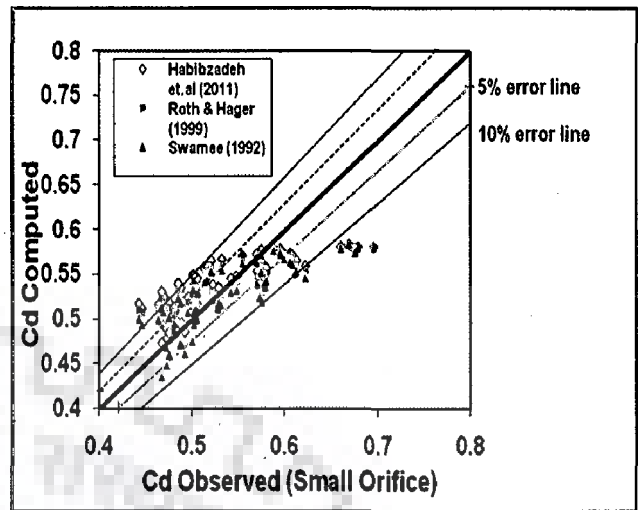


Lip I

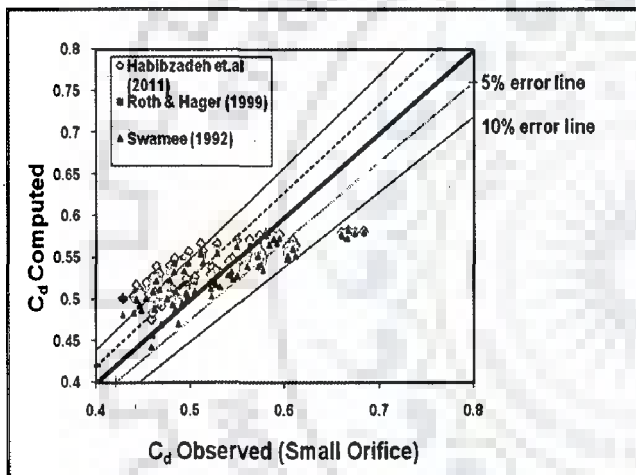
Fig. 6.1 a: Agreement between observed and computed discharge coefficient using small orifice formula for different lip types F, G, H, and I in a gate located over a weir of upstream slope 1H:3V



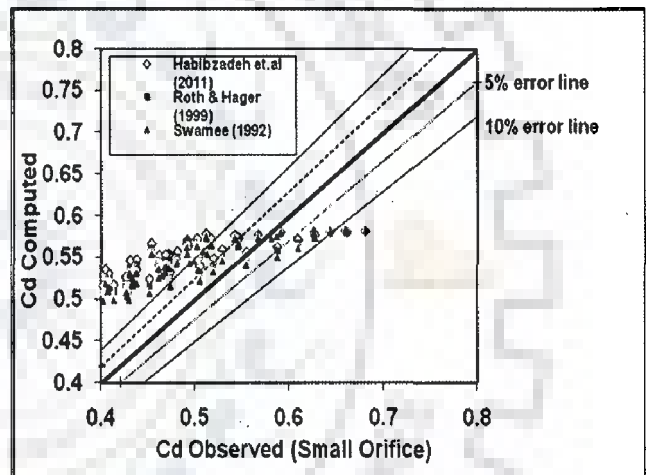
Lip J



Lip K

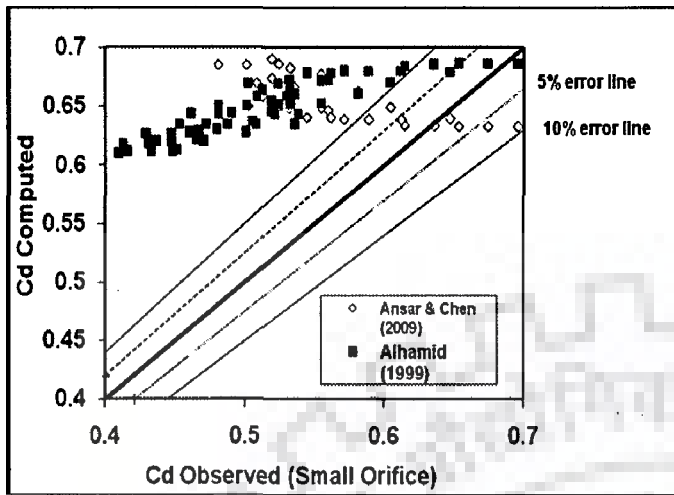


Lip L

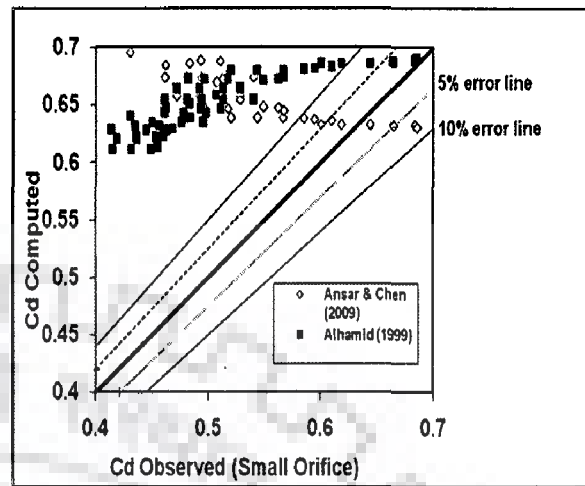


Lip N

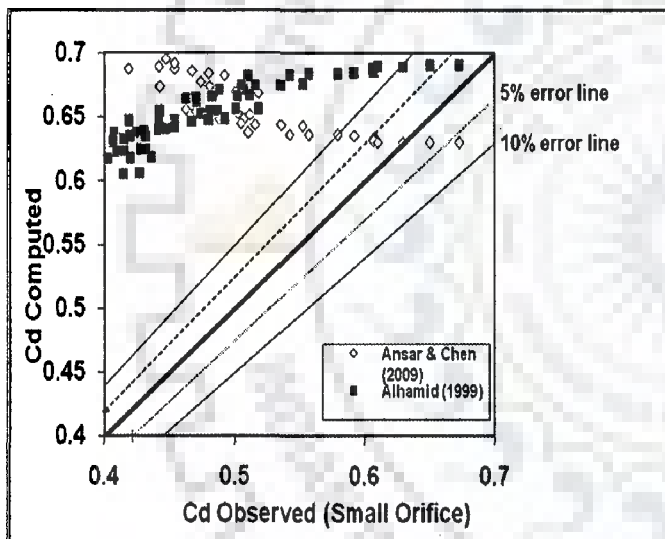
Fig. 6.1 b: Agreement between observed and computed discharge coefficient using small orifice formula for different lip types J,K,L,and N in a gate located over a weir of upstream slope 1H:3V



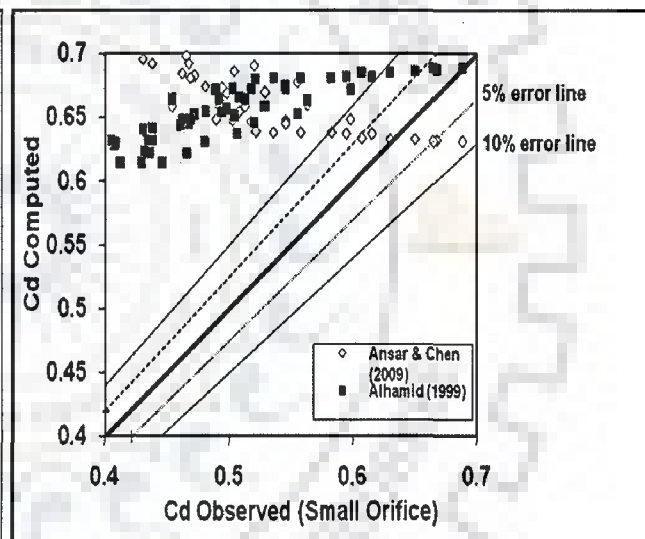
Lip F



Lip G



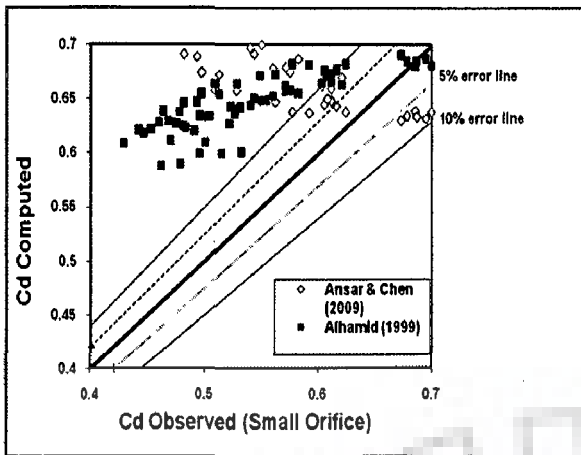
Lip H



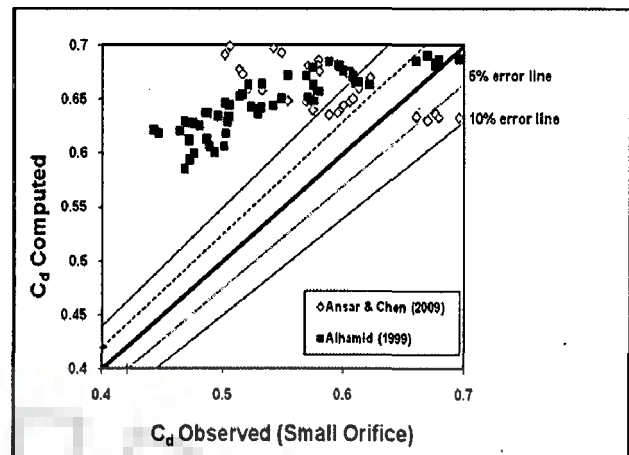
Lip I

Fig. 6.1 c: Agreement between observed and computed discharge coefficient using small orifice formula for different lip types F,G, H and I in a gate located over a weir of upstream slope 1H:3V

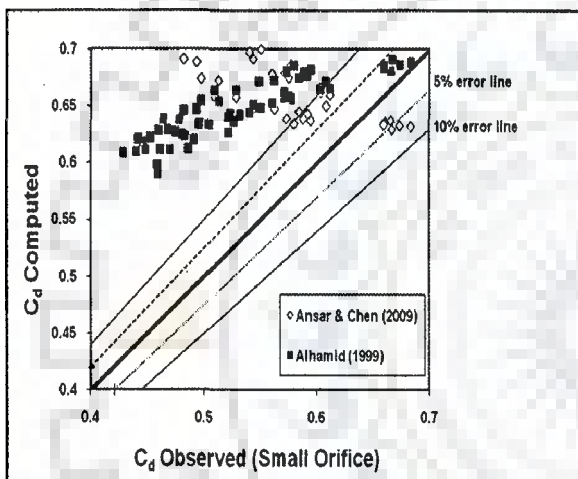




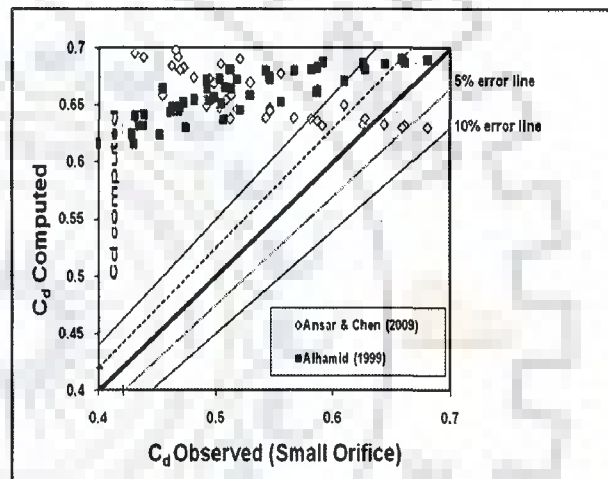
Lip J



Lip K



Lip L



Lip N

Fig. 6.1 d: Agreement between observed and computed discharge coefficient using small orifice formula for different lip types J,K,L and N in a gate located over a weir of upstream slope 1H:3V

It is again observed that  $C_d$  values computed using Ansar and Chen (2009) and Alhamid (1999) do not show good agreement with the observed  $C_d$ . Also, the performance of Ansar and Chen (2009) and Alhamid(1999) are inferior to those computed using Habibzadeh et al. (2011), Roth and Hager (1999) and Swamee (1992). Similar analysis is done for raised crest (2H: 3V), raised

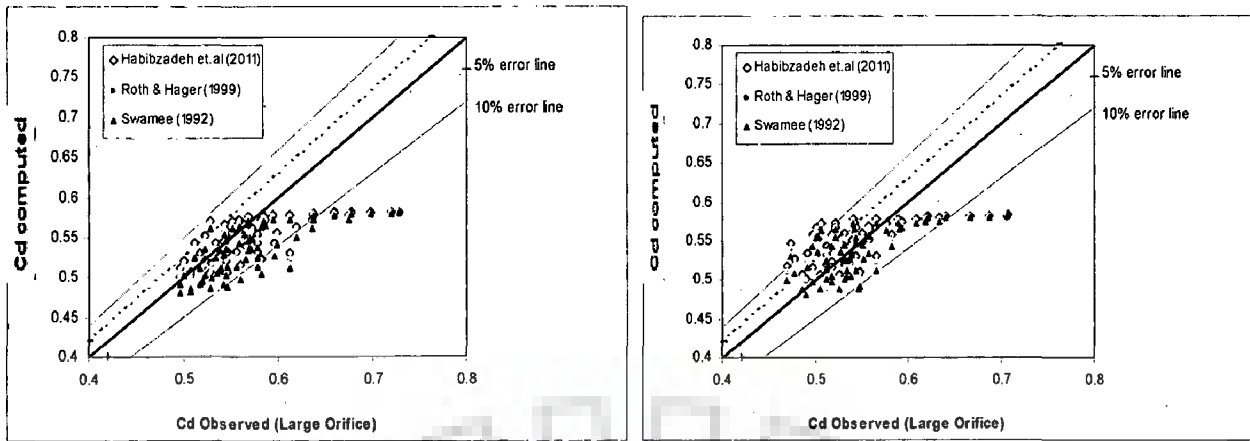
crest (upstream face vertical) and for plane bed. These agreement diagrams are given in the appendix attached in C.D. form with the present thesis.

### 6.2.2 Use of Large Orifice Formula

The agreement diagram between computed and observed  $C_d$  is shown for eight lip shapes and raised crest (1H: 3V). Fig 6.2a shows the agreement diagram for lip F,G,H and I using three approaches Habibzadeh et.al(2011),Roth and Hager (1999) and Swamee(1992) . Again, many values are found to deviate from the error band width of  $\pm 10\%$ . However, when compared with Fig 6.1.a, it can be seen that the agreements have been relatively better when large orifice formula is used.

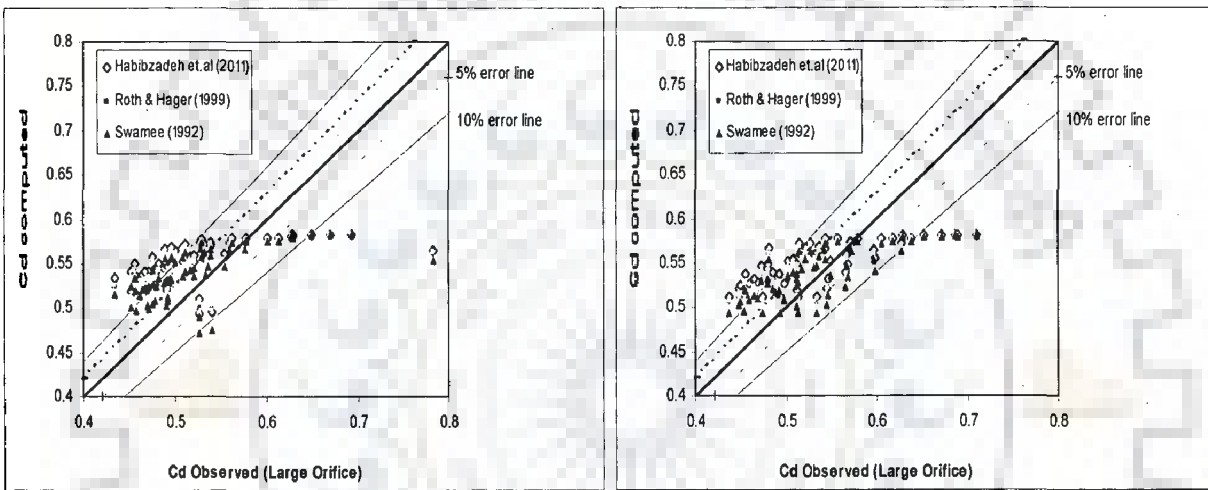
A comparison between Figs. 6.1.b and 6.2.b again indicates that large orifice formula has a tendency to shift the points below the line of perfect agreement, particularly in lip J,K and L. For lip N only few points deviate from the  $\pm 10\%$  error band width . For example for lip J, K, L, Swamee relationship predicts low values of discharge coefficient in the lip types used in Fig 6.2.b.

Fig 6.2.c helps in assessing the merit of Ansar and Chen (2009) and Alhamid (1999) relationship for lip type F, G, H and I. It can be seen that for lip F when the  $C_d$  observed lies in the range of 0.5 to 0.6, the  $C_d$  computed using Ansar and Chen and Alhamid relationship lies between 0.6 to 0.8. Thus, these relationships overestimate the value of discharge coefficient. Similar trend is observed for other lip types G, H, and I.



**Lip F**

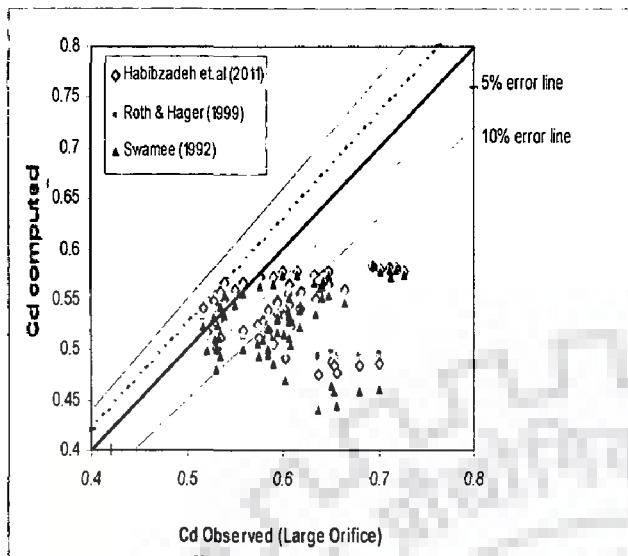
**Lip G**



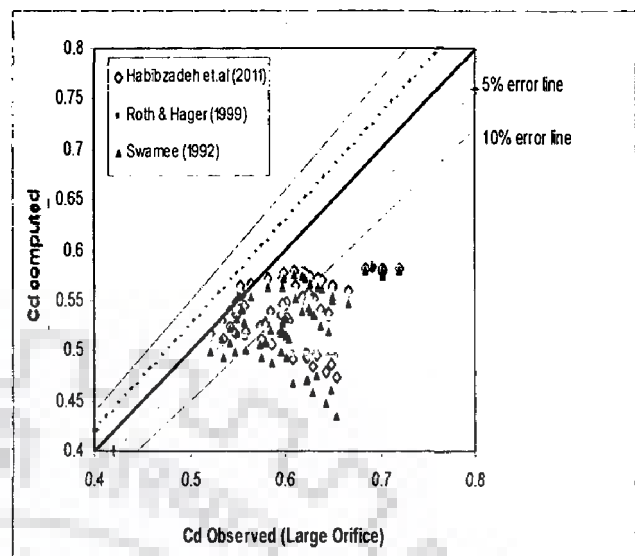
**Lip H**

**Lip I**

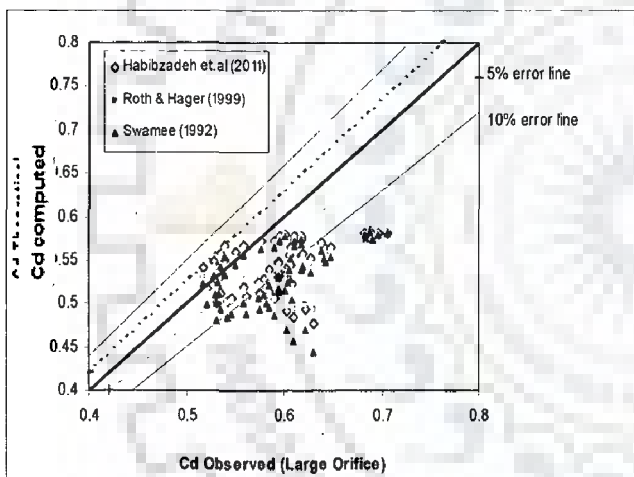
Fig. 6.2 a: Agreement between observed and computed discharge coefficient using Large orifice formula for different lip types F,G,H and I in a gate located over a weir of upstream slope 1H:3V



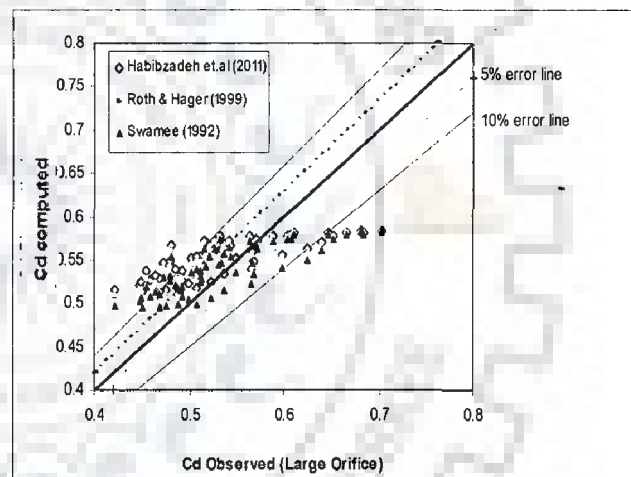
**Lip J**



**Lip K**

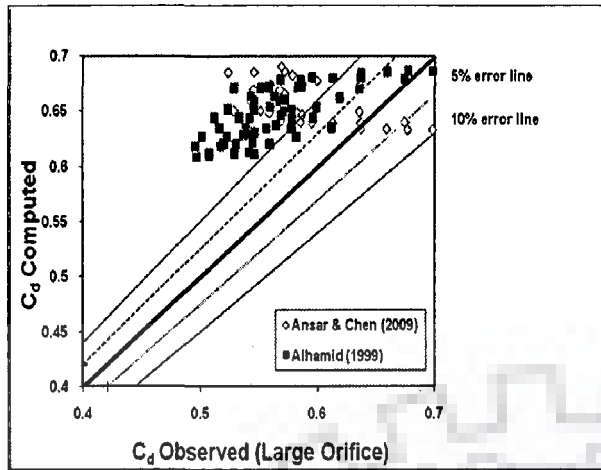


**Lip L**

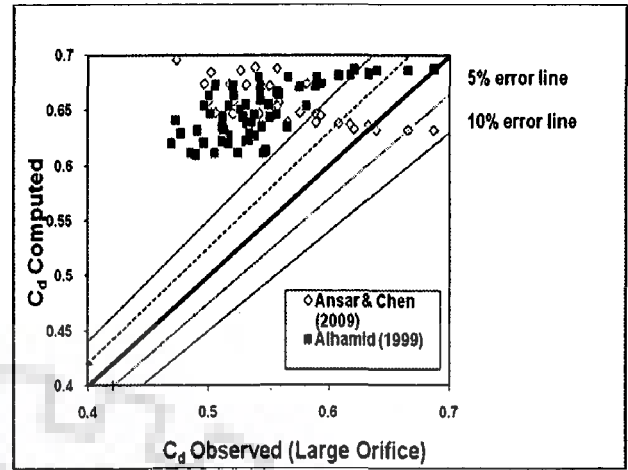


**Lip N**

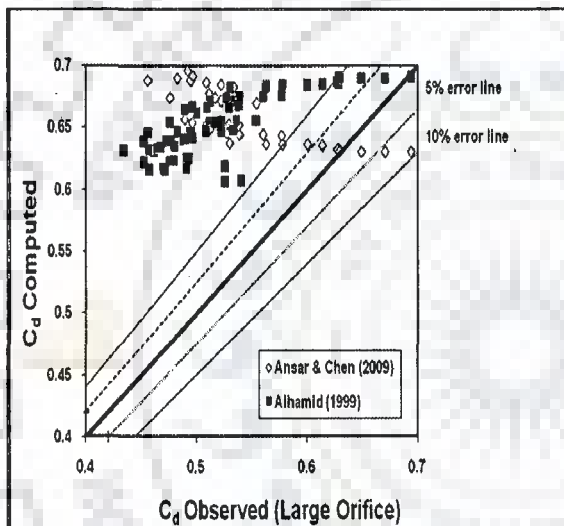
Fig. 6.2 b: Agreement of discharge coefficient using large orifice formula for lip types J,K,L and N for 1H:3V bed type



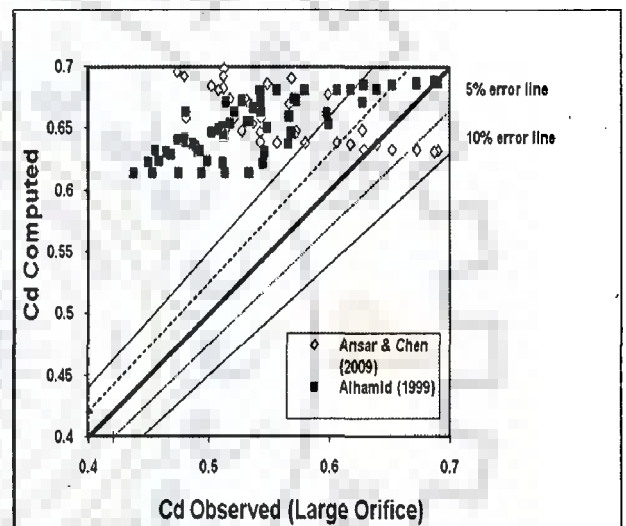
Lip F



Lip G

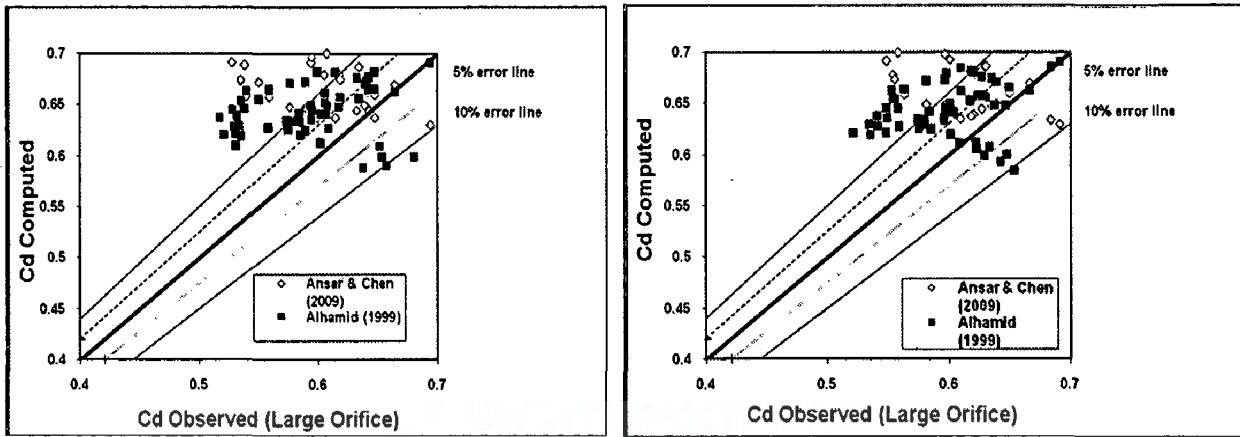


Lip H



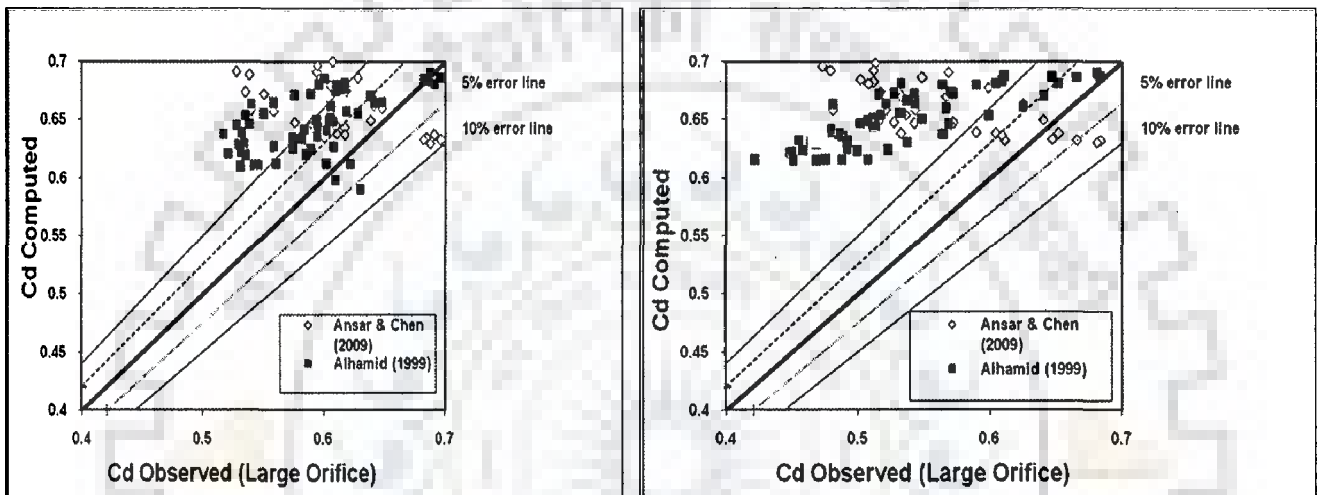
Lip I

Fig. 6.2 C: Agreement of discharge coefficient using large orifice formula for lip types F,G,H and I for 1H:3V bed



Lip J

Lip K



Lip L

Lip N

**Fig. 6.2 d:** Agreement between observed and computed discharge coefficient using Large orifice formula for different lip types J,K,L and N in a gate located over a weir of upstream slope 1H:3V

To further substantiate the relative performance of Ansar and Chen and Alhamid relationship Fig. 6.2d is developed for lip types J,K,L and N. A relative comparison between Fig. 6.1d and 6.2d reveals that the agreement is certainly not better in case of raised crest with the use of raised crest relationship for discharge computations.

On the contrast, the performance of Habibzadeh et.all (2011), Roth and Hager (1999) and Swamee (1992) seem to work better. For other weir types, the agreement diagrams using large orifice formula are given in Appendix.

### 6.3 DEVELOPMENT OF CORRECTION FACTORS

Considering that there was a lot of deviation between the observed and computed  $C_d$  using different relationships, correction factors are developed for different types of lips, as given in Tables 6.1a to 6.1d for different bed types. The formula of Alhamid which is only available formula for raised crest, can be multiplied with the correction factors generated from experimental data for various lip and bed profile combinations.

**Table 6.1a: Correction factors for Raised Crest Profile (1H: 3V)**

Lip Shape	Correction Factor (Large Orifice)	Correction Factor (Small Orifice)
Lip F	$1.2502 A^{0.0528}$	$1.5973 A^{0.1349}$
Lip G	$1.3056 A^{0.0521}$	$1.6549 A^{0.1305}$
Lip H	$1.4534 A^{0.0818}$	$1.8171 A^{0.1545}$
Lip I	$1.4522 A^{0.0963}$	$1.811 A^{0.1678}$
Lip J	$1.0618 A^{-0.0036}$	$1.4235 A^{0.1016}$
Lip K	$1.0512 A^{-0.0077}$	$1.4036 A^{0.095}$
Lip L	$1.1166 A^{0.0131}$	$1.4648 A^{0.1074}$
Lip N	$1.4836 A^{0.1051}$	$1.8404 A^{0.1742}$

**Raised Crest Profile (2H: 3V)**

**Table 6.1b: Correction factors for Raised Profile (2H: 3V)**

Lip Shape	Correction (Large Orifice) Factor	Correction (Small Orifice) Factor
Lip F	1.2604 A <sup>0.0335</sup>	1.5954 A <sup>0.1109</sup>
Lip G	1.4331 A <sup>0.0691</sup>	1.7836 A <sup>0.1593</sup>
Lip H	1.4967 A <sup>0.08</sup>	1.8501 A <sup>0.1473</sup>
Lip I	1.4671 A <sup>0.0805</sup>	1.8205 A <sup>0.1496</sup>
Lip J	1.1892 A <sup>0.0252</sup>	1.5341 A <sup>0.1118</sup>
Lip K	1.289 A <sup>0.0356</sup>	1.6298 A <sup>0.1127</sup>
Lip L	1.3536 A <sup>0.0449</sup>	1.695 A <sup>0.1176</sup>
Lip N	1.3439 A <sup>0.0543</sup>	1.6809 A <sup>0.1265</sup>



**Table 6.1c: Correction factors for Raised Crest Profile (Vertical)**

Lip Shape	Correction Factor (Large Orifice)	Correction Factor (Small Orifice)
Lip F	$1.2847 A^{0.0552}$	$1.6327 A^{0.135}$
Lip G	$1.317 A^{0.0807}$	$1.6639 A^{0.1378}$
Lip H	$1.5101 A^{0.0886}$	$1.866 A^{0.1558}$
Lip I	$1.4477 A^{0.092}$	$1.8035 A^{0.163}$
Lip J	$1.1327 A^{0.0218}$	$1.488 A^{0.1173}$
Lip K	$1.1163 A^{0.0102}$	$1.4632 A^{0.104}$
Lip L	$1.1163 A^{0.0102}$	$1.4632 A^{0.104}$
Lip N	$1.4809 A^{0.1012}$	$1.837 A^{0.1703}$

**Table 6.1d: Correction factors for Plane Bed Profile**

Lip Shape	Correction (Large Orifice) Factor	Correction (Small Orifice) Factor
Lip F	$0.7779 A^{-0.0293}$	$0.9033 A^{0.0126}$
Lip G	$0.7196 A^{-0.0728}$	$0.8508 A^{-0.0223}$
Lip H	$0.9773 A^{0.0089}$	$1.1834 A^{0.0717}$
Lip I	$0.6819 A^{-0.0618}$	$0.8134 A^{-0.0077}$
Lip J	$0.9433 A^{-0.0876}$	$1.1807 A^{-0.0099}$
Lip K	$0.911 A^{-0.0746}$	$1.1439 A^{0.0058}$
Lip L	$1.0346 A^{-0.0598}$	$1.2664 A^{0.0064}$
Lip N	$1.0346 A^{-0.0598}$	$1.2664 A^{0.0064}$

Multiplying the discharge coefficient (computed using Alhamid formula) and the correction factor, the agreement diagrams are developed and shown for illustrative purposes only for few cases, as shown in Figs. 6.3 a-d.

It can be seen from Figs. 6.3 a-d and Figs. 6.1 and 6.2, that use of correction factors brings a closer agreement between observed and computed discharge coefficients. The agreement diagrams are presented for the use of small orifice formula as well as large orifice formula. Essentially, by small orifice formula, it is meant that it can be used in case of smaller opening,

whereas the large orifice formula means that it can be used for large gate openings. In the literature, however, all the investigators have only used small orifice formula. Therefore, correction factors have been developed for both cases. However, in the agreement diagrams, using large orifice formula, we have only multiplied the correction factors of large orifice formula, with the small gate opening based equation of Alhamid (1999). It would have also possible to develop similar correction factors using other approaches. However, the same was avoided considering that Alhamid approach was more rational to use as it had been already tested on several types of bed.

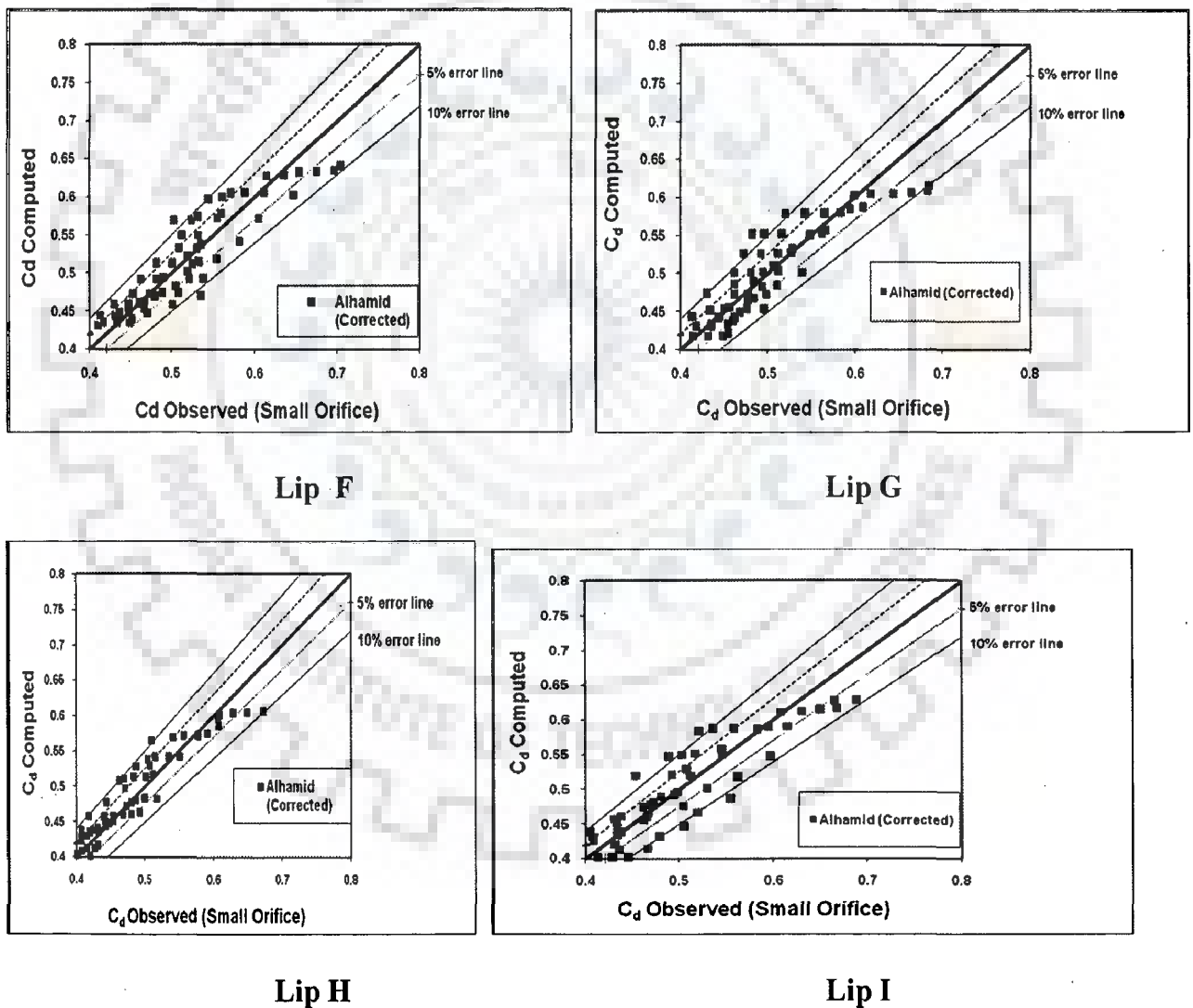
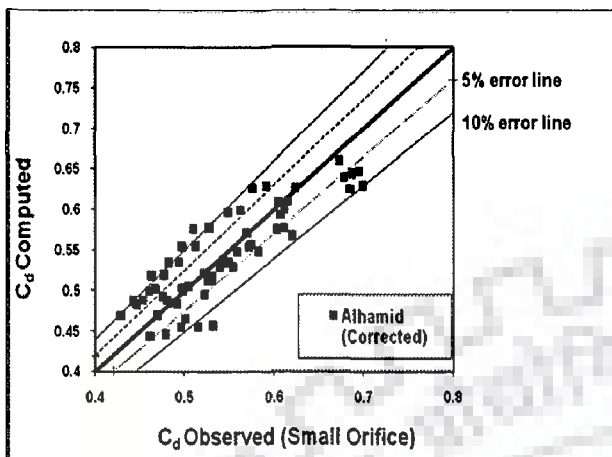
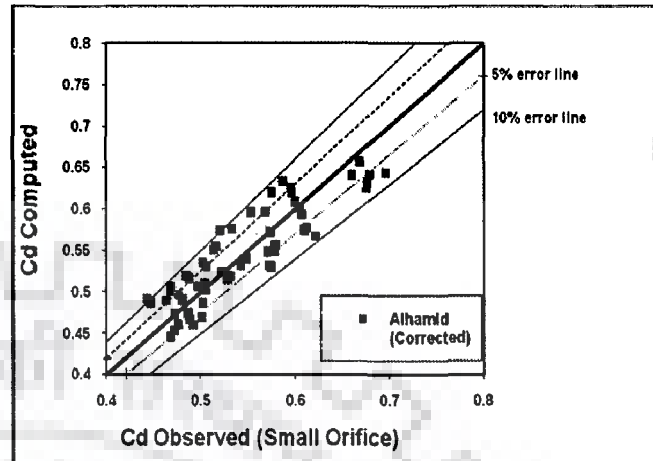


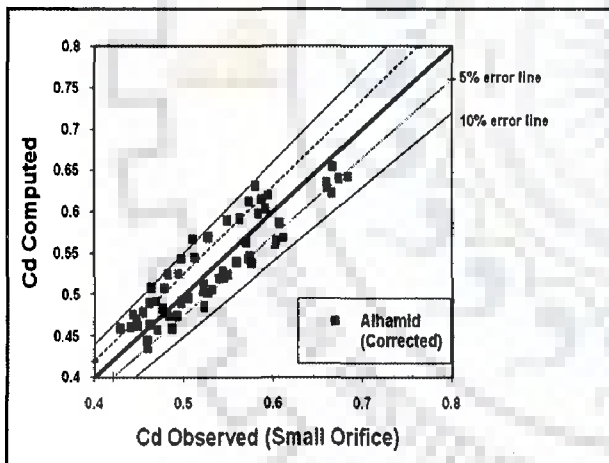
Fig. 6.3 a: Agreement between observed and computed  $C_d$  using correction factors for bed type (1H:3V)



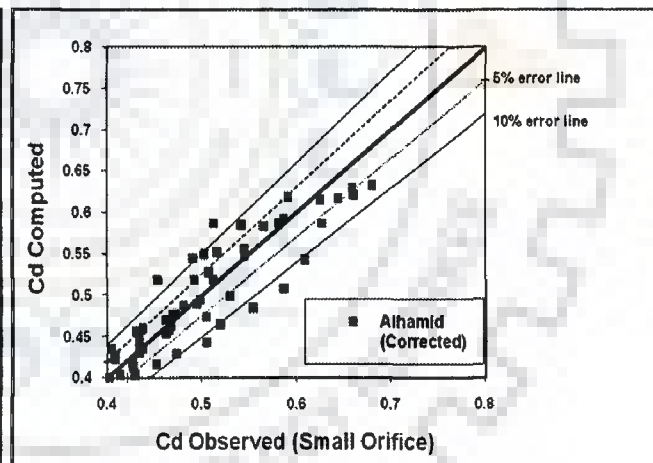
Lip J



Lip K

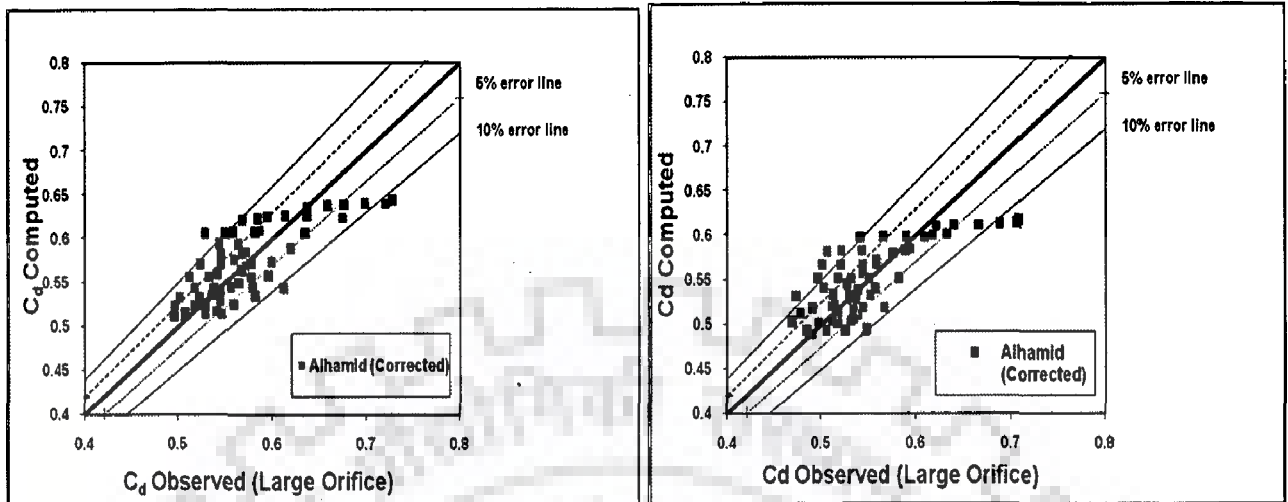


Lip L



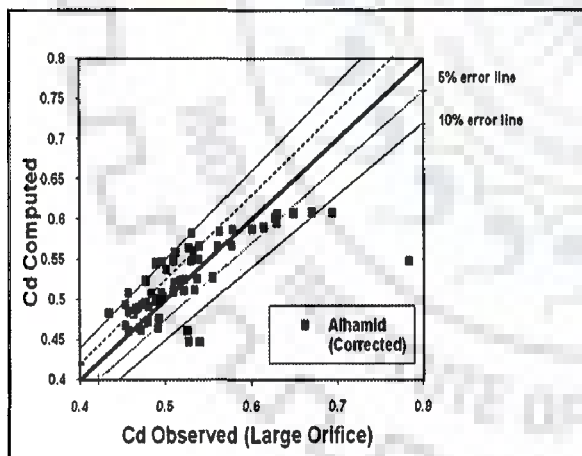
Lip N

Fig. 6.3 b: Agreement between observed and computed  $C_d$  (small orifice formula) for lips J, K, L and N using correction factors for bed type (1H:3V)

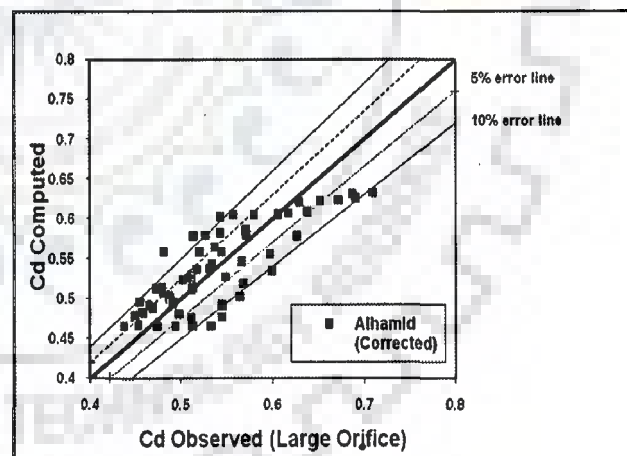


Lip F

Lip G

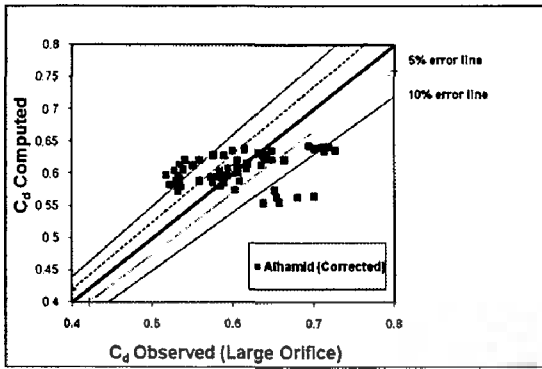


Lip H

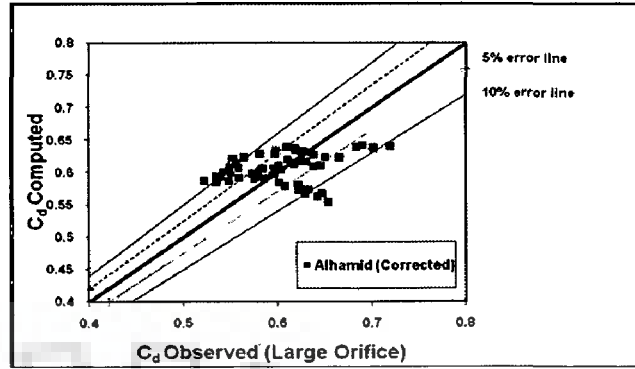


Lip I

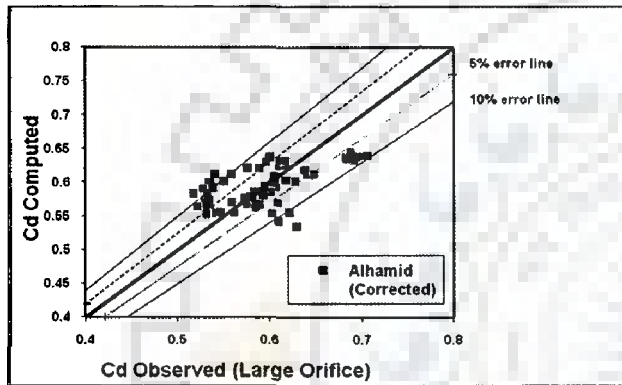
Fig. 6.3c: Agreement between observed and computed  $C_d$  (large orifice formula) for lips F,G,H and I using correction factors for bed type (1H:3V)



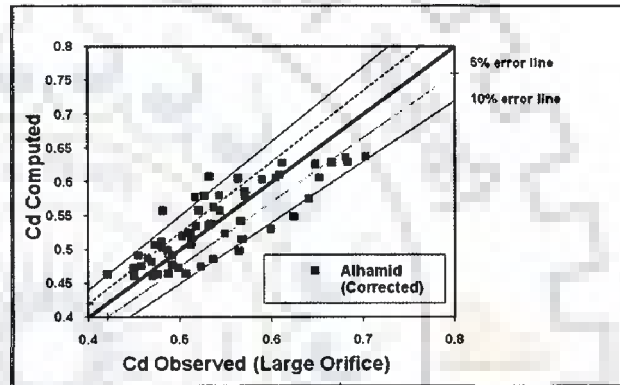
Lip J



Lip K



Lip L



Lip N

Fig. 6.3 d: Agreement between observed and computed  $C_d$  (large orifice formula) for lips J,K,L and N, using correction factors for bed type (1H:3V)

#### 6.4 SUMMARY

In this chapter, eight types of streamlined shapes for four types of bed configurations below gate. The use of small orifice formula using the approach of Swamee (1992), Roth and Hager (1999), Alhamid (1999) and Ansar and Chen (2009), and Habibzade et al. (2011) are tested. The agreement between observed and computed discharge coefficient using various approaches indicated a poor agreement and therefore to account for the lip shape effects correction factors

are proposed with the use of Alhamid (1999) formula. The use of this formula is considered because it is valid for plain as well as raised crest bed conditions .with the use of correction factors the agreement between observed and computed discharge coefficient is found to improve significantly. As far as the  $C_d$  variations are concerned these are found to exhibit similar variations with relative gate opening as described in chapter 4. Also the  $C_d$  values have been found to be higher in case of raised crest in comparison to plane bed. In case of lip H and K,  $C_d$  values are also observed to be more than the other streamlined lip shapes.







---

# PRESSURE CHARACTERISTICS OF STREAM LINED LIP SHAPES

---

### 7.1 INTRODUCTION

In this Chapter, the pressure characteristics of sluice gates having stream lined lips are considered. In Chapter 5, the variation of pressure on the lips was shown as a function of relative gate opening. In addition, the use of dimensionless terms involving two depth terms, as given by Anwar and Chen (2009) are also used. Use of specific energy ( $E$ ) based term,  $E/a$ , with gate opening 'a' was also related with the ratio of observed to hydrostatic pressure. The shape of the lip, plays an important role in the uplift pressure experienced by the sluice gate. This is in part due to the fact that lip shape affects stream lines and the point of flow separation of the oozing water. Thus, in view of analysis presented in Chapter 5, the variations of observed to hydrostatic pressures are shown with respect to various dimensionless parameters including relative gate opening and  $E/a$ . The stream lined lip shapes which lead to minimum pressures throughout the operational range of relative gate opening are identified for different types of bed profile under the sluice gate.

### 7.2 PRESSURE MEASUREMENTS

In case of stream lined lip shapes, the steps involved for pressure measurements have been essentially similar to what has been done for non-streamlined shapes. To be brief, the measurements of the pressure were taken using piezometer connected to nine holes spread across and along the lip portion. The arrangement of these holes is symmetric; three holes each on the extreme edges of the lip and three at the center of the lip.

### **7.3 VARIATION OF PRESSURE**

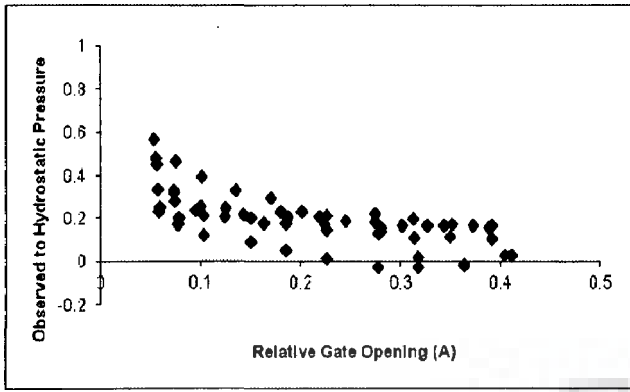
As discussed, in the first step, the average pressure on the lip is computed using all the measurements. The idea is that average pressure can easily give preliminary idea about effective lip shape. Although averaging can have its own limitations, particularly in those conditions, where some pressures are positive and some are negative. For this reason, it is also essential that uniformity tests must be applied to finally select a suitable stream lined lip shape. Thus, in the first step, only the variation of average pressure, also termed as observed pressure, is considered for processing.

#### **7.3.1 Variation of Observed to Hydrostatic Pressure with Relative Gate Opening**

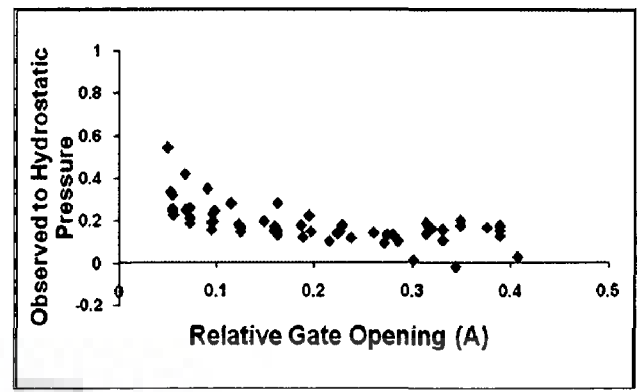
The relevance of relative gate opening has been shown in Chapters 4 and 5. As a total of eight stream-lined shapes and four types of bed profile are considered in the present experiments, a total of 32 plots indicating the variation of observed to hydrostatic pressures with relative gate opening are presented next. For the sake of presentation, the sequence is kept as follows: (i) Weir type (1H:3V). This means that bed profile below the gate is given by the top profile of the weir. (ii) Weir type (2H:3V) (iii) Weir with vertical upstream face and (iv) Flat bed. Thus, according to the profile of the bed below the gate, variations of observed to hydrostatic pressures are described for eight types of stream lined lip shapes.

##### **7.3.1.1 Raised crest (1H: 3V)**

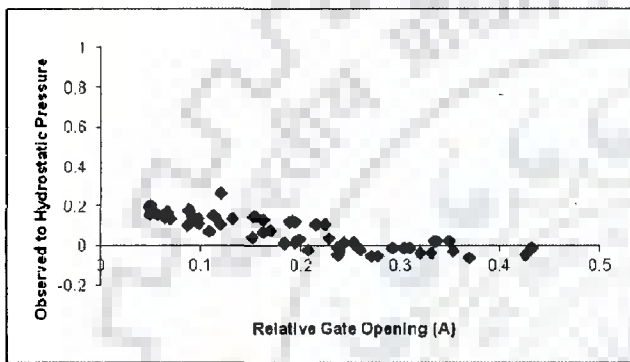
The relative gate opening has been plotted on x-axis against ratio of observed pressure head to the hydrostatic pressure head (equal to the upstream depth) on y-axis for raised crest of 1H:3V type and is shown in Figs. 7.1(a) and (b).



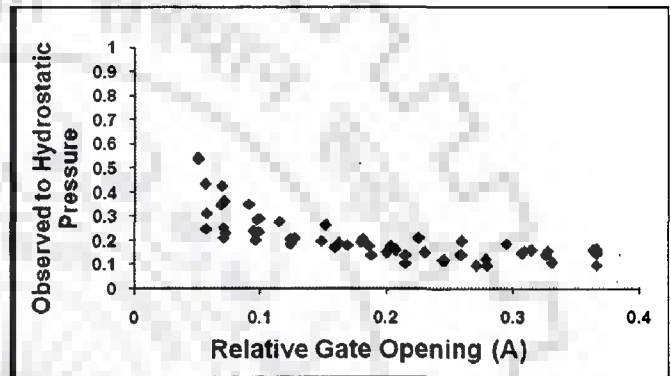
(Lip F)



(Lip G)



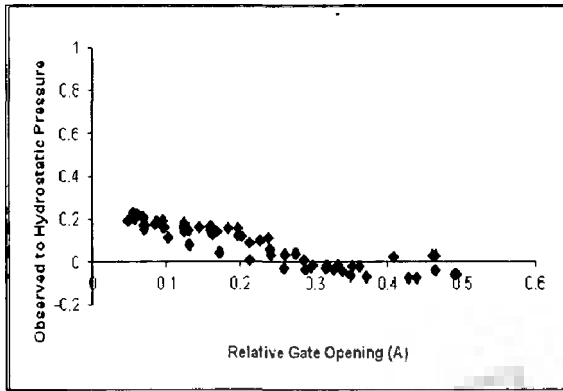
(Lip H)



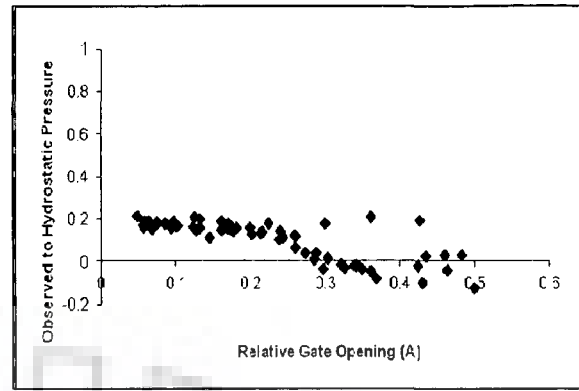
(Lip I)

Fig. 7.1a : Variation of observed to hydrostatic pressure for lip types F, G, H and I

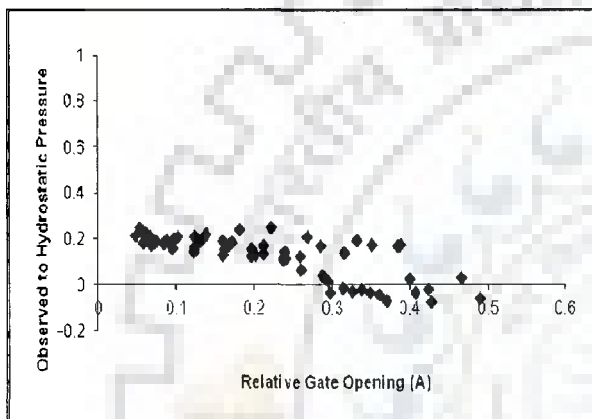
Fig. 7.1a shows that among four lip types, the performance of lip type I always experiences positive pressure that is uplift pressure. Among lip shapes, F, G and H, F and G behave very similar to each other and the uplift pressures prevail in general at all relative gate opening. However, in certain runs, negative pressures do develop. Lip H experiences minimum uplift pressure and it also experiences down pull (negative pressure) in the range of relative opening greater than 0.2:



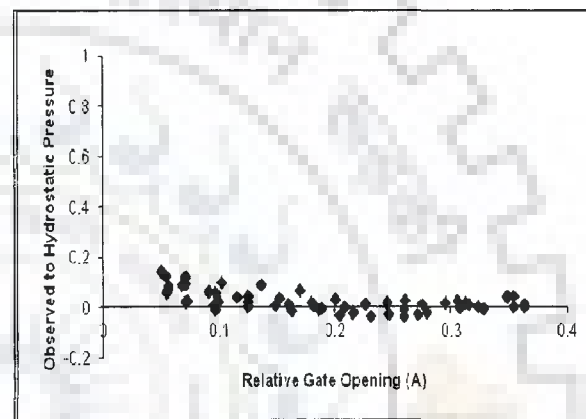
(Lip J)



(Lip K)



(Lip L)



(Lip N)

Fig. 7.1(b): Variation of observed to hydrostatic pressure for lip types J, K, L and N

Fig. 7.1b shows that among four lip types, i.e., J, K, L and N, none of the lip always experiences positive pressure that is uplift pressure. Lips J, K and L show very similar trend of variation of observed to hydrostatic pressure and the magnitude also vary similar to that of lip H. For these lip shapes, the uplift pressure works for the relative gate opening less than 0.2. In lip type, N, there is relatively lower uplift pressure as well as negative pressure, when compared with the remaining lip types.

### 7.3.1.2 Raised crest (2H:3V)

Fig. 7.2a represents variation of observed to hydrostatic pressure in Lip types F,G,H and I for sluice gate placed above raised crest (2H:3V).

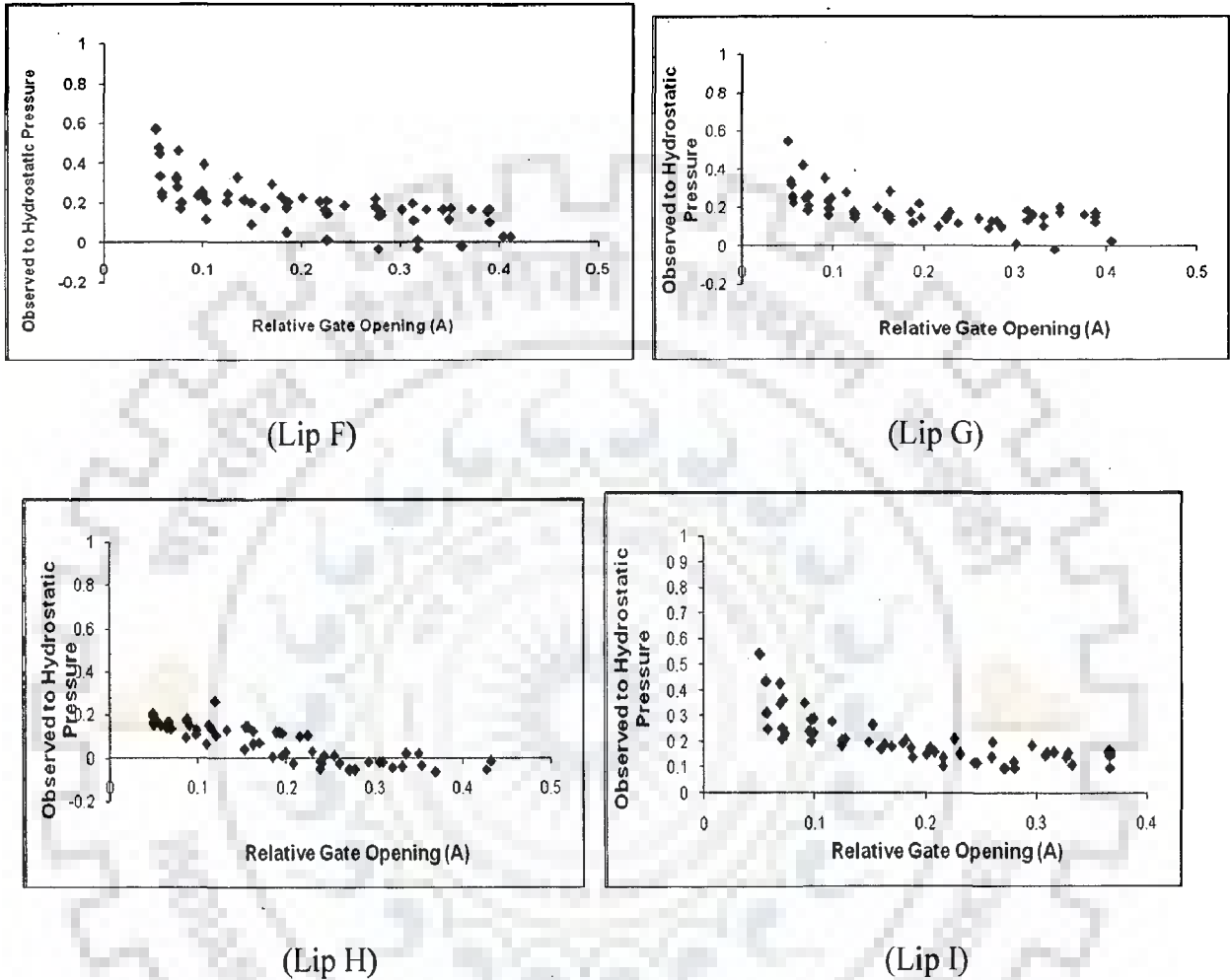


Fig. 7.2a: Variation of observed to hydrostatic pressure in Lip types F,G,H and I for sluice gate placed above raised crest (2H:3V)

Comparative evaluation of performance of lip types F, G, H and I indicates that lowest pressure is achieved in lip type H. For very low opening, say around 0.05, the observed pressure can be about 40% of hydrostatic pressure, even in lip H. In comparison, lips F,G, and I experience

pressures which are as high as 60% of observed hydrostatic pressure. Very few data points also indicate the presence of negative pressures for lip H, which are of course very low in magnitude.

Fig. 7.2 b shows the variation of observed to hydrostatic pressure in Lip types J, K, L and N for sluice gate placed above raised crest (2H:3V)

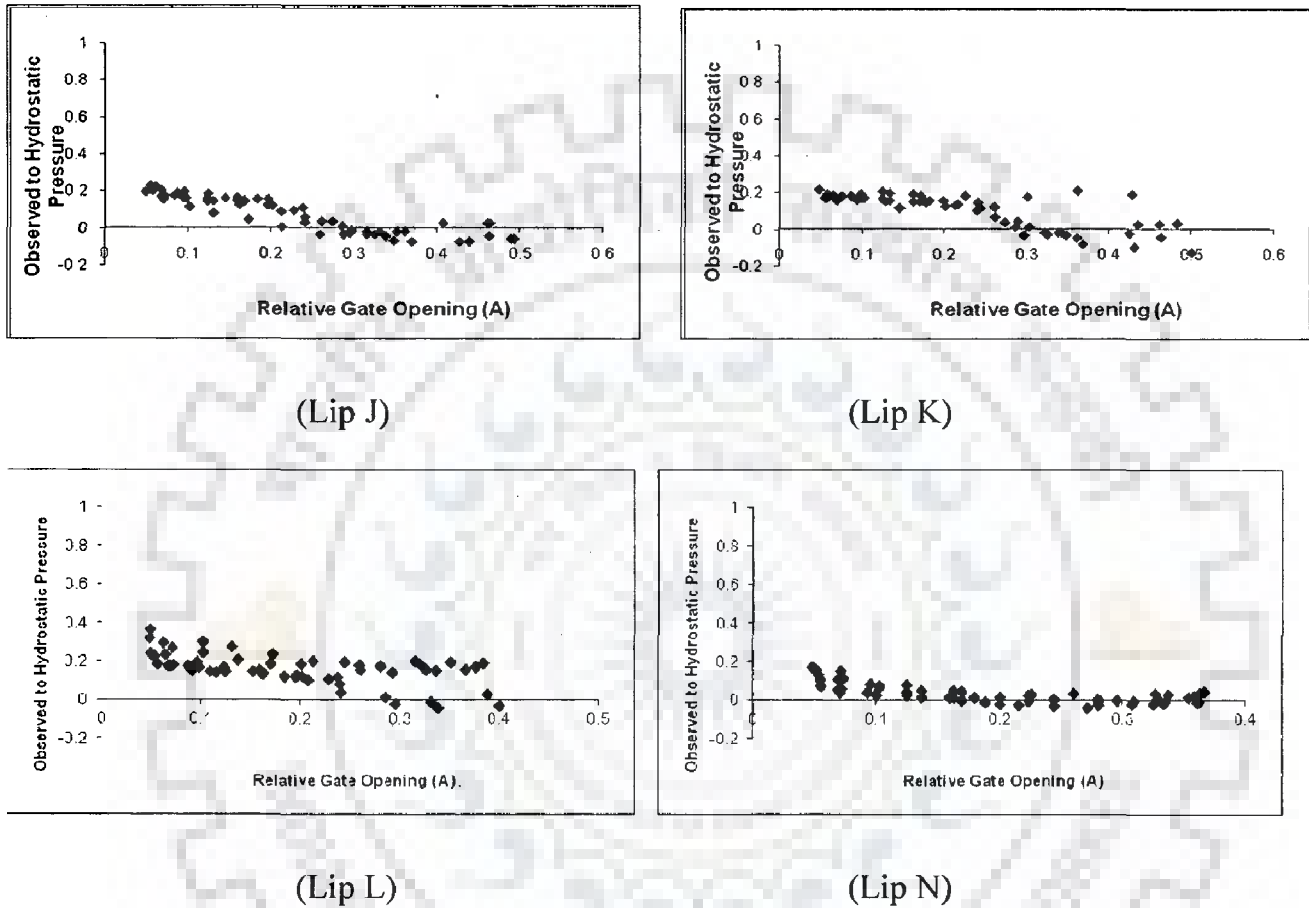


Fig. 7.2b: Variation of observed to hydrostatic pressure in Lip types J, K, L and N for sluice gate placed above raised crest (2H:3V)

Compared to lip type H, Lip J, K and L experience similar amount of positive pressures, though the value in Lip L is towards higher side. Lip N experiences lowest pressure and gives an indication that this is the most effective lip shape. However, this is not so and the reasons for rejection of this lip shape will be discussed at a later stage in this chapter.

A comparison of Figs. 7.1a and 7.2a is also relevant here. For example, if lip type H is considered, the magnitude of observed pressure is less for the gate located above weir with profile 1H:3V than the one located above weir of type 2H:3V.

### 7.3.1.3 Raised crest (vertical)

Comparison of the pressure characteristics of gates located over two types of ogee shaped weirs indicated to examine the third ogee type weir, which essentially had vertical upstream crest. Figs. 7.3 a and b show the variation of observed to hydrostatic pressure for eight lip types in total.

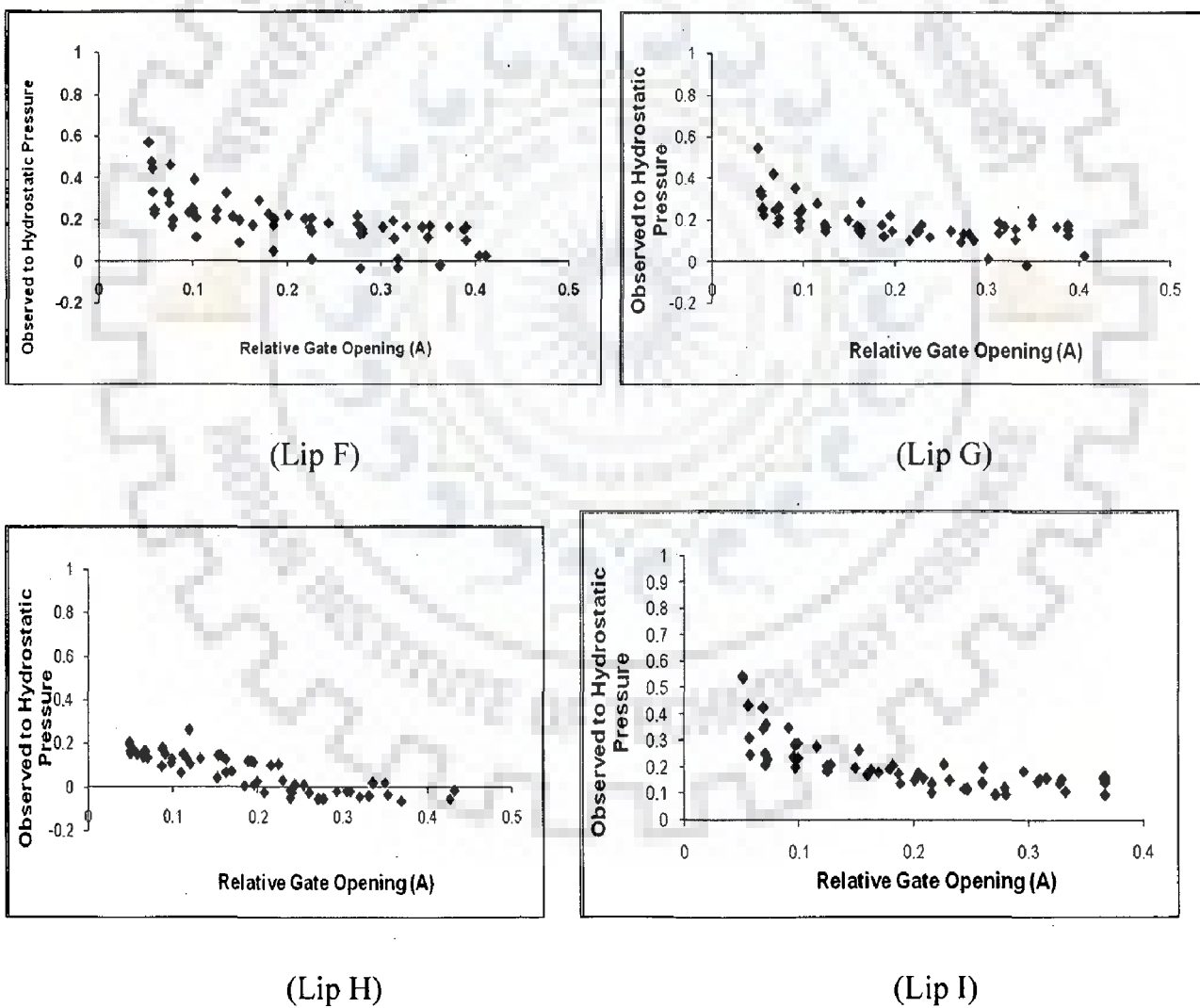
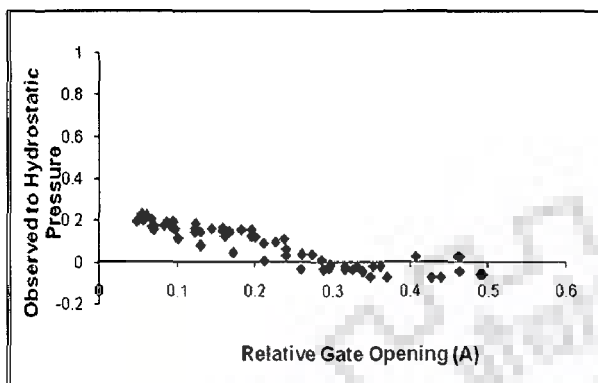
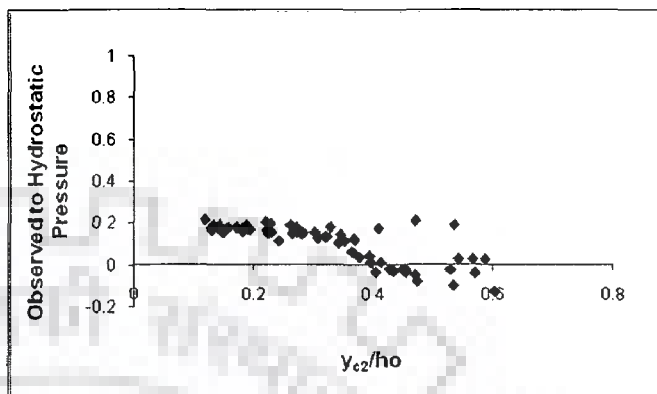


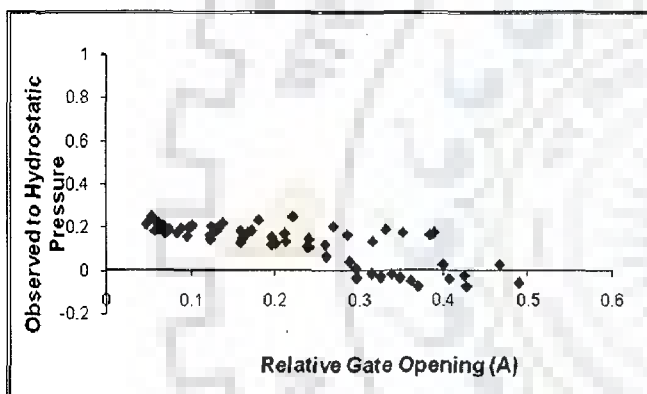
Fig. 7.3a: Variation of observed to hydrostatic pressure in Lip types F, G, H and I for sluice gate placed above vertical raised crest



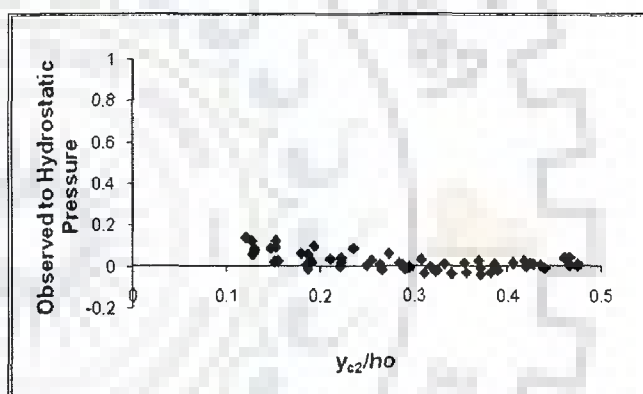
(Lip J)



(Lip K)



(Lip L)



(Lip N)

Fig. 7.3b: Variation of observed to hydrostatic pressure in Lip types J, K, L and N for sluice gate placed above raised crest (Vertical upstream face)

From Figs. 7.3 a and 7.3 b, it can be seen that lip shapes G, H, J, K, L and N experience negative pressure. From magnitude considerations, lip N again becomes the first choice followed by Lip H. It is noted that performance of other lip shapes, i.e. J, K and L are also very comparable to lip H. Further, the performance of lip type H in case of gate located above weir having upstream face with slope 1H:3V is comparable to that with the gate located above weir having upstream vertical face.



#### 7.3.1.4 Plane bed

Occurrence of plane bed is also common in many situations. However, experiments on plane bed with different lip shapes did not indicate much reduction in pressures on lip as compared to that on gates located above raised crest. Fig. 7.4 presents a combined performance of different streamlined shapes. It can be seen from this figure that lip type L achieves the lowest pressure. The performance of lip shape N is not shown. Because of hemispherical shape, this lip type has been previously reported to be non-suitable because of occurrence of separation, non-uniform pressure distribution along the lip width and severe vibration problems in case of gates located on flat bottoms. After limited experiments on this lip shape, it was decided to exclude it for rigorous experimental work and for this reason, the performance of lip N is not shown in Fig. 7.4.

Among the other lip shapes tested for flat bed, lip L appears to work better in terms of low pressure development along lip bottom. However, prior to recommending any lip type, the variation of pressure along the lip bottom is to be studied. To study this, a dimensionless parameter  $K_B$  has been often used in literature. The parameter  $K_B$  is defined as

$$K_B = 2(h_o - h)/(\rho v_o^2) \quad (7.1)$$

Where  $h_o$  = Hydrostatic Pressure Head

$h$  = Observed Pressure Head

$\rho$  = Density of water

$v_o$  = Velocity of water in the flume

The units of  $K_B = m^2 s^2 / kg$  It can be converted to dimensionless  $k_B$  where  $k_B = \rho g K_B$

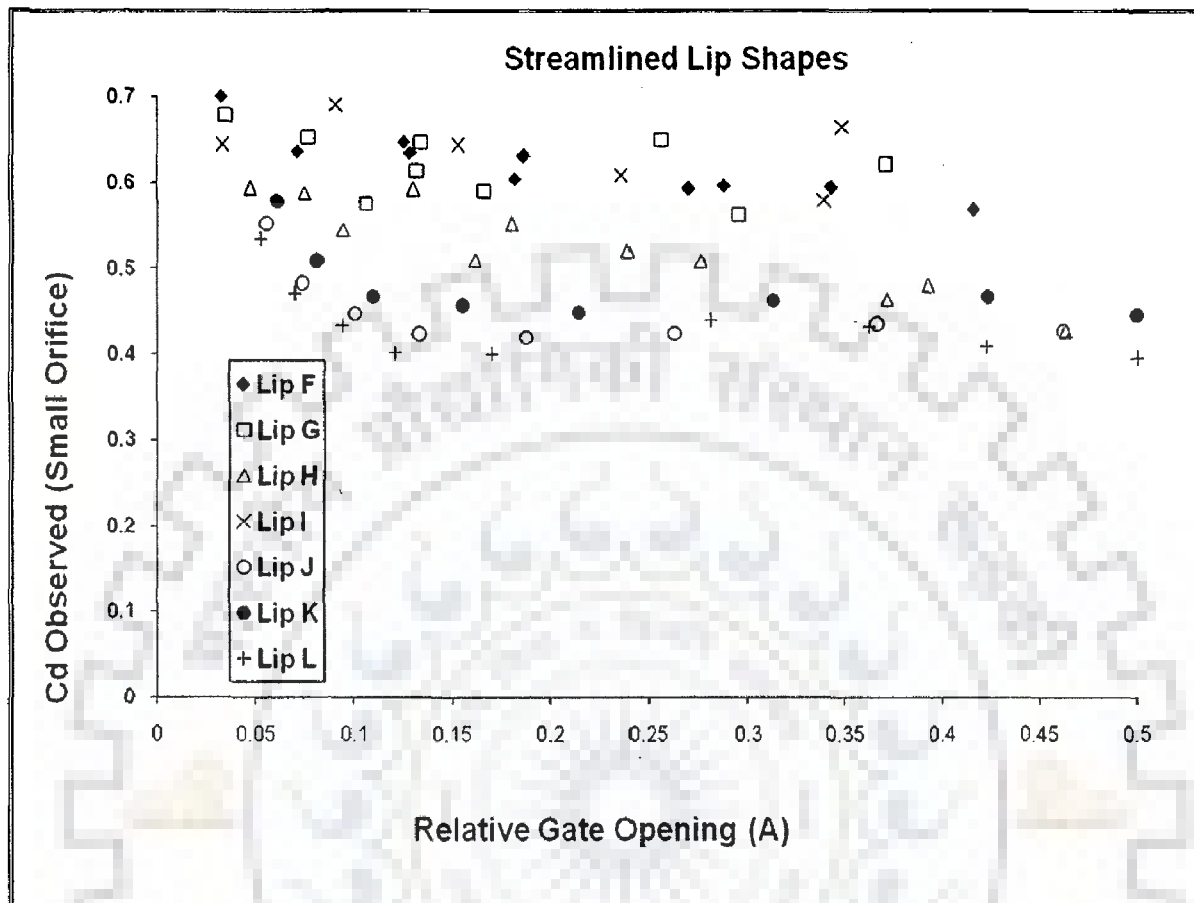


Fig. 7.4: A typical variation of observed  $C_d$  on stream lined lip shapes for gate located above raised crest.

#### 7.4 A COMPARATIVE EVALUATION OF STREAMLINED LIP TYPES USING PRESSURES ALONG THE LIP

Similar to Fig. 7.4, Figs. 7.5, 7.6 and 7.7 are developed and these are also shown here so that a better comparison of different stream lined shapes as well as type of bed below gate is feasible. To further assist with the selection of suitable lip shape, uniformity diagrams are also shown with

summary graphs. Uniformity diagrams are essentially pressure diagrams or K diagrams along the lip base in the direction of flow.

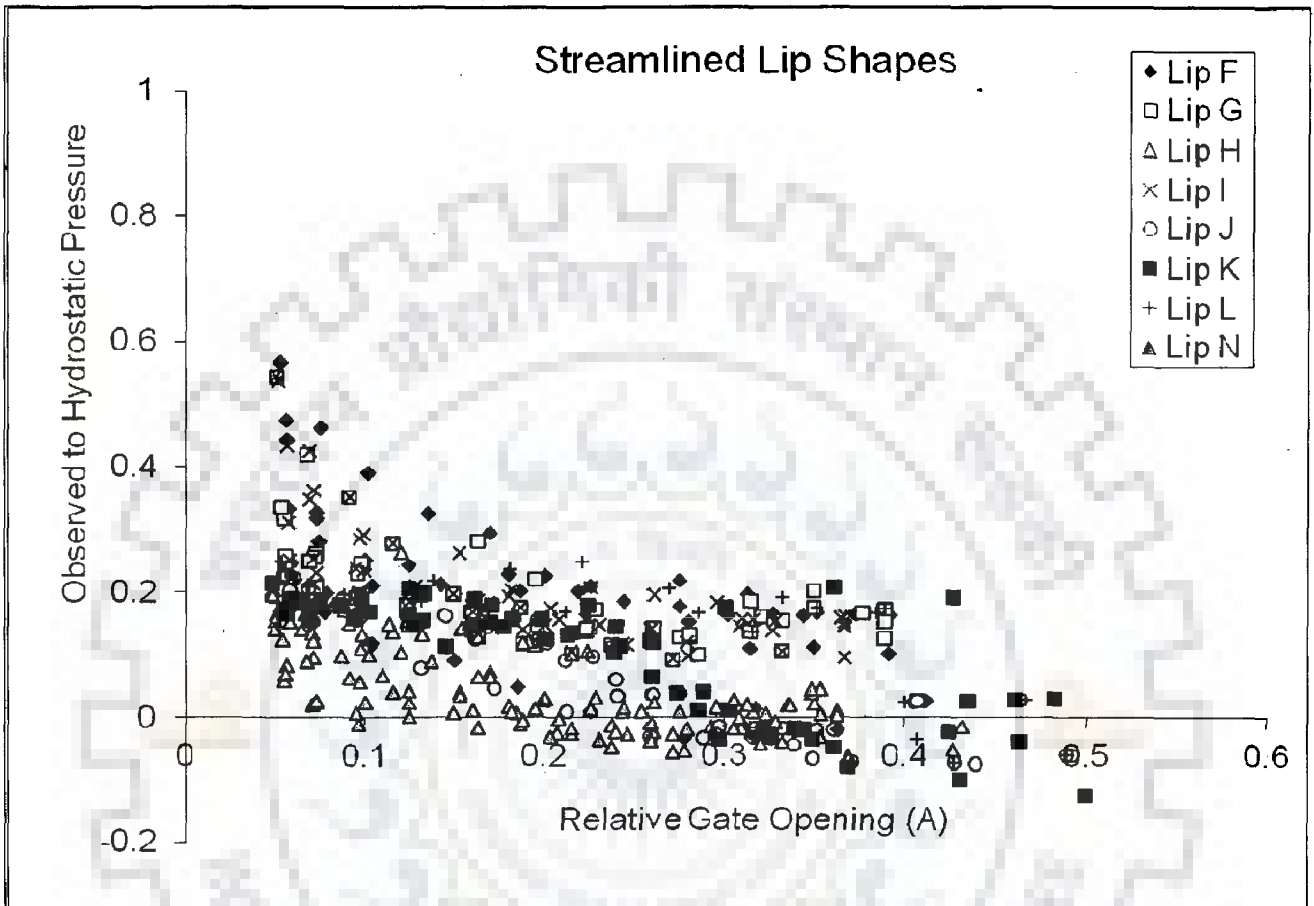


Fig. 7.5 a: Summary graph showing pressure variations for raised crest (1H:3V)

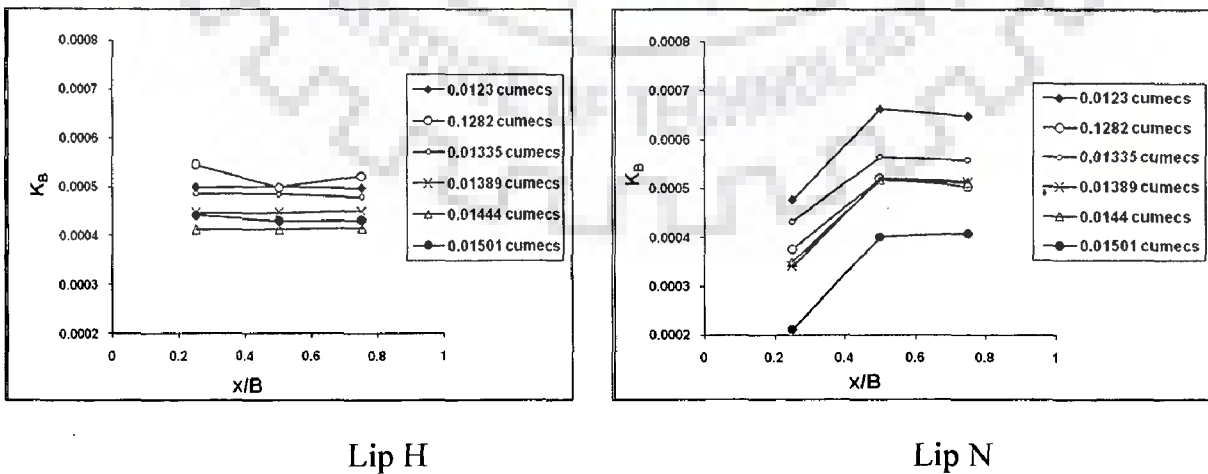


Fig. 7.5 b: Pressure variations along lip H and N (for raised crest 1H:3V)

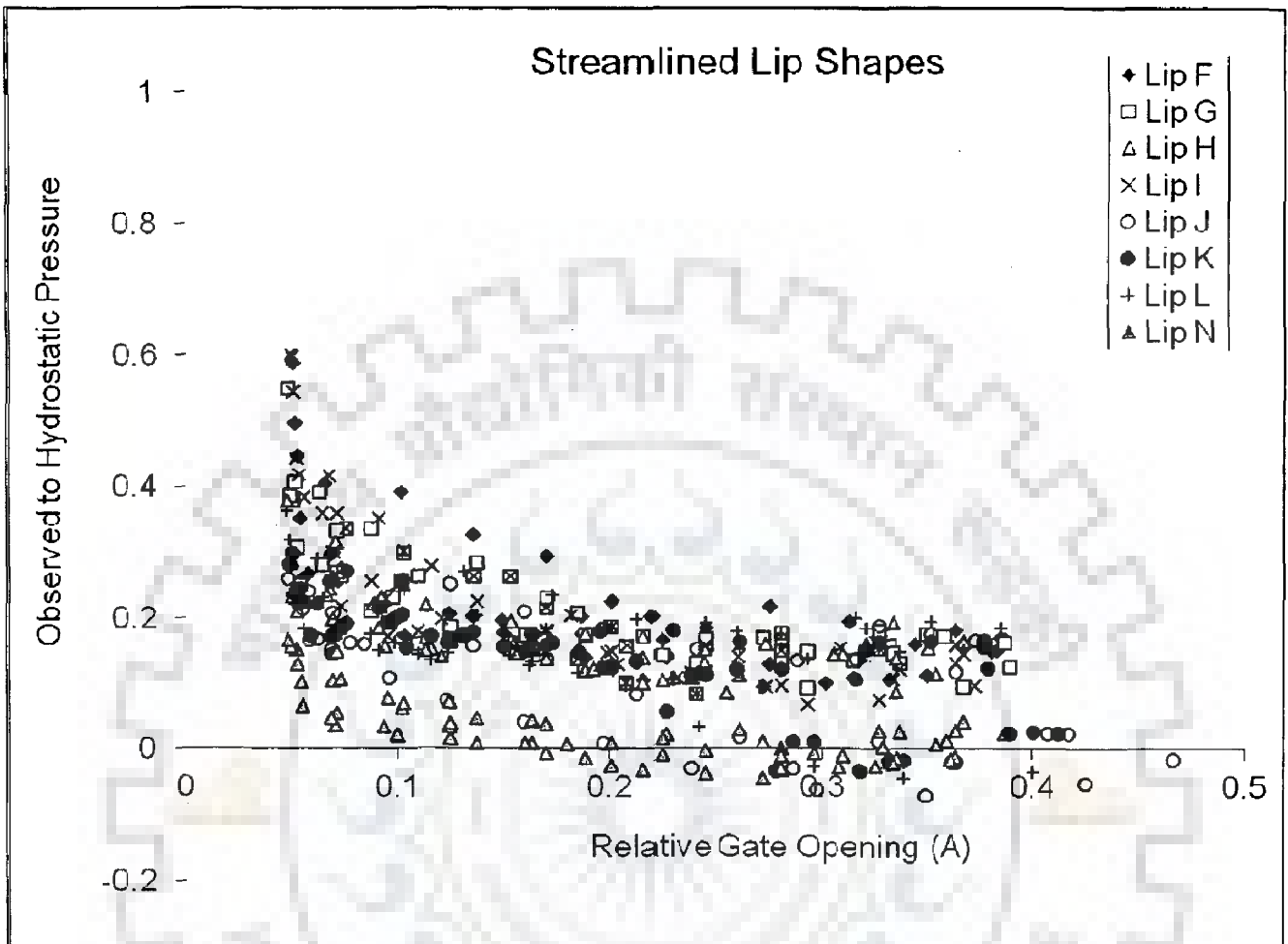


Fig. 7.6 a: Summary graph showing pressure variations for raised crest (2H:3V)

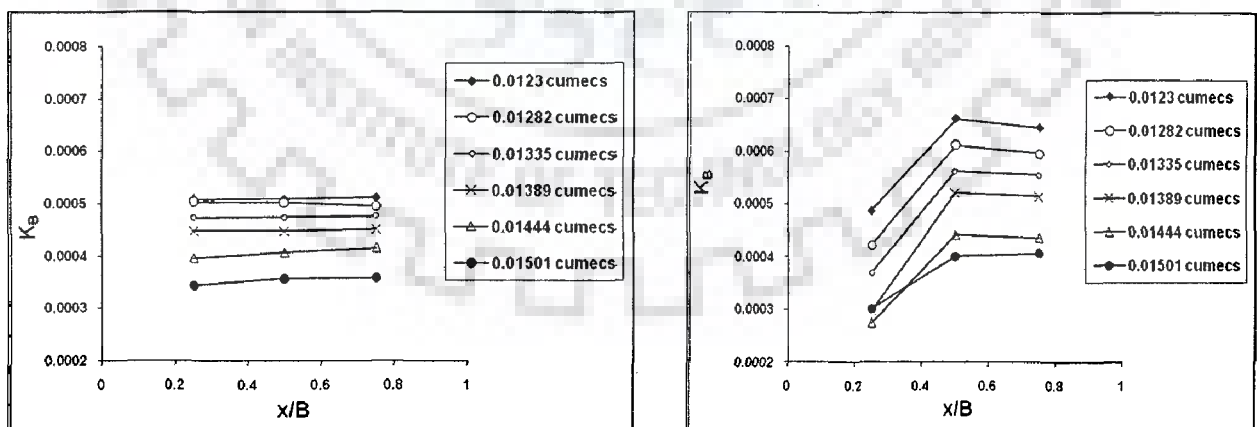


Fig. 7.6 b: Pressure variations along lip H and N (for raised crest 2H:3V)

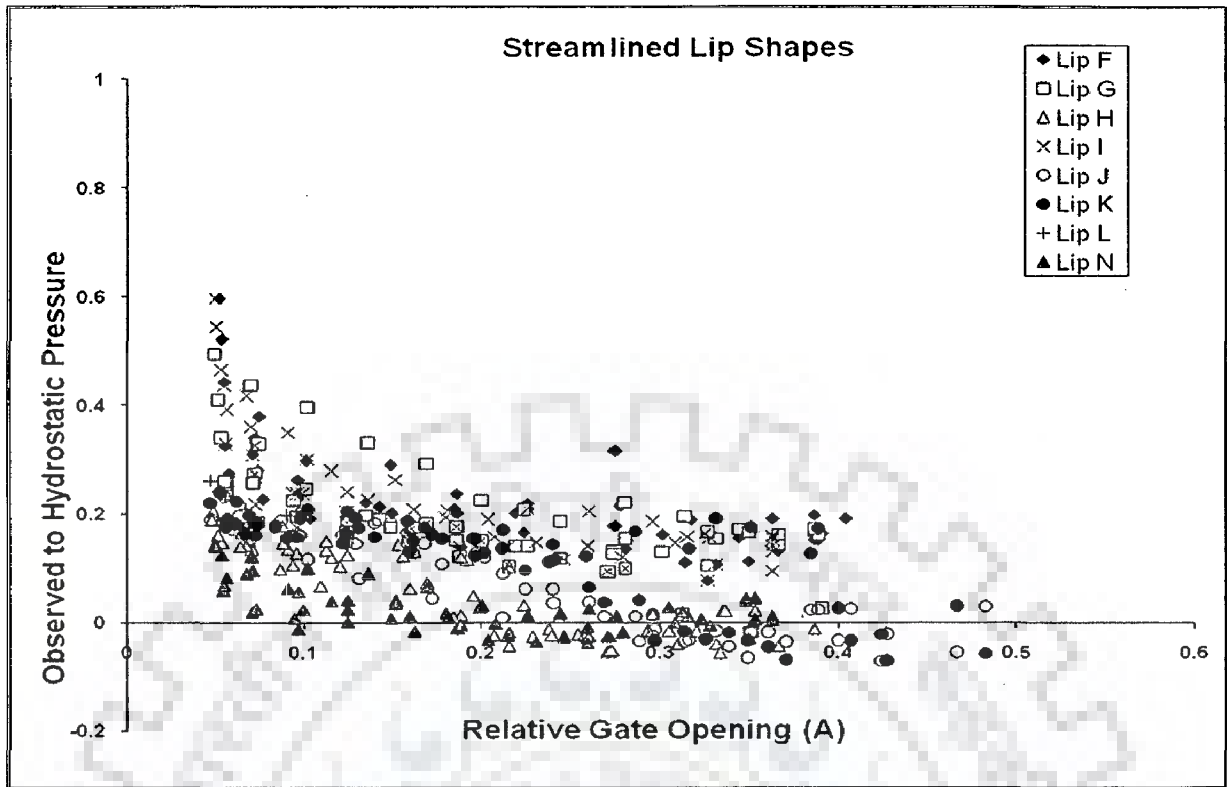


Fig. 7.7 a: Summary graph showing pressure variations for raised crest (upstream vertical face)

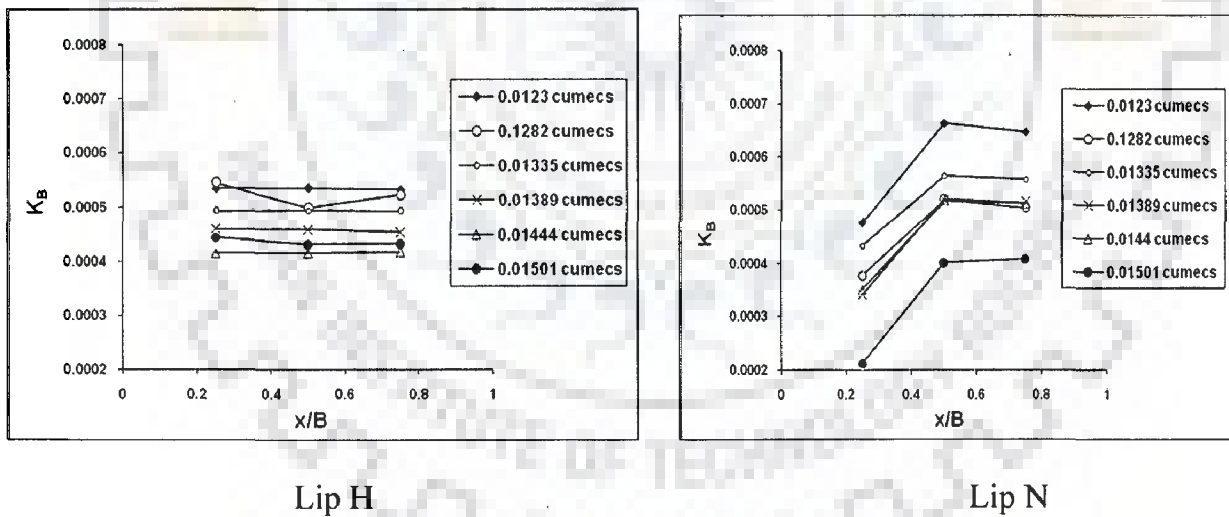


Fig. 7.7 b: Pressure variations along lip H and N (for raised crest vertical upstream face)

Figs. 7.5b, 7.6b and 7.7b indicate that there is merit in using lip type H as the pressure distribution is also uniform below the lip bottom lip K was also found to have uniform pressure distribution. In case of flat bed, lip type G and H are found to have uniform distribution around the lip bottom.

## 7.5 USE OF OTHER DIMENSIONLESS PLOTS FOR PRESSURE VARIATION

In Chapter 5, several plots were made to represent pressure variations using two dimensionless terms  $y_{c1}/a$  and  $y_{c2}/a$ , where  $y_{c1}$  and  $y_{c2}$  are two depth terms used by Anwar and Chen (2009) in their study on flow characteristics over raised crests. These depth terms have been defined in Chapter 5. Just to have an idea how the ratio of observed to hydrostatic pressure diagram gets modified in terms of these dimensionless numbers, few plots are shown for lip type H in Figs. 7.8 and b. It is apparent from Fig. 7.8 that plots are still scattered with the use of  $y_{c1}/h_0$ .

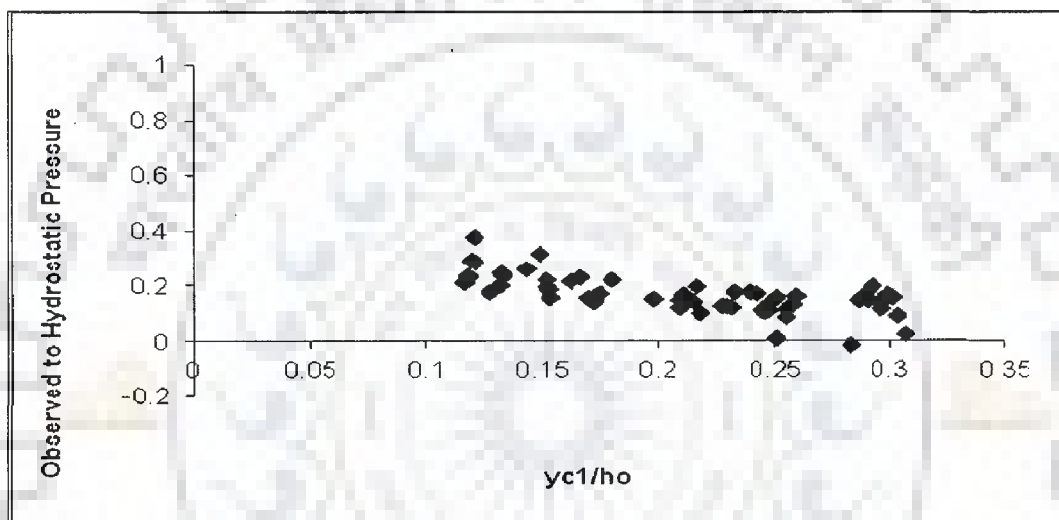


Fig. 7.8 a: Pressure ratio versus  $y_{c1}/h_0$  for lip H and raised crest (2H:3V)

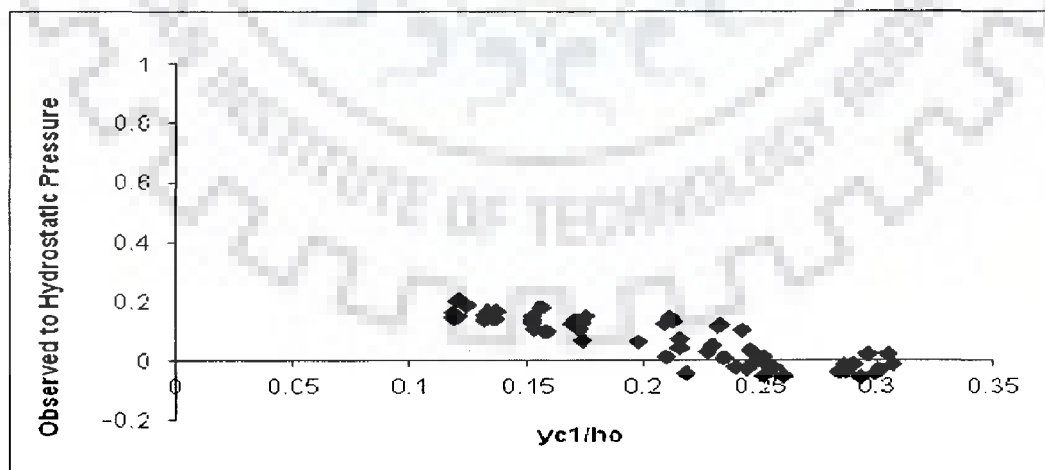


Fig. 7.8 b: Pressure ratio versus  $y_{c1}/h_0$  for lip H and raised crest (vertical upstream face)

Similarly, plots are made between ratio of observed to hydrostatic pressure and  $y_{c2}/h_0$ . Fig. 7.9 a and b again reflect that the use of  $y_{c2}$  also does not help in reducing the scatter of data points.

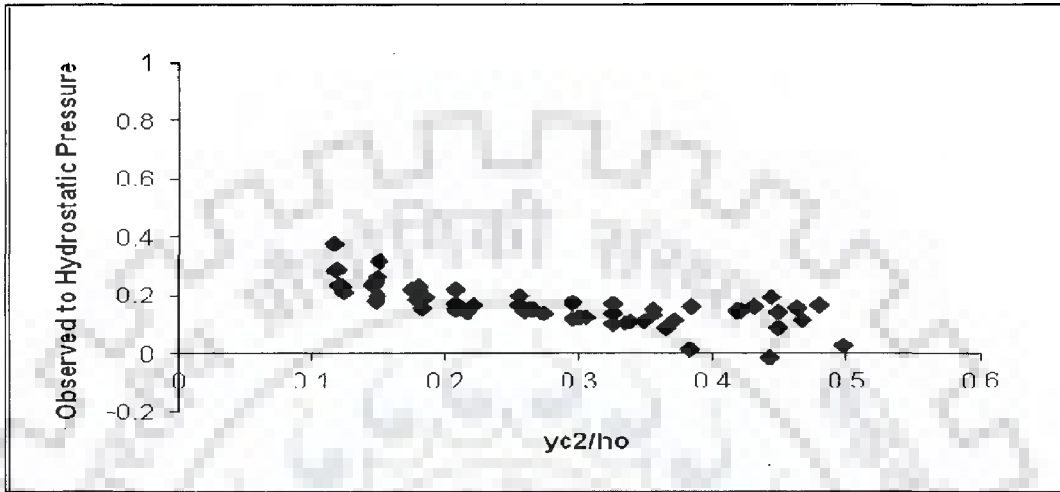


Fig. 7.9 a: Pressure ratio versus  $y_{c2}/h_0$  for lip H and raised crest (2H:3V)

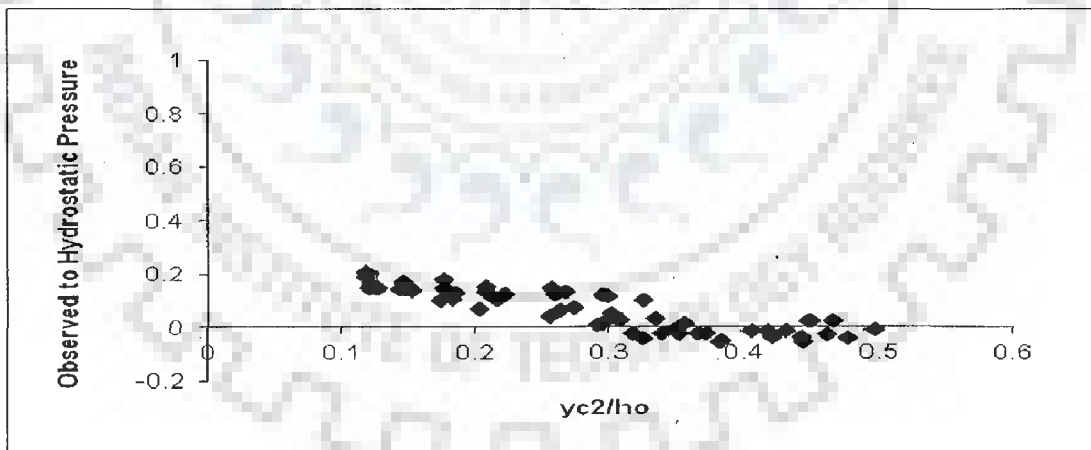


Fig. 7.9 b: Pressure ratio versus  $y_{c1}/h_0$  for lip H and raised crest (vertical upstream face)

Plots in respect of other bed types are not shown as these also did not support the use of dimensionless terms based on two depth terms of Anwar and Chen (2009).

Plots using dimensionless term  $E/a$  are also made and few plots for lip H are shown to indicate the trend of variation of pressure /gate opening( $P/a$ ) with the  $E/a$ .

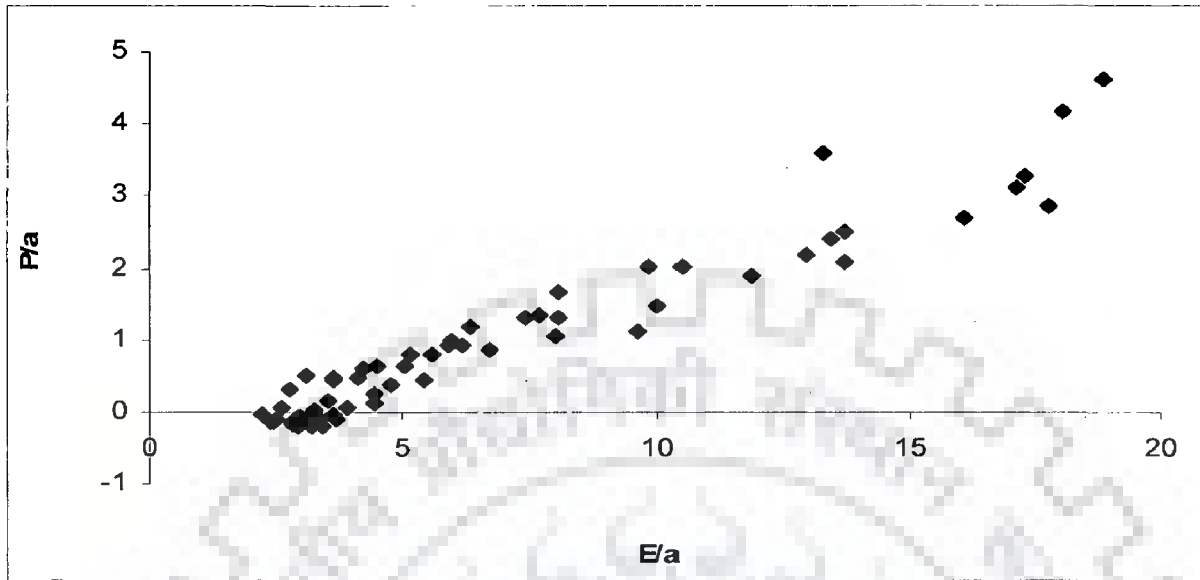


Fig. 7.10 a:  $P/a$  versus  $E/a$  variation for lip H on ogee crest (1H:3V)

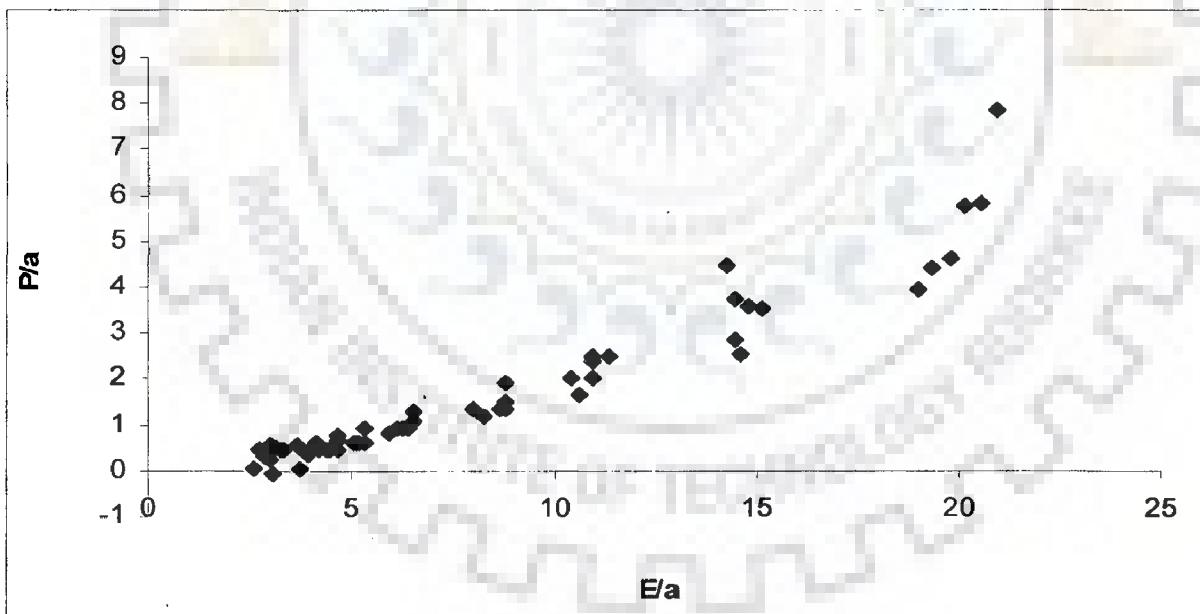


Fig. 7.10 b:  $P/a$  versus  $E/a$  variation for lip H on ogee crest (2H:3V)



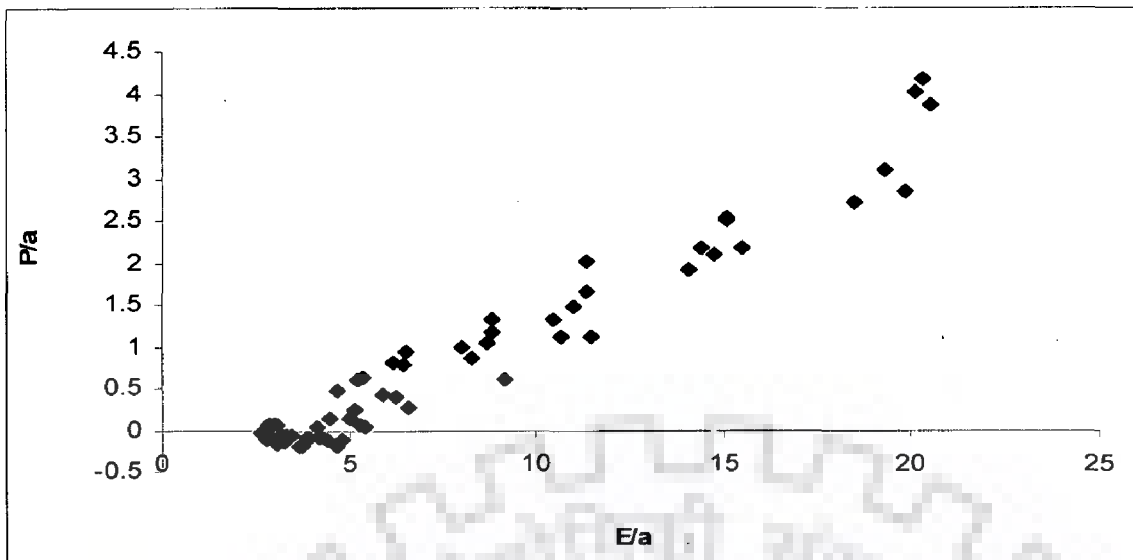


Fig. 7.10 c: P/a versus E/a variation for lip H on ogee crest (upstream vertical face)

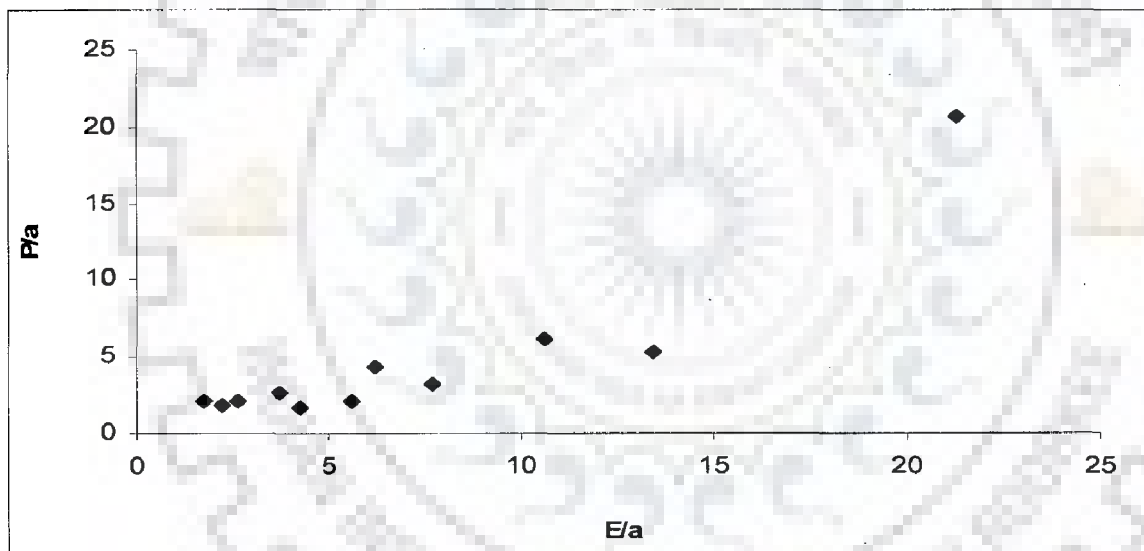
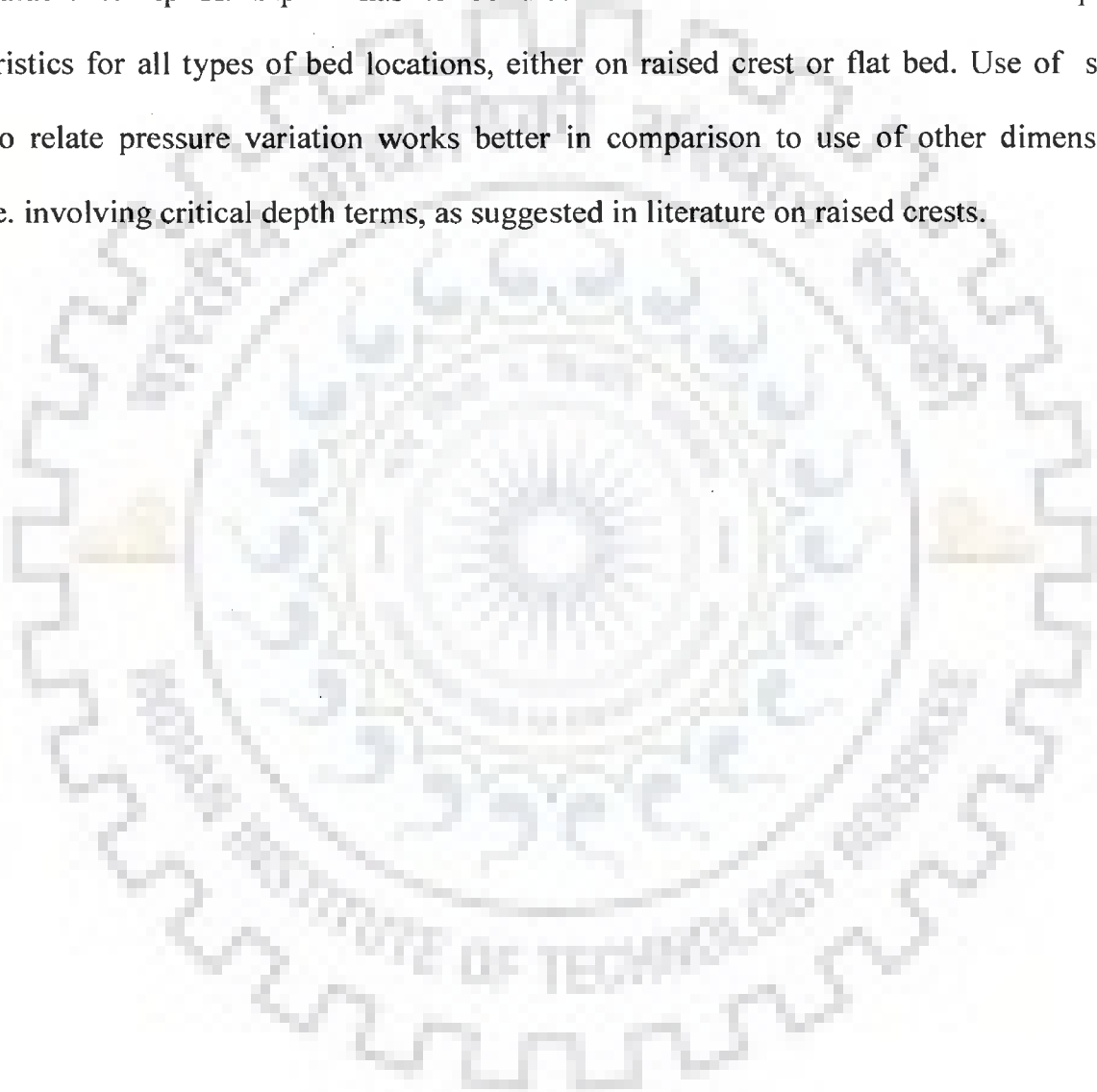


Fig. 7.10 d: P/a versus E/a variation for lip H on flat bed

From Figs. 7.10 a-d, it is observed that P/a plot is having well defined variations in certain situations. For example, in Fig. 7.10 b for ogee crest type 2H:3V, there is very less scatter between P/a versus E/a plot. Thus, a comparison of different dimensionless plots does suggest the superiority of P/a versus E/a plot over other dimensionless plots.

## 7.6 SUMMARY

In this chapter, pressure characteristics of different stream lined shapes have been investigated. Of the various lip types, use of lip type H and K are recommended in case of gates located above raised crests as well as plane bed. In plane or flat bed, lip G also works well and its performance is comparable to lip H. Lip N has to be discarded in view of its non-uniform pressure characteristics for all types of bed locations, either on raised crest or flat bed. Use of specific energy to relate pressure variation works better in comparison to use of other dimensionless terms, i.e. involving critical depth terms, as suggested in literature on raised crests.



---

**EVALUATION OF PERFORMANCE OF LIPS**

---

**8.1 INTRODUCTION**

In the preceding chapters, discharge and pressure characteristics of non streamlined lip shapes(chapters 4 and 5) and streamlined lip shapes (chapters 6 and 7) have been analyzed for various bed types. In this chapter, the evaluation of performance of the same has been presented.

**8.2 METHODOLOGY**

To gauge the overall effectiveness of a lip shape, three criteria have been chosen: (1) Discharge Coefficient (2) Ratio of Observed to Hydrostatic Pressure at lip of gate bottom, and (3) Uniformity of pressure along the thickness of lip. The basic premise is that a lip with maximum discharge coefficient, least ratio of observed to hydrostatic pressure and uniformity of pressure distribution along the thickness is the best available option. To make comparisons, scores are allotted on a scale of zero to ten for these three criteria within the maximum and minimum values for each criteria. The lips were scrutinized using summary diagrams of discharge coefficient, ratio of observed to hydrostatic pressure and uniformity of pressure. The lips were given ranks on the basis of their relative behavior.

**8.3 EVALUATION OF LIP TYPES**

Table 8.1a-h show the necessary computations for non-stream lined (Tables 8.1a-d) and stream lined lips (tables 8.1e-h) on different bed types. Similarly, Figs. 8.1-h show the corresponding score of different lips under different bed conditions for non-stream lined lip types (Figs. 8.1a-d) and stream lined lips (Figs. 8.1e-h).

To assign the scores for  $C_d$ , the following methodology is adopted. The lower and upper ranges of  $C_d$  are used to assign lowest score of 1 and highest score of 10. Intermediate variations of  $C_d$  have been interpolated. For other parameters, similar procedure has been followed and thus for three parameters, a score has been assigned out of 30. For example. With reference to table 8.1a, for lip a, the sum of scores is 20 out of 30 which equals 6.67 on a scale of 10. It is possible that one may use different scales and different ways of adding the scores, however, for simplicity, a procedure based on equal weightage to all the parameters is suggested.

Table 8.1a : Overall score for different non-streamlined lips on a bed type (1H:3V)

<b>1H:3V</b>	Lip A	Lip B	Lip C	Lip D	Lip E	Lip M
Cd	8	6	10	2	4	1
h/h <sub>o</sub>	2	1	8	6	4	10
Uniformity	10	10	8	10	6	4
Sum Total	20	17	26	18	14	15
Cumulative Score	6.666667	5.666667	8.666667	6	4.666667	5

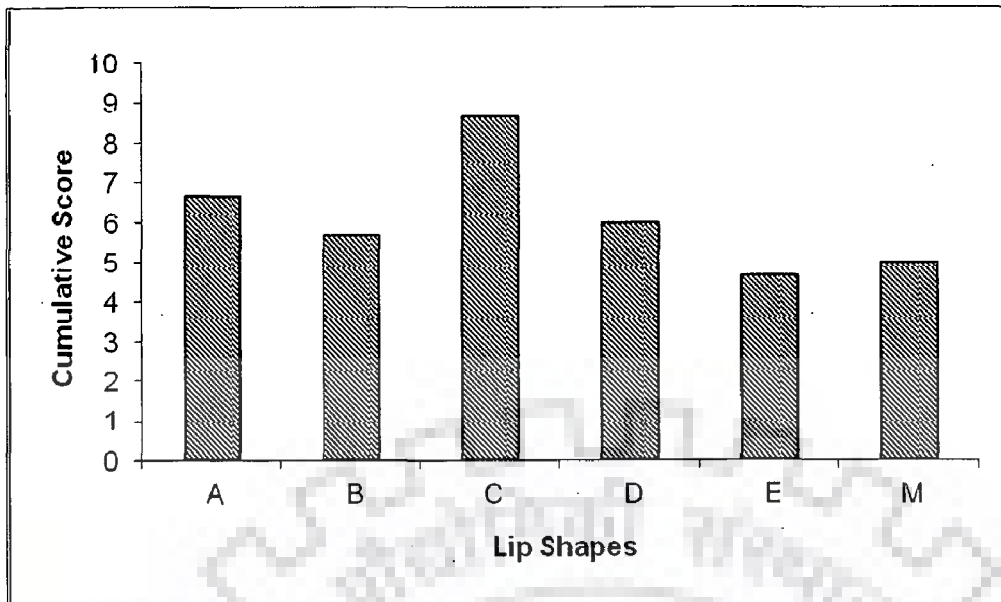


Fig 8.1a : Overall score for different non-streamlined lips on a bed type (1H:3V)

Table 8.1b : Overall score for different non-streamlined lips on a bed type (2H:3V)

2H:3V	Lip A	Lip B	Lip C	Lip D	Lip E	Lip M
Cd	1	8	10	2	4	6
h/h <sub>o</sub>	2	1	8	6	4	10
Uniformity	8	10	10	10	10	1
Sum Total	11	19	28	18	18	17
Cumulative Score	3.666667	6.333333	9.333333	6	6	5.666667

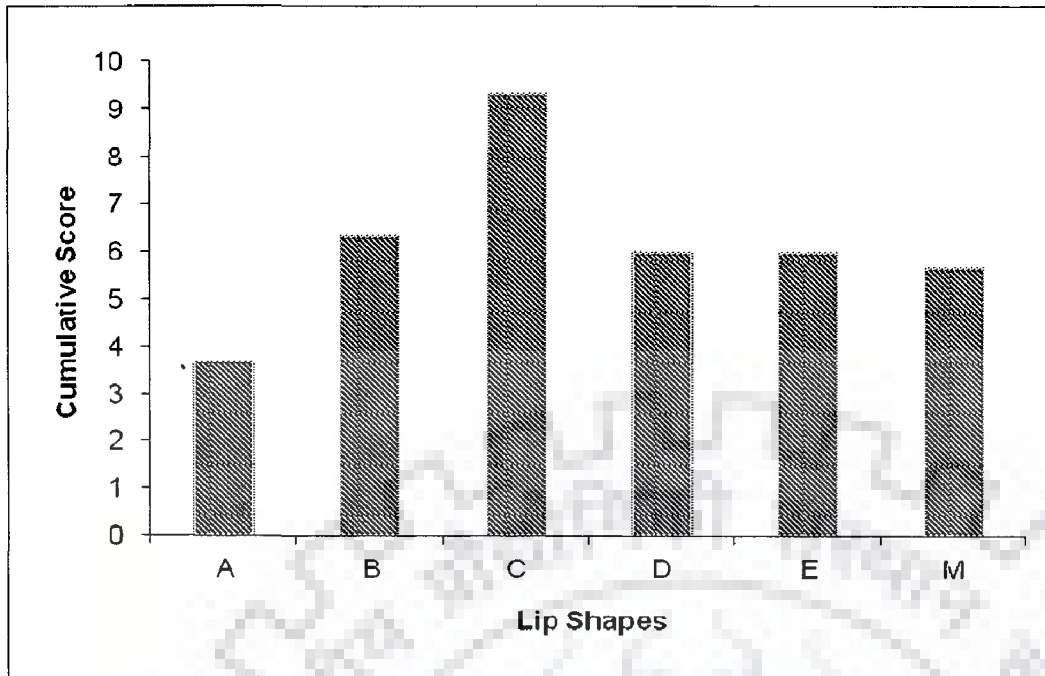


Fig 8.1b : Overall score for different non-streamlined lips on a bed type (2H:3V)

Table 8.1c : Overall score for different non-streamlined lips on a bed type (vertical)

Vertical	Lip A	Lip B	Lip C	Lip D	Lip E	Lip M
Cd	6	8	10	2	6	2
h/h <sub>o</sub>	4	6	8	8	2	10
Uniformity	10	8	8	8	8	1
Sum Total	20	22	26	18	16	13
Cumulative Score	6.666667	7.333333	8.666667	6	5.333333	4.333333

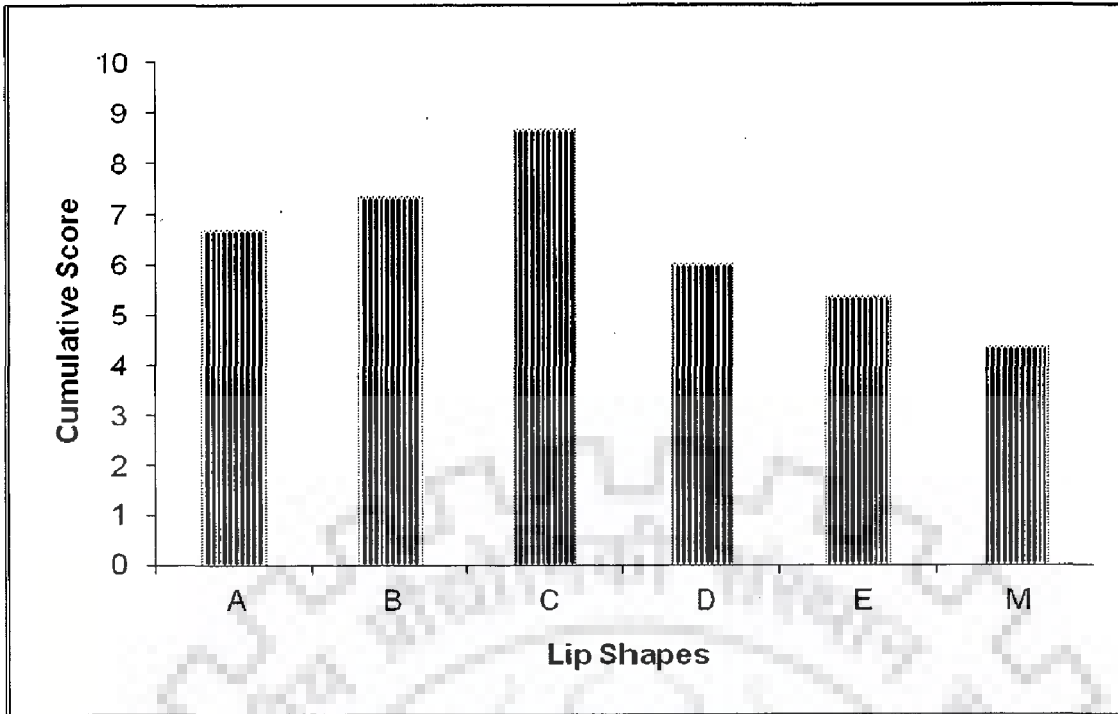


Fig 8.1c : Overall score for different non-streamlined lips on a bed type (vertical)

Table 8.1d : Overall score for different non-streamlined lips on a bed type (plane bed)

Plane Bed	Lip A	Lip B	Lip C	Lip D	Lip E
Cd	2	8	10	6	4
$h/h_o$	2	6	8	10	4
Uniformity	2	6	10	8	4
Sum Total	8	20	28	24	12
Cumulative Score	2.666667	6.666667	9.333333	8	4

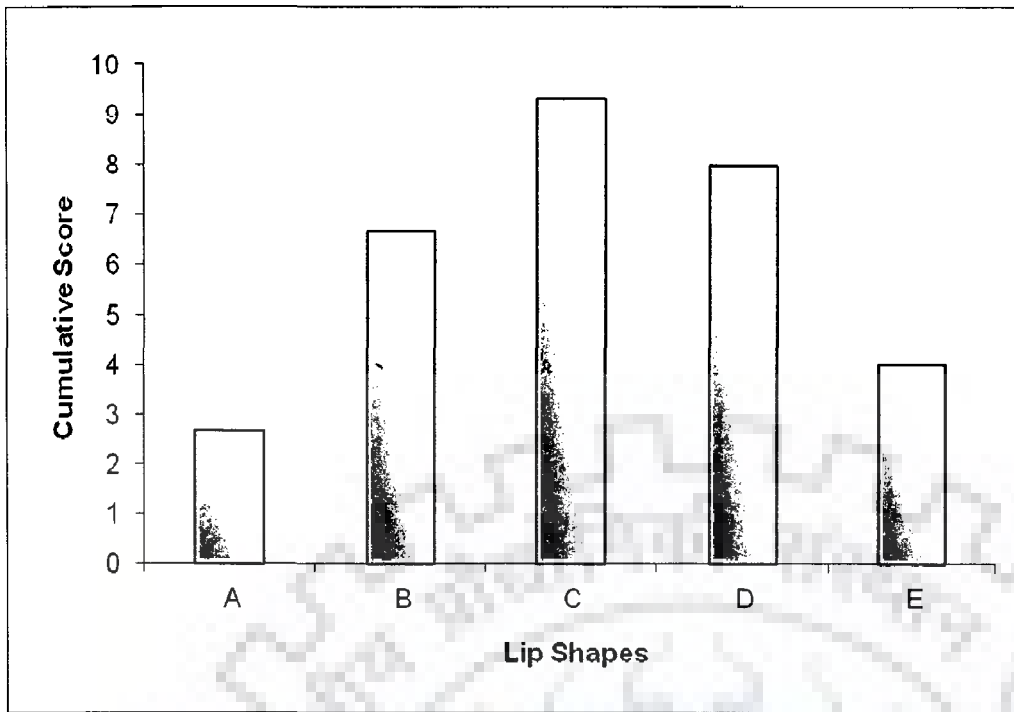


Fig 8.1d : Overall score for different non-streamlined lips on a bed type (plane bed)

The above figures(Figs.8.1a-d) and tables(tables Figs.8.1a-d) show that for the given bed types, lip C shows the best results of all the non-streamlined lip shape types.

Table 8.1e : Overall score for different -streamlined lips on a bed type (1H:3V)

1H:3V	Lip F	Lip G	Lip H	Lip I	Lip J	Lip K	Lip L	Lip N
Cd	6	4	1	2	8	10	4	1
h/h <sub>o</sub>	0	2	8	0	6	4	1	10
Uniformity	10	10	8	6	4	6	4	2
Sum Total	16	16	17	8	18	20	9	13
Cumulative Score	5.333333	5.333333	5.666667	2.666667	6	6.666667	3	4.333333



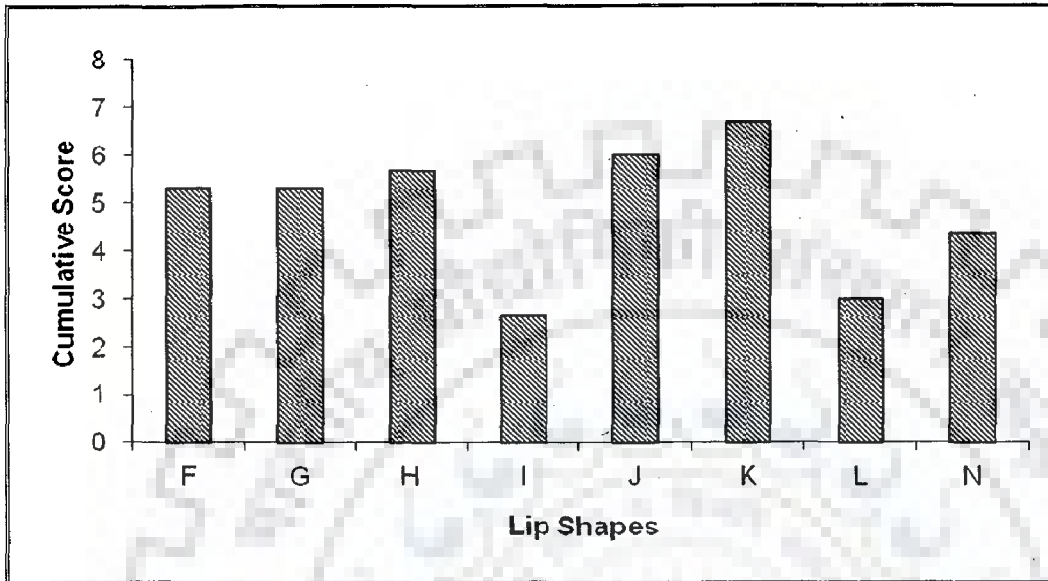


Fig 8.1e : Overall score for different -streamlined lips on a bed type (1H:3V)

Table 8.1f : Overall score for different streamlined lips on a bed type (2H:3V)

2H:3V	Lip F	Lip G	Lip H	Lip I	Lip J	Lip K	Lip L	Lip N
Cd	8	2	0	1	8	10	4	6
h/h <sub>o</sub>	0	2	8	4	8	6	1	10
Uniformity	8	10	10	8	8	10	10	1
Sum Total	16	14	18	13	24	26	15	17
Cumulative Score	5.333333	4.666667	6	4.333333	8	8.666667	5	5.666667

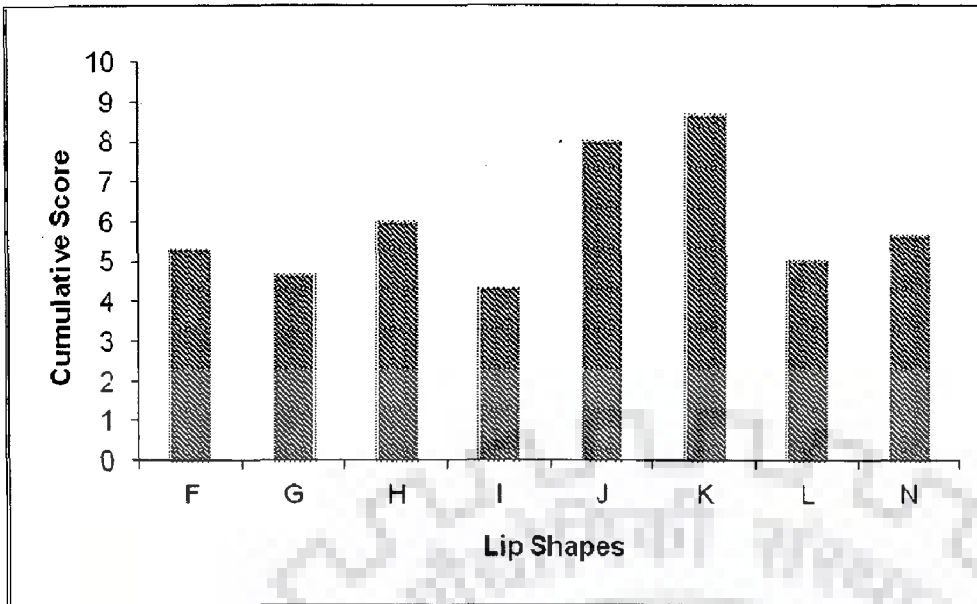


Fig 8.1f : Overall score for different streamlined lips on a bed type (2H:3V)

Table 8.1g : Overall score for different streamlined lips on a bed type (Vertical upstream face)

Vertical	Lip F	Lip G	Lip H	Lip I	Lip J	Lip K	Lip L	Lip N
Cd	6	6	2	4	8	10	10	8
h/h <sub>o</sub>	2	1	8	4	8	6	4	10
Uniformity	8	10	10	8	6	8	8	1
Sum Total	16	17	20	16	22	24	22	19
Cumulative Score	5.33333 3	5.66666 7	6.66666 7	5.33333 3	7.33333 3	8.00000 8	8.33333 3	6.33333 3

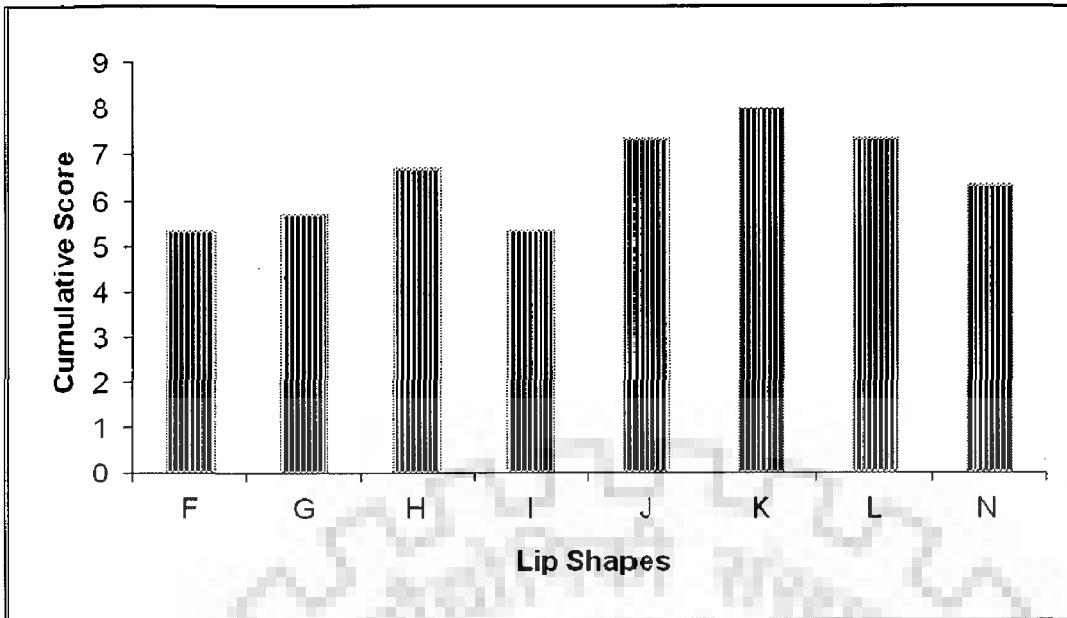


Fig 8.1g : Overall score for different streamlined lips on a bed type (Vertical upstream face)

Table 8.1h : Overall score for different streamlined lips on a bed type (plane bed)

Plane Bed	Lip F	Lip G	Lip H	Lip I	Lip J	Lip K	Lip L
Cd	10	6	4	8	2	4	1
$h/h_0$	2	6	4	4	8	8	10
Uniformity	6	4	1	6	8	10	8
Sum Total	18	16	9	18	18	22	19
Cumulative Score	6	5.333333	3	6	6	7.333333	6.333333

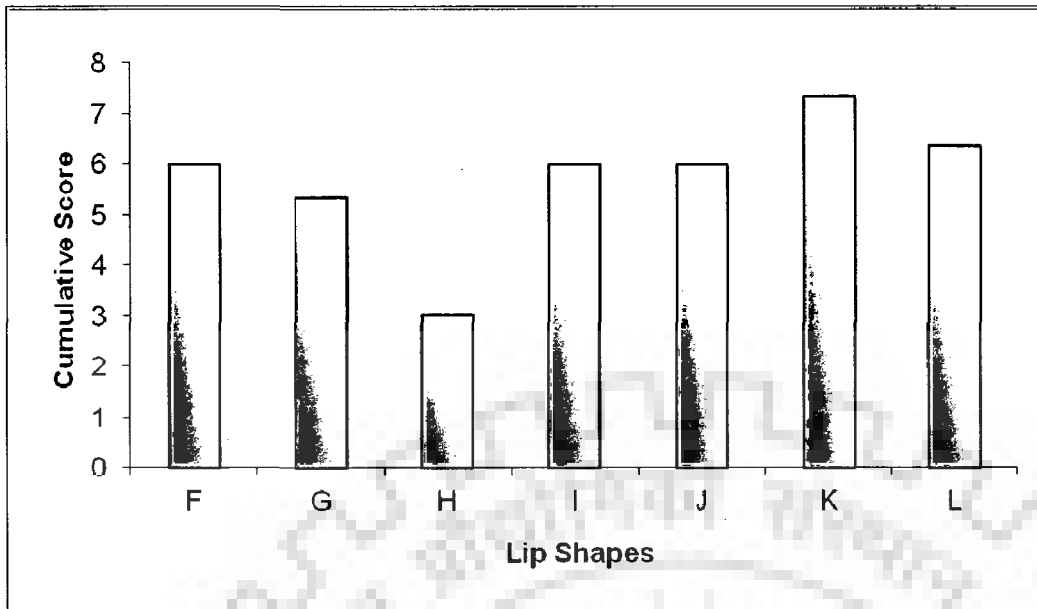


Fig 8.1h : Overall score for different streamlined lips on a bed type (plane bed)

As per the above tabulation and charts, it can be seen that of all the streamlined lip types, lip K has the best characteristics for the given bed types.

#### 8.4 RANKING OF LIP SHAPES

The ranking of the lip shapes is done here based on the consolidated scores assigned in the previous section. The table 8.2 and Fig 8.2 show the ranking of streamlined lips for various bed types and the better performance of lip K is evident from Fig. 8.2. Similarly, Fig. 8.3 shows the variation for non streamlined lips.

Table 8.2: Ranking Of Streamlined Lips

Lip Shapes	1H:3V	2H:3V	Vertical	Plane bed
F	5.33	5.33	6.67	6
G	5.33	4.67	7.33	5.33
H	5.67	6	8.67	3
I	2.67	4.33	6	6
J	6	8	5.33	6
K	6.67	8.67	4.33	7.33
L	3	5		6.33
N	4.33	5.67		

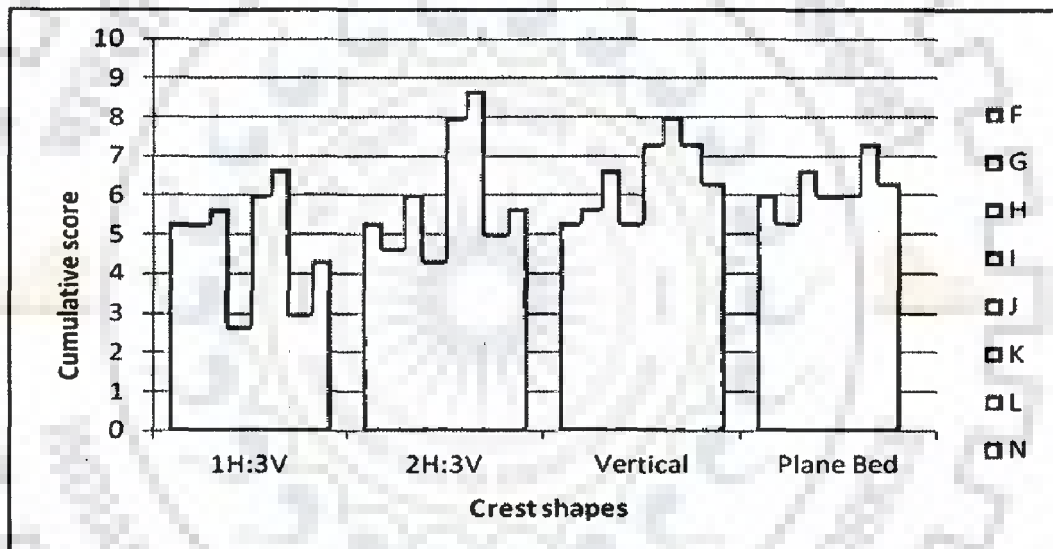


Fig. 8.2: Comparative Performance Chart Of Streamlined Lips.

Table 8.3: Ranking Of Non Streamlined Lips

lip Shapes	1H:3V	2H:3V	Vertical	Plane bed
A	6.67	3.67	6.67	2.67
B	5.67	6.33	7.33	6.67
C	8.67	9.33	8.67	9.33
D	6	6	6	8
E	4.67	6	5.33	4
M	5	5.67	4.33	

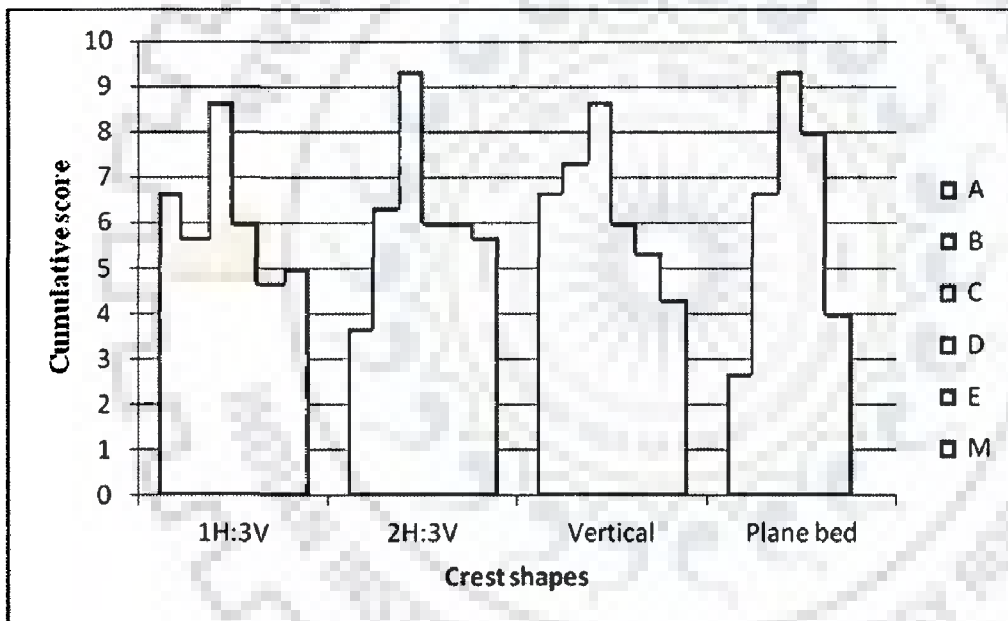


Fig. 8.3: Comparative Performance Chart Of Non Streamlined Lips.

The performance of the lip shapes is evaluated based on the above tabulated scores. For the streamlined lips, lip K showed minimum uplift pressure, maximum  $C_d$  and uniformity of pressure at the bottom of the lips and similar output performance was shown by lip C for non streamlined lips.

---

## CONCLUSIONS

---

### 9.1 INTRODUCTION

The present work has been mainly an experimental investigation with the broad objectives of studying the discharge and pressure characteristics of various types of non-stream lined and stream lined lip shapes. These lips have been placed at the gate bottom and experiments have been conducted in total for fourteen lip types and four bed conditions including three raised ogee crests, marked by variations in the upstream face and one plane bed. Experiments on certain lip types, such as M and N were not extensive as it was observed that these always lead to non-uniform pressure distributions about the base. Similarly, plane bed experiments were not extensive when it was observed that higher discharge coefficients were obtained in the case of weirs located above raised crest. Thus, based on the analysis of these experiments, the following can be inferred:

#### 9.1.1 Variation of Discharge Coefficient

- Discharge coefficient depends on the lip type and bed type below the gate. This is found to vary with the relative gate opening and in general, it has a decreasing trend with the increase in relative gate opening.
- Discharge coefficient relationships proposed by Swamee (1992), Roth and Hager (1999) and Habibzadeh et al. (2011) represent similar type of functional form when certain simplifying assumptions are invoked. Habibzadeh et al. (1992) approach seems to be

more general as it is represented by a third order polynomial variation. The relationships of Swamee, and Roth and Hager are represented by a second order polynomial.

- Discharge coefficient variations are not well predicted using the existing relationships in view of the lip effects. To account for lip effects, correction factors are developed which when multiplied with the existing relationships of discharge coefficient lead to a better match with the observed values of discharge coefficient.
- Among non-streamlined lip types, lip C is found effective as leads to higher coefficient of discharge than other non-streamlined lip types for a given relative gate opening.
- Among stream lined lip shapes, lips H and K are found effective as these lead to higher coefficient of discharge than other stream lined lip types for a given relative gate opening.
- The discharge coefficient is found to be higher when the gate is located above raised crest than the plane bed. This behavior is observed for all the lip types.

### **9.1.2 Variation of Pressure**

- The ratio of observed to hydrostatic pressure is found below one. This is influenced by the type of bed profile. For example: type 2H: 3V experiences lesser pressure than type 1H: 3V and upstream face vertical. Thus, the increase in the slope of upstream face has been found to cause an increase in the ratio of observed to hydrostatic pressure.
- Ratio of observed pressure ( $P$ ) to gate opening ( $a$ ) shows an increasing trend with the ratio of upstream specific energy ( $E$ ) to gate opening.
- When the upstream velocity head is negligible, a relationship is developed to relate  $P/a$  versus  $E/a$  variations in terms of ratio of observed to hydrostatic pressure versus relative gate opening.



- Lip type M and N experience too much too much non uniformity in the pressure distribution along the lip width. Such type of profiles should be discarded in practice, because this will lead to vibrations of the gate.
- In case of lips C (non-stream lined lip ), lip H and lip K (streamlined lip), the pressure variations are found to be uniform along the lip width.

### 9.1.2 Ranking of Lips

Using the Cd variation, ratio of observed to hydrostatic pressure and uniformity of pressure variation, scores are assigned to rank performance of various lip shapes. Among non-stream lined lips, lip C having an inclination of 45 degree from horizontal is found to score better than other lip shapes. Among stream-lined lip shapes, lip K and H do better. Overall, lip C scores more than lip K and H. Considering that score assignment may be subjective, it is possible that scores may vary for these lips. However, a comparative evaluation among the lips tested in this work is expected to be not sufficiently very different than concluded in favour of lips C, K and H.

### 9.2 LIMITATIONS OF THE STUDY AND FUTURE WORK

- It is possible that certain errors in collection of discharge might have been introduced because of measurement over V-notch. However, this will not change the conclusions regarding relative ranking of lips. Nevertheless, there may be a need to go for advanced discharge measurement techniques.
- It is also possible that certain errors might have crept in during measurements of particularly smaller opening, which might have slightly influenced the computations of observed coefficient of discharge. This error may be more pronounced at lesser values of relative gate opening.

- It was planned to do shifting of gate locations and see the corresponding effect on pressure and discharge characteristics. Certain observations did show further increase in discharge coefficient as a result of this shift. More work on this may be planned for future.



---

## BIBLIOGRAPHY AND REFERENCES

---

1. Akoz, M., Kirkgoz, M., and Oner, A. (2009). "Experimental and numerical modeling of a sluice gate flow." *J. Hydraul. Res.*, 47(2), 167–176.
2. Alhamid, A.A., Negm, A.M. and Al-Brahim, A.M.,(1997),"Discharge Equation for Proposed Self-Cleaning Device", Journal of King Sand University, Engineering ,Science, Riyadh, Saudia Arabia, Vol.9,No.1, pp.13-24.
3. Alminagorta, O., and Merkley, G. P. (2009). "Transitional flow between orifice and nonorifice regimes at a rectangular sluice gate." *J. Irrig. Drain Eng.*, 135(3), 382–387.
4. Ansar, M. (2001). "Discussion of 'Simultaneous flow over and under a gate' by V. Ferro." *J. Irrig. Drain Eng.*, 127(5), 325–326.
5. Ansar, M. and Chen, Z.(2009). "Generalized Flow Rating Equations at Prototype Gated Spillways." *Journal of Hydraulic Engineering*, Vol. 135, No. 7, July 2009, pp. 602-608.
6. Barghei, Jalili, Ghodsian M. (1999) "Discharge coefficient for sharp crested weir in sub critical flow" *ASCE Hy. Eng.*, vol 125 (10) oce 1999, pp 1051-1056.
7. Belaud, G., Cassan, L., and Baume, J.-P. (2009). "Calculation of contraction coefficient under sluice gates and application to discharge measurement." *J. Hydraul. Eng.*, 135(12),1086–1091.
8. Belaud, G., and Litrico, X. (2008). "Closed-form solution of the potential flow in a contracted flume." *J. Fluid Mech.*, 000, 1–9.
9. Benjamin, T. B. (1956). "On the flow in channels when rigid obstacles are placed in the stream." *J. Fluid Mech.*, 1, 227–248.
10. Binnie, A. (1952). "The flow of water under a sluice gate." *Q. J. Mech.Appl. Math.*, 5, 395–407.

11. Bearman, P.W., (1971) "An investigation of the forces on flat plates normal to a turbulent flow," journal of fluid mechanics, London, England, vol 46, pp 177-198.
12. Bearman P.W., (1972) "Some measurements of distortion of turbulence approaching a two dimensional bluff bodyb," journal of fluid mechanics,London, England, vol 53, pp 451-467.
13. Bergholz J, (1981) "Bestimmung der turbulence and Geschwindigkeitsverteilungen mittels laser Doppler aneometrie und deren einfluss auf die druckverteilung an einem understromen schutzmodell," vertiferarbeit No. 483, Institute of Hydromechanik Universitat Karlsruhe,Germany.
14. Bombardelli, F. A., Hirt, C. W., and García, M. H. (2001). "Discussion on 'computations of curved free surface water flow on spiral concentrators'." J. Hydraul. Eng., 122(7), 629–630.
15. Bos, M. (1989). Discharge Measurement Structures. Third edition. International Institute for Land Reclamation and Improvement. Wageningen, The Netherlands.
16. Buyalski, C.P. (1983), " Discharge alogarthims for canal Radial Gates", REC-ERC, 83-,Engineering and Research centre, U.S.Bureau of Reclamation, Denver.
17. Carollo, F. G., Ferro, V., and Termini, D. (2002). "Flow velocity measurements in vegetated channels." J. Hydraul. Eng., 128(7), 664–673.
18. Cassan, L. and Belaud, G., (2010). "Experimental and numerical studies of the flow structure generated by a submerged sluice gate." Proc. 1st Eur. IAHR Cong., Edinburgh, UK.
19. Cassan, L. and Belaud, G. (2008). "Rans simulation of the flow generated by sluice gates." Hydraulic structure : proc. 2nd Int. Junior Res. and Eng. Workshop on Hydraulic Structure (IJREW'08), S. Pagliara (ed.), Pisa, Italy. 217–225.

20. Castro-Orgaz, O., Lozano, D., and Mateos, L. (2010). "Energy and momentum velocity coefficients for calibrating submerged sluice gates in irrigation canals." *J. Irrig. Drain. Eng.*, 136(9), 610–616.
21. Cheng, A.H.D., Liggett, J.A., and Liu, P. (1981). "Boundary calculations of sluice and spillway flows." *J. Hydraulics Div.*, ASCE, Vol. 107, No. 10, pp. 1163-1178.
22. Cherry N.J., Hitler R., (1983), "the unsteady structure of two dimensional separated and reattaching flow", *Journal of wind engineering and industrial Aerodynamics*, 11, 95-105.
23. Chung, Y. (1972). "Solution of flow under sluice gates." *J. Engrg. Mech. Div.*, 98(1), 121–140.
24. Clemmens, A. J., Strelkoff, T., and Repogle, J. (2003). "Calibration of submerged radial gates." *J. Hydraul. Eng.*, 129(9), 680–687.
25. Clemmens A.J., Wahl, T.L., Bos, M.G. and Replogle, J.A. (2001) , " Water measurements with flumes and weirs" , Publication-58 International Institute for land reclamation and improvement, Wageningen. The Netherland.
26. Cruise J.F., Sheriff M.M., Singh V.P. (2006) "Elementary Hydraulics", Thomson Nelson,
27. Department of army, engineer manual EM 1110-2-1602, 1963. Hydraulic design of reservoir outlet structures.
28. De Vries F. (1988), "Model study on the emergency closure of a high head wheel gate" *Proceedings of the int. symposium on model prototype correlation of hydraulic structures*" ASCE, Colorado Springs, Colorado, pp 325-333.
29. Defina, A., and Susin, F. (2003). "Hysteretic behavior of the flow under a vertical sluice gate." *Phys. Fluid.*, 15(9), 2541–2548. Fluent Inc. (2006). "FLUENT 6.3 User's Guide"
30. Dhillon, G.S. (1978), "Modern Trends in Design and Research of Highhead Gates With Reference to Downpull" , All India Seminar on Hydraulic Gates, Hyderabad.

31. Ouma J.H.,( 1951) “Hydraulic design of slide, vertical lift and tainter gates,” International conference on large dams.
32. “Downpull and vibration studies on high head gates” poondi irrigation research station India. 32<sup>nd</sup> research committee meeting, central board of irrigation and power,1962
33. Durst F., Schmitt F.,(1985),”Experimental studies of high Reynolds no. backward facing step flow”, proceedings of 5<sup>th</sup> symposium on turbulent shear flow, Cornell University, USA.
34. Falvey, H.T. (1980), “Air, water flow in hydraulic structures”, U.S. Deptt. of interior, water and power resources service, Engineering Monograph No-41
35. Fangmeier, D., and Strelkoff, T. (1968). “Solution for gravity flow under a sluice gate.” *J. Engrg. Mech. Div.*, 94(EM1), 153–176.
36. Ferro, V. (2000). “Simultaneous flow over and under a gate.” *J. Irrig. Drain Eng.*, 126(3), 190–193.
37. Ferro, V. (2001). “Closure to ‘Simultaneous flow over and under a gate’ by V. Ferro.” *J. Irrig. Drain Eng.*, 127(5), 326–328.
38. Franke, J., Hirsch, C., Jensen, A., Krus, H., Schatzmann, M., Westbury, P., Miles, S., Wisse, J., and Wright, N. (2004). “Recommendations on the use of CFD in wind engineering.” The International Conference Urban Wind Engineering and Building Aerodynamics, von Karman Institute.
39. Frizell, K.B. (1988), “Prototype tests of an emergency gate closure” Proceedings of the int. symposium on model prototype correlation of hydraulic structures” ASCE, Colorado Springs, Colorado, pp 373-380.
40. Garbrecht, G. (1977). “Discussion of ‘Discharge computations at river control structures’ by L. Dannie.” *J. Hydr. Div.*, 103(2), 1481–1484.

41. Garcia, C., Cantero, M., Nino, Y., and Garcia, M. (2007). "Closure to "turbulence measurements with acoustic doppler velocimeters"." J. Hydraul. Eng., 133(11), 1289–1292.
42. Gartshore I.S., "the effects of free stream turbulence on the drag of rectangular two dimensional prisms," research report BLWT-4-73, boundary layer wind tunnel laboratory, faculty of engineering science , univ. of western Ontario, Ontario, Canada, 1973
43. Ghodsian, M. , Borghei, S.M. and Jalili M.R. (1999), " Discharge Coefficient for sharp crested side weir in sub critical flow" ASCE J. of Hydraulic Eng. Vol 125 No-10 pp 17141
44. Gole, C.V., Desai S.C. and Patnage, P.M. (1969). "Flow conditions and study of non-closure of emergency gates for diversion tunnel at elevation 91.44 m, nagarjun-sagar dam project, Andhra Pradesh." Proc. 39<sup>th</sup> Ann. Res. Sess. Of central board of Irrigation and power, new delhi (India), vol. 1-A (hydr), 72-87.
45. Habibzadeh, A., Vatankhah, Ali R. and Rajaratnam, N. (2011). "Role of Energy Loss on Discharge Characteristics of Sluice Gates." Journal of Hydraulic Engineering, Vol. 137, No. 9, September 2011, pp. 1079-1084
46. Hager, W.H. and Roth, A. (1999), "Underflow of standard sluice gate" Exp. Fluids 27, pp 339-350.
47. Henderson, F. M. (1966). Open channel flow, Macmillan, New York.
48. Henry, H. (1950), "Discussion: diffusion of submerged jets" Trans. Am soc Civ. Eng., 687-697.
49. Hirt, C. and Nichols, B. (1981). "Volume of fluid (VOF) method for the dynamics of free boundaries." J. Comput. Phys., 39(1), 201–225.
50. "Hydraulic design of reservoir outlet structures,": "Department. of army engineering manual EM 1110-2-1602, 1963.

51. "Hydraulic model studies of downpull forces that act on palisades type regulating gate and glendo type fixed wheel gate," US Bureau of reclamation , hydraulic laboratory report no. hyd 421 1957.
52. "Hydraulic model studies of 7ft 6in X 9ft palisades regulating gate," US bureau of reclamation, hydraulic lab report no. hyd-387 1954.
53. "Hydraulic downpull forces on large gates," US bureau of reclamation, report no-4 166.
54. "Hydraulic model study of penstor coaster gates," US bureau of reclamation hyd 130
55. "Hydraulic model studies of diversion tunnel coaster gates, Shasta dam," US bureau of reclamation, lab report no 107, 1942.
56. Issacs, L.T. and Allen P.H. (1994), "Contraction coefficient for Radial sluice Gates" , Proc. 1994 int. conference on hydraulics in civil engg., National conf. publ.no. 94/1, Institution of engineers,Barton ACT Astralia 262-265.
57. Iwasa, Y. (1957). "Boundary layer growth of open channel flows on a smooth bed and its contributions to practical application to channel design." *Memoirs of Fac. of Engrg.*, Kyoto Univ., Kyoto, Japan, 19(3), 229-254.
58. Kavianpour M.R., (2000)), "Effect of air on the structure of flow downstreams of ramp", 4<sup>th</sup> international conference on hydroscience engineering, Seoul,Korea.
59. Kavianpour M.R.,Khosrojerdi A.,(2001),"Review the physical model studies of new bottom outlet in Iran, proceeding of 29<sup>th</sup> IAHR Congress, Beijing,China
60. Khosrojerdi and Kavianpour (2003), "Experimental Investigation of Pressure Distribution In Bottom Outlet Lift Gate", Proceeding of waterpower XIII Congress, New York,Buffalo,USA.
61. Khosrojerdi (2003), "Determination of Downpull Force in Bottom Outlet Lift Gate Base on Hydraulic Model Studies", national conference on hydropower, Tehran, Iran.



62. Kim, D. (2007). "Numerical analysis of free flow past a sluice gate." *KSCE J. Civil Eng.*, 11,127–132.
63. Knight, D. W., Demetriou, J. D., and Hamed, M. E. (1984). "Boundary shear in smooth rectangular channels." *J. Hydr. Engrg.*, ASCE, 110(4), 405-422.
64. Larock, B. (1969). "Gravity-affected flow sluice gate." *J. Hydr. Div.*, 95(HY4), 153–176.
65. Launder, B. (1989). "Second-moment closure: present... and future?." *Int. J. Heat Fluid Flow*, 10(4), 282–300.
66. Launder, B. and Spalding, D. (1974). "The numerical computation of turbulent flows." *Comput. Meth. Appl. Mech. Eng.*, 3(2), 269–289.
67. Leutheusser, H. J., and Kartha, V. C. (1972). "Effect of inflow condition on hydraulic jump." *J. Hydr. Div.*, ASCE, 98(8), 1367-1385.
68. Lin, C. H., Yen, J. F., and Tsai, C. T. (2002). "Influence of sluice gate contraction coefficient on distinguishing condition." *J. Irrig. Drain Eng.*, 128(4), 249–252.
69. Lozano, D., Mateos, L., Merkley, G. P., and Clemmens, A. J. (2009). "Field calibration of submerged sluice gates in irrigation Canals." *J. Irrig. Drain. Eng.*, 135(6), 763–772.
70. Ma, F., Hou, Y., and Prinos, P. (2001). "Numerical calculation of submerged hydraulic jumps." *J. Hydraulic Research*, 39(5), 493–501.
71. Marchi, E. (1953). "Sui fenomeni di efflusso piano da luci a battente." *Ann. Mat. Pura Appl.*, 35(1), 327–341 (in Italian).
72. Masliyah, J.H., Nandakumar, K., Hemphill, F., and Fung, L. (1985). "Body fitted coordinates for flow under sluice gates." *J. Hydraulic Eng.*, ASCE, Vol. 111, No. 6, pp. 922-933.
73. Montes J.S. (1997), "Irrotational flow and real fluid effects under planner sluice gates", *J. of Hydraulic Eng.*, 123(3), 219-232

74. Montes J.S. (1999), Closure to "Irrotational flow and real fluid effects under planar sluice gates", *J. of Hydraulic Eng.*, 125(2), 212-213
75. Narayan N., Kavianpour M.R.,(2000)," wall pressure field in the reattaching flow past deflectors-without aeration",*Proc. Institute of civil engineers, Water and Maritime engineering, London* ,142,79-86.
76. Narayan R., Reynolds A.J., (1972), "reattaching flow downstream of leaf gate", *journal of hydraulic division*, 98(HY5), 913-934.
77. Narsimhan S., Bhargava V.P., (1989)," pressure fluctuation on gates ",*Journal of hydraulic research*, 27(2),215-231.
78. Naudascher E., (1984)," scale effects in model tests",*proceeding IAHR symposium on scale effects in modeling hydraulic structures*, H.Kobus (ed), Institut für Wasserbau, Universität Stuttgart, Germany, Paper 1-1.
79. Naudascher, E. (1991), "Hydrodynamic Forces" *IAHR Structures Design Manual*, International Association of Hydro Research, Stockholm, Sweden.
80. Negm, A.M.; Abdellatef, M. and Owais, T.M., (1993) " Effect of under gate sill crest shapes on the flow characteristics" *Proc. of AEIC-93*, 18-21 Dec., Faculty of Eng., Al-Azhar University, Naser City, Cairo , Egypt, vol. 4, pp 230-241.
81. Negm, A.M. (1995), " Free and Submerged Flow Below Sluice Gate with Sill." *Proc. of ICHE-95 Conf.* 22-26 March, Beijing, China, Vol. II pp. 283-300.
82. Nezu, I. and Nakagawa, H. (1993). *Turbulence in open-channel flows*. A. A. Balkema; IAHR Monograph Series.
83. Ohtsu, I., Yasuda, Y., and Awazu, S. (1990). "Free and submerged hydraulic jump in rectangular channels." *Report No. 35*, Res. Inst. of Sci. and Tech., Nihon Univ., Tokyo, Japan, 1-50.

84. Ohtsu, I., Yasuda, Y., and Yamanaka, Y. (1992). Reply to discussion of "Drag on vertical sill of forced jump." *J. Hydr. Res.*, Delft, the Netherlands, 30(2), 277-288.
85. Ohtsu, I. and Yasuda, Y., (1994). Characteristics of supercritical flow below Sluice Gate. *J. Hydr. Engg., Proc. ASCE*, 120-3 March pp332-346
86. Paul, T.C. and Dhillon, G.S. (1986). "Dimensionless vertical lift gates". *Int. water pow. And dam constr.*, 38(11) 45-47.
87. Peter M. and Smith, "Hydraulic downpull on lee harbour power house gate. A paper presented at the may 1963 ASCE water resources engineering conference.
88. Poondi irrigation research station, India 32<sup>nd</sup> research committee meeting, central board of irrigation and power, 1962. Downpull and vibrational studies on high head gates.
89. Rangaraju, K.G. and Visavadia, D.S. (1979). "Discharge characteristics of a sluice gate located on a raised crest." *Proc. IMEKO in Industry Tokyo, Japan, Nov.*, pp.39-43.
90. Rajaratnam, N. and Humphries, J. (1982). "Free flow upstream of vertical sluice gates." *J. Hydraul. Res.*, 20(5), 427-437.
91. Rajaratnam, N. (1977). "Free flow immediately below sluice gates." *J. Hydr. Div., ASCE*, 103(4), 345-351.
92. Rajaratnam, N. and Subramanya, K. (1967). "Flow equation for the sluice gate." *J. Irrigation and Drainage Eng.*, ASCE, Vol. 93, No. 3, pp. 167-186.
93. Rao, P.V. (1968) "Boundary layer development at curved conduit entrances" *Proceedings of ASCE, J. of Hydraulic Div.* vol 94 no HY 1 January 1968 pp 195
94. RAO R.P.R., "effect of gate and conduit geometry upon the hydrodynamic forces acting on high head gates," Thesis state university of Iowa, USA 1963.

95. Robertson, J.A. and Crowe, C.T. (1993). *Engineering Fluid Mechanics*, 5th edition, Houghton Mifflin, Boston, MA.
96. Robertson R.A and Ball J.W.” Model study poer intake gate of mussy rock dam” journal of hydraulic division,proceedings of ASCE, July 1971.
97. Rodi, W. (1984). “Turbulence models and their application in hydraulics.” IAHR, Delft, the Netherlands.
98. Roth, A. and Hager, W. (1999). “Underflow of standard sluice gate.” *Exp. Fluids.*, 27(4), 339–350.
99. Sagar B.T.A., (1997),” Downpull in high-head gate installation”,Part 1,2 and 3 *Water power and Dam construction* (3-5)
100. Sagar B.T.A.,(1999),” Gate lip hydraulic”,proceedings of 28<sup>th</sup> IAHR Congress, Graz Austria,23-27 August. Venard J., Street R.L.,(1975),*Elementary Fluid Mechanics*, John Wiley and Sons,Inc Sixth Edition.
101. Sagar, B.T.A. (1977), “Downpull in Highhead Gate Installations, Parts 1,2 and 3”, *Water Power and Dam Construction* (3-5).
102. Sagar B.T.A. (1999), “Gate Lip Hydraulic” *Proceedings of 28<sup>th</sup> IAHR Congress, Graz, Austria, 23-27 August.*
103. Sagar, B.T.A.,and Tullis, J.P.(1970).”problems with machinery, equipment and cavitation section , IAHR, Part I, paper F1, 1-8.
104. Sagar B.T.A and Tullis J.P.”problems in recent high head gates installations,” *international association of hydraulic research symposium. Stockholm,Sweden 1970.*
105. Salama, M. (1987), “ Flow Below Sluice Gate with Sill.” *Juornal of Egyptian Society of Engineering*, Vol. 26 No. 4 , pp. 31-36.

106. Savage, B.M. and Johnson, M.C. (2001). "Flow over ogee spillway: Physical and numerical model case study." *J. Hydraulic Eng.*, ASCE, Vol. 127, No. 8, pp. 640-649.
107. Sepúlveda, C., Gómez, M., Rodellar, J., (2009) "Benchmark of Discharge Calibration Methods for Submerged Sluice Gates." *Journal of Irrigation and Drainage Engineering*, Vol. 135, No. 5, September/October 2009, pp. 676-682.
108. Simmons W.P., "Air model studies on large gates," *journal on hydraulics division proceedings of ASCE*, January 1959.
109. Slide Gate Tests of norfok dam" US army corps of engineers, technical memorandum no. 2-389, Waterways experiment station, Vicksburg, Missouri, USA, 1954.
110. Spreeli and Hager (1999), "Discussion: Irrotational flow and real fluid effects under planner sluice gates", *J. of Hydraulic Eng.* 125(2) 210-212.
111. Schlichting, H. (1979). *Boundary-layer theory*. McGraw-Hill, New York, N.Y.
- Tominaga, A., and Nezu, I. (1992). "Velocity profiles in steep open-channel." *J. Hydr. Engrg.*, ASCE, 118(1), 73-90.
112. Swamee P.K. (1992) , " Sluice Gates discharge equations" *J. Irrig. Drainage Eng.*, 118(1) 56-60.
113. Uppal H.L. and Paul T.C., "Design of gate for high head reservoir outlets", *Indian journal of power and river valley development*, October 1964.
114. US army corps of engineers, technical report no. 2-528, waterways experiment station, Vicksburg, Missouri, USA 1959 Spilway and outlet works, fort randall dam.
115. US army corps of engineers technical memorandum No.- 2-389 waterways experiment station, vicksbure, Missouri, USA, 1954. Slide gate tests of Norfok Dam.

116. US bureau of reclamation, hydraulic laboratory report no. Hyd-287, 1954. Hydraulic model studies of 7<sup>th</sup> 6inx2ft palisades regulating gate, Rao, R.P.R. Effect of gate and conduit geometry upon the hydrodynamic forces acting on high head gates, thesis, State University of Iowa, USA 1963.
117. US Bureau of reclamation, laboratory report no. 107, 1942 hydraulic model studies of diversion tunnel coaster gates, Shasta dam.
118. U.S. Bureau of Reclamation (1957), "Model Studies of Hydraulic Downpull Forces That Act on Palisades Type Regulating Slide Gate and on the Glendo Fixed Wheel Gate", Hydraulic Laboratory Report M, Hyd-421.
119. Vanden-Broeck, J. (1997). "Numerical calculation of the free-surface flow under sluice gate." *J. Fluid Mech.*, 130, 339–347.
120. Von Helmholtz H.L. (1868), " Ueber diskontinuirliche flussigkeithewegungen", Monatsberichten der koiniglich pressichen Akademie der Wissenschaften Berlin Germany 215-228.
121. Wahl, T. (2005). "Refined energy correction for calibration of submerged radial gates." *J. Hydraul. Eng.*, 131(6), 457–466.
122. Wilson, E., and Turner, A. (1972). "Boundary layer effects on hydraulic jump location." *J. Hydr. Div., ASCE*, 98(7), 1127-1142.
123. Webby, M.G. (1950), "Discussion: Irrotational flow and real fluid effects under planner sluice gates", *J. of Hydraulic Eng.* 125(2) 210-212.
124. White, F.M. (1994). *Fluid Mechanics*, 3rd edition, McGraw-Hill, Inc., New York, N.Y.
125. Yen, J., Lin, C., and Tsai, C. (2001). "Hydraulic characteristics and discharge control of sluice gates." *J. Chin.Inst. Eng.*, 24(3), 301–310.